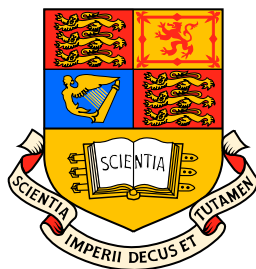


UNIVERSITY OF LONDON



Imperial College of Science, Technology and Medicine
The Blackett Laboratory
Theoretical Physics Group

A CAUSAL PERSPECTIVE ON RANDOM GEOMETRY

Stefan Zohren

Thesis submitted in partial fulfilment of the
requirements for the degree of
Doctor of Philosophy
of the University of London
and the Diploma of Membership of Imperial College.

October 2008

Supervisor: Dr. Helen Fay Dowker

Examiners: Prof. Dr. Kellog Stelle (Imperial College)
Prof. Dr. John Wheeler (University of Oxford)

A CAUSAL PERSPECTIVE ON RANDOM GEOMETRY

Stefan Zohren

Imperial College
London

Stefan Zohren
Blackett Laboratory
Imperial College London
Prince Consort Road
SW7 2AZ London
United Kingdom

© Stefan Zohren, London, 2008

All rights reserved. No part of this publication may be reproduced in any form without prior written permission of the author.

Printed in The Netherlands
PrintPartners Ipskamp B.V.

ISBN 978-90-9023894-4

Abstract

One of the biggest challenges of present day theoretical physics is to find a consistent theory of quantum gravity. There are however obvious problems in constructing a quantum theory of general relativity. It has already been shown in the seventies by 't Hooft and Veltman that perturbative quantum gravity is non-renormalizable in four dimensions. However, this does not mean that it is impossible to formulate quantum gravity by use of field theoretic techniques, on the contrary, it suggests that special, so-called non-perturbative methods have to be applied. In this thesis we investigate the importance of causality in such non-perturbative approaches to quantum gravity.

Firstly, causal sets are introduced as a simple kinematical model for causal geometry. It is shown how causal sets could account for the microscopic origin of the Bekenstein entropy bound. Holography and finite entropy emerge naturally from the interplay between causality and discreteness.

Going beyond causal set kinematics is problematic however. It is a hard problem to find the right amplitude to attach to each causal set that one needs to define the non-perturbative quantum dynamics of gravity. One approach which is ideally suited to define the non-perturbative gravitational path integral is dynamical triangulation. Without causality this method leads to unappealing features of the quantum geometry though. It is shown how causality is instrumental in regulating this pathological behavior. In two dimensions this approach of causal dynamical triangulations has been analytically solved by transfer matrix methods.

In this thesis considerable progress has been made in the development of more powerful techniques for this approach. The formulation through matrix models and a string field theory allow us to study interesting generalizations. Particularly, it has become possible to define the topological expansion. A surprising twist of the new matrix model is that it partially disentangles the large- N and continuum limit. This

makes our causal model much closer in spirit to the original idea by 't Hooft than the conventional matrix models of non-critical string theory.

The power of the here introduced techniques greatly extends the scope of analytical calculations for causal quantum gravity. This ranges from simple matter coupling to a new causal perspective on non-critical string theory.

Acknowledgments

First of all I would like to thank my supervisor Fay Dowker for guiding me through this research, as well as for giving me the freedom to follow different themes during my research. Fay has been supporting me and my career in quantum gravity already since my time at Queen Mary in 2003.

Further, I would like to thank Jan Ambjørn and Renate Loll at Utrecht University for supervising me during my regular visits to Utrecht. With respect to this I would like to thank the Theoretical Physics Institute at Utrecht University for the kind hospitality during my many visits there.

Special thanks also to my main collaborator and good friend Willem Westra without whom my work would have been only half as enjoyable as it was now. Thanks also to my other collaborators: Richard Gill, Romuald Janik, David Rideout and Yoshiyuki Watabiki, as well as my friends and colleagues at Imperial College and Utrecht University. I am also grateful to Rafael Sorkin for stimulating discussions.

With respect to my visit in Japan I would like to thank everyone at the Particle Physics Group at Ochanomizu University as well as at the Theoretical High Energy Physics Group at Tokyo Institute of Technology for the nice time we spent together. I am particularly grateful to Akio Sugamoto and Yoshiyuki Watabiki. Many thanks also to Ishiro Oda for inviting me to the University of the Ryukyus in Okinawa.

I would also like to thank the Niels Bohr Institute at Copenhagen University, the Thiele Center For Applied Mathematics in Natural Science at Århus University, the Perimeter Institute in Waterloo, the Department of Physics at Reykjavik University, the Service de Physique Théorique at CEA Saclay, the Institute of Physics at Jagellonian University and the Mathematical Institute at Leiden University for hospitality during short visits.

Financial support through ENRAGE (European Network on Random Geometry), a Marie Curie Research Training Network in the European Community's Sixth Framework Programme, network contract MRTN-CT-2004-005616 as well as through the JSPS (Japan Society for the Promotion of Science) is kindly acknowledged. Additional financial support to visit GRG18 and Perimeter Institute was provided through the Imperial College Trust and Perimeter Institute.

To my family and Maru.

Contents

Abstract	i
Acknowledgments	iii
Contents	v
List of Figures	ix
1 Introduction	1
I Motivating causality: Causal sets	7
2 Causal sets: Discrete causal geometry	9
2.1 Introducing causal sets	9
2.2 Towards a continuum approximation	11
2.3 Discussion and outlook	12
3 Entropy bounds from causal sets	15
3.1 Entropy bounds in gravity	15
3.2 An entropy bound from causal set theory	17
3.3 Evidence for the claim	19
3.3.1 The ball in Minkowski space-time	20
3.3.2 Generalizations to different spatial hypersurfaces	30
3.4 Discussion and outlook	34

II	2D causal dynamical triangulations	35
4	Path integrals and quantum gravity	37
4.1	Random paths and one-dimensional gravity	37
4.2	Random surfaces and strings	41
4.3	A path integral for quantum gravity	43
4.4	Two-dimensional Euclidean quantum gravity and Liouville theory	45
5	Two-dimensional dynamical triangulations	49
5.1	Geometry from simplices	49
5.2	The disc function	53
5.2.1	Discrete solution	53
5.2.2	Continuum limit	58
5.3	Geodesic distance and the two-loop amplitude	60
5.3.1	Defining geodesic distance and the two-loop function	60
5.3.2	The peeling procedure	62
5.3.3	The transfer matrix approach	67
5.4	Physical observables	70
5.5	Discussion and outlook to higher dimensions	72
6	Two-dimensional causal dynamical triangulations	75
6.1	Incorporating causality in dynamical triangulations	75
6.2	The discrete solution	77
6.3	The continuum limit	81
6.4	Marked amplitudes	82
6.5	Hamiltonians in causal quantum gravity	85
6.6	Physical observables: Comparing CDT and DT	87
6.7	Summary and outlook to higher dimensions	89
7	Relating Euclidean and causal dynamical triangulations	93
7.1	Introducing spatial topology changes: From CDT to DT	93
7.2	Integrating out baby universes: From DT to CDT	101
7.3	The renormalization relation	104
7.4	Discussion and outlook	106

8	The emergence of background geometry in two dimensions	109
8.1	Two-dimensional Euclidean quantum gravity with non-compact space-time	109
8.2	The emergence of background geometry	110
8.3	The classical effective action	112
8.4	Quantum fluctuations	113
8.5	Discussion and outlook	116
III	Third quantization of 2D causal dynamical triangulations	119
9	A field theoretic perspective of spatial topology changes	121
9.1	Taming spatial topology changes	121
9.2	The disc amplitude	124
9.3	The loop-loop amplitude and the consistency condition	126
9.4	Discussion and outlook	129
10	A causal string field theory	133
10.1	The string field theory framework	133
10.2	The genus zero limit	138
10.2.1	The disc amplitude	138
10.2.2	Inclusive amplitudes	139
10.3	Dyson-Schwinger equations	140
10.4	Application of the DSE	141
10.5	Discussion	146
IV	Matrix models for 2D causal dynamical triangulations	149
11	Matrix models for two-dimensional Euclidean quantum gravity	151
11.1	Counting triangulations with matrix models	151
11.2	Loop equations from matrix models	155
11.3	The loop insertion operator and higher loop amplitudes	159
11.4	Discussion and outlook	160
12	A loop equation and matrix model for CDT	163
12.1	Geometrical loop equations for CDT	163

12.2 A matrix model for generalized 2D causal quantum gravity	165
12.3 Taking the continuum limit	167
12.4 The finite time propagator	168
12.5 Discussion and outlook	169
13 A continuum matrix model for CDT	171
13.1 Mapping the DSE	171
13.2 Matrix loop equations	173
13.3 Relation to the discrete matrix model	174
13.4 Discussion and Outlook	175
14 Summary and conclusions	179
A Annexes: Causal sets	183
A.1 Basic definitions regarding the causal structure	183
A.2 Volume of the causal region between two events	184
A.3 Asymptotics of the generalized hypergeometric function	185
B Annexes: Causal dynamical triangulations	187
B.1 Lorentzian angles and simplicial building blocks	187
B.2 Analyzing Hamiltonians for causal quantum gravity	189
Bibliography	195
Index	208
Curriculum Vitae	211

List of Figures

2.1	A so-called Hasse diagram of a partially order set. In this example $x \prec y$ and $y \prec z$ and hence $x \prec z$ through transitivity.	10
3.1	Illustration of a spacelike hypersurface Σ , its boundary $\mathcal{B}(\Sigma)$, its future domain of dependence $D^+(\Sigma)$ and its future Cauchy horizon $H^+(\Sigma)$. . .	18
3.2	Shown is the expected number of maximal elements $\langle n \rangle$ as a function of the total number of elements in the domain of dependence of the unit disk in 2+1 dimensional Minkowski space-time, on a logarithmic scale. Besides the analytical result and its asymptotics, data points with error bars from Monte-Carlo simulations are also shown.	22
3.3	A snapshot from a simulation showing $N = 7806$ space-time elements forming the domain of dependence of the two-dimensional ball in 2+1 dimensional Minkowski space-time (illustrated in red) and $n = 126$ maximal elements therein (illustrated in green).	23
3.4	Shown is the expected number of maximal elements $\langle n \rangle$ as a function of the total number of elements in the domain of dependence of the 3-dimensional unit ball in 3+1 dimensional Minkowski space-time on a logarithmic scale. The plot shows the analytical result, its asymptotics, and numerical results from Monte-Carlo simulation.	25
3.5	Shown is the plot of the number of maximal elements $\langle n \rangle$ as a function of the total number of elements in the domain of dependence of the 4-dimensional ball in 4+1 dimensional Minkowski space-time on a logarithmic scale, its asymptotics, and numerical results.	27

3.6	Shown is the plot of the fundamental length scale l_f in Planck units ($l_p = (\hbar G_N/c^3)^{(d-2)/2}$) as a function of the dimensions d for even and odd dimensions and the analytic continuation.	29
3.7	Illustration of the different hyperbolic spherically symmetric spatial hypersurfaces Σ parameterized by a , and the domain of dependence $D^+(\Sigma)$.	30
3.8	Shown is the plot of the expected number of maximal elements $\langle n \rangle$ in the domain of dependence as a function of the length of the boundary A for different hyperbolic spherical symmetric spacelike hypersurfaces parameterized by a in 2+1 dimensional Minkowski space-time. One sees that all functions approach the same asymptotic $\langle n \rangle = A/4$	32
3.9	Shown is the plot of the expected number of maximal elements $\langle n \rangle$ as a function of the length of the boundary A for different hyperbolic spherical symmetric spacelike hypersurfaces in 3+1 dimensional Minkowski space-time parameterized by a . One sees that all functions approach the same asymptotics $\langle n \rangle = A/4$	33
4.1	Illustration of the path integral for a one-dimensional relativistic quantum mechanical problem, e.g. a propagating particle. One possible path of the configuration space (path space) is drawn. The “virtual” particle is propagating from x to y in a piecewise linear path of n steps each of size a .	38
4.2	(a) A worldline parametrized by ξ is embedded into \mathbb{M}^D by the mapping x^μ . (b) Analogous to the worldline a two-dimensional worldsheet of a closed string parametrized by ξ_1 and ξ_2 is embedded into \mathbb{M}^D by the mapping x^μ	42
5.1	Illustration of a positive (a) and negative (b) deficit angle ϵ_v at a vertex v .	50
5.2	Shown is a triangulation and its dual triangulation (dashed line). Highlighted is a vertex v of the triangulation and its dual cell of volume V_v .	51
5.3	Shown is a regular triangulation with topology of the disc (a) and a unrestricted triangulation with topology of a disc (b).	54
5.4	Elementary decomposition moves: If the marked edge on the boundary belongs to a triangle this triangle is removed (a), if the mark corresponds to a double link the double link is removed and the triangulation splits into two (b).	55
5.5	Graphical representation of the loop equation (5.10) for the disc function.	56

5.6	A rooted branched polymer created by gluing double links with one marked link.	57
5.7	Fixed geodesic distance two-loop amplitude $G(l_1, l_2; g; t)$	61
5.8	Decomposition of the triangulation for the fixed geodesic distance two-loop amplitude by a peeling procedure	63
5.9	The peeling decomposition moves are the same as already used in the loop equation for the disc function (recall Fig. 5.5): If the marked edge on the initial loop belongs to a triangle the triangle is removed. If it belongs to a double link then the double link is removed causing the triangulation to split. The off-splitting part of the triangulation with the final loop has topology of a cylinder, whereas the other part has topology of a disc. . .	64
5.10	Graphical illustration of the composition law (5.60) for the fixed geodesic distance two-loop amplitude.	68
5.11	A typical quantum geometry of two-dimensional Euclidean quantum gravity [1].	71
5.12	The phase diagram of four-dimensional Euclidean quantum gravity defined through DT.	73
6.1	Section of a two-dimensional Lorentzian triangulation consisting of space-time strips of height $\Delta t = 1$. Each spatial slice is periodically identified, such that the simplicial manifold has topology $[0, 1] \times S^1$. One sees that the lower strip with initial boundary length $l(t)$ and final boundary length $l(t + 1)$ consists exactly of $l(t)$ up-pointing triangles and $l(t + 1)$ down-pointing triangles.	76
6.2	A typical two-dimensional Lorentzian space-time. The compactified direction shows the spatial hypersurfaces of length $\langle L \rangle$ and the vertical axis labels proper time T . Technically, the picture was generated by a Monte-Carlo simulation, where a total volume of $N = 18816$ triangles and a total proper time of $t = 168$ steps was used. Further, initial and final boundary has been identified.	89
7.1	Illustration of the double light cone causal structure at a Morse point in an up-side down trousers geometry.	94
7.2	Illustration of the one-step propagator with an off-splitting “baby universe”.	95

7.3	Decomposition of the disc function with a marked point in the bulk into a propagator with arbitrary time and a disc function with a mark on the boundary.	97
7.4	(a) At every point in the quantum geometry there is an infinitesimal baby universe. (b) When trying to draw the baby universes on a plane one is forced to draw smaller and smaller triangles reflecting the fractal structure of the geometry.	99
7.5	Illustration of the peeling relation (7.36). In each step of the decomposition either a triangle is removed or a double link which results into an off-splitting of a branched polymer.	103
9.1	Feynman rules: (a) shows a vertex of φ^3 -theory which is assigned a coupling g . (b) shows the analogous interaction term for a splitting string. Similar to φ^3 -theory we assign a string coupling g to this interaction. . .	122
9.2	In all four graphs, the geodesic distance from the final to the initial loop is given by T . Differentiating with respect to T leads to eq. (9.8). Shaded parts of graphs represent the full, g_s -dependent propagator and disc amplitude, and non-shaded parts the CDT propagator.	123
9.3	Graphical illustration of eq. (9.10). Shaded parts represent the full disc amplitude, unshaded parts the CDT disc amplitude and the CDT propagator.	124
9.4	Two different ways of decomposing the loop-loop amplitude into proper-time propagators and a disc amplitude. Two points touch in the disc amplitude W , pinching the boundary to a figure-8, which combinatorially implies a substitution $W_{\Lambda, g_s}(L) \rightarrow L W_{\Lambda, g_s}(L)$ in the formulas. The time variables are related by $T_1 + T_2 = T$	127
10.1	The elementary terms of the string field theory Hamiltonian (10.10): (a) the single spatial universe propagator, (b) the term corresponding to splitting into two spatial universes, (c) the term corresponding to the merging of two spatial universes and (d) the tadpole term.	136
11.1	Building blocks for Feynman graphs: (a) the scalar propagator and (b) the scalar three-point vertex.	152

11.2 Building blocks for fat-graphs: (a) the Hermitian matrix propagator and (b) the Hermitian matrix three-point vertex.	153
11.3 The contour C encloses counterclockwise the cut $[c_-, c_+]$ but not z	157
12.1 Illustration of the two composition moves to add a triangle. The white dot on the right-hand-side shows the position of the mark before the triangle was added whereas the black dot shows the mark after the triangle was added.	164
12.2 Graphical representation of the loop equation (12.2).	165
12.3 Graphical representation of the loop equation (12.8).	166
B.1 Illustration of a space-like (a) and a time-like (b) Lorentzian deficit angle ϵ_v at a vertex v	188

CHAPTER 1

Introduction

Finding a consistent theory of quantum gravity is a notoriously hard problem. Such a theory should give a fundamental quantum description of space-time geometry with general relativity as a classical limit. However, more than ninety years have passed since Einstein's discovery of general relativity, and still very little is known about the ultimate structure of space-time at very small scales.

Quantum field theory on the other hand has proven to be a marvelously successful way to describe three of the four fundamental forces of nature: the electro-magnetic, the weak and the strong force. For the gravitational force however one does not have a well-defined predictive quantum field theoretic description yet, but one does have a very successful classical field theoretic description in the form of Einstein's theory of general relativity. Since the other forces can be described by quantum field theories, it seems natural that there also exists a quantum theory for the gravitational field.

Another reason which supports the existence of such a theory of quantum gravity is the fact that gravity couples to all forms of energy. Hence, one expects the energy fluctuations at small distances due to Heisenberg's uncertainty relations to induce also quantum fluctuations in the gravitational field. This leads to the prediction that space-time geometry has a highly non-trivial microstructure at extremely small scales close to the Planck length, $l_p = \sqrt{\hbar G_N c^{-3}} \approx 1.616 \times 10^{-35} m$.

There are however obvious problems in constructing a quantum theory of general

relativity (see [2] for an overview). It has already been shown in the seventies by 't Hooft and Veltman that perturbative quantum gravity is non-renormalizable in four dimensions [3]. There are several ways to confront this problem:

One of the most prominent approaches to quantum gravity is string theory (see standard text books [4, 5, 6, 7]). In this unifying theory the worldlines of propagating particles are replaced by worldsheets of propagating strings. The issue of non-renormalizability is thought to be resolved from the start in string theory, since the point-like interactions which cause the divergencies are replaced by extended interactions which cannot be localized. Whereas string theory has recently had some successes such as the calculation of strongly coupled gauge theories using the AdS/CFT correspondence (see for instance [8]), as a theory of quantum gravity it still relies on supersymmetry and extra dimensions.

Another approach is loop quantum gravity [9, 10] in which one uses a Dirac (constraint) quantization [11] of Ashtekar's connection variables [12]. Recent advances in this approach have been made by use of covariant spin-foam models [10, 13]. These approaches suggest that the ultraviolet divergences can be resolved by the existence of a minimal length scale, commonly expressed in terms of the Planck length l_p . Finiteness of gravitational entropy can be seen as evidence for such fundamental discreteness of space-time.

A more radical approach is causal set theory [14, 15] which postulates fundamental discreteness from the outset. In this approach discrete sets of space-time events are viewed as fundamental objects underlying continuum space-times. Even though some interesting phenomenological models using causal sets have been proposed, there has been little progress in formulating a quantum path integral for causal sets.

There are other approaches which define quantum gravity non-perturbatively. Renormalizability of the non-perturbative theory could be achieved by a nontrivial fixed point scenario as described by Weinberg [16]. One possible example of such a scenario is the exact renormalization group flow method for Euclidean quantum gravity in the continuum [17].

Another famous attempt to non-perturbatively define quantum gravity is dynamical triangulations (DT), a covariant path integral formulation, in which quantum gravity is obtained as a continuum limit of a superposition of simplicial space-time geometries (see for instance [18]). Two-dimensional DT has also been used as a worldsheet regularization of the bosonic string. A particular strength of this approach is that it ex-

presses the theory as a statistical sum over entirely geometric objects. Since the path integral assigns a probability to each contributing geometry, we also call it a model of random geometry. To perform the statistical sum one usually starts off in the Euclidean sector including many “acausal” geometries. This leads to unappealing features of the quantum geometries in dimensions higher than two. It can be shown within the approach of causal dynamical triangulations (CDT) that causality is essential to regulate this pathological behaviour. In CDT one starts off with a sum over Lorentzian geometries and then analytically continues to the Euclidean sector to perform the summation [19]. Numerical simulations indicate that CDT in contrast to DT leads to a well-behaved continuum limit in four dimensions [20, 21].

In this thesis we focus on the implementation of causality in models of random geometry.

In Part I of this thesis we concentrate on the approach of causal sets. In Chap. 2 causal sets are introduced as a simple and instructive model of causal random geometry. After defining causal sets we show how they can correspond to continuum space-times in the continuum approximation. Although we are not able to define a path integral for causal sets, we describe a simple phenomenological model where causal sets are randomly embedded in a fixed space-time. From this model we show in Chap. 3 how causal sets could account for the microscopic origin of the Bekenstein or Susskind entropy bound.

It seems that to define random geometry in terms of a non-perturbative path integral over geometries more structure is needed. Such structure is provided by causal dynamical triangulations (CDT) on which we focus in Part II, III and IV of this thesis.

Part II gives an introduction to CDT as a model of causal quantum gravity with emphasis on analytical results in two dimensions. In Chap. 4 we give a brief introduction into path integrals in general with emphasis on the gravitational path integral. In Chap. 5 we introduce dynamical triangulations (DT) as a non-perturbative definition of the path integral for two-dimensional Euclidean quantum gravity. At the end of this chapter we comment on the problems one encounters in higher-dimensional DT. In the next chapter, Chap. 6, CDT are introduced as a model of two-dimensional causal quantum gravity. A comparison to the Euclidean model (DT) is given as well as a brief outlook to results in higher dimensions. In Chap. 7 several relations between DT and CDT in two dimensions are discussed. In particular, we describe how CDT and DT can be

related by respectively introducing or “integrating out” baby universes, i.e. spatial topology changes. In Chap. 8 we discuss CDT for the case of non-compact geometries. We see how a semi-classical background emerges from quantum fluctuations yielding a simple model of two-dimensional quantum cosmology.

In Part III we introduce a generalized CDT model. This is formulated as a third quantization of two-dimensional CDT, i.e. a model in which spatial universes or strings can be annihilated and created from the vacuum. In Chap. 9 we show how by introducing a coupling constant to the process of off-splitting baby-universes one can non-perturbatively solve for the disc function with an arbitrary number of baby-universes. In Chap. 10 this result is embedded in the framework of a string field theory (SFT) model of CDT. As an application of the resulting Dyson-Schwinger equations (DSE) of the SFT we calculate amplitudes of higher genus.

The last Part IV deals with the development of matrix models for CDT. After a brief introduction to matrix models in the context of DT in Chap. 11, we formulate a matrix model description for the contributing triangulations in CDT in Chap. 12. In the continuum limit one recovers the results of the generalized CDT model introduced in Chap. 9 giving a combinatorial interpretation of this model. In Chap. 13 we show that also the continuum CDT model is described by a matrix model. This is particularly interesting, since contrary to DT the size of the matrices N does not have to scale with the cut-off in the so-called double scaling limit. Further, the expansion in $1/N^2$ reorganizes the power expansions in terms of topology, where terms with powers N^{-2h+2} can be identified with the *continuum* surfaces of genus h . This makes the new matrix model much closer to the original proposal by 't Hooft for QCD than the conventional matrix models of non-critical string theory.

In Chap. 14 we conclude this thesis by summarizing the results. Further, we comment on possible applications of the newly discovered matrix model to simple matter coupling in CDT. Interestingly, it might be possible to give a simple derivation of the Onsager exponents from CDT.

Finally App. A and B provide supplementary information to the chapters on causal sets and causal dynamical triangulations respectively.

Most of the novel results of this thesis have been published in research articles. In particular, the following chapters are based on the following articles:

- Chapter 3 on D. Rideout and S. Zohren, *Class. Quantum Grav.* **23** (2006) 6195–6213;
- Chapter 8 on J. Ambjørn, R. Janik, W. Westra, and S. Zohren, *Phys. Lett. B* **641** (2006) 94–98;
- Chapter 9 on J. Ambjørn, R. Loll, W. Westra, and S. Zohren, *JHEP* **0712** (2007) 017;
- Chapter 10 on J. Ambjørn, R. Loll, W. Westra, Y. Watabiki and S. Zohren, *JHEP* **0805** (2008) 032;
- Chapter 12 on J. Ambjørn, R. Loll, W. Westra, Y. Watabiki and S. Zohren, *Phys. Lett. B* **670** (2008) 224-230;
idem, to appear in *Acta Phys. Polon. B* **39** (2008) 3355-3364.
- Chapter 13 on J. Ambjørn, R. Loll, W. Westra, Y. Watabiki and S. Zohren, *Phys. Lett. B* **665** (2008) 252–256.

The remaining chapters are mainly introductory parts which review existing literature. These are included to make the thesis self-contained, but do not represent new work done by the author of this thesis.

Part I

Motivating causality: Causal sets

CHAPTER 2

Causal sets: Discrete causal geometry

In this chapter we introduce causal sets as a simple model of causal random geometry. After giving a mathematical definition of causal sets we show how those can correspond to continuum space-times in the continuum approximation. Even though we are not able to define a path integral for causal sets we describe a simple phenomenological model where causal sets are randomly embedded in a fixed space-time [14]. In the next chapter we will use this model to give a microscopic understanding of the Susskind or Bekenstein entropy bound.

2.1 | Introducing causal sets

Causal order suggests itself as a fundamental principle for quantum gravity because of the enormous amount of topological and geometrical information which it contains [15].

There are several reasons to support the assumption of causal structure as primary in quantum gravity. It has been shown that, given merely the causal relations of events in a space-time manifold, one needs only the volume measure to recover the full geometry in the continuum [22, 23].

Being faced with the non-renormalizability of perturbative quantum gravity in four dimensions 't Hooft already proposed in 1978 several radical ideas to possibly define

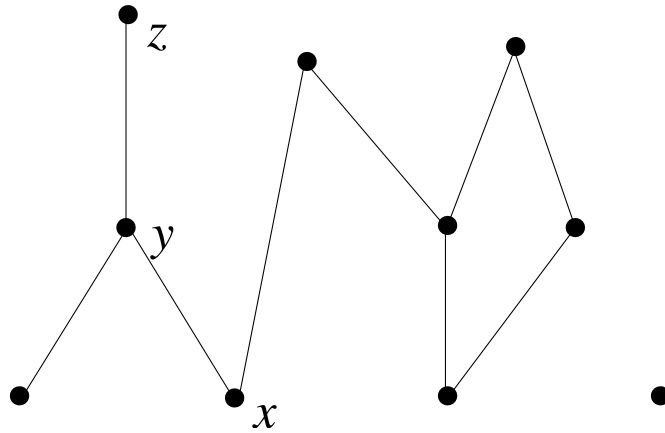


Figure 2.1: A so-called Hasse diagram of a partially order set. In this example $x \prec y$ and $y \prec z$ and hence $x \prec z$ through transitivity.

a theory of quantum gravity [24], of which one was to view quantum gravity as a theory of causal sets of space-time events (see also [25]). This idea was later picked up again by Bombelli et al. [14] and further developed by many others to what is sometimes referred to as causal set theory (see for instance [26, 27] for some reviews).

Mathematically speaking, a *causal set* is defined to be a locally finite partially ordered set $\mathcal{C} = (C, \prec)$, namely a set C together with a relation \prec , called “precedes”, which satisfy the following axioms:

Transitivity: If $x \prec y$ and $y \prec z$ then $x \prec z$, $\forall x, y, z \in C$;

Irreflexivity: $x \not\prec x$;

Local Finiteness: For any pair of fixed elements x and z of C , the set of elements lying between x and z is finite, $\text{card}\{y | x \prec y \prec z\} < \infty$, where $\text{card}X$ means the cardinality of the set X .

Fig. 2.1 shows a graphical representation of a causal set as an example. Of these axioms, the first two say that $\mathcal{C} = (C, \prec)$ is a partially ordered set or poset. The last expression, local finiteness, is related to the “radical idea” of this approach, namely that space-time is fundamentally discrete. The motivation for introducing fundamental

discreteness is that it provides us with a way to account for the missing volume information. However, from a phenomenological point of view there are also other reasons, for example the finiteness of gravitational entropy which suggests that space-time might be fundamentally discrete.

In the following we summarize some basic definitions for intrinsic causal set quantities of which most are “discrete” versions of analogous concepts used to describe the causal structure of continuum space-times (cf. App. A.1).

The *past* of an element $x \in C$ is the subset $\mathbf{past}(x) = \{y \in C \mid y \prec x\}$. This corresponds to the causal past $J^-(x)$ in the continuum approximation. The past of a subset of C is the union of the pasts of its elements. The *future* of an element $x \in C$ is the subset $\mathbf{future}(x) = \{y \in C \mid x \prec y\}$ which respectively corresponds to the causal future $J^+(x)$ in the continuum approximation.

An important concept for the formulation of the entropy bound from causal set theory is that of a *maximal element* in a causal set $\mathcal{C} = (C, \prec)$. This is an element which has no successors, i.e. an element x for which $\nexists y \in C$ such that $x \prec y$. The set of all maximal elements in \mathcal{C} is denoted by $\mathbf{max}(\mathcal{C}) = \{x \in C \mid \nexists y \in C \text{ s.t. } x \prec y\}$. In analogy, a *minimal element* is one which has no ancestors, i.e. an element x for which $\nexists y \in C$ such that $y \prec x$ and the set of all minimal elements in \mathcal{C} is denoted by $\mathbf{min}(\mathcal{C}) = \{x \in C \mid \nexists y \in C \text{ s.t. } y \prec x\}$.

2.2 | Towards a continuum approximation

Having given the precise definition of a causal set one might ask the questions: How could one actually be able to formulate a theory of quantum gravity using causal sets, and how do causal sets relate to the known classical notion of smooth Lorentzian manifolds? In the following we give a definition of what it means for a causal set \mathcal{C} to be approximated by a Lorentzian space-time (\mathcal{M}, g) .

Consider a strongly causal space-time (\mathcal{M}, g) . The map $\phi : C \rightarrow \mathcal{M}$ from a causal set $\mathcal{C} = (C, \prec)$ into a space-time (\mathcal{M}, g) is called a *conformal embedding* if $x \prec y \iff \phi(x) \in J^-(\phi(y))$, $\forall x, y \in C$. Consider the Alexandrov neighborhood $J^+(p) \cap J^-(q)$, for every $p, q \in \mathcal{M}$, which forms a basis for the manifold topology of (\mathcal{M}, g) if (\mathcal{M}, g) is strongly causal, which we assume throughout. *sprinkling* The map ϕ is called a *faithful embedding* or *sprinkling* if it has the following property: The number of elements n mapped into an Alexandrov neighborhood is equal to its space-time volume V times

the space-time density, up to Poisson fluctuations. Thus, the probability of finding n elements in this region is given by the Poisson distribution

$$P(n) = \frac{(\rho V)^n e^{-\rho V}}{n!}, \quad (2.1)$$

where $\rho = l_f^{-d}$ is the density set by the fundamental length scale l_f in d dimensions. In other words, this means that in a space-time region of volume V one finds on average $N = V\rho$ elements of the causal set embedded into this region, and the fluctuations are typically of the order \sqrt{N} . Further, the properties of the Poisson distribution lead to local Lorentz invariance in the continuum space-time [28, 29].

Using the above definitions, we say that a space-time (\mathcal{M}, g) *approximates* a causal set \mathcal{C} if there exists a faithful embedding of \mathcal{C} into (\mathcal{M}, g) . This notion gives a correspondence between causal sets and continuum space-times. In terms of this correspondence continuum causal structure arises from the microscopic order relations of the causal set elements and the continuum volume measure of a region arises from counting the number of elements comprising this region. Nevertheless, one still has to prove the uniqueness of this correspondence (up to small fluctuations). In general the precise formulation of such a uniqueness proof is a difficult mathematical problem. However, it has been proven to hold for the limiting case $\rho \mapsto \infty$ [30] and certain progress has been made in the generalization to large but finite ρ [31].

2.3 | Discussion and outlook

The ultimate aim of causal set theory is to formulate a theory of quantum gravity using a path integral approach, where the single histories are causal sets. Continuum physics would then be supposed to emerge in a suitable continuum approximation. However, since there is basically no information on spatial distances of space-time events, there is no obvious way to find a discretized version of the gravitational action in this context. And even if such an action would be found it is not clear how the sum over different causal sets in the path integral could be performed.

A different path in the search for causal set dynamics has been taken by analyzing certain sequential growth models of the causal sets [32, 33, 34, 35]. These growth models aimed to determine an effective *classical* dynamics of causal sets. One interesting result is that the “early universe” phase of such growth models closely resem-

bles de Sitter space, at least in the way that volumes of causal intervals scale with their length [36].

From the above discussion we can say that it is still very ambitious to view causal sets as a model for quantum gravity, but nevertheless, it still gives a very simple and instructive model of causal random geometry. In particular, we can take a fixed Lorentzian space time and view it as a continuum approximation of a causal set. Using the Poisson distribution, as mentioned in the previous section, we are then able to randomly draw causal sets which can be faithfully embedded in this space-time. From a phenomenological point of view we can now study certain properties of such an ensemble, as will be done in the next chapter with view on entropy bounds. Even though some of these phenomenological models give interesting predictions [37, 28, 38, 39, 40], one should still treat them with a bit of care for the following reason: Already in the case of a quantum mechanical particle we know that even though the classical path is smooth and nice, single histories of the path integral look nothing like this and are not even described by differentiable functions. Hence, it is not a priori clear, that classical space-times should approximate a *single* causal sets history. Keeping this in mind we use causal sets as a phenomenological model of fundamentally discrete space-time.

Entropy bounds from causal sets

In this chapter we propose a measure for the maximal entropy of spherically symmetric spacelike space-time regions in terms of the ensemble of causal sets approximating this continuum space-time [39, 41]. A bound for the entropy contained in this region is obtained from a counting of potential “degrees of freedom” associated to the Cauchy horizon of its future domain of dependence. For different spherically symmetric spacelike regions in Minkowski space-time of arbitrary dimension, we show that this proposal leads, in the continuum approximation, to Susskind’s or Bekenstein’s well-known spherical entropy bound up to a numerical factor.

3.1 | Entropy bounds in gravity

In the history of general relativity there has been a long discussion regarding the thermodynamics of gravitational systems. One of the most famous examples is the *Bekenstein-Hawking formula* for black hole entropy [42, 43, 44, 45], stating that the entropy of a black hole is given by a quarter of the area of the event horizon in Planckian

units¹

$$S_{BH} = \frac{A}{4}. \quad (3.1)$$

This bound is truly universal, meaning that it is independent of the characteristics of the matter system and can be derived without any knowledge of the actual microstates of the quantum statistical system.

Along this line there have been several generalizations of this entropy bound. One is *Susskind's spherical entropy bound* [46], stating that the upper bound for the entropy of the matter content of an arbitrary spherically symmetric spacelike region (of finite volume) is,

$$S_{\text{matter}} \leq \frac{A}{4}, \quad (3.2)$$

where A is the area of the boundary of the region.² Even though this spacelike entropy bound cannot be generalized to arbitrary non-spherically symmetric spacelike regions, there exists a generalization in terms of light-sheets, namely the *Bousso or covariant entropy bound* [49, 50]. More precisely, let $A(\mathcal{B})$ be the area of any $(d-2)$ -dimensional surface \mathcal{B} , then the $(d-1)$ dimensional hypersurface L is called the light-sheet of \mathcal{B} if L is generated by light rays which begin at \mathcal{B} , extend orthogonally away from \mathcal{B} and have everywhere non-negative expansion. The entropy flux through the light-sheet is then bounded by

$$S(L) \leq \frac{A(\mathcal{B})}{4}. \quad (3.3)$$

¹As a convention we will throughout the discussion regarding entropy bounds work in Planck units with

$$c = k_B = G_N = \hbar = 1,$$

where c, k_B, G_N, \hbar denote the speed of light, Boltzmann's constant, Newton's constant and Planck's constant respectively. In these units the Planck length is given by

$$l_p = \left(\frac{\hbar G_N}{c^3} \right)^{\frac{d-2}{2}} = 1, \quad \text{for } d \geq 3.$$

²There was an earlier proposed bound by Bekenstein [47] stating that the entropy of any weakly gravitating matter system obeys $S_{\text{matter}} \leq 2\pi ER$, where E is the energy of the matter system and R the circumferential radius of the smallest sphere that contains it. If one further assumes that this bound is valid for strongly gravitating matter systems, then gravitational stability in four dimensions implies that $2E \leq R$ and hence $S_{\text{matter}} \leq 2\pi ER \leq A/4$. One sees that in four dimensions the Bekenstein bound is stronger than the Susskind bound, however, in $d > 4$ gravitational stability and the Bekenstein bound only imply that $S_{\text{matter}} \leq (d-2)A/8$ [48]. Hence, the geometrical Susskind bound is arguably more fundamental.

This entropy bound is also widely regarded as evidence for the *holographic principle* [51, 46, 50], stating that the maximum number of degrees of freedom carried by L is given by $A(\mathcal{B})/4$.

These entropy bounds suggest that an underlying theory of quantum gravity should predict the bounds from a counting of microstates (see for example [52]). This verification of the thermodynamic laws is an important consistency check for any approach to quantum gravity. Further, the finiteness of the entropy might already give some indications about the actual microstructure of space-time. There is a semi-classical argument that the description of a quantum theory of gravity by a local quantum field theory in the continuum, in the absence of a high frequency cut-off, leads to infinitely many degrees of freedom in a finite region, and therefore to a divergence in the entropy of this region [38, 53]. The entropy bounds therefore suggest that space-time might possess a fundamental discreteness at scales of order of the Planck scale. Continuum physics would then have to emerge from this fundamental theory when making a continuum approximation at large scales. This suggests that to obtain a theory of quantum gravity one does not have to quantize the metric fields of the continuum geometries, but should rather find a quantum theory of the discrete structure underlying those continuum geometries [54].

In the following we show how using causal sets as a phenomenological model of causal random geometry one can derive a notion of maximum entropy from a counting of potential horizon “degrees of freedom” of the fundamental theory reminiscent of former ideas in the context of black hole entropy [55, 38]. Using this measure we formulate an entropy bound for spherically symmetric spacelike regions within the causal set approach. We then show that in the continuum approximation, for different spherically symmetric spacelike regions in Minkowski space-time of arbitrary dimension, this leads to Susskind’s spherical entropy bound up to a numerical factor.

3.2 | An entropy bound from causal set theory

In the previous chapter we introduced causal sets as a phenomenological model of causal random geometry. As explained earlier space-time volume arises from a counting of fundamental space-time elements. In the following we show how entropy bounds could arise from a counting of potential horizon “degrees of freedom” at the fundamental level, giving a microscopic origin for Susskind’s spherical entropy bound.

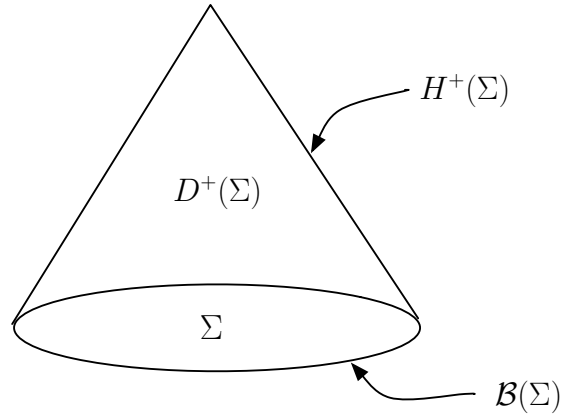


Figure 3.1: Illustration of a spacelike hypersurface Σ , its boundary $\mathcal{B}(\Sigma)$, its future domain of dependence $D^+(\Sigma)$ and its future Cauchy horizon $H^+(\Sigma)$.

As already mentioned in the previous section, the spherical entropy bound states that the entropy of the matter content of a spherically symmetric spacelike region Σ (of finite volume) is bounded by a quarter of the area of the boundary of Σ in Planck units

$$S \leq \frac{A}{4}, \quad (3.4)$$

in full units $S \leq Ak_B c^3 / (4G_N \hbar)$, where $A = \text{Vol}(\mathcal{B}(\Sigma))$ is the area of the boundary of this region.

Surprisingly, the maximum entropy in (3.4) can be determined without any knowledge of the microscopic properties of the thermodynamic system. A theory of quantum gravity however should be able to deduce (3.4) purely from a counting of the fundamental degrees of freedom at the microscopic level. (One may wonder in what manner a counting of degrees of freedom measures the entropy of a system. In a discrete context “degrees of freedom” are generally finite, and a state counting can be expected to yield something proportional to the exponential of the number of degrees of freedom. Thus measuring the entropy as the logarithm of the number of states can be seen to be equivalent to counting the number of degrees of freedom of the system.) In the following we want to give a notion of those fundamental degrees of freedom in the context of causal set theory leading to the formulation of an entropy bound within this approach.

Consider a spherically symmetric spacelike region of space-time, potentially containing some matter system. We assume that the “back reaction” of the matter content

upon the space-time geometry can be neglected, so that different states of the matter system lead to the same spherically symmetric space-time geometry. The entropy of that system must eventually “flow out” of the region by passing over the boundary of its future domain of dependence. But because space-time is fundamentally discrete, the amount of such entropy flux is bounded above by the number of discrete elements comprising this boundary. This is a fundamental limit imposed by discreteness on the amount of information flux which can emerge from the region, and therefore on the amount of entropy which it can contain. Thus we have argued that an entropy bound arises from causal sets.

Proposal *Consider a spherically symmetric spacelike hypersurface Σ of finite volume in a strongly causal space-time \mathcal{M} of dimension $d \geq 3$. Denote the future domain of dependence of this hypersurface by $D^+(\Sigma)$ (c.f. App. A.1 and Fig. 3.1). Let $\mathcal{C} = (C, \prec)$ be a causal set which can be faithfully embedded into $D^+(\Sigma)$. Then the maximum entropy contained in Σ is given by the number of maximal elements of \mathcal{C} ,*

$$S_{\max} = \mathbf{card}\{\mathbf{max}(\mathcal{C})\}. \quad (3.5)$$

Claim *This proposal leads to Susskind’s entropy bound in the continuum approximation,*

$$S_{\max} = \frac{A}{4}, \quad (3.6)$$

where $A = \text{Vol}(\mathcal{B}(\Sigma))$ is the area of the boundary of this region Σ , if the fundamental discreteness scale is fixed at a dimension dependent value to be calculated.

3.3 | Evidence for the claim

In this section we provide analytical and numerical evidence for the claim that the entropy bound (3.5) leads to Susskind’s bound in the continuum. In all discussed examples we consider $(d - 1)$ -dimensional spherically symmetric spacelike hypersurfaces Σ in d -dimensional Minkowski space \mathbb{M}^d , and calculate the number of maximal elements in its domain of dependence $D^+(\Sigma)$. Since we assume that $D^+(\Sigma)$ arises as a continuum approximation of a causal set \mathcal{C} , we know from the phenomenological model described above that the elements of \mathcal{C} are faithfully embedded into $D^+(\Sigma)$ according to the Poisson distribution (2.1). Hence the expected number of maximal elements in

$D^+(\Sigma)$ is given by

$$\langle n \rangle = \rho \int_{D^+(\Sigma)} dx^d \exp \left\{ -\rho \text{Vol} \left(J^+(x) \cap D^+(\Sigma) \right) \right\}, \quad (3.7)$$

where again ρ is the fundamental density of space-time. On the right-hand-side of (3.7) one integrates over all points $x \in D^+(\Sigma)$, where every point is first weighted by the probability of finding an element of \mathcal{C} embedded at this point and further weighted by the probability of not finding any other element of \mathcal{C} embedded in $J^+(x) \cap D^+(\Sigma)$. Note that because of the fundamentally random nature of the discrete-continuum correspondence in causal sets we calculate the expected number of maximal elements in a sprinkling, even though the proposal (3.5) is phrased in terms of a fixed causal set.

3.3.1 | The ball in Minkowski space-time

In this section we want to calculate the expected number of maximal elements $\langle n \rangle$ in $D^+(\Sigma)$, where Σ is chosen to be a $(d-1)$ -dimensional ball $S_{d-1}(R)$ with radius R in Minkowski space-time \mathbb{M}^d . Due to the spherical symmetry of the problem it is useful to introduce spherical coordinates $x = (t, r, \theta_1, \dots, \theta_{d-2})$, where we choose the origin to be the futuremost event of $D^+(\Sigma)$. The volume element $\text{Vol}(J^+(x) \cap D^+(\Sigma))$ is equal to the volume of the Alexandrov neighborhood of x and 0, $\text{Vol}_d(\tau) \equiv \text{Vol}(J^+(x) \cap J^-(0))$, where we denote proper time by $\tau = \sqrt{t^2 - r^2}$. Using the result for $\text{Vol}_d(\tau)$ as calculated in App. A.2 and integrating out the spherical symmetry in (3.7) one obtains a general expression for the expected number of maximal elements in $D^+(S_{d-1}(R))$,

$$\langle n \rangle = \rho \frac{(d-1)\pi^{\frac{d-1}{2}}}{\Gamma(\frac{d+1}{2})} \int_0^R dt \int_0^t dr r^{d-2} e^{-\rho D_d(t^2-r^2)^{\frac{d}{2}}}, \quad (3.8)$$

where the dimension dependent constant D_d is defined in App. A.2.

In the following we evaluate (3.8) for various dimensions by analytical and numerical methods.

2+1 dimensions

In $d = 3$ dimensions one can explicitly evaluate (3.8). It is useful to express the result in terms of the expected total number of space-time elements faithfully embedded into $D^+(S_2(R))$, $N = \rho V$, where $V = \frac{\pi}{3} R^3$ is the volume of the domain of dependence

$D^+(S_2(R))$. The expected number of maximal elements is

$$\langle n \rangle = 8 \left(e^{-\frac{N}{4}} - 1 \right) - 2NE_{\frac{1}{3}} \left(\frac{N}{4} \right) + 4\Gamma \left(\frac{2}{3} \right) \sqrt[3]{2N}, \quad (3.9)$$

where $E_n(x)$ is the exponential integral defined by

$$E_n(x) = \int_1^\infty t^{-n} e^{-xt} dt. \quad (3.10)$$

We also measured the expected number of maximal elements numerically by “sprinkling” a causal set into a 2+1-dimensional $2 \times 2 \times 1$ square box, which contains $D^+(S_2(1))$. By sprinkling we mean simply selecting N_c elements at random with uniform distribution within the box, and computing the causal relation between each pair from the Minkowski metric. For each of 100 trials $i = 1 \dots 100$, we deduce the set of elements which fall within $D^+(S_2(1))$, compute its cardinality N_i , and count the number of such elements n_i which are maximal within that region. From these we compute the sample mean and its error, and repeat this computation for a range of values of N_c . These computations were greatly facilitated by utilizing causal set and Monte-Carlo toolkits within the Cactus computational framework [56].

The plot of the expected number of maximal elements $\langle n \rangle$ as a function of N for the unit disk is shown in Fig. 3.2, on a logarithmic scale. The agreement of analytical and numerical results justifies the numerical methods.

For a large number of elements $N \rightarrow \infty$ we can use the asymptotic expansion of the exponential integrals

$$E_n(x) \propto \frac{e^{-x}}{x} \left(1 - \frac{n}{x} + \dots \right) \quad \text{for } |x| \rightarrow \infty \quad (3.11)$$

yielding

$$\langle n \rangle = 4\Gamma \left(\frac{2}{3} \right) \sqrt[3]{2N} + \dots \quad \text{for } N \rightarrow \infty, \quad (3.12)$$

where $+\dots$ are lower order terms in N . The asymptotics are also displayed in Fig. 3.2 together with the full expression for the expected number of maximal elements. In terms of the density ρ and the radius R of $S_2(R)$ this result reads

$$\langle n \rangle = \frac{16\sqrt[3]{2\pi}}{3^{5/6}\Gamma \left(\frac{1}{3} \right)} \rho^{\frac{1}{3}} \frac{2\pi R}{4}, \quad (3.13)$$

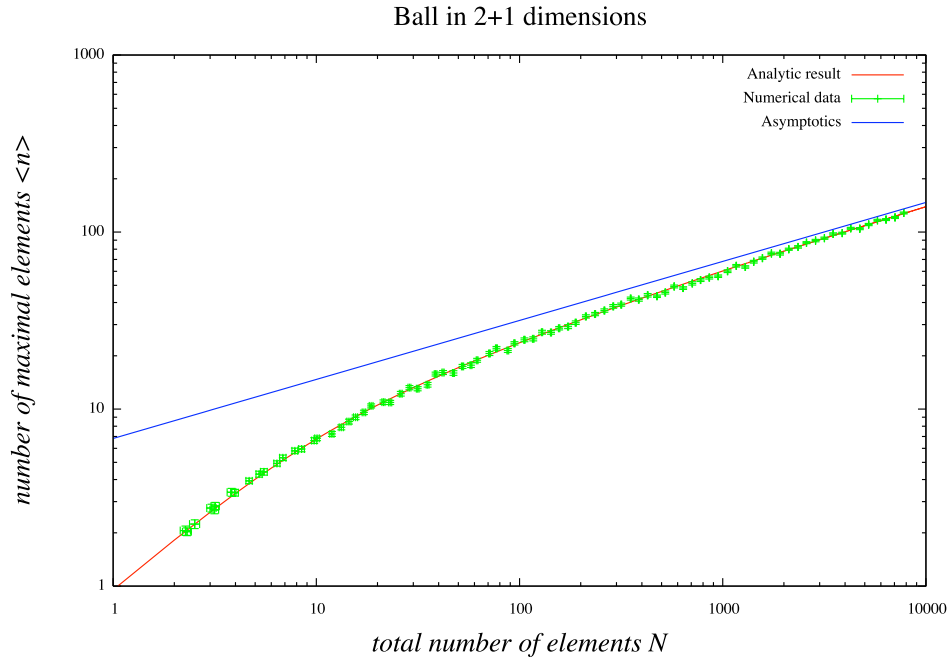


Figure 3.2: Shown is the expected number of maximal elements $\langle n \rangle$ as a function of the total number of elements in the domain of dependence of the unit disk in 2+1 dimensional Minkowski space-time, on a logarithmic scale. Besides the analytical result and its asymptotics, data points with error bars from Monte-Carlo simulations are also shown.

up to lower order corrections. It is important to see that $\langle n \rangle \propto A/4$, where $A = 2\pi R$ is the length of the boundary of $S_2(R)$. This is highly non-trivial, as one can see by looking at a snapshot of a numerical simulation (Fig. 3.2). There one observes that the maximal elements do not align along the one-dimensional boundary $\mathcal{B}(S_2(R))$. Instead they are distributed along a hyperbola close to the two-dimensional Cauchy horizon $H^+(S_2(R))$, with a density of maximal elements which *decreases* with distance from the center. Hence the fact that the expected number of maximal elements is indeed proportional to the length A of the one-dimensional boundary $\mathcal{B}(S_2(R))$ for large A already gives very non-trivial evidence for the proposed entropy bound.

To have the precise confirmation of the $\mathcal{O}(1)$ constant in $\langle n \rangle \propto A/4$ one has to choose the fundamental length scale $l_f = \rho^{-1/3}$ to be $l_f = 16\sqrt[3]{2\pi}/(3^{5/6}\Gamma(1/3)) \approx 4.41$. This gives support to the belief that the fundamental discreteness scale of space-time

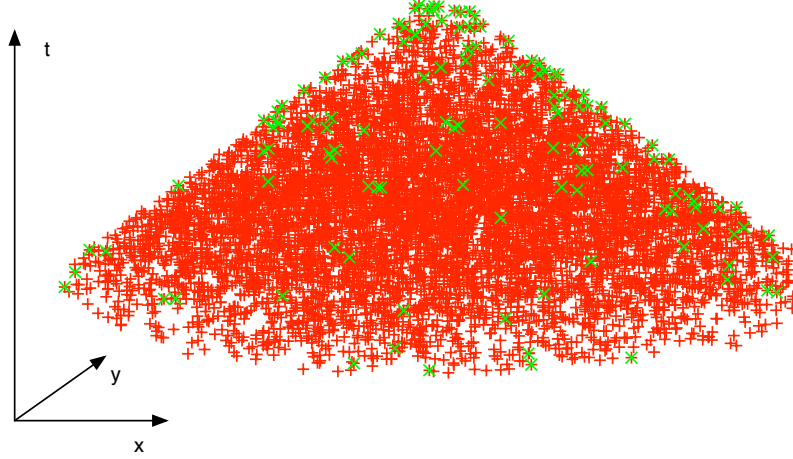


Figure 3.3: A snapshot from a simulation showing $N = 7806$ space-time elements forming the domain of dependence of the two-dimensional ball in 2+1 dimensional Minkowski space-time (illustrated in red) and $n = 126$ maximal elements therein (illustrated in green).

is of the order of the Planck length.

Hence, using this value for the fundamental discreteness scale we have confirmed our claim, namely in the continuum approximation we have

$$S_{\max} = \langle n \rangle = \frac{2\pi R}{4} \quad (3.14)$$

or $S_{\max} = k_B 2\pi R / (4\sqrt{\hbar G_N / c^3})$ in full units, when we set $l_f = 16\sqrt[3]{2\pi} / (3^{5/6}\Gamma(1/3))$. One now sees that the assumption of large but finite N used to obtain the asymptotic behavior is equivalent to saying that A is much larger than the Planck length. However, one can see that even for relatively small values of the length A , such as 10^3 in Planck units, the approximation of $\langle n \rangle$ by its asymptotic expansion is already very accurate. For even smaller values of the length scale the Planck corrections become significant. However, as one can see in Fig. 3.2, the corrections always decrease the expected number of maximal elements, such that $\langle n \rangle$ never exceeds the bound (3.14).

3+1 dimensions

Clearly from a physical point of view the evaluation of (3.8) in 3+1 dimensions is the most interesting case. For $d = 4$ one can write (3.8) as follows,

$$\langle n \rangle = 2\pi\rho \int_0^R dt \int_0^{t^2} dz \sqrt{t^2 - z} e^{-\rho D_4 z^2} \quad (3.15)$$

One can perform the first integration in (3.15) by using the following integral relation [57]

$$\int_0^u x^{\nu-1} (u-x)^{\mu-1} e^{\beta x^n} dx = B(\mu, \nu) u^{\mu+\nu-1} \times \\ \times {}_nF_n \left(\frac{\nu}{n}, \frac{\nu+1}{n}, \dots, \frac{\nu+n-1}{n}; \frac{\mu+\nu}{n}, \frac{\mu+\nu+1}{n}, \dots, \frac{\mu+\nu+n-1}{n}; \beta u^n \right), \quad (3.16)$$

for $\Re(\mu) > 0$, $\Re(\nu) > 0$ and $n = 2, 3, \dots$, where $B(\mu, \nu)$ denotes Euler's beta function and ${}_pF_q(a_1, \dots, a_p; b_1, \dots, b_q; z)$ is the generalized hypergeometric function defined through

$${}_pF_q(a_1, \dots, a_p; b_1, \dots, b_q; z) = \sum_{k=0}^{\infty} \frac{z^k \prod_{i=1}^p (a_i)_k}{k! \prod_{j=1}^q (b_j)_k}, \quad (3.17)$$

and $(a)_n = \Gamma(a+n)/\Gamma(a)$ are the usual Pochhammer polynomials. The second integration, namely the one of the generalized hypergeometric function, can be obtained by use of the following relation [57]

$$\int z^{\alpha-1} {}_pF_q(a_1, \dots, a_p; b_1, \dots, b_q; z) dz = \frac{z^\alpha}{\alpha} {}_{\rho+1}F_{q+1}(a_1, \dots, a_p, \alpha; b_1, \dots, b_q, \alpha+1; z). \quad (3.18)$$

Expressed in terms of the number of causal set elements sprinkled into $D^+(S_3(R))$, $N = \rho V$, where the volume of $D^+(S_3(R))$ is given by $V = \frac{\pi}{3} R^4$, the final result reads

$$\langle n \rangle = N {}_3F_3 \left(\frac{1}{2}, 1, 1; \frac{5}{4}, \frac{7}{4}, 2; -\frac{1}{8} N \right). \quad (3.19)$$

For a large number of elements N we can use the asymptotic expansion of the generalized hypergeometric functions (cf. App. A.3), yielding the asymptotic expression for the expected number of maximal elements,

$$\langle n \rangle = 3\sqrt{2\pi} N^{\frac{1}{2}} + \dots \quad \text{for } N \rightarrow \infty. \quad (3.20)$$

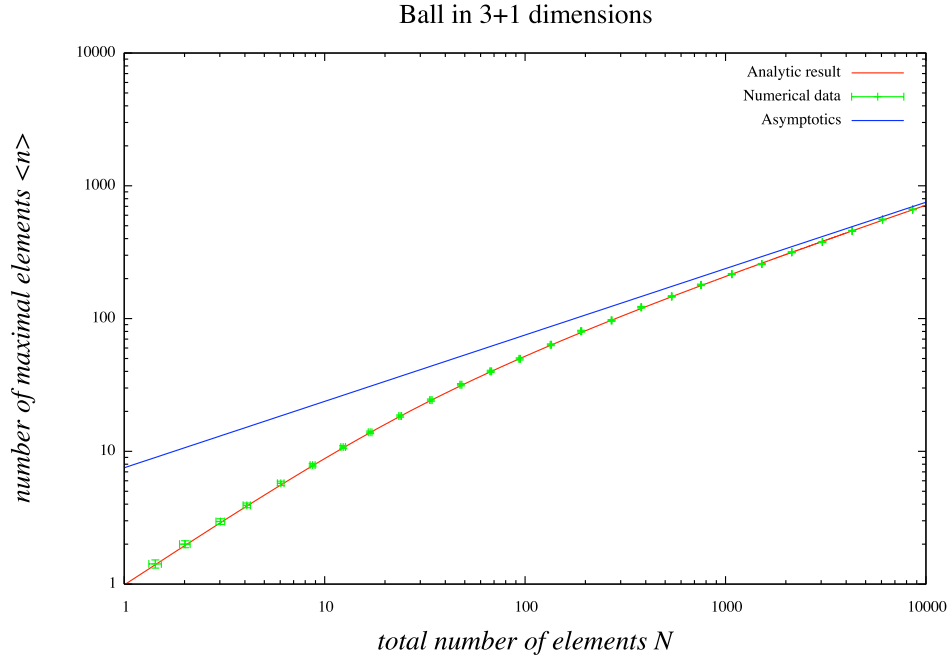


Figure 3.4: Shown is the expected number of maximal elements $\langle n \rangle$ as a function of the total number of elements in the domain of dependence of the 3-dimensional unit ball in 3+1 dimensional Minkowski space-time on a logarithmic scale. The plot shows the analytical result, its asymptotics, and numerical results from Monte-Carlo simulation.

In terms of the fundamental density of space-time ρ and the radius R of $S_3(R)$ this result translates into

$$\langle n \rangle = \sqrt{6} \rho^{\frac{1}{2}} \frac{4\pi R^2}{4}. \quad (3.21)$$

As in the previous case the number of maximal elements follows the right scaling according to the entropy bound, namely $\langle n \rangle \propto A/4$, where the area of the boundary of $S_3(R)$ is given by $A = 4\pi R^2$. The factor of proportionality is a $\mathcal{O}(1)$ constant as in the previous case, supporting the assumption that the fundamental length scale l_f is proportional to the Planck length l_p . More precisely, to have an exact agreement with the Susskind bound the fundamental length scale in four dimensions will be given by $l_f = \sqrt[4]{6}$ in Planck units. Using this value for the fundamental length scale the asymptotic expansion for the expected number of maximal elements reads

$$S_{\max} = \langle n \rangle = \frac{4\pi R^2}{4} \quad (3.22)$$

or $S_{\max} = 4\pi R^2 k_B c^3 / (4\hbar G)$ in full units. At first sight one might feel uncomfortable in absorbing the order one constant into the fundamental length scale to exactly confirm the Susskind bound. However, as discussed in the previous case, the scaling $\langle n \rangle \propto A/4$ is nontrivial and already serves as a confirmation of the bound. Taking the phenomenological law $S_{\max} = A/4$ (spherical entropy bound) as “data” gives the fundamental length scale in four dimensions to be

$$l_f = \sqrt[4]{6} \approx 1.57 \quad (\text{in four dimensions}). \quad (3.23)$$

In comparison to the previous case of 2+1 dimensions one observes that the fundamental discreteness scale l_f depends on the dimension. In Sec. 3.3.1 we will derive an expression for the factor for arbitrary (even) dimensions, showing that this factor tends exactly to one as $d \rightarrow \infty$. It is important to check that l_f is universal for all cases with the same space-time dimension. In Sec. 3.3.2 we will provide evidence that this is indeed the case.

At this point it is interesting to note that a similar method of fixing the fundamental discreteness scale to obtain the right factor of proportionality in the entropy bound is followed in loop quantum gravity in the context of black hole entropy (cf. [58]). There one fixes the Immirzi parameter which can be regarded as a measure for the discreteness scale (through its relation to the lowest eigenvalue of the area operator) to obtain the right factor of a quarter in the black hole entropy. However, since there are several ambiguities in the relation between the Immirzi parameter and the fundamental discreteness scale in the sense one uses it in causal set theory, it is hard to compare the numerical values in any sense.

4+1 dimensions

In $d = 5$ dimensions one can also evaluate the integral in (3.8) in a similar way to the calculation in 2+1 dimensions. As in the previous cases the result is expressed in terms of the number of causal set elements sprinkled into $D^+(S_4(R))$, $N = \rho V$, with the volume of $D^+(S_4(R))$ given by $V = \frac{\pi^2}{10} R^5$. The final result reads

$$\begin{aligned} \langle n \rangle = & \frac{4}{3} \left(32 \left(1 - e^{-\frac{N}{16}} \right) + 3NE_{\frac{1}{5}} \left(\frac{N}{16} \right) - NE_{\frac{3}{5}} \left(\frac{N}{16} \right) + \right. \\ & \left. + 5(2N)^{\frac{3}{5}} \Gamma \left(\frac{7}{5} \right) - 30(2N)^{\frac{1}{5}} \Gamma \left(\frac{9}{5} \right) \right). \end{aligned} \quad (3.24)$$

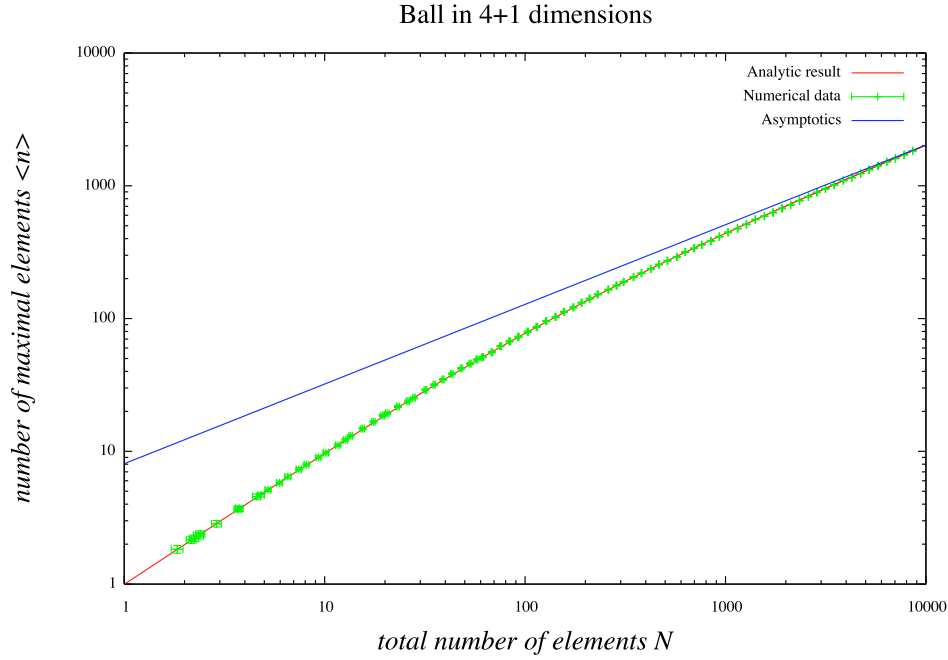


Figure 3.5: Shown is the plot of the number of maximal elements $\langle n \rangle$ as a function of the total number of elements in the domain of dependence of the 4-dimensional ball in 4+1 dimensional Minkowski space-time on a logarithmic scale, its asymptotics, and numerical results.

The plot of $\langle n \rangle$ as a function of N is shown in Fig. 3.5 on a logarithmic scale as well as the numerical results obtained from Monte-Carlo simulation and the asymptotic behavior. As in the previous cases there is agreement between analytical and numerical results.

For large N one can expand (3.24) using the asymptotic expansion for the exponential integral (3.11), yielding

$$\langle n \rangle = \frac{20}{3} \Gamma\left(\frac{7}{5}\right) (2N)^{\frac{3}{5}} + \dots \quad \text{for } N \rightarrow \infty. \quad (3.25)$$

Re-expressed in terms of the density ρ and the radius R of $S_4(R)$ this result reads

$$\langle n \rangle = \frac{32\pi^{1/5}}{5^{8/5}\Gamma\left(\frac{8}{5}\right)} \sqrt{\frac{2}{5 + \sqrt{5}}} \rho^{\frac{3}{5}} \frac{2\pi^2 R^3}{4}. \quad (3.26)$$

As for the lower dimensional cases this result gives the correct behavior $\langle n \rangle \propto A/4$, where $A = 2\pi^2 R^3$ is the volume of the boundary of $S_4(R)$, providing further evidence

for the claim. Further, we can use the coefficient in (3.26) to fix the fundamental length scale in 4+1 dimensions $l_f = \rho^{-1/5}$ to be $l_f = 2^{11/6}\pi^{1/15}/(5^{8/15}(5+\sqrt{5})^{1/6}\Gamma(8/5)^{1/3}) \approx 1.22$ in Planck units. Using this fundamental length scale the number of maximal elements (3.26) reads

$$S_{\max} = \langle n \rangle = \frac{2\pi^2 R^3}{4}, \quad (3.27)$$

or in full units $S_{\max} = 2\pi^2 R^3 k_B / (4(\hbar G_N / c^3)^{3/2})$, which confirms our claim.

Generalizations to higher dimensions

In the previous sections we have seen that causal set theory can provide a fundamental explanation for Susskind's entropy bound for the spacelike hypersurface $S_{d-1}(R)$ in 2+1, 3+1 and 4+1-dimensional Minkowski space-time. In this section we want to generalize these results to arbitrary dimensions. For the case of odd space-time dimension, it turns out that one can easily calculate the expected number of maximal elements, but one cannot write the results in a closed form. However, for even dimensions one can find a closed expression.

As in the previous cases we will express the result of the expected number of maximal elements in terms of $N = \rho V$, where V is the volume of the domain of dependence of $S_{d-1}(R)$, given by

$$V \equiv \text{Vol}(D^+(S_{d-1}(R))) = \frac{\pi^{\frac{d-1}{2}}}{d\Gamma(\frac{d+1}{2})} R^d. \quad (3.28)$$

Using the integration relations (3.16) and (3.18) one can integrate (3.8) for even dimensions, yielding

$$\langle n \rangle = N^{\frac{d}{2}+1} F_{\frac{d}{2}+1} \left(\frac{2}{d}, \frac{4}{d}, \dots, \frac{d}{d}, 1; \frac{d+1}{d}, \frac{d+3}{d}, \dots, \frac{2d-1}{d}, 2; -2^{1-d} N \right). \quad (3.29)$$

Note that this result is also valid for the case of $d = 2$ dimensions, however it is not related to any entropy of the system, and is thus excluded from the proposal.

For large N one can use the asymptotic expansion of the generalized hypergeometric function (App. A.3) to derive the asymptotics of the number of maximal elements for arbitrary even dimensions, yielding

$$\langle n \rangle = \frac{2^{\frac{2d-2}{d}} \pi(d-1)}{d \sin\left(\frac{2\pi}{d}\right) \Gamma\left(\frac{2d-2}{d}\right)} N^{\frac{d-2}{d}} + \dots, \quad \text{for } N \rightarrow \infty. \quad (3.30)$$

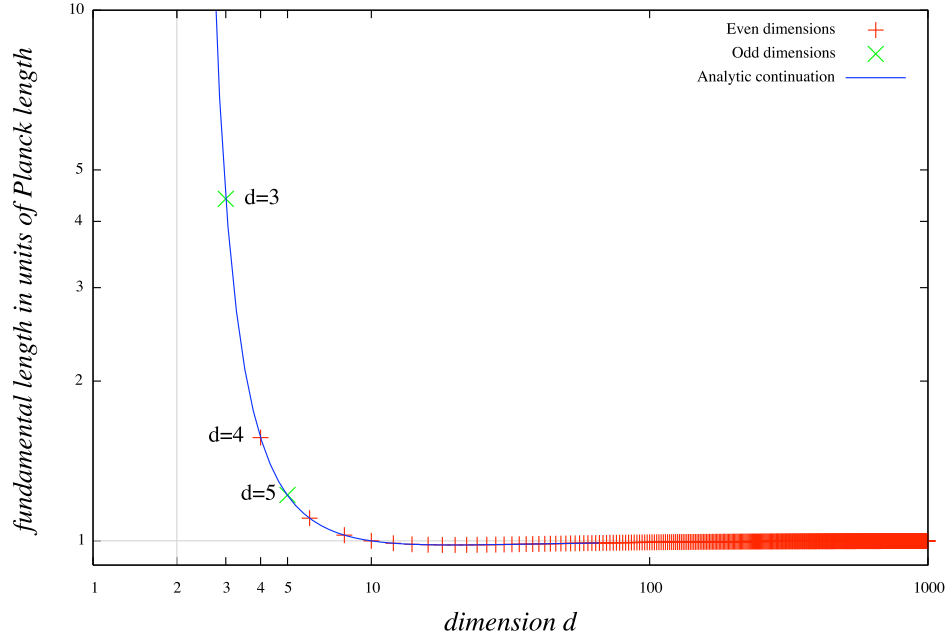


Figure 3.6: Shown is the plot of the fundamental length scale l_f in Planck units ($l_p = (\hbar G_N/c^3)^{(d-2)/2}$) as a function of the dimensions d for even and odd dimensions and the analytic continuation.

From this result one can see that the number of maximal elements scales like $\langle n \rangle \sim A/4$, where A is the volume of the boundary of $S_{d-1}(R)$, i.e.

$$A \equiv \text{Vol}(\mathcal{B}(S_{d-1}(R))) = \frac{\pi^{\frac{d-1}{2}}(d-1)}{\Gamma(\frac{d+1}{2})} R^{d-2}. \quad (3.31)$$

Further, we obtain $\langle n \rangle = A/4$ precisely for the following value of the fundamental length scale,

$$l_f = \left[\frac{16 \left(\frac{\pi d^2}{4} \Gamma\left(\frac{d+1}{2}\right)^2 \right)^{\frac{1}{d}}}{d^2 \sin\left(\frac{2\pi}{d}\right) \Gamma\left(2\frac{d-1}{d}\right)} \right]^{\frac{1}{d-2}} \quad (3.32)$$

The analytic continuation of (3.32) as a function of the dimension is shown in Fig. 3.6 together with the explicit values for 2+1 and 4+1 dimensions as determined in the previous sections. One observes that the expression (3.32) agrees with these values. This suggests that (3.32) also holds for arbitrary odd dimensions. For $d = 2$ the value

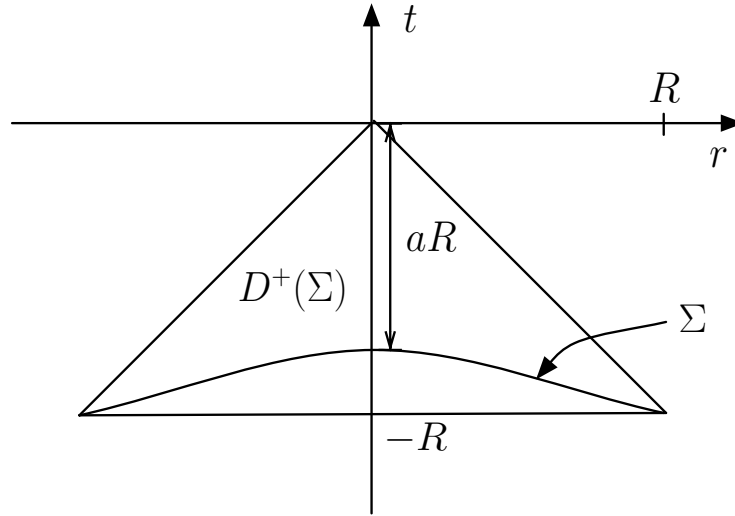


Figure 3.7: Illustration of the different hyperbolic spherically symmetric spatial hypersurfaces Σ parameterized by a , and the domain of dependence $D^+(\Sigma)$.

of (3.32) diverges, since the Planck length $l_p = (\hbar G_N / c^3)^{(d-2)/2}$ is not well defined in two dimensions. This also reflects the fact that the entropy bound only holds for dimensions $d \geq 3$. For all values $d \geq 3$ the fundamental length scale is of order of the Planck length.

3.3.2 | Generalizations to different spatial hypersurfaces

In the previous section we have derived the Susskind bound for the case where the spacelike hypersurface was chosen to be a $(d - 1)$ -dimensional ball in d dimensional Minkowski space-time. Further, from this we determined the fundamental discreteness scale of space-time. However, it is important to prove that the fundamental discreteness scale so determined yields the same entropy bound for all spacelike hypersurfaces of a certain dimension.

In this section we show that the claim also holds for spacelike hypersurfaces in Minkowski space-time different from those discussed in the previous section. We investigate hyperbolic spherically symmetric spacelike hypersurfaces given by

$$t = -\sqrt{r^2 + a^2(R^2 - r^2)}, \quad 0 \leq a \leq 1, \quad (3.33)$$

as shown in Fig. 3.7 together with its domain of dependence. For the special case of

$a=1$ the spacelike hypersurface given by (3.33) is equivalent to the $(d-1)$ -dimensional ball $S_{d-1}(R)$ for which we have determined an analytic expression for the expected number of maximal elements $\langle n \rangle$ in the previous section. For other values $0 < a < 1$ one cannot determine the number of maximal elements analytically. In the following we will investigate this problem numerically for the physically most important cases of 2+1 and 3+1 dimensions.

2+1 dimensions

For $d = 3$ dimensions we use Monte-Carlo methods to numerically obtain the number of maximal elements in the domain of dependence of the spacelike hypersurfaces Σ defined by (3.33) for different values of a as a function total number N of elements in the domain of dependence. Since all these spacelike hypersurfaces Σ have the same boundary $\mathcal{B}(\Sigma)$, it is useful to express $\langle n \rangle$ as a function of the length of the boundary $A = 2\pi R$. One can do this by using that $N = \rho V$, where the volume of the domain of dependence of Σ is given by

$$V = \frac{2\pi}{3} \frac{a^2}{1+a} R^3. \quad (3.34)$$

Further, we use the value for the fundamental density of space-time as obtained in Sec. 3.3.1, i.e. $\rho = (3^{5/2} \Gamma(1/3)^3) / (8192\pi)$.

The results of the simulations are summarized in Fig. 3.8. Shown is the expected number of maximal elements $\langle n \rangle$ as a function of the boundary length A . For the special case of $a = 1$ in (3.33) we know that the result is given by (3.9), where N is replaced by $N = A^3 / (2^{13} \Gamma(2/3)^3)$. The asymptotics of this analytic result is given by $\langle n \rangle = A/4$ as shown earlier. For different values of $0 < a < 1$ the simulations show that even though the number of maximal elements as a function of A differs for small values $A \lesssim 10^3$ in Planck units, in the expansion for large A , corresponding to the continuum approximation, all functions $\langle n \rangle$ for different a enter the same asymptotic expansion $\langle n \rangle = A/4$, yielding Susskind's entropy bound. In addition, it shows that the prediction of the fundamental discreteness scale is universal in 2+1 dimensions, at least for all investigated cases of spacelike hypersurfaces in Minkowski space-time. A generalization to examples in curved space-time has still to be shown and will be investigated in future work.

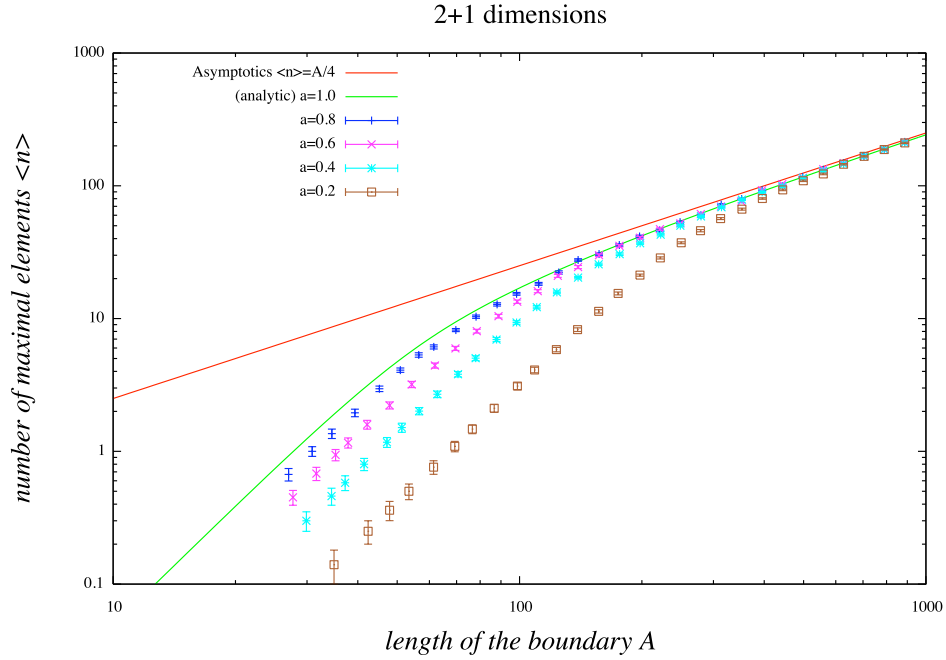


Figure 3.8: Shown is the plot of the expected number of maximal elements $\langle n \rangle$ in the domain of dependence as a function of the length of the boundary A for different hyperbolic spherical symmetric spacelike hypersurfaces parameterized by a in 2+1 dimensional Minkowski space-time. One sees that all functions approach the same asymptotic $\langle n \rangle = A/4$.

3+1 dimensions

As in the case of 2+1 dimensions we use Monte-Carlo methods to numerically obtain the number of maximal elements in the domain of dependence of the spacelike hypersurfaces Σ defined by (3.33) for $d = 4$ and different values of a . Again, the result is expressed as a function of the area of the boundary of Σ , i.e. $A = 4\pi R^2$. This can be done by using the relation $N = \rho V$ and noticing that the volume of the domain of dependence of Σ is given by

$$V = R^4 \left[\frac{\pi}{3} - \frac{\pi}{6(1-a^2)^{\frac{3}{2}}} \left(\sqrt{1-a^2}(2-5a^2) + 3a^4 \log \left(\frac{1+\sqrt{1-a^2}}{a} \right) \right) \right], \quad (3.35)$$

where we use $\rho = 1/6$ for the value of the fundamental density of four dimensional space-time.

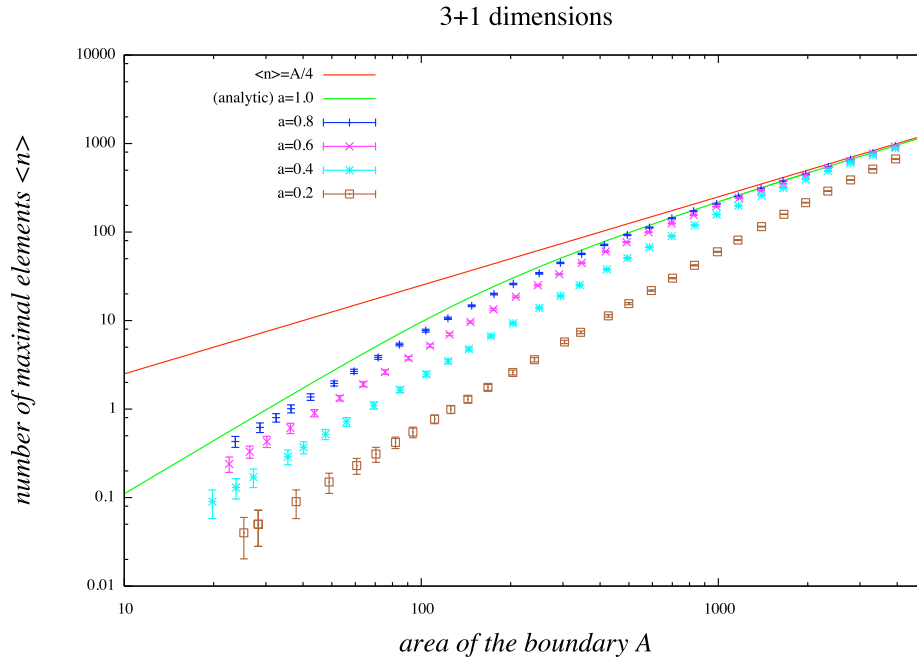


Figure 3.9: Shown is the plot of the expected number of maximal elements $\langle n \rangle$ as a function of the length of the boundary A for different hyperbolic spherical symmetric spacelike hypersurfaces in 3+1 dimensional Minkowski space-time parameterized by a . One sees that all functions approach the same asymptotics $\langle n \rangle = A/4$.

The numerical and analytical results are shown in Fig. 3.9. Displayed is the expected number of maximal elements $\langle n \rangle$ as a function of the area A of the boundary. For the special case of $a = 1$ the analytical result was given by (3.19), with N replaced by $N = A^2/(2\pi 12^2)$. The simulations show that for different values of $0 < a < 1$ all functions $\langle n \rangle$ enter the same asymptotics, $\langle n \rangle = A/4$, in the continuum limit, giving further evidence for the claim. For very small values of a the expected number of maximal elements enters the asymptotic regime only very slowly. However, the upper value for A of the simulations is still very small ($\sim 10^{-33}m$). As in the lower dimensional case the simulations show that the prediction for the value of the fundamental discreteness scale of four-dimensional space-time, namely $l_f = \sqrt[4]{6}$, is a universal quantity for this dimension, at least for all investigated cases of spherically symmetric spacelike hypersurfaces in Minkowski space-time.

3.4 | Discussion and outlook

Using the phenomenological model of causal set theory as introduced in the previous chapter we argued for a bound on the entropy in a spherically symmetric spacelike region from a counting of potential horizon “degrees of freedom” of the fundamental theory, namely the maximal elements of the future domain of dependence of the region. It was then shown that, for different spherically symmetric spacelike regions in Minkowski space-time of arbitrary dimension, this leads to Susskind’s spherical entropy bound. The evidence was given in terms of analytical results for spatial $(d - 1)$ -dimensional balls in d -dimensional Minkowski space-time, and in terms of numerical results obtained from Monte-Carlo simulations for the case of hyperbolic spherically symmetric hypersurfaces in Minkowski space-time.

So far results were given only in terms of examples in flat Minkowski space-time. Clearly this is a very restricted class and further evidence should be provided in different space-times. Spherically symmetric spacelike regions in curved space-time such as in Friedmann-Robertson-Walker cosmology will be investigated in future work.

Another step would be to formulate the proposal intrinsically in terms of order invariants, without making explicit reference to the continuum. Such a formulation may be fruitful in providing a fundamental understanding of Bousso’s covariant entropy bound.

Further work in progress in the direction of entropy bounds from causal sets is the implementation of entropy evaluation through link counting as proposed in [38, 53] for black holes, to other situations such as dS space-time.

Part II

2D causal dynamical triangulations

CHAPTER 4

Path integrals and quantum gravity

In Part I of this thesis we introduced causal sets as a simple model of causal random geometry. The remaining three parts of this thesis will be centered around the approach of causal dynamical triangulations. As already discussed in the introduction, one way to confront the non-renormalizability of perturbative quantum gravity in four dimensions is to find a proper non-perturbative definition of the gravitational path integral. Before describing dynamical triangulations as such, we first give a brief introduction to path integrals in general. Specifically, we comment on problems one encounters when formulating the gravitational path integral.

4.1 | Random paths and one-dimensional gravity

Path integrals were first introduced by Dirac and Feynman [59, 60] as a quantization scheme to first quantize physical systems. One of the most instructive examples is the free relativistic particle in D -dimensional Minkowski space-time \mathbb{M}^D . The amplitude of a particle moving from x to y can be expressed by the so-called propagator,

$$G_m(x, y) = \int_x^y \mathcal{D}P(x, y) e^{iS[P(x, y)]} \quad (4.1)$$

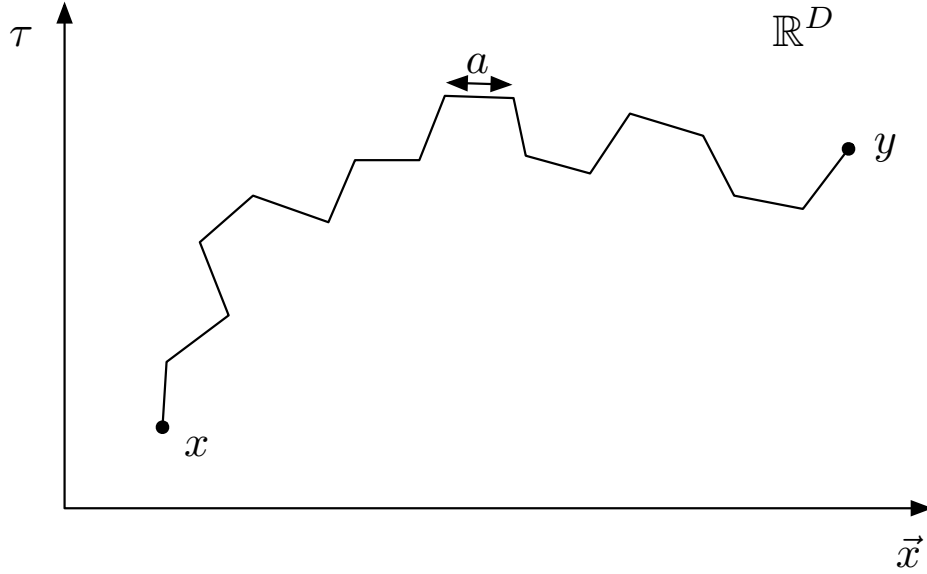


Figure 4.1: Illustration of the path integral for a one-dimensional relativistic quantum mechanical problem, e.g. a propagating particle. One possible path of the configuration space (path space) is drawn. The “virtual” particle is propagating from x to y in a piecewise linear path of n steps each of size a .

where the action is simply given by the mass m times the length of the path

$$S[P(x, y)] = m \int_{P(x, y)} dl. \quad (4.2)$$

The classical equations of motion are derived by choosing a specific parametrization

$$x(\xi) : [0, 1] \rightarrow \mathbb{M}^D, \quad x(0) = x, \quad x(1) = y. \quad (4.3)$$

The action now reads

$$S[P(x, y)] = m \int_0^1 d\xi \sqrt{(\dot{x}^\mu(\xi))^2}, \quad (4.4)$$

where we defined $\dot{x}^\mu := dx^\mu/d\xi$. The classical equations of motion can be easily obtained by varying the action

$$\frac{\delta S}{\delta x^\mu(\xi)} = \frac{d}{d\xi} \frac{\dot{x}^\mu}{|\dot{x}|} = 0 \quad (4.5)$$

which are simply straight lines from x to y and reparametrizations of it.

To be able to define the path integral (4.1) one usually performs a Wick rotation by taking time imaginary

$$t \rightarrow -i\tau = -ix^D. \quad (4.6)$$

One now deals with the corresponding Euclidean model in \mathbb{R}^D .

One way to define the path integral (4.1) is to introduce a “geometrical” discretization scheme where one directly discretizes the length of the worldline (see for instance [18]). Therefore it is useful to work with the action (4.2), since its definition does not depend on parametrized quantities. Specifically, in the employed discretization each worldline consists of a piecewise linear path, where each edge is of size a (see Fig. 4.1). Here a serves as a reparametrization invariant cut-off which will be taken to zero in the continuum limit. For a piecewise linear path of length n the action simply becomes $S = m_0 a n$, where m_0 is the bare mass. Further, the path integral can be written as a sum over all possible paths connecting x and y :

$$\int_x^y \mathcal{D}P(x, y) \rightarrow \sum_{n=1}^{\infty} \int \prod_{i=0}^n d\hat{e}_i \delta(a \sum_{i=0}^n \hat{e}_i - (y - x)). \quad (4.7)$$

Here the $a\hat{e}_i$ denote the vectors of the linear parts of the discretized worldline, where the \hat{e}_i 's are unit vectors in \mathbb{R}^D . The propagator can now be defined as follows

$$G_{m_0}(x, y) = \sum_{n=1}^{\infty} e^{-m_0 a n} \int \prod_{i=0}^n d\hat{e}_i \delta(a \sum_{i=0}^n \hat{e}_i - (y - x)). \quad (4.8)$$

To perform the integration it is helpful to use the Fourier transform

$$G_{m_0}(p) = \int dx e^{-ip(x-y)} G_{m_0}(x, y) = \sum_{n=1}^{\infty} e^{-m_0 a n} \int \prod_{i=0}^n d\hat{e}_i e^{-iap\hat{e}_i}. \quad (4.9)$$

The integral in the above expression can be expanded as

$$\int d\hat{e} e^{-iap\hat{e}} \equiv f(a|p|) = f(0)(1 - c^2(ap)^2 + \mathcal{O}(a^4)), \quad (4.10)$$

where $f(0) \equiv \text{Vol}(S_{D-1}(1))$ is given in (A.5) and c is an irrelevant constant. We can now perform the summation leading to

$$G_{m_0}(p) = \sum_{n=1}^{\infty} (e^{-m_0 a} f(a|p|))^n = \frac{1}{1 - e^{-m_0 a} f(a|p|)}. \quad (4.11)$$

One can define the continuum limit by taking the cut-off a to zero and at the same time taking the number of steps in the discretized path to infinity. The latter is fulfilled when $\mu \equiv m_0 a$ is taken to its critical value $\mu_c = \log f(0)$ at which $G_{m_0}(p)$ approaches its radius of convergence. Hence, we renormalize the bare mass m_0 such that

$$\mu - \mu_c = m^2 c^2 a^2 \quad (4.12)$$

where m is the physical mass. Using this renormalization we obtain

$$G_{m_0}(p) \xrightarrow{a \rightarrow 0} \frac{1}{a^2 c^2} \frac{1}{p^2 + m^2}. \quad (4.13)$$

After a wave function renormalization the continuum propagator $G_m^c(p)$ becomes the well-known expression for the Feynman propagator

$$G_m^c(p) = a^2 c^2 G_{m_0}(p) = \frac{1}{p^2 + m^2}. \quad (4.14)$$

In terms of its Fourier transform this is precisely the solution of the field equation for the Green function of a Klein-Gordon field,

$$(-\partial_y^2 + m^2)G_m(x, y) = \delta^{(D)}(y - x). \quad (4.15)$$

In the above description we used a discretization scheme where we directly discretized the length of the worldline. A different prescription is to use the parametrized action (4.4) and to introduce a cut-off on the worldline coordinates (see for instance [61]). However, since the square root in this expression is very difficult to handle, it is useful to look at an alternative action for the free relativistic particle first introduced in [62],

$$S[x, g]_{(x,y)} = \int_0^1 d\xi \sqrt{|g(\xi)|} (g^{-1}(\xi) \dot{x}^2 + m^2), \quad (4.16)$$

where $g(\xi)$ is the internal metric of the one-dimensional worldline. The action (4.16) can also be viewed as the action of one-dimensional gravity coupled to D scalar fields x^μ . Solving for the equations of motion for g and plugging the result back into the equations of motion for x one finds (4.5). This shows that the systems described by both actions (4.4) and (4.16) are equivalent on the classical level. Whether this is also true on the quantum level remains to be checked. To obtain the propagator we now also have to integrate over the worldline metric g ,

$$G_m(x, y) = \int \mathcal{D}[g] \int_x^y \mathcal{D}_g x e^{iS[x, g]_{(x,y)}}, \quad (4.17)$$

where $\mathcal{D}[g]$ refers to the measure of the space of worldline metrics modulo diffeomorphisms, i.e. coordinate transformations on the worldline. Let us in the following briefly sketch how to calculate the propagator (4.17) (for details see [61]). The first step is to perform the Wick rotation. One proceeds by defining the integral over \mathcal{D}_{g^X} for fixed g . Therefore one discretizes the worldline coordinates by forming $N + 1$ slices of arbitrary small parameter differences

$$\epsilon_n = \xi_n - \xi_{n-1}, \quad \xi_0 = 0, \quad \xi_N = 1. \quad (4.18)$$

The integration over \mathcal{D}_{g^X} and the continuum limit $\epsilon_n \rightarrow 0$ can now be performed in a similar manner as one usually does for the non-relativistic particle. The remaining integral over $\mathcal{D}[g]$ can then be done after a suitable gauge fixing. The result is precisely given by (4.14). This indicates that both actions (4.4) and (4.16) not only lead to the same classical equations of motion, but also to the same dynamics on the quantum level. A comparison of the two discretization schemes further shows that the “geometrical” discretization employed above is computationally rather simple in comparison to the continuum method. Dynamical triangulations, as will be introduced in the next chapter, is an analogous “geometrical” discretization scheme for surfaces and higher-dimensional manifolds.

4.2 | Random surfaces and strings

The natural generalization to the random paths, as considered in the previous section, are random surfaces or worldsheets of propagating (closed) strings (Fig. 4.2). In analogy to the relativistic particle we expect those to describe the relativistic string. The simplest action for a surface F is given by its area

$$S[F] = \lambda \int_F dA(F), \quad (4.19)$$

where λ is a (cosmological) constant conjugate to the area. The action (4.19) is a direct analog of (4.2). The parametrized form of (4.19) is called the Nambu-Goto action [63] and reads

$$S[F] = \lambda \int_F d^2\xi \sqrt{h}, \quad (4.20)$$

where

$$h = \det h_{ab} = \det \frac{\partial x^\mu}{\partial \xi^a} \frac{\partial x^\mu}{\partial \xi^b} \quad (4.21)$$

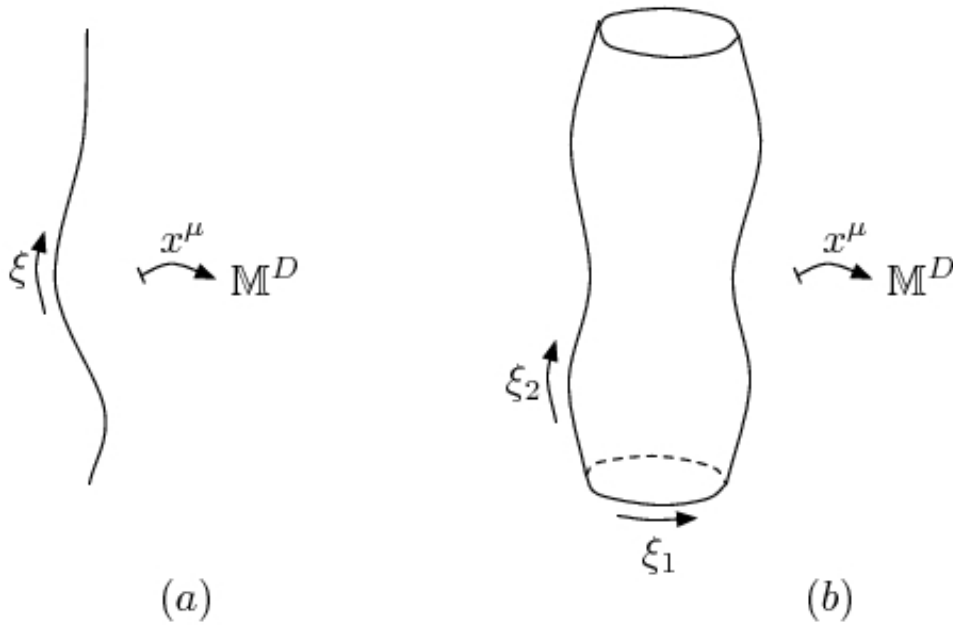


Figure 4.2: (a) A worldline parametrized by ξ is embedded into \mathbb{M}^D by the mapping x^μ . (b) Analogous to the worldline a two-dimensional worldsheet of a closed string parametrized by ξ_1 and ξ_2 is embedded into \mathbb{M}^D by the mapping x^μ .

is the determinant of the metric h_{ab} , $a, b = 1, 2$, of the embedded worldsheet induced by the mapping x .

As for the relativistic particle we can also write an action in terms of the internal metric g_{ab} , $a, b = 1, 2$, of the worldsheet. This is the so-called Polyakov action [62], the analog of (4.16),

$$S[g, x] = \int_M d^2\xi \sqrt{|g(\xi)|} (g^{ab} h_{ab} + \lambda), \quad (4.22)$$

where one should integrate over both g and x in the path integral [64]. Both (4.19) and (4.22) are equivalent on the classical level, however, it is not so obvious that this also holds at the quantum level (see for instance [18]).

We will see in the following two sections how (4.22) can also be viewed as the action for two-dimensional quantum gravity coupled to D scalar fields. An explicit “geometrical” discretization to define the corresponding path integral will be discussed in the next chapter.

4.3 | A path integral for quantum gravity

In the previous section we discussed the Polyakov and Nambu-Goto action as simple generalizations of random paths to random surfaces. The natural action for a theory of quantum gravity in d -dimensions is the so-called Einstein-Hilbert action,

$$S_{EH}([g_{ab}]) = \frac{1}{16\pi G_N} \int_M d^d \xi \sqrt{|g(\xi)|} (2\Lambda - R), \quad (4.23)$$

where G_N is the Newton's constant, Λ the cosmological constant, R the scalar curvature of the metric g_{ab} and $g = \det g_{ab}$ the determinant of the metric. For manifolds with boundaries one also has to include the Gibbons-Hawking-York boundary term [65, 66]

$$S_{GHY}([g_{ab}]) = \frac{1}{8\pi G_N} \int_{\partial M} d^{d-1} \xi \sqrt{|h(\xi)|} K, \quad (4.24)$$

where h and K are the induced metric and curvature on the boundary. All physical degrees of freedom are encoded in the equivalence class $[g_{ab}]$ which is g_{ab} modulo diffeomorphisms, i.e. coordinate transformations.

The expression of the gravitational path integral for the partition function is then formally written as

$$\mathcal{Z}(G_N, \Lambda) = \int_{\text{Geom}(M)} \mathcal{D}[g_{ab}] e^{iS_{EH}([g_{ab}])}, \quad (4.25)$$

where the integration should be taken over the space of all closed geometries, i.e. the coset space $\text{Geom}(M) = \text{Metrics}(M)/\text{Diff}(M)$. Generalizations to geometries with boundaries are also possible. When trying to define the formal expression (4.25) several problems arise:

First of all, $\mathcal{D}[g_{ab}]$ has to be defined in a covariant way to preserve the diffeomorphism invariance. Unfortunately, to perform further calculations one would then have to gauge fix the field tensors which would give rise to Faddeev-Popov determinants [67] whose non-perturbative evaluation is exceedingly difficult.¹

The second problem is due to the complex nature of the integrand. In quantum field theory this problem is solved by doing the Wick rotation $t \mapsto -i\tau$, where t is the time coordinate in Minkowski space (\vec{x}, t) . Clearly, a prescription like this does not work out

¹See [68, 69, 70] for an evaluation in the setting of two-dimensional Euclidean quantum gravity in the light-cone gauge. In [71] a calculation for three- and four-dimensional Lorentzian quantum gravity in the proper-time gauge is presented. It is anticipated there that the Faddeev-Popov determinants cancel the divergences coming from the conformal modes of the metric non-perturbatively.

in the gravitational setting, since all components of the metric field tensor depend on time. Further $t \mapsto -i\tau$ is certainly *not* diffeomorphism invariant (as a simple example consider the coordinate transformation $t \mapsto t^2$ for $t > 0$). Hence, the question arises: What is the natural generalization of the Wick rotation in the gravitational setting? This problem is often circumvented in the approach of *Euclidean* quantum gravity, where one does an ad hoc substitution

$$e^{iS_{EH}([g_{ab}^{(lor)}])} \rightarrow e^{-S_{EH}([g_{ab}^{(eu)}])}. \quad (4.26)$$

In this substitution the path integral over Lorentzian manifolds $M^{(lor)}$ is replaced by an integral over Euclidean manifolds $M^{(eu)}$. Clearly, the path integral now also includes many “acausal” manifolds and we will see in the next chapter when discussing two-dimensional Euclidean quantum gravity what consequences this brings with it. The main interest of this thesis is however to analyze ways to define the gravitational path integral in a Lorentzian setting including a proper definition of the Wick rotation.

Another problem in the definition of (4.25) is the following. Since we are working in a field theoretical context, some kind of regularization and renormalization will be necessary, and again, has to be formulated in a covariant way. In quantum field theory the use of lattice methods provides a powerful tool to perform non-perturbative calculations, where the lattice spacing a serves as a cut-off of the theory. An important question to ask at this point is whether or not the theory becomes independent of the cut-off. Consider for example QCD and QED on the lattice. All evidence suggests that QCD in four space-time dimensions is a genuine continuum quantum field theory. By genuine continuum quantum field theory we mean a theory which needs a cut-off at an intermediate step, but whose continuum observables will be *independent* of the cut-off at arbitrarily small scales. In QED the situation seems to be different, one is not able to define a non-trivial theory with the cut-off removed, unless the renormalized coupling $e_{ren} = 0$ (trivial QED). Therefore, QED is considered as a low-energy effective theory of a fundamental theory at the Planck scale.

Finally, one could argue to also include a sum over topologies in the path integral (4.25). However, in higher dimensions such a sum over topologies is quite intractable, since for $d \geq 3$ there does not even exist an obvious classification of topologies in terms of a finite set of parameters.

These are some of the reasons to first look at the simpler case of two dimensions.

4.4 | Two-dimensional Euclidean quantum gravity and Liouville theory

One of the big advantages of the two-dimensional Einstein-Hilbert action is that the curvature term is a topological invariant. This follows from the Gauss-Bonnet theorem which states that

$$\int_M d^2\xi \sqrt{|g(\xi)|} R = 4\pi\chi(M), \quad (4.27)$$

where $\chi(M) = 2 - 2h - b$, is the so-called *Euler-characteristic*, h is the genus of the manifold M , i.e. the number of holes in the surface, and b the number of boundary components of M .

Using the Gauss-Bonnet theorem we can write the partition function for two-dimensional Euclidean quantum gravity including a sum over topologies (using a rescaling of the couplings)

$$\mathcal{Z}(G_N, \Lambda) = \sum_{h=0}^{\infty} e^{-\chi(M_h)/G_N} \mathcal{Z}_h(\Lambda), \quad (4.28)$$

where the partition function for manifolds with fixed genus h is given by

$$\mathcal{Z}_h(\Lambda) = \int_{\text{Geom}(M_h)} \mathcal{D}[g] e^{-S(g, \Lambda)} \quad (4.29)$$

and

$$S(g, \Lambda) = \Lambda V_g, \quad V_g = \int_{M_h} d^2\xi \sqrt{|g(\xi)|}. \quad (4.30)$$

Here V_g is the volume of the manifold M_h . Eq. (4.28) is called the *topological expansion*. Note that since the sum is taken over closed surfaces, we have $\chi(M) = 2 - 2h$. Often one is only interested in the genus zero contribution, i.e. the sum over surfaces with topology of S^2 . In this case we denote the partition function by $\mathcal{Z}(\Lambda) \equiv \mathcal{Z}_0(\Lambda)$.

If the path integral is taken over surfaces with b boundaries the Euler characteristic reads $\chi(M) = 2 - 2h - b$. Further, it is natural to include boundary terms in the action

$$S(g, \Lambda, Z_1, \dots, Z_b) = \Lambda V_g + \sum_{i=1}^b Z_i L_i(g), \quad (4.31)$$

where $L_i(g)$ is the length of the i th boundary loop \mathcal{L}_i with respect to the metric g . Here the Z_i take the role of boundary cosmological constants. One should notice that in two

dimensions the intrinsic boundary geometry is completely determined by its lengths $L_i(g)$. The partition function for the case of boundaries is given thus by

$$W(\Lambda, Z_1, \dots, Z_b) = \int_{\text{Geom}(M)} \mathcal{D}[g] e^{-S(g, \Lambda, Z_1, \dots, Z_b)} \quad (4.32)$$

and is called the multi-loop amplitude. Instead of fixing the boundary cosmological constants Z_i one could have alternatively also fixed the boundary lengths,

$$W(\Lambda, L_1, \dots, L_b) = \int_{\text{Geom}(M)} \mathcal{D}[g] e^{-S(g, \Lambda)} \prod_{i=1}^b \delta(L_i - L_i(g)). \quad (4.33)$$

The length space versions of the multi-loop amplitudes are also called the Hartle-Hawking wave functions [72]. For the case of one boundary component we also call it the disc function. One observes that (4.33) and (4.32) are related by Laplace transforms,

$$W(\Lambda, Z_1, \dots, Z_b) = \int_0^\infty \prod_{i=1}^b dL_i e^{-Z_i L_i} W(\Lambda, L_1, \dots, L_b). \quad (4.34)$$

So far we discussed only pure two-dimensional Euclidean quantum gravity, i.e. without any coupling to matter fields. If one would like to couple D scalar fields x^μ one should add the following term in the action

$$S_M(g, x) = \int_{M_h} d^2\xi \sqrt{|g(\xi)|} g^{ab} \frac{\partial x^\mu}{\partial \xi^a} \frac{\partial x^\mu}{\partial \xi^b}. \quad (4.35)$$

It is interesting to notice that $S_M(g, x) + S(g, \Lambda)$ is precisely the Polyakov action (4.22), discussed in the previous section. Hence we see that pure two-dimensional Euclidean quantum gravity corresponds to string theory in zero-dimensional target space, i.e. non-critical string theory.

In the following section we explain how to define the path integral for two-dimensional Euclidean quantum gravity using a discretization scheme called dynamical triangulations. Before doing so let us briefly mention a different way of computing the gravitational path integral using continuum methods. This is done by fixing the metric to the conformal gauge

$$g = e^\phi \hat{g}, \quad (4.36)$$

where \hat{g} is the reference metric. One sees that the theory is now expressed in terms of a single field, the so-called Liouville field ϕ . There are interesting analytical results

for Liouville field theory on the quantized level (see for example [73, 74]). Further, whenever the continuum theory and the discretized theory (as described in the next chapter) can be compared the results agree [75]. However, contrary to what one might have expected the discretized theory allows one to compute many quantities which are not accessible from the continuum theory.

Two-dimensional dynamical triangulations

In this chapter we introduce dynamical triangulations as a discretization of the Euclidean gravitational path integral. In the special case of two dimensions analytical results can be obtained. In particular, we show how both the Hartle Hawking wave function as well as the gravitational propagator can be calculated explicitly within this approach. The results agree with those of the continuum formulation of two-dimensional Euclidean quantum gravity through Liouville theory as briefly mentioned in the previous chapter.

5.1 | Geometry from simplices

The use of discrete approaches to quantum gravity has a long history [76]. In classical general relativity, the idea of approximating a space-time manifold by a triangulation of space-time goes back to the early work of Regge [77] and was first used in [78, 79] to give a path integral formulation of gravity. By a triangulation we mean a piecewise linear space-time obtained by a gluing of simplicial building blocks. This one might think of as the natural analogue of the piecewise linear path we used to describe the relativistic particle. In two dimensions these simplicial building blocks are *flat* Euclidean

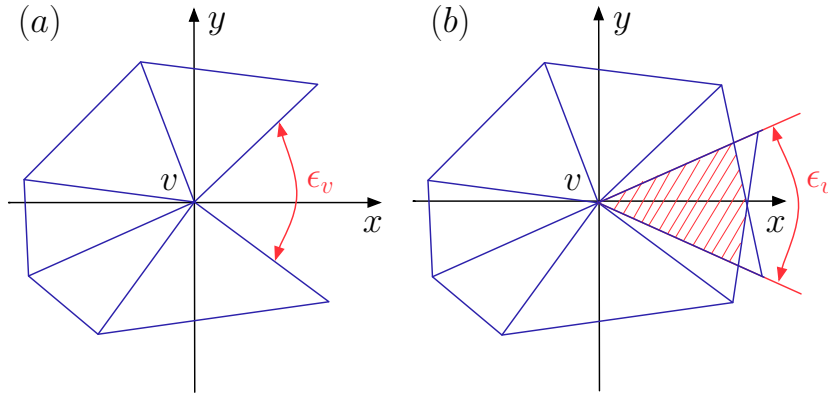


Figure 5.1: Illustration of a positive (a) and negative (b) deficit angle ϵ_v at a vertex v .

triangles¹, where flat means isomorphic to a piece of Euclidean space respectively. One could in principle assign a coordinate system to each triangle to recover the metric space $(M, g_{\mu\nu})$, but the strength of this ansatz lies just in the fact that even without the use of coordinates, each geometry is completely described by the set of edges length squared $\{l_i^2\}$ of the simplicial building blocks. This provides us with a regularized parametrization of the space of all geometries $\text{Geom}(M)$ in a diffeomorphism invariant way, and hence, is the first step towards defining the gravitational path integral.

For the further discussion it is essential to understand how a geometry is encoded in the set of edges length squared $\{l_i^2\}$ of the simplicial building blocks of the corresponding triangulation. In the case of two dimensions this can be easily visualized, since the triangulation consists just of triangles. Further, the Riemann scalar curvature $R(x)$ coincides with the Gaussian curvature $K(x)$ up to a factor of $1/2$. There are several ways to reveal curvature of a simplicial geometry. The most convenient method is by parallel transporting a vector around a closed loop. Since all building blocks are flat, a vector parallel transported around a vertex v always comes back to its original orientation unless the angles θ_i of the surrounding triangles do not add up to 2π , but differ by the so-called *deficit angle* $\epsilon_v = 2\pi - \sum_{i \supset v} \theta_i$ (Figure 5.1). The Gaussian curvature located at the vertex v is then given by

$$K_v = \frac{\epsilon_v}{V_v}, \quad (5.1)$$

¹In the next chapter, when discussing two-dimensional causal dynamical triangulations, we will consider a similar construction with Minkowskian triangles.

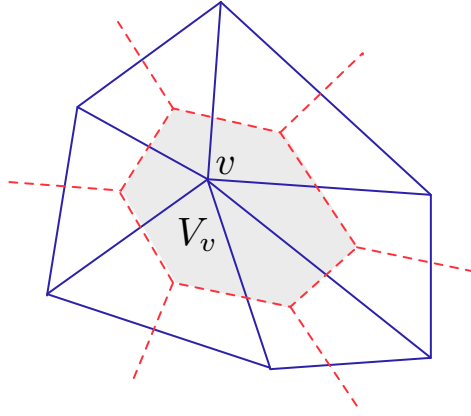


Figure 5.2: Shown is a triangulation and its dual triangulation (dashed line). Highlighted is a vertex v of the triangulation and its dual cell of volume V_v .

where V_v is the volume associated to the vertex v ; more precisely, the dual volume of the vertex as shown in Fig. 5.2. Note that the curvature at each vertex takes the form of a conical singularity. Then one can write the simplicial discretization of the usual curvature and volume terms appearing in the two-dimensional Einstein-Hilbert action,

$$\frac{1}{2} \int_M d^2x \sqrt{|\det g|} R(x) \rightarrow \sum_{v \in \mathcal{R}} \epsilon_v, \quad (5.2)$$

$$\int_M d^2x \sqrt{|\det g|} \rightarrow \sum_{v \in \mathcal{R}} V_v, \quad (5.3)$$

where $\mathcal{R} \equiv \{l_i^2\}$ is a triangulation of the manifold M described by the set of edge lengths squared. From this one can write down the simplicial discretization of the two-dimensional Einstein-Hilbert action, the so-called *Regge action*,

$$S_{\text{Regge}}(\mathcal{R}) = \sum_{v \in \mathcal{R}} V_v \left(\lambda - k \frac{\epsilon_v}{V_v} \right), \quad (5.4)$$

where k is the inverse Newton's constant and λ the cosmological constant. It is then an easy exercise of trigonometry to evaluate the right hand side of (5.4) in terms of the squared edge lengths.

From this notion of triangulations one can now write the gravitational path integral as the integral over all possible edge lengths $\int \mathcal{D}l$, where each configuration \mathcal{R} is weighted by the corresponding Regge action (5.4). In this approach the triangulation

is fixed and only the length of the edges is varied. A potential problem one encounters with this ansatz is a possible overcounting of triangulations, due to the fact that one can continuously vary each edge length, as is clear from flat space-time. Further, one still has to introduce a suitable cut-off for the length variable l . Among other things, this motivated the approach of “rigid” Regge calculus or (Euclidean) dynamical triangulations (DT) where one considers a certain class \mathcal{T} of simplicial space-times as an explicit, regularized version of Euclidean geometries, where each triangulation $T \in \mathcal{T}$ only consists of simplicial building blocks whose edges have all the same edge length squared $L_a^2 = a^2$. Here, the geodesic distance a serves as the short-distance cut-off, which will be sent to zero in the continuum limit.

Following early work by Tutte [80, 81, 82, 83] and Brezin et al. [84], DT have in a quantum gravity context first been introduced as an regularization of the bosonic string [85, 86, 87, 88, 89]. Further developments have been made in many contributions, for an overview the reader is referred to [18]. The motivation for using a discretization of Euclidean geometries instead of Lorentzian geometries is mainly to avoid the need to define a gravitational Wick rotation. One simply starts off with a sum over Euclidean triangulations weighted by the Euclidean (real) Regge action. In the continuum limit this theory of (Euclidean) DT corresponds to two-dimensional Euclidean quantum gravity. It is important to notice that this theory is distinct from two-dimensional Lorentzian quantum gravity which we will introduce in the next chapter.

Putting the above discussion into formulas we can give a definite meaning to the formal continuum path integral of two-dimensional Euclidean quantum gravity as a discrete sum over inequivalent triangulations,

$$\mathcal{Z} = \int_{\text{Geom}(M)} \mathcal{D}[g_{\mu\nu}] e^{-S_{\text{EH}}[g_{\mu\nu}]} \rightarrow \sum_{T \in \mathcal{T}} \frac{1}{C(T)} e^{-S_{\text{Regge}}(T)}, \quad (5.5)$$

where $1/C(T)$ is the measure on the space of discrete geometries, with $C(T) = |\text{Aut}(T)|$ the dimension of the automorphism group of the triangulation T .

Now the problem of calculating the gravitational path integral reduces to a statistical physics problem. Here the weight $e^{-S_{\text{Regge}}(T)}$ is the so-called Boltzmann factor and the sum together with the measure factor determines the entropy of configurations with equal weight. In the following section we solve this statistical problem analytically for the two-dimensional model.

5.2 | The disc function

In this section we calculate the disc function or Hartle-Hawking wave function of two-dimensional Euclidean quantum gravity defined through DT. The disc function is defined as a sum over all triangulations with topology of a disc with fixed boundary of length l . In other words the disc function describes the amplitude for the creation of a universe from nothing [72]. Although rather “global” it is a simple observable which can be used to calculate other interesting observables.

5.2.1 | Discrete solution

As we are in two space-time dimensions we have seen that the curvature term in the Einstein-Hilbert action is a purely topological quantity. Hence, if we are interested in computing sums over triangulations of fixed space-time topology, the contribution from the curvature term reduces to an irrelevant normalization constant.

The Regge action (5.4) is thus simply given by

$$S_{\text{Regge}}(T) = \lambda \sum_{v \in T} V_v = \lambda a^2 N(T), \quad (5.6)$$

where λ is the bare (dimensionfull) cosmological constant and $N(T)$ is the number of triangles in the triangulation T . The factor of a^2 comes from the volume of a single triangle where the order one constant has been absorbed into λ .

The expression for the disc function $w_l(g)$ now becomes

$$w_l(g) = \sum_{T \in \mathcal{T}(l)} e^{-\lambda a^2 N(T)} = \sum_{T \in \mathcal{T}(l)} g^{N(T)}, \quad (5.7)$$

where we defined $g = e^{-a^2 \lambda}$ as the fugacity of a triangle. The sum is taken over all triangulations with boundary length l and a mark on one boundary edge. The mark is introduced for convenience to remove a symmetry factor of $1/l$ in the sum which corresponds to the factor $1/C(T)$ in the above expression. We can further write (5.7) as

$$w_l(g) = \sum_N w_{l,N} g^N, \quad (5.8)$$

where $w_{l,N}$ is the number of triangulations with l boundary edges and N triangles. We now see that the problem of determine the disc function reduces to a purely combinatorial problem, namely finding the number $w_{l,N}$ of all possible triangulations with l

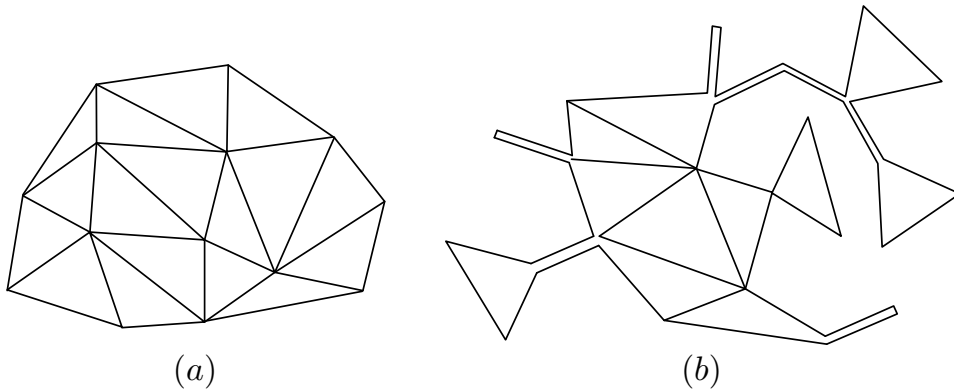


Figure 5.3: Shown is a regular triangulation with topology of the disc (a) and a unrestricted triangulation with topology of a disc (b).

boundary edges and N triangles. Fig. 5.3 (a) shows an example of one triangulation with $l = 9$ boundary edges and $N = 16$ triangles. This combinatorial problem was first studied by Tutte in 1962 [80, 81, 82, 83].

In the following we will not follow the procedure by Tutte but rather count the number of all possible triangulations of a wider class, so-called *non-restricted* triangulations. Non-restricted triangulations are more general than the ones considered above in the sense that they can include double links (see Fig. 5.3 (b)). The double links are mainly included to facilitate the calculation and to be able to map the results to those of matrix models. The use of matrix models will be an important part of this thesis and we will discuss them in detail at a later stage. The justification for being able to include double links is that when taking the continuum limit the contribution coming from the double links will be “washed away” as they do not carry a factor of g . Further, using the results of Tutte it can be checked explicitly that both regular and non-restricted triangulations lead to the same continuum expression for the disc function (see for example [18]).

When trying to solve a combinatorial problem it is often useful to introduce generating functionals,

$$\tilde{w}(g, x) = \sum_{l=0}^{\infty} w_l(g) x^l. \quad (5.9)$$

Here x can be understood as the fugacity of a boundary edge or in other terms as being related to a boundary cosmological constant λ_l via $x = e^{-a\lambda_l}$.

Generating functionals are very useful tools especially since there are helpful to

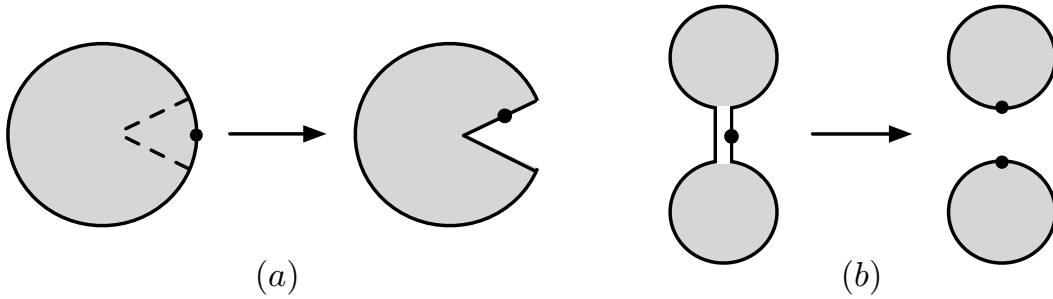


Figure 5.4: Elementary decomposition moves: If the marked edge on the boundary belongs to a triangle this triangle is removed (a), if the mark corresponds to a double link the double link is removed and the triangulation splits into two (b).

find recursion equations for $\tilde{w}(g, x)$, the so-called loop equations. Let us first make the observation that whenever one removes triangles from a triangulation for each volume decrement of one triangle the generating function is decreased by a factor of g and for each decrement in boundary length it is decreased by a factor of x .

Starting with a triangulation one can now uniquely decompose it step-by-step to a single dot by the following two elementary moves: Firstly, if the marked edge on the boundary belongs to a triangle this triangle is removed (see Fig. 5.4 (a)). Thus one boundary edge is removed and two new edges are created of which by convenience the one further counterclockwise is marked again. In this move the power of g in $\tilde{w}(g, x)$ is decreased by one and the power of x is increased by one. The second move corresponds to the case where the mark belongs to a double link (see Fig. 5.4 (b)). In this case the double link is removed and the triangulation splits into two, each with a mark next to where the double link was attached.

The step-by-step procedure described above leads to the following recursion relation (see Fig. 5.5)

$$\tilde{w}(g, x) = \frac{g}{x} (\tilde{w}(g, x) - w_1(g)x - 1) + x^2 \tilde{w}^2(x, g), \quad (5.10)$$

where the first term corresponds to the first move and the last term to the second move. The term $w_1(g)x + 1$ in the bracket is subtracted to be in accordance with the initial conditions of the the recursion relation. One can now solve for $\tilde{w}(g, x)$, however, the solution is implicit since $w_1(g)$ still has to be determined.

To be in accordance with the notation adopted in matrix models and also in later

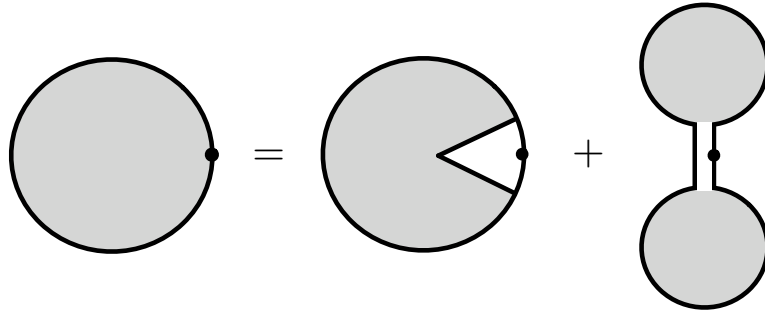


Figure 5.5: Graphical representation of the loop equation (5.10) for the disc function.

parts of this thesis one often rewrites this equation using a slightly different definition of the generating functional

$$w(g, z) = \sum_{l=0}^{\infty} w_l(g) z^{-l-1} = \frac{\tilde{w}(g, 1/z)}{z}. \quad (5.11)$$

Here z^{-1} takes the roles of the fugacity of a boundary edge. The formal solution to the recursion relation (5.10) reads in terms of the newly defined generating function

$$w(g, z) = \frac{1}{2} \left(V'(z) - \sqrt{(V'(z))^2 - 4Q(z)} \right), \quad (5.12)$$

where anticipating the discussion of matrix models in later chapters we introduced the notation

$$V'(z) = z - gz^2, \quad Q(z) = 1 - w_1(g) - gz. \quad (5.13)$$

The sign in front of the square root is determined by the initial condition $w_{0,0} = 1$ which leads to the requirement $w(g, z) = 1/z + \mathcal{O}(1/z^2)$. In principle one would now have to find a combinatorial solution for $w_1(g)$, however, there exists a way of determining an explicit solution for $w(g, z)$ by making use of the analytic structure of (5.12). Therefore we first solve (5.12) for the limiting case of $g = 0$, where only double links are present. In this case $w(z) \equiv w(g = 0, z)$ corresponds to the generating function of rooted branched polymers (see Fig. 5.6). The implicit solution (5.12) becomes explicit in this special case

$$w(z) = \frac{1}{2} \left(z - \sqrt{z^2 - 4} \right). \quad (5.14)$$

This is precisely the generating function of the Catalan numbers

$$w(z) = \sum_{l=0}^{\infty} \frac{w_{2l}}{z^{2l+1}}, \quad w_{2l} = \frac{(2l)!}{(l+1)!l!}. \quad (5.15)$$

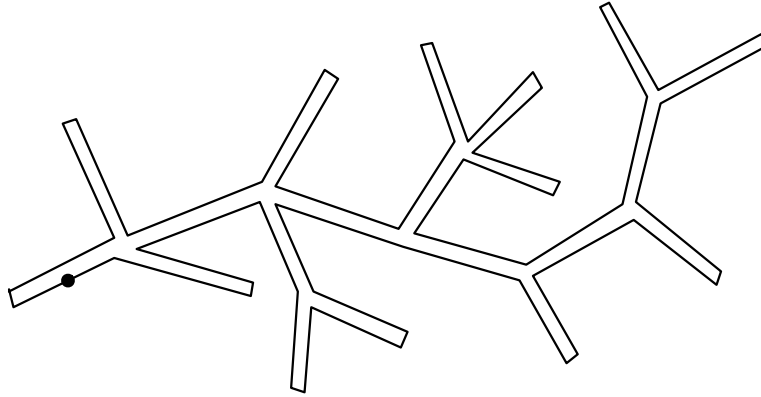


Figure 5.6: A rooted branched polymer created by gluing double links with one marked link.

Hence we see that the number of rooted branched polymers with l links is given by the Catalan numbers w_{2l} .

Anticipating the general solution for $g \neq 0$ it is instructive to analyze the analytic structure of (5.14). The generating function $w(z)$ is analytic in \mathbb{C} with a branch cut on the real axis along the interval $[c_-(0), c_+(0)] \equiv [-2, 2]$. The endpoints of the cut precisely determine the radius of convergence of $w(z)$ which is needed to find the critical points when taking the continuum limit later on.

The key to finding the solution for the general case of $g \neq 0$ is to notice that the analytic structure of $w(g, z)$ as a function of z cannot change discontinuously at $g = 0$. For $g = 0$ the branch cut is determined by the following expression under the square root

$$(V'(z))^2 - 4Q(z) = (z - c_+(0))(z - c_-(0)) = (z - 2)(z + 2) \quad (5.16)$$

For $g \neq 0$ this expression becomes fourth order in z ,

$$(V'(z))^2 - 4Q(z) = [z - (2 + 2g) + \mathcal{O}(g^2)] \times [z + (2 - 2g) + \mathcal{O}(g^2)] [gz - (1 - 2g^2) + \mathcal{O}(g^3)]^2. \quad (5.17)$$

Since the analytic structure of $w(g, z)$ should not change in the neighborhood of $g = 0$, this implies that the term under the square root must be of the general form

$$(V'(z))^2 - 4Q(z) = (c(g) - gz)^2(z - c_+(g))(z - c_-(g)), \quad (5.18)$$

where we labeled the roots such that $c_-(g) \leq c_+(g) \leq c(g)$. The solution for the disc function then reads

$$w(g, z) = \frac{1}{2} \left(z - gz^2 - (c(g) - gz) \sqrt{(z - c_+(g))(z - c_-(g))} \right). \quad (5.19)$$

Matching the coefficients of (5.18) in the expansion in z yields four equations which completely determine $c_-(g)$, $c_+(g)$, $c(g)$ and $w_1(g)$. This gives the full combinatorial solution for the disc function in DT.

5.2.2 | Continuum limit

Having solved the gravitational path integral as a statistical sum over triangulations we now have to perform the continuum limit to extract the continuum physics. This is done by taking the lattice spacing a to zero while at the same time taking the number of triangles N and the discrete boundary length l to infinity, such that physical area A and length L stay finite.

In terms of critical phenomena the continuum limit relates to a fine-tuning of the coupling constants, generally denoted by g , to the critical point g_c of the phase transition. This means a divergence of the correlation length l in the scaling limit

$$l(g) \sim \frac{1}{|g - g_c|^\nu} \xrightarrow{g \rightarrow g_c} \infty, \quad (5.20)$$

while the cut-off a goes to zero as

$$a(g) \sim |g - g_c|^\nu \xrightarrow{g \rightarrow g_c} 0, \quad (5.21)$$

where ν is a critical exponent. In terms of the cut-off a and the correlation length l , the physical correlation length is given by $L = l(g) \cdot a(g)$ and the continuum limit is defined as the simultaneous limit

$$a(g) \rightarrow 0, \quad l(g) \rightarrow \infty \quad \text{for fixed} \quad L = l(g) \cdot a(g). \quad (5.22)$$

From standard techniques of renormalization theory, we expect the couplings with positive mass dimension, i.e. the cosmological constant λ and the boundary cosmological constant λ_i to undergo an additive renormalization,

$$\lambda = \frac{A_\lambda}{a^2} + \Lambda, \quad \lambda_i = \frac{A_{\lambda_i}}{a} + Z, \quad (5.23)$$

where Λ , Z denote the corresponding renormalized values. Introducing the critical values

$$g_c = e^{-A\lambda}, \quad z_c = e^{A\lambda_i}, \quad (5.24)$$

it follows that

$$g = g_c e^{-a^2 \Lambda}, \quad z = z_c e^{a Z}. \quad (5.25)$$

The critical point for the coupling g can be extracted from the radius of convergence of $w_1(g)$ at which the number of triangles N diverges. Using the result for $w_1(g)$ which can be derived easily as described below (5.2.2) one finds $g_c = 1/\sqrt[4]{432}$. To obtain the critical value for z at which also the boundary length diverges we look at the radius of convergence of $w(g_c, z)$ as a function of z . From the analysis of the analytic structure we know that the radius of convergence is precisely given by the endpoints of the branch cut and hence we conclude that $z_c = c_+(g_c)$ (in the following we omit the precise numerical values of the critical couplings, since they are not of essential importance for the discussion).

Inserting the scaling relations (5.25) and the critical values into the discrete solution of the disc function yields

$$w(g, z) = w_{ns} + a^{3/2} \left(Z - \frac{1}{2} \sqrt{\Lambda} \right) \sqrt{Z + \sqrt{\Lambda}} + \mathcal{O}(a^2), \quad (5.26)$$

where $w_{ns} = V'(z)/2$ is the so-called non-scaling part of the disc function which consists of terms of lower order in the cut-off, more precisely an order one constant and a term proportional to aZ . Further, for convenience we rescaled Λ and Z by positive multiplicative constants to simplify the result.

Introducing a wave function renormalization of the continuum disc function

$$W_\Lambda(Z) = a^{-3/2} w(g, z) \quad (5.27)$$

we obtain

$$W_\Lambda(Z) = \left(Z - \frac{1}{2} \sqrt{\Lambda} \right) \sqrt{Z + \sqrt{\Lambda}}, \quad (5.28)$$

where we dropped the non-scaling part. This is precisely the result obtained from Liouville theory.

We can now also go back to the physical length L . The continuum limit of the defining equation for the generating function (5.11) is precisely the Laplace transform,

$$W_\Lambda(Z) = \int_0^\infty dL W_\Lambda(L) e^{-LZ}. \quad (5.29)$$

Hence performing the inverse Laplace transform

$$W_\Lambda(L) = \int_{-i\infty}^{+i\infty} \frac{dZ}{2\pi i} W_\Lambda(Z) e^{LZ} \quad (5.30)$$

of (5.28) we obtain

$$W_\Lambda(L) = L^{-5/2} (1 + \sqrt{\Lambda L}) e^{-\sqrt{\Lambda L}}. \quad (5.31)$$

Further we can also calculate the resulting disc function without a mark on the boundary by simply dividing (5.32) by L , yielding

$$W_\Lambda^{(u)}(L) = L^{-7/2} (1 + \sqrt{\Lambda L}) e^{-\sqrt{\Lambda L}}, \quad (5.32)$$

where the (u) stands for “unmarked”.

5.3 | Geodesic distance and the two-loop amplitude

5.3.1 | Defining geodesic distance and the two-loop function

In the previous section we calculated the disc function of two-dimensional Euclidean quantum gravity using the framework of dynamical triangulations. This is in a sense a rather “global” observable and in the following we are interested in calculating more “local” observables. The quantity we calculate is the fixed geodesic distance two-loop amplitude which we also sometimes refer to as the gravitational propagator or simply propagator.

To be able to calculate this quantity we first need to make some definitions of basic concepts. Firstly, we have to give a proper definition of geodesic distance. If we would reintroduce coordinates on the simplicial building blocks one could simply employ the standard continuum definition as used in general relativity. However, we have seen that the strength of this approach lies in the fact that we have a coordinate independent representation of geometries. Hence, we should better look for a geodesic distance definition intrinsic to dynamical triangulations. There are several such definitions. The one we employ here defines the geodesic distance $d(e, e')$ between two links (edges) e and e' in a triangulation as the number of links of the shortest path between the corresponding links of the dual triangulation. Now we want to extend the above definition for the case of geodesic distance of boundaries of the triangulation, where each boundary consists of a collection of links. In particular, we define the geodesic distance of a

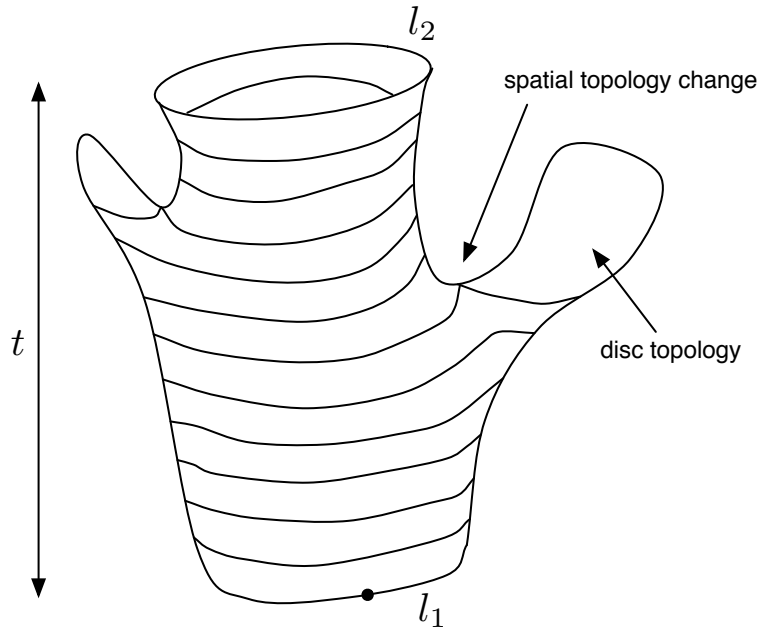


Figure 5.7: Fixed geodesic distance two-loop amplitude $G(l_1, l_2; g; t)$.

boundary loop \mathcal{L} to a link e as $\min_{e' \in \mathcal{L}} d(e, e')$. Finally, we say that a boundary loop \mathcal{L}_1 has geodesic distance t to another boundary loop \mathcal{L}_2 if all links $l \in \mathcal{L}_1$ have a geodesic distance t to \mathcal{L}_2 . One should notice that this definition is not symmetric in \mathcal{L}_1 and \mathcal{L}_2 .

As an example, Fig. 5.7 shows an amplitude with a boundary of length l_1 and another boundary of length l_2 at geodesic distance t to the first boundary. One observes that the geodesic distance induces a natural foliation or time-slicing for the triangulations by following the sequence of loops of geodesic distance $r = 0, 1, 2, \dots, t$ to \mathcal{L}_1 .² Whereas the space-time topology of the triangulation is fixed to $S_1 \times [0, 1]$, the topology of the spatial sections changes in general as a function of geodesic distance r . We call these *spatial topology changes*. One should notice that spatial topology changes are naturally present in Euclidean dynamical triangulations. However, as we will argue in the next chapter, in a proper theory of Lorentzian quantum gravity the branching points of changing spatial topology relate essentially to points in the continuum geometry of

²This notion of time essentially suggests the existence of a Hamiltonian for two-dimensional Euclidean quantum gravity. The formulation of such Hamiltonian dynamics lead to interesting results in the field of string field theory [90, 91, 92, 93]. We will not review this work, however, in Chap. 10 we will propose an analogous string field theory formulation for Lorentzian quantum gravity.

anomalous causal structure. This is one motivation for studying triangulations without spatial topology change as we will do in the next chapter.

We now have all ingredients at hand to define the fixed geodesic two-loop amplitude

$$G(l_1, l_2; g; t) = \sum_{T \in \mathcal{T}(l_1, l_2, t)} g^{N(T)}, \quad (5.33)$$

where the sum is taken over all triangulations with an initial boundary of length l_1 and a final boundary of length l_2 at geodesic distance t to the initial boundary. For $t=0$ the initial and final loop coincide which leads to the following initial condition

$$G(l_1, l_2; g; t=0) = \delta_{l_1, l_2}. \quad (5.34)$$

As for the disc function it will be useful to introduce generating function

$$G(z, w; g; t) = \sum_{l_1, l_2=0}^{\infty} G(l_1, l_2; g; t) z^{-l_1-1} w^{-l_2-1}, \quad (5.35)$$

with the initial condition equivalent to (5.34),

$$G(z, w; g; t=0) = \frac{1}{zw} \frac{1}{zw - 1}. \quad (5.36)$$

Solving (5.33) is a purely combinatorial problem. In the following we describe two different methods to solve this problem. The first method of solving the geodesic two-loop amplitude is the so-called peeling procedure due to Watabiki [94]. It is very simple and instructive, since it essentially uses the above loop equations and only views them as a “time-dependent” process. The disadvantage however is that not all steps of the calculation are rigorous. The second method due to Kawai et al. [95] uses transfer matrices (see also [96, 97]). Though more complicated it is on the other hand better defined. Further, it introduces important techniques which will be essential to study problems arising in the next chapter.

5.3.2 | The peeling procedure

In Fig. 5.7 we illustrate the fixed geodesic distance two-loop amplitude as decomposed in slices of thickness $\Delta r = 1$. In the spirit of the loop equation for the disc function, as discussed in the previous section, we can also decompose the triangulation by a peeling procedure, a sequel of elementary decomposition moves (see Fig. 5.8).

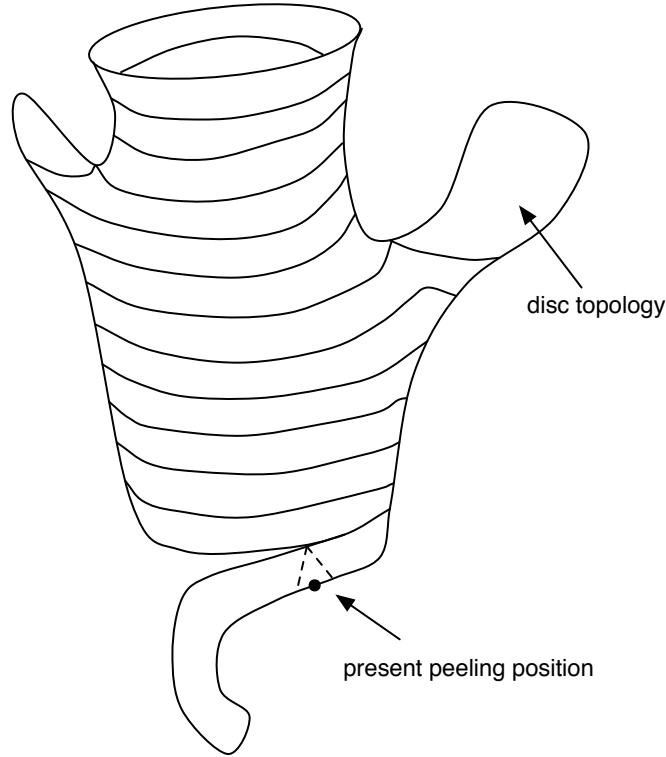


Figure 5.8: Decomposition of the triangulation for the fixed geodesic distance two-loop amplitude by a peeling procedure .

Similar to the loop equation for the disc function we can write down a recursion relation for the geodesic two-loop amplitude (see Fig. 5.9)

$$G'(l_1, l_2; g; t) = gG(l_1 + 1, l_2; g; t) + 2 \sum_{l=0}^{\infty} w_l(g) G(l_1 - l - 2, l_2; g; t). \quad (5.37)$$

Here the two decomposition moves are essentially the same as for the disc function. The factor of two comes from the two possibilities of having the final boundary on either of the two off-splitting triangulations. The prime on the expression on the left-hand-side means that the surfaces contributing to this quantity do not exactly have \mathcal{L}_2 at geodesic distance t from \mathcal{L}_1 .

Rather than giving a precise definition of $G'(l_1, l_2; g; t)$ one makes a proposal which approximates $G'(l_1, l_2; g; t)$ for large t . When comparing to the exact transfer matrix calculation in the next section we shall see that this approximation indeed leads to

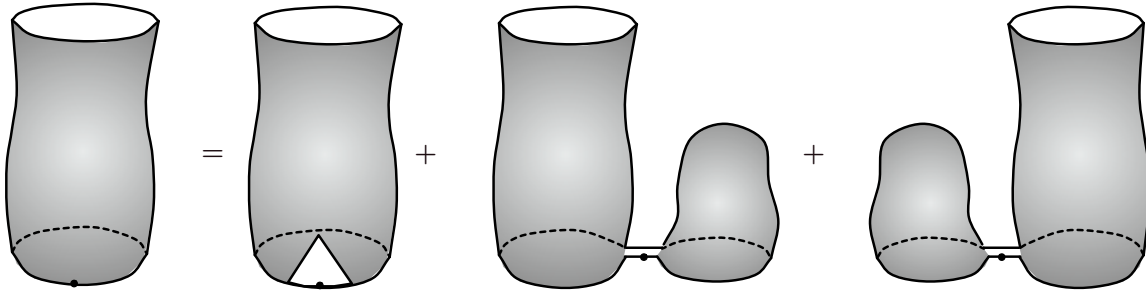


Figure 5.9: The peeling decomposition moves are the same as already used in the loop equation for the disc function (recall Fig. 5.5): If the marked edge on the initial loop belongs to a triangle the triangle is removed. If it belongs to a double link then the double link is removed causing the triangulation to split. The off-splitting part of the triangulation with the final loop has topology of a cylinder, whereas the other part has topology of a disc.

the correct result. The basic idea in approximating $G'(l_1, l_2; g; t)$ is that when applying the elementary decomposition moves l_1 times on $G(l_1, l_2; g; t)$ we will on average get $G(l_1, l_2; g; t - 1)$, since roughly speaking we peeled off a whole slice. Ignoring the fact that t is an integer we can then view $G'(l_1, l_2; g; t) = G(l_1, l_2; g; t + 1/l_1)$. For large l_1 one can Taylor expand

$$G(l_1, l_2; g; t + 1/l_1) = G(l_1, l_2; g; t) + 1/l_1 \partial_t G(l_1, l_2; g; t) + \dots \quad (5.38)$$

Inserting this into (5.37) gives

$$\begin{aligned} \frac{\partial}{\partial t} G(l_1, l_2; g; t) &= -l_1 G(l_1, l_2; g; t) + g l_1 G(l_1 + 1, l_2; g; t) + \\ &\quad + 2l_1 \sum_{l=0}^{\infty} w_l(g) G(l_1 - l - 2, l_2; g; t), \end{aligned} \quad (5.39)$$

or in terms of the generating functions

$$\frac{\partial}{\partial t} G(z, w; g; t) = \frac{\partial}{\partial z} [(z - gz^2 - 2w(g, z))G(z, w; g; t)]. \quad (5.40)$$

Plugging in the result for the disc function (5.2.2) we see that the first term in the bracket cancels the non-scaling part of the disc function and we get

$$\frac{\partial}{\partial t} G(z, w; g; t) = -2 \frac{\partial}{\partial z} [f(g, z)G(z, w; g; t)], \quad (5.41)$$

where we defined

$$f(g, z) = w(g, z) - \frac{1}{2}(z - gz^2) = \frac{1}{2}(gz - c(g))\sqrt{(z - c_+(g))(z - c_-(g))}. \quad (5.42)$$

Instead of trying to solve the differential equation and then take the continuum limit of the result, we will in the following take the continuum limit directly of the differential equation (5.41) and its initial condition (5.36). Therefore we extend the scaling relations (5.25) to

$$g = g_c e^{-a^2 \Lambda}, \quad z = z_c e^{aZ}, \quad w = z_c e^{aW}, \quad (5.43)$$

using the same critical values as described above. Inserting these relations into the initial conditions (5.36) gives

$$G_\Lambda(Z, W; T=0) = \frac{1}{Z + W}, \quad (5.44)$$

where we introduced the following wave function renormalization for the geodesic two-loop amplitude

$$G_\Lambda(Z, W; T) = aG(z, w; g; t). \quad (5.45)$$

Further, inserting the scaling relations (5.43) and (5.45) into (5.41) we observe that the geodesic distance should scale as

$$T \sim t\sqrt{a}, \quad (5.46)$$

yielding the following continuum differential equation for the geodesic distance two-loop amplitude

$$\frac{\partial}{\partial T} G_\Lambda(Z, W; T) = -\frac{\partial}{\partial Z} [W_\Lambda(Z) G_\Lambda(Z, W; T)]. \quad (5.47)$$

One observes that time does not scale canonically as maybe expected. We will see in the next section that this is due to the fractal structure of the quantum geometry.

This partial differential equation can be solved under the above initial condition, yielding

$$G_\Lambda(Z, W; T) = \frac{W_\Lambda(\bar{Z}(T, Z))}{W_\Lambda(Z)} \frac{1}{Z + W}, \quad (5.48)$$

where $\bar{Z}(T, Z)$ is the solution to the characteristic equation

$$\frac{\partial}{\partial T} \bar{Z}(T, Z) = -W_\Lambda(\bar{Z}(T, Z)), \quad \bar{Z}(T=0, Z) = Z. \quad (5.49)$$

Equivalently we can write

$$T = \int_{\bar{Z}(T,Z)}^Z \frac{dX}{W_\Lambda(X)}. \quad (5.50)$$

One can now insert the solution for the disc function (5.28) into this equation and perform the integral,

$$T = -\frac{2}{\alpha^4\sqrt{\Lambda}} \left[\operatorname{arctanh} \left(\frac{1}{\alpha^4\sqrt{\Lambda}} \sqrt{X + \sqrt{\Lambda}} \right) \right]_{X=\bar{Z}(T,Z)}^{X=Z}, \quad (5.51)$$

where $\alpha = \sqrt{3/2}$. Inverting this formula gives

$$\bar{Z}(T, Z) = \alpha^2\sqrt{\Lambda} \tanh \left(\frac{\alpha^4\sqrt{\Lambda}}{2} T + \operatorname{arctanh} \left(\frac{1}{\alpha^4\sqrt{\Lambda}} \sqrt{X + \sqrt{\Lambda}} \right) \right)^2 - \sqrt{\Lambda}, \quad (5.52)$$

which together with (5.48) yields the explicit solution for $G_\Lambda(Z, W; T)$.

The geodesic two-loop amplitude is a useful quantity from which many other quantities can be calculated. For the discussion of the quantum geometry in the next section we will be especially interested in the dependence on the geodesic distance. For simplicity, we shall analyze this dependence by shrinking both boundaries to zero. The resulting quantity is called the geodesic distance two-point function and was introduced in [98]. It is much simpler than the full two-loop amplitude, but still contains all essential dependence on the geodesic distance.

Let us first shrink the outer boundary to zero. Performing the inverse Laplace transform we get

$$G_\Lambda(Z, L_2; T) = \frac{W_\Lambda(\bar{Z}(T, Z))}{W_\Lambda(Z)} e^{-LZ} \quad (5.53)$$

and hence

$$G_\Lambda(Z, L_2 = 0; T) = \frac{W_\Lambda(\bar{Z}(T, Z))}{W_\Lambda(Z)} \quad (5.54)$$

One could have also obtained this result directly from the Laplace transformed quantity (5.48) by taking $\lim_{W \rightarrow \infty} W^\beta G_\Lambda(Z, W; T)$, where the coefficient is $\beta = 1$ which lead to a finite expression. The quantity $G_\Lambda(Z, L_2 = 0; T)$ is in a sense similar to $W_\Lambda(Z)$ with the difference that it has a marked point in the bulk which has a geodesic distance T to the entrance loop. This marked point comes from the boundary which was shrunken to zero. If we would integrate over $T \in [0, \infty]$ this expression should correspond to the

disc function with a marked point anywhere in the bulk, given by $-\partial_\Lambda W_\Lambda(Z)$. A quick check reveals that this is indeed true, i.e. that

$$-\frac{\partial}{\partial \Lambda} W_\Lambda(Z) \sim \int_0^\infty dT G_\Lambda(Z, L_2 = 0, T). \quad (5.55)$$

From (5.54) we then get for the two-point function $G_\Lambda(T) := G_\Lambda(L_1 = 0, L_2 = 0, T)$,

$$G_\Lambda(T) = \lim_{Z \rightarrow \infty} Z^\beta \frac{W_\Lambda(\bar{Z}(T, Z))}{W_\Lambda(Z)} = W_\Lambda(\bar{Z}(T, Z = \infty)), \quad (5.56)$$

where we chose $\beta = 3/2$ to get a finite expression.³ Using (5.52) one gets

$$G_\Lambda(T) = (\alpha \sqrt[4]{\Lambda})^3 \frac{\cosh \frac{\alpha}{2} \sqrt[4]{\Lambda} T}{\sinh^3 \frac{\alpha}{2} \sqrt[4]{\Lambda} T} \quad (5.57)$$

5.3.3 | The transfer matrix approach

In this subsection we want to rederive the continuum result for the fixed geodesic distance two-loop function as obtained by (5.48) in the previous subsection using the so-called *transfer matrix* approach. This exact method is more rigorous than the peeling method described in the previous subsection. Further, it employs useful techniques which will be of importance in the forthcoming chapters.

It was argued in [95] that any triangulation $\mathcal{T}(l_1, l_2, t)$ can in principle be uniquely decomposed into triangulations of geodesic distance one, i.e. $\mathcal{T}(l_1, l_2, t = 1)$, by slicing it in the way described above. This situation is shown in Fig. 5.7.

A nice feature of this construction is that it implies the following semi-group property or composition law for the propagator

$$G(l_1, l_2; g; t_1 + t_2) = \sum_l G(l_1, l; g; t_1) G(l, l_2; g; t_2), \quad (5.58)$$

or in terms of the generating functions

$$G(z, w; g; t_1 + t_2) = \oint \frac{dx}{2\pi i} G(z, x^{-1}; g; t_1) G(x, w; g; t_2). \quad (5.59)$$

Fig. 5.10 gives an graphical interpretation of the composition law. Setting $t_1 = 1$ and $t_2 = t - 1$ one obtains

$$G(l_1, l_2; g; t) = \sum_l G(l_1, l; g; t = 1) G(l, l_2; g; t - 1). \quad (5.60)$$

³The different values for β when shrinking the initial and final loop to a point (i.e. $3/2$ and 1) come from the fact that the initial loop was marked and the final loop not.

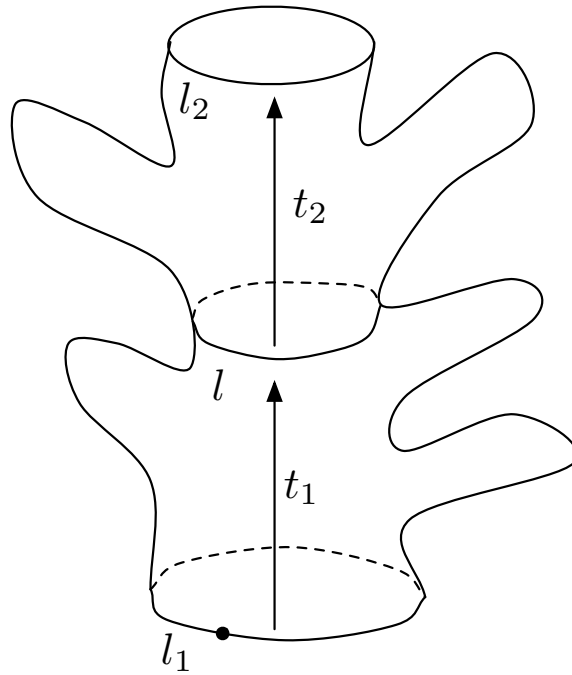


Figure 5.10: Graphical illustration of the composition law (5.60) for the fixed geodesic distance two-loop amplitude.

Here $G(l_1, l_2; g; t = 1)$ is the so-called one-step propagator which can be seen as the matrix element of the so-called transfer matrix $\mathcal{T}(g)$,

$$G(l_1, l_2; g; t = 1) = \langle l_2 | \mathcal{T}(g) | l_1 \rangle. \quad (5.61)$$

Knowing the transfer matrix one can in principle iterate (5.60) t -times to obtain the fixed geodesic distance two-loop amplitude

$$G(l_1, l_2; g; t) = \langle l_2 | \mathcal{T}^t(g) | l_1 \rangle. \quad (5.62)$$

If one is however only interested in calculating the continuum expressions there exists a shortcut to obtain $G_\Lambda(L_1, L_2, T)$ directly from the continuum limit of (5.60) without having to perform the iteration as we will see in the following.

Our first task is now to calculate the one-step propagator $G(l_1, l_2; g; t = 1)$ by combinatorial methods. So far we have been working with amplitudes which have a mark on the initial boundary. In some cases it is however useful to work with amplitudes without

a mark on the boundary. The marked and unmarked propagators are related as follows

$$G(l_1, l_2; g; t) = l_1 G^{(u)}(l_1, l_2; g; t), \quad (5.63)$$

where the (u) stands for unmarked. Remember that the marked amplitude has only the initial loop marked and not the final loop. In terms of generating functionals, (5.63) reads

$$G(z, w; g; t) = -\frac{\partial}{\partial z} z G^{(u)}(z, w; g; t). \quad (5.64)$$

For the unmarked propagator the composition law (5.60) becomes

$$G^{(u)}(l_1, l_2; g; t_1 + t_2) = \sum_l l G^{(u)}(l_1, l; g; t_1) G^{(u)}(l, l_2; g; t_2), \quad (5.65)$$

where the measure factor l in the sum is the direct manifestation of the symmetry factor $C(T)$ in (5.5).

We will now follow the results of [95] to combinatorially determine $G^{(u)}(z, w; g; t)$. It was shown there that every one-step propagator is made out of the following four elementary building blocks:

$$\begin{array}{c} \triangle \\ \hline \triangle \end{array} = \frac{g}{zw^2} \quad (5.66)$$

$$\begin{array}{c} \triangle \\ \hline \bigcirc \end{array} = \frac{gw(g, z)}{z^2 w} \quad (5.67)$$

$$\begin{array}{c} \triangle \\ \hline \bigcirc \end{array} = \frac{g(zw(g, z) - 1)}{z^2} \quad (5.68)$$

$$\begin{array}{c} \text{blob} \\ \hline \bigcirc \end{array} = \frac{w(g, z)}{z^2}. \quad (5.69)$$

Here the dotted lines refer to the initial boundary with weight $1/z$ per edge and the dashed lines refer to final boundary with weight $1/w$ per edge. Again each triangles carries a weight g . Further, the blobs represent the DT disc function $w(g, z)$ as derived in Sec. 5.2.1.

Now we can write the one-step propagator as the composition of all these terms

$$\begin{aligned} G^{(u)}(z, w; g; 1) &= \sum_{k=1}^{\infty} \frac{1}{k} \left(\begin{array}{c} \triangle \\ \hline \triangle \end{array} + \begin{array}{c} \triangle \\ \hline \bigcirc \end{array} + \begin{array}{c} \triangle \\ \hline \bigcirc \end{array} + \begin{array}{c} \text{blob} \\ \hline \bigcirc \end{array} \right)^k \\ &= -\log \left(1 - \frac{g}{zw^2} - \frac{gw(g, z)}{z^2 w} - \frac{g(zw(g, z) - 1)}{z^2} - \frac{w(g, z)}{z^2} \right) \end{aligned} \quad (5.70)$$

Here the factor of $1/k$ reflects the circular symmetry, i.e. $1/C(T)$.

In the following we perform the continuum limit using the same scaling relations as in the previous subsection

$$g = g_c e^{-a^2 \Lambda}, \quad z = z_c e^{aZ}, \quad w = z_c e^{aW}, \quad (5.71)$$

with the same critical values. Inserting the scaling relations and the solution for $G^{(u)}(z, w; g; 1)$, i.e. (5.70), into (5.64) we get to lowest order in a

$$G(z, w; g; t=1) = \frac{1}{a} \frac{1}{Z+W} - \frac{1}{\sqrt{a}} \frac{\partial}{\partial Z} \left(\frac{W_\Lambda(Z)}{Z+W} \right) + \mathcal{O}(1). \quad (5.72)$$

Hence we introduce the following wave function renormalization for the geodesic two-loop amplitude to match the desired initial condition (5.44),

$$G_\Lambda(Z, W; T) = aG(z, w; g; t). \quad (5.73)$$

From the second term in the expansion of (5.72) we see that time has to scale as

$$T \sim t\sqrt{a}. \quad (5.74)$$

Inserting the full scaling relations and the solution (5.72) for the one step propagator into the composition law (5.59) we obtain

$$\frac{\partial}{\partial T} G_\Lambda(Z, W; T) = -\frac{\partial}{\partial Z} [W_\Lambda(Z) G_\Lambda(Z, W; T)]. \quad (5.75)$$

This is precisely the differential equation for the fixed geodesic distance two-loop function as derived in the previous subsection, i.e. (5.47). Thus, we rederived the previous result obtained from the peeling method using the transfer matrix formalism. The solution to the differential equation (5.75) is again given by (5.48).

5.4 | Physical observables

One of the simplest observables in two-dimensional Euclidean quantum gravity is the disc function or Hartle-Hawking wave function which describes the amplitude of creation of a universe from nothing. The result was obtained to be

$$W_\Lambda(Z) = \left(Z - \frac{1}{2}\sqrt{\Lambda} \right) \sqrt{Z + \sqrt{\Lambda}} \quad (5.76)$$

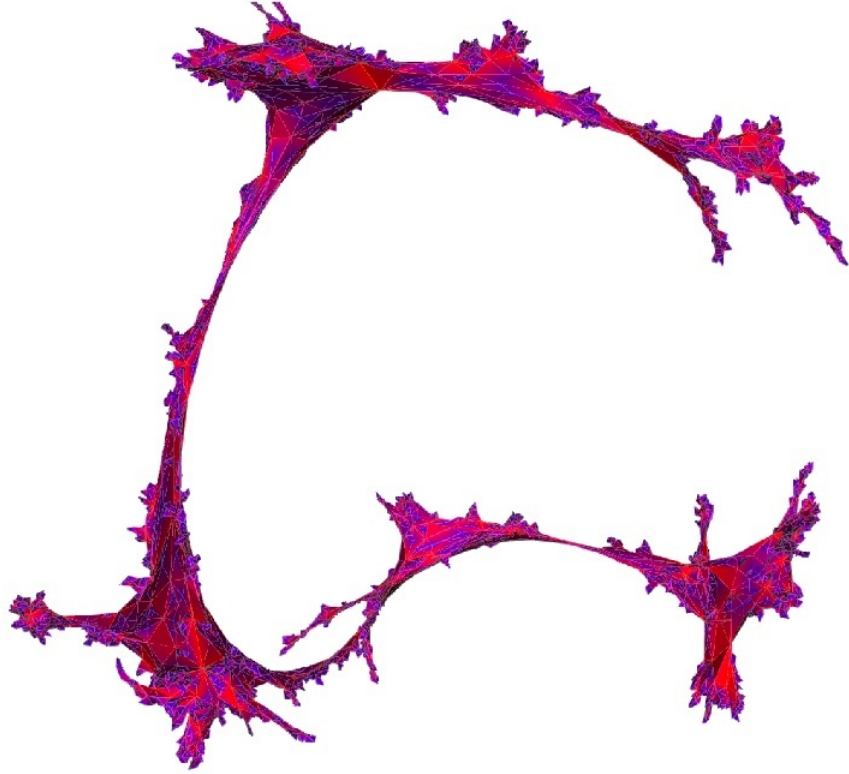


Figure 5.11: A typical quantum geometry of two-dimensional Euclidean quantum gravity [1].

or

$$W_\Lambda(L) = L^{-5/2}(1 + \sqrt{\Lambda}L)e^{-\sqrt{\Lambda}L}. \quad (5.77)$$

Having determined the dependence on the geodesic distance through the two-point function in Sec. 5.3.2 we can further calculate the *Hausdorff dimension* d_H of the quantum geometry. This dimension estimator is formally defined as

$$\langle V(T) \rangle \sim T^{d_H} \quad \text{for } T \rightarrow \infty. \quad (5.78)$$

Using the expression for the two-point function, i.e. (5.57),

$$G_\Lambda(T) \sim e^{-\sqrt[4]{\Lambda}T/\alpha} \quad \text{for } T \rightarrow \infty. \quad (5.79)$$

we obtain

$$\langle V(T) \rangle = -\frac{1}{G_\Lambda(T)} \frac{\partial}{\partial \Lambda} G_\Lambda(T) \sim \frac{T}{\Lambda^{3/4}}. \quad (5.80)$$

This equation reflects the fact that at large T the quantum geometry looks effectively one-dimensional, i.e. the volume is proportional to the length. Further one can extract from this expression that the average spatial length of the quantum geometry at intermediate T behaves as

$$\langle L \rangle = \frac{\langle V(T) \rangle}{T} \sim \frac{1}{\Lambda^{3/4}}. \quad (5.81)$$

Hence for typical time scales of $T \sim 1/\sqrt[4]{\Lambda}$ we have

$$\langle V(T) \rangle \sim T^4 \quad \text{for } T \sim \frac{1}{\sqrt[4]{\Lambda}}. \quad (5.82)$$

Thus we conclude that the Hausdorff dimension of two-dimensional Euclidean quantum gravity is given by $d_H = 4$. This result is somehow unexpected since we started off with a theory of two-dimensional triangulations. In fact, this is an indication that the quantum geometry is fractal [99, 95, 100, 101]. As we will see explicitly in Sec. 7.1 the quantum geometry is dominated by a proliferation of baby universes at the cut-off scale, meaning that at every point in the geometry there splits off a geometry with disc topology. The infinite number of baby universes causes the increment in the Hausdorff dimension. This fractal structure can be nicely observed in Fig. 5.11, which shows a typical configuration of the path integral obtained from a Monte Carlo simulation [1].

5.5 | Discussion and outlook to higher dimensions

In this chapter we introduced dynamical triangulations as a regularization scheme to define the Euclidean gravitational path integral. In particular, we considered the case of two dimensions in which analytical results can be obtained. We calculated the disc or Hartle-Hawking wave function, the fixed geodesic distance two-loop amplitude as well as the two-point function. Using these quantities we were able to analyze several properties of the quantum geometry. One very interesting observation is the fractal structure of the quantum geometry which manifests itself in a proliferation of baby universes at the cut-off scale. This is related to the unexpected value of the Hausdorff dimension of $d_H = 4$. Fig. 5.11 illustrates this situation by showing a typical configuration of the path integral obtained from a Monte Carlo simulation [1].

It is interesting to note how this situation translates to higher dimensions. In an analogous manner to two dimensions one can define the gravitational path integral as a sum over d -dimensional simplicial complexes (see for example [18] for a detailed

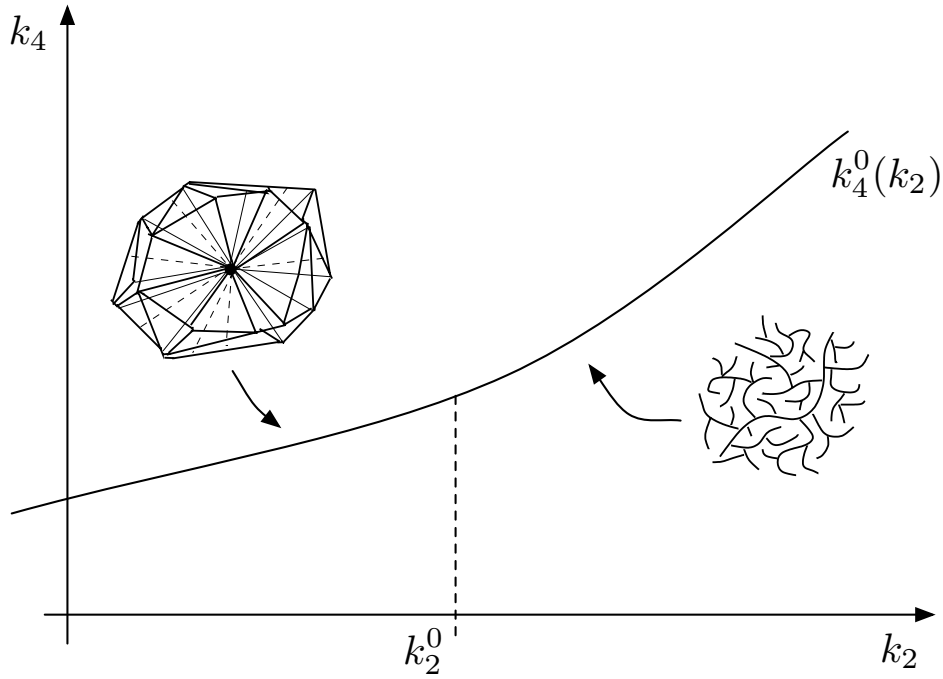


Figure 5.12: The phase diagram of four-dimensional Euclidean quantum gravity defined through DT.

exposition). The corresponding Regge action takes the following simple form

$$S_T(k_{d-2}, k_d) = k_d N_d(T) - k_{d-2} N_{d-2}(T), \quad (5.83)$$

where $N_d(T)$ denotes the number of d -simplices and $N_{d-2}(T)$ the number of $(d-2)$ -simplices in the triangulation T . The analog expression to (5.5) for the partition function is then written as the sum over closed d -dimensional triangulations \mathcal{T}_d ,

$$\mathcal{Z}(k_{d-2}, k_d) = \sum_{T \in \mathcal{T}_d} \frac{1}{C_T} e^{-S_T(k_{d-2}, k_d)}. \quad (5.84)$$

Since analytical methods are absent in $d > 2$, one has to perform Monte Carlo simulations of the quantum geometry (see for instance [18]). DT in three dimensions were considered in [102, 103, 104, 105]. The four-dimensional case was first analyzed in [106, 107, 108], followed by further progress in [109, 110, 111, 112, 113, 114]. The results for $d=4$ are summarized by the following schematic phase diagram (Fig. 5.12).⁴

⁴Although we only consider the case of $d=4$ here, the picture turns out to be essentially the same in

One observes that the model possesses an infinite-volume limit everywhere along the critical line $k_4^0(k_2)$, which fixes the bare cosmological constant as a function of the inverse Newton constant $k_2 \sim G_N^{-1}$. Along this critical line, there is a critical point k_2^0 . Below this critical point the geometries generically have a very large Hausdorff dimension $d_H \approx \infty$. This can be understood in terms of a situation where every point in the quantum geometry is effectively at Planck distance to any other point. We call this the *crumpled phase* of the quantum geometry. Above k_2^0 we find the opposite situation where a configuration contributing to the state sum looks like a branched polymer with Hausdorff dimension $d_H = 2$ (see Fig. 5.6). This is called the *branched polymer phase* of the quantum geometry.

One could hope that right at the transition point k_2^0 genuine extended triangulations with a finite Hausdorff dimension might be dominating. For this to happen the phase transition at this point should be of second or higher order. Unfortunately, it was found to be of first kind⁵ which leaves us with little hope that a sensible continuum theory of Euclidean quantum gravity can be obtained from DT for $d > 2$.

This unsatisfactory situation is one of the reasons for incorporating causality in DT. We have already seen above that many of the unappealing features of the quantum geometry were related to the proliferation of baby universes at the cut-off scale. In a genuine Lorentzian framework we expect such “acausal” configurations to be suppressed and the path integral should be much better behaved. The development of such a genuine Lorentzian framework by so-called causal dynamical triangulations is the subject of the next chapter.

the case of $d=3$.

⁵Evidence that the phase transition is of first order was given both in three dimensions [105, 115] as well as in four dimensions [116, 117, 118].

CHAPTER 6

Two-dimensional causal dynamical triangulations

In the previous chapter we introduced the reader to the concept of dynamical triangulations (DT). As we discussed at the end of the chapter, DT seems to be incompatible with a well-behaved continuum limit in three and higher dimensions. This problem is related to the failure of incorporating the Lorentzian signature into the gravitational path integral. In this chapter we see how this issue can be resolved in the framework of Lorentzian quantum gravity defined through causal dynamical triangulations [19]. The presentation of this chapter closely follows [19, 119, 120].

6.1 | Incorporating causality in dynamical triangulations

Inspired by early ideas of Teitelboim [121, 122], we want to construct a gravitational path integral, where we insist in starting from space-times with Lorentzian signature. However, to address the Lorentzian nature of the path integral it is essential to look at geometries that have an intrinsically defined notion of time. In the approach of causal dynamical triangulations (CDT), introduced by Ambjørn and Loll in 1998 [19] for the case of two dimensions¹, this problem is addressed by studying piecewise linear

¹Further developments for two-dimensional CDT have been made in [123, 124, 125, 126, 127, 128, 129, 130, 131, 132, 133] which will be partially discussed in more detail in the following chapters. References to results in higher dimensions will be given in the last section of this chapter.

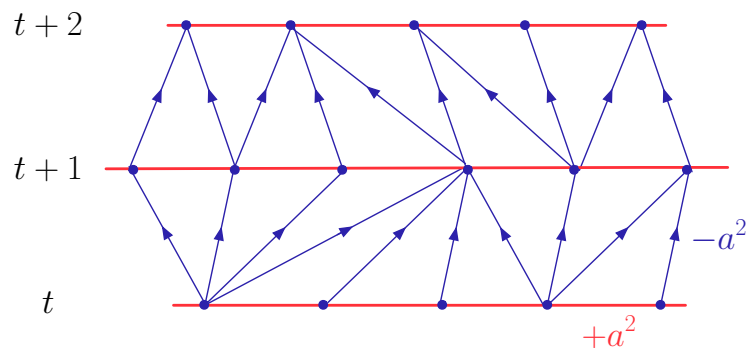


Figure 6.1: Section of a two-dimensional Lorentzian triangulation consisting of space-time strips of height $\Delta t = 1$. Each spatial slice is periodically identified, such that the simplicial manifold has topology $[0, 1] \times S^1$. One sees that the lower strip with initial boundary length $l(t)$ and final boundary length $l(t + 1)$ consists exactly of $l(t)$ up-pointing triangles and $l(t + 1)$ down-pointing triangles.

geometries that have an entirely time-sliced structure. By virtue of the time-slicing one can globally distinguish timelike and spacelike edges. We will see that this distinction is essential to define a consistent Wick rotation.

As in the case of DT one uses triangles at cut-off length to discretize the geometries. However, in contrary to DT, CDT uses Minkowskian instead of Euclidean triangles. These have one spacelike edge of length squared $L_s^2 = +a^2$ and two timelike edges of length squared $L_t^2 = -a^2$. By construction one chooses triangulations with topology of $S^1 \times [0, 1]$. Each triangulation consists of t time slices of height $\Delta t = 1$. The geometry of an individual time slice is now determined by the composition of $l(t)$ up-pointing triangles and $l(t + 1)$ down-pointing triangles as illustrated in Fig. 6.1.

In this formulation the time t by definition takes the role of geodesic distance. Further, there are no spatial topology changes with respect to the time-slicing. Hence, the layered structure does not only introduce an intrinsic time-direction that enables us to define a Wick rotation, but it also excludes spatial topology changes which in the Lorentzian picture lead to singular points with ill-defined signature.²

Since the triangles are simply patches of flat Minkowski space, they are naturally

²In the next chapter we will relax this constraint and we will show how one can make sense of spatial topology changes in a Lorentzian setting.

equipped with a local light cone structure. Furthermore, due to the sliced structure of the triangulations which glues spacelike to spacelike and timelike to timelike edges, the triangulation is naturally equipped with a global causal structure. By virtue of this global causal structure it is possible to define a Wick rotation for curved manifolds on the discretized level. In the triangulation context this is done by performing a Wick rotation on the timelike edges, i.e. $L_t \rightarrow iL_t$. The Wick rotation acting on the whole manifold is then defined as

$$\mathcal{W} : \mathcal{T}^{lor} = \{T, L_s^2 = a^2, L_t^2 = -a^2\} \mapsto \mathcal{T}^{eu} = \{T, L_s^2 = a^2, L_t^2 = a^2\}. \quad (6.1)$$

As in the continuum case this rotation should be treated with some care and one must show that the Lorentzian action defined with $L_t^2 = -a^2$ can be analytically continued to the Euclidean action defined with $L_t^2 = a^2$. This is done in appendix B.1, where we discuss in more detail the Regge action for two-dimensional Lorentzian triangulations. It is shown there that under the above defined Wick rotation the Boltzmann weight for each triangulation indeed transforms as

$$\mathcal{W} : e^{i S_{\text{Regge}}(\mathcal{T}^{lor})} \mapsto e^{-S_{\text{Regge}}(\mathcal{T}^{eu})}. \quad (6.2)$$

We shall see in the forthcoming section that the above defined kinematical structure reduces the computation of the path integral for the fixed geodesic distance correlator or finite-time propagator to a simple statistical mechanics problem.

6.2 | The discrete solution

As for DT we fix the space-time topology of the triangulation to be of the form $S^1 \times [0, 1]$. The Regge action is then simply proportional to the volume of the triangulation,

$$S_{\text{Regge}}(T) = \tilde{\lambda} a^2 N(T), \quad (6.3)$$

where $\tilde{\lambda}$ is the bare cosmological constant and $N(T)$ the number of triangles in the triangulation T . Note that an order one factor coming from the volume term has been absorbed into $\tilde{\lambda}$. Since all slices have the same geodesic distance, the propagator or fixed geodesic distance two-loop function can be defined in a simple manner

$$G_{\tilde{\lambda}}^{(u)}(l_1, l_2; t) = \sum_{\mathcal{T}_c(l_1, l_2, t)} \frac{1}{C_T} e^{i \tilde{\lambda} a^2 N(T)}, \quad (6.4)$$

where \mathcal{T}_c denotes the causal triangulations with initial boundary length l_1 and final boundary length l_2 constructed out of t time-slices. Again, C_T denotes the volume of the automorphism group of a triangulation. As for DT we add a superscript (u) to denote the propagator with no marked points on the boundary. As discussed above, after the Wick rotation the discrete sum over complex amplitudes is converted to a genuine statistical model with a real Boltzmann weight,

$$G_\lambda^{(u)}(l_1, l_2; t) = \sum_{\mathcal{T}_c(l_1, l_2, t)} \frac{1}{C_T} e^{-\lambda a^2 N(T)}, \quad (6.5)$$

where λ and $\tilde{\lambda}$ differ by an order one constant due to the different volume of Minkowskian and Euclidean triangles (see App. B.1). As for the fixed geodesic distance two-loop amplitude in the case of DT the propagator satisfies the following semi-group property or composition law (e.g. (5.65)),

$$G_\lambda^{(u)}(l_1, l_2; t_1 + t_2) = \sum_l l G_\lambda^{(u)}(l_1, l; t_1) G_\lambda^{(u)}(l, l_2; t_2), \quad (6.6)$$

where again the measure factor l in the composition law comes from the periodic boundary conditions. Writing the composition law for $t_1 = 1$ we find the following relation for the one-step propagator,

$$G_\lambda^{(u)}(l_1, l_2; t + 1) = \sum_l l G_\lambda(l_1, l; 1) G_\lambda(l, l_2; t). \quad (6.7)$$

As for DT we introduce a generating function for $G_\lambda(l_1, l_2; t)$

$$G_\lambda^{(u)}(x, y; t) \equiv \sum_{k, l} x^k y^l G_\lambda^{(u)}(k, l; t), \quad (6.8)$$

where x and y can again be related to the boundary cosmological constants of individual triangles,

$$x = e^{-\lambda_i a}, \quad y = e^{-\lambda_o a}. \quad (6.9)$$

The analogous fugacity of a triangle is again given by,

$$g = e^{-\lambda a^2}. \quad (6.10)$$

The total Boltzmann weight of one strip can be determined by noting that for the one-step propagator in CDT a factor of gx is assigned for triangles that have the space-like edge on the initial loop and a factor gy for triangles where the spacelike edge is

on the final loop. This relation is much simpler than in the case of DT. The one-step propagator is now easily computed by,

$$\begin{aligned} G^{(u)}(x, y; g; 1) &= \triangle + \nabla + \triangle + \dots \\ &= \sum_{k=1}^{\infty} \frac{1}{k} \left(\sum_{m=1}^{\infty} (gx)^m \sum_{n=1}^{\infty} (gy)^n \right)^k, \end{aligned} \quad (6.11)$$

where the factor $1/k$ comes again from dividing by the volume $C(T)$ of the automorphism group for circular triangulations. Performing the summations in (6.11) we readily obtain

$$G^{(u)}(x, y; g; 1) = \sum_{k=1}^{\infty} \frac{1}{k} \left(\frac{gx}{1-gx} \frac{gy}{1-gy} \right)^k = -\log \left(1 - \frac{gxy}{(1-gx)(1-gy)} \right). \quad (6.12)$$

From the inverse discrete Laplace transform of (6.12) it can be seen that the one-step propagator with fixed boundary lengths is given by

$$G^{(u)}(l_1, l_2; g; 1) = g^{l_1+l_2} \frac{1}{l_1+l_2} \binom{l_1+l_2}{l_1}, \quad (6.13)$$

where the division by the volume of the automorphism group now makes its appearance in the factor $1/(l_1+l_2)$. Similar expressions for different boundary conditions can for instance be found in [119].

Instead of obtaining the continuum limit directly of the one-step propagator as done in the previous chapter we want to iteratively compute the finite-time propagator $G(x, y; g; t)$ and then perform the continuum limit. To do so we rewrite the composition law (6.6) in terms of generating functions and obtain,

$$G^{(u)}(x, y; g; t_1 + t_2) = \oint \oint \frac{dz}{2\pi i} \frac{dz'}{2\pi i} \frac{1}{(1-zz')^2} G(x, z; g; t_1) G(z', y; g; t_2). \quad (6.14)$$

Setting $t_2 = 1$ and performing the contour integration over z one gets

$$G^{(u)}(x, y; g; t) = \oint \frac{dz'}{2\pi iz'^2} \left[\frac{d}{dz} G^{(u)}(x, z; g; 1) \right]_{z=1/z'} G^{(u)}(z', y; g; t-1). \quad (6.15)$$

Inserting the expression for the one-step propagator, i.e. (6.12), yields

$$G^{(u)}(x, y; g; t) = G^{(u)} \left(\frac{g}{1-gx}, y; g; t-1 \right) - G^{(u)}(g, y; g; t-1). \quad (6.16)$$

This equation can be iterated and the implicit solution written as

$$G^{(u)}(x, y; g; t) = \log \left(\frac{1}{1 - F_t(x)y} \right) - \log \left(\frac{1}{1 - F_{t-1}(g)y} \right), \quad (6.17)$$

where F_t is defined iteratively by

$$F_t(x) = \frac{g}{1 - gF_{t-1}(x)}, \quad F_0(x) = x. \quad (6.18)$$

The fixed point F of this equation as defined by $F_t(x) = F_{t-1}(x)$ is given by

$$F = \frac{1 - \sqrt{1 - 4g^2}}{2g}, \quad g = \frac{1}{F + 1/F}. \quad (6.19)$$

By standard techniques one can use the fixed point to give the explicit solution to the iterative equation (6.18)

$$F_t(x) = \frac{B_t - xC_t}{A_t - xB_t}, \quad F_{t-1}(g) = \frac{B_t}{A_t}, \quad (6.20)$$

where we have defined

$$A_t = 1 - F^{2t+2}, \quad B_t = F - F^{2t+1}, \quad C_t = F^2 - F^{2t}. \quad (6.21)$$

The explicit solution for the propagator is now obtained by substituting (6.20) in (6.17), yielding

$$G^{(u)}(x, y; g; t) = -\log(1 - Z(x, y; g; t)), \quad (6.22)$$

where we have defined

$$Z(x, y; g; t) = \left(1 - \frac{A_t C_t}{B_t^2}\right) \frac{\frac{B_t}{A_t} x \frac{B_t}{A_t} y}{\left(1 - \frac{B_t}{A_t} x\right) \left(1 - \frac{B_t}{A_t} y\right)}. \quad (6.23)$$

The combined region of convergence of this result as an expansion in powers $g^k x^l y^m$ is

$$|g| < \frac{1}{2}, \quad |x| < 1, \quad |y| < 1. \quad (6.24)$$

As in the case of DT we will use the radius of convergence to obtain the critical points.

6.3 | The continuum limit

To define the continuum limit of the theory we assume canonical scaling dimensions for the bulk and boundary cosmological constants as in the case of DT,

$$g = g_c e^{-a^2 \Lambda/2}, \quad x = x_c e^{-aX}, \quad y = y_c e^{-aY}. \quad (6.25)$$

The critical values for these couplings are again determined by the region of convergence of the propagator, i.e. (6.24), yielding

$$g_c = 1/2, \quad x_c = 1, \quad y_c = 1, \quad (6.26)$$

One can quickly convince oneself that these are the correct critical values by looking at the average number of triangles in one strip

$$\langle N \rangle = g \frac{d}{dg} G^{(u)}(x, y; g; 1) = 1 - \frac{1}{1 - gx} - \frac{1}{1 - gy} + \frac{1}{1 - g(x + y)}. \quad (6.27)$$

We see that the average number of triangles diverges at the critical point $(g_c, x_c, y_c) = (1/2, 1, 1)$. We hence arrive at the following scaling relations

$$g = \frac{1}{2} e^{-a^2 \Lambda/2}, \quad x = e^{-aX}, \quad y = e^{-aY}. \quad (6.28)$$

The continuum limit of the propagator can now be determined by inserting these scaling relations into (6.22). To get a sensible continuum limit we require time to scale as

$$T \sim at. \quad (6.29)$$

which yields the following result

$$G_\Lambda^{(u)}(X, Y, T) = -\log(1 - Z_\Lambda(X, Y, T)), \quad (6.30)$$

where

$$Z_\Lambda(X, Y, T) = \frac{\Lambda}{\sinh^2 \sqrt{\Lambda} T (X + \sqrt{\Lambda} \coth \sqrt{\Lambda} T) (Y + \sqrt{\Lambda} \coth \sqrt{\Lambda} T)}. \quad (6.31)$$

As in the case of DT the propagator undergoes a wave function renormalization

$$G_\Lambda^{(u)}(X, Y, T) = a G^{(u)}(x, y; g; t). \quad (6.32)$$

Again the power of a is uniquely determined by the initial condition coming from the composition law, i.e. (6.14).

The continuum expression for the propagator, where the boundary lengths are fixed instead of the boundary cosmological constants can now be obtained by an inverse Laplace transformation of (6.30) with respect to both X and Y ,

$$G_\lambda^{(u)}(L_1, L_2; T) = \frac{e^{-\sqrt{\lambda} \coth \sqrt{\lambda} T (L_1 + L_2)}}{\sinh \sqrt{\lambda} T} \frac{\sqrt{\lambda}}{\sqrt{L_1 L_2}} I_1 \left(\frac{2\sqrt{\lambda L_1 L_2}}{\sinh \sqrt{\lambda} T} \right), \quad (6.33)$$

where $I_1(x)$ is a modified Bessel function of the first kind. The continuum version of the composition law (6.14) for fixed lengths then reads

$$G_\lambda^{(u)}(L_1, L_2; T_1 + T_2) = \int_0^\infty dL L G_\lambda^{(u)}(L_1, L; T_1) G_\lambda^{(u)}(L, L_2; T_2). \quad (6.34)$$

An interesting observation is that in contrast to the Euclidean model the time or geodesic distance scales canonically. We will further comment on this when discussing the physical observables of the model.

6.4 | Marked amplitudes

To better compare to the results of the previous chapter for Euclidean DT it is important to introduce the same convention of a marked edge on the initial boundary in CDT. In terms of the propagator this convention reads,

$$G_\lambda(l_1, l_2; 1) = I_1 G_\lambda^{(u)}(l_1, l_2; 1). \quad (6.35)$$

As before this marking removes the measure factor in the composition law for the propagator (6.6)

$$G_\lambda(l_1, l_2; t_1 + t_2) = \sum_l G_\lambda(l_1, l; t_1) G_\lambda(l, l_2; t_2), \quad (6.36)$$

which corresponds to the following composition law for the generating function,

$$G_\lambda(x, y; t_1 + t_2) = \oint \frac{dz}{2\pi i z} G_\lambda(x, z^{-1}; t_1) G_\lambda(z, y; t_2). \quad (6.37)$$

The one-step propagator with a mark on the boundary can easily be computed from (6.12) by taking a derivative with respect to the boundary cosmological constant,

$$G(x, y; g; 1) = x \frac{d}{dx} G^{(u)}(x, y; g; 1) = \frac{g^2 xy}{(1 - gx)(1 - g(x + y))}. \quad (6.38)$$

Inserting this expression into the composition law (6.36) gives an iterative equation analogous to (6.16) ,

$$G(x, y; g; t) = \frac{g^x}{1 - gx} G\left(\frac{g}{1 - gx}, y; g; t - 1\right). \quad (6.39)$$

The explicit solution can be obtained from (6.22) by taking a derivative with respect to the boundary cosmological constant,

$$G(x, y; g; t) = x \frac{d}{dx} G^{(u)}(x, y; g; t) = \frac{F^{2t}(1 - F^2)^2 xy}{(A_t - B_t x)(A_t - B_t(x + y) + C_t xy)}, \quad (6.40)$$

where F , A_t , B_t and C_t were defined in (6.19) and (6.21).

To obtain the continuum marked propagator we could now apply the scaling relations (6.28) to this expression. Instead, one can also apply the scaling relations directly to (6.39) in the manner we proceeded for DT. Doing so one finds the following differential equation for the continuum marked propagator,

$$\frac{\partial}{\partial T} G_\Lambda(X, Y, T) = -\frac{\partial}{\partial X} \left[\hat{W}(X) G_\Lambda(X, Y, T) \right], \quad (6.41)$$

where

$$\hat{W}(X) = X^2 - \Lambda. \quad (6.42)$$

The notation $\hat{W}(X)$ is introduced in analogy to the Euclidean result, however, it should be noted that in the case of CDT $\hat{W}(X)$ is *not* the disc function.

Solving the differential equation (6.41) with initial condition

$$G_\Lambda(X, Y; T=0) = \frac{1}{X + Y}. \quad (6.43)$$

gives

$$G_\Lambda(X, Y; T) = \frac{\hat{W}(\bar{X}(T, X))}{\hat{W}(X)} \frac{1}{\bar{X}(T, X) + Y}, \quad (6.44)$$

where $\bar{X}(T, X)$ is the solution to the characteristic equation

$$\frac{d\bar{X}(T, X)}{dT} = -\hat{W}(\bar{X}(T, X)), \quad \bar{X}(T=0, X) = X. \quad (6.45)$$

Proceeding as in Sec. 5.3.2 we obtain,

$$\bar{X}(T, X) = \sqrt{\Lambda} \frac{(\sqrt{\Lambda} + X) - e^{-2\sqrt{\Lambda}T}(\sqrt{\Lambda} - X)}{(\sqrt{\Lambda} + X) + e^{-2\sqrt{\Lambda}T}(\sqrt{\Lambda} - X)}. \quad (6.46)$$

Inserting this expression in (6.44) gives the explicit solution for the continuum marked propagator. Further, one can check that if one marks the unmarked propagator (6.30) by taking a derivative with respect to the initial boundary cosmology constant X , the resulting expression precisely coincides with this result. Inverse Laplace transforming (6.44) with respect to X and Y yields the continuum marked propagator in the length representation,

$$G_\Lambda(L_1, L_2; T) = \frac{e^{-\sqrt{\Lambda} \coth \sqrt{\Lambda} T (L_1 + L_2)}}{\sinh \sqrt{\Lambda} T} \frac{\sqrt{\Lambda} L_1}{\sqrt{L_1 L_2}} I_1 \left(\frac{2\sqrt{\Lambda} L_1 L_2}{\sinh \sqrt{\Lambda} T} \right), \quad (6.47)$$

which is simply (6.33) multiplied by L_1 as expected.

As in the case of DT we can also calculate the disc function from the propagator. In CDT it can be defined as follows from the finite-time propagator with one boundary shrunken to zero,

$$W_\Lambda(L) = \int_0^\infty dT G_\Lambda(L, L_2 = 0, T). \quad (6.48)$$

One notices that this definition differs slightly from the corresponding relation in the Euclidean setting, i.e. (5.55). This is due to the fact that the mark coming from the zero-length boundary is always at latest T and cannot be anywhere in the bulk as in the case of DT. Therefore we do not have to differentiate with respect to $-\partial/\partial\Lambda$.

Using (6.33) we get

$$G_\Lambda(L, L_2 = 0, T) = \frac{\Lambda}{\sinh^2 \sqrt{\Lambda} T} e^{-\sqrt{\Lambda} L \coth \sqrt{\Lambda} T}. \quad (6.49)$$

Inserting this into (6.48) one readily arrives at the simple expression

$$W_\Lambda(L) = e^{-\sqrt{\Lambda} L} \quad (6.50)$$

or in Laplace transform language

$$W_\Lambda(X) = \frac{1}{X + \sqrt{\Lambda}}. \quad (6.51)$$

The corresponding result for the disc function without mark reads

$$W_\Lambda^{(u)}(L) = \frac{e^{-\sqrt{\Lambda} L}}{L}. \quad (6.52)$$

From (6.49) we can also easily compute the two-point function for CDT, i.e.

$$G_\Lambda(T) = G_\Lambda(L_1 = 0, L_2 = 0, T) = \frac{\Lambda}{\sinh^2 \sqrt{\Lambda} T}. \quad (6.53)$$

6.5 | Hamiltonians in causal quantum gravity

As mentioned earlier the concept of time or geodesic distance directly relates to a notion of Hamiltonian dynamics. This can be seen explicitly when viewing the differential equation for the continuum marked propagator (6.41) as a Wick rotated Schrödinger equation,

$$-\frac{\partial}{\partial T} G_\Lambda(X, Y, T) = \hat{H}_X G_\Lambda(X, Y, T). \quad (6.54)$$

Here \hat{H}_X can be interpreted as the *effective quantum Hamiltonian* of the system and is given by

$$\hat{H}_X = (X^2 - \Lambda) \frac{\partial}{\partial X} + 2X. \quad (6.55)$$

The effective quantum Hamiltonian in length space can be obtained from (6.54) by inverse Laplace transformation, yielding

$$\hat{H}_L = -L \frac{\partial^2}{\partial L^2} + \Lambda L. \quad (6.56)$$

The corresponding Hamiltonian for the case of unmarked amplitudes reads

$$\hat{H}_L^{(u)} = -L \frac{\partial^2}{\partial L^2} - 2 \frac{\partial}{\partial L} + \Lambda L. \quad (6.57)$$

These kind of Hamiltonians are analyzed in detail in App. B.2, where several properties such as the spectrum and eigenfunctions are computed. In particular, it is shown there that the Hamiltonian (6.57) is self-adjoint with respect to the measure LdL . This is also reflected in the corresponding semi-group property, where the integration is taken over the same measure. As we will see later for some comparisons it is useful to transform this Hamiltonian to one which is self-adjoint on a flat measure. This can be done by absorbing the measure in the wave functions corresponding to the initial and final loop, i.e. $\psi_n(L) = \frac{1}{\sqrt{L}} \varphi_n(L)$. Commuting (6.57) with $1/\sqrt{L}$ gives³

$$\hat{H}_L^{\text{flat}} = -L \frac{\partial^2}{\partial L^2} - \frac{\partial}{\partial L} + \frac{1}{4L} + \Lambda L. \quad (6.58)$$

In the following we present a calculation by Nakayama [134] which reproduces the effective quantum Hamiltonian of CDT, i.e. (6.58) from a continuum calculation. More precisely, Nakayama considered the non-local “induced” action of two-dimensional

³See App. B.2 for more details.

quantum gravity in the proper time gauge. The general form of this action was first introduced by Polyakov [64] and reads

$$S[g] = \int dt dx \sqrt{g} \left(\frac{1}{16} R_g \frac{1}{-\Delta_g} R_g + \Lambda \right), \quad (6.59)$$

where R is the scalar curvature corresponding to the metric g , t denotes time and x the spatial coordinate. In the proper time gauge the metric has the form

$$g = \begin{pmatrix} 1 & 0 \\ 0 & \gamma(t, x) \end{pmatrix}. \quad (6.60)$$

This is in contrast to the conformal gauge with $g = e^\phi \hat{g}$. It was shown by Nakayama that in this gauge the classical dynamics is described entirely by the following effective action

$$S_\kappa = \int_0^T dt \left(\frac{(\dot{l}(t))^2}{4l(t)} + \Lambda l(t) + \frac{\kappa}{l(t)} \right), \quad (6.61)$$

where

$$l(t) = \frac{1}{\pi} \int dx \sqrt{\gamma}, \quad (6.62)$$

and where κ is an integration constant coming from the solution for the energy-momentum tensor component $T_{01} = 0$. As can be seen from Eq. (6.62) $L_{cont} \equiv \pi l(t)$ is precisely the length of a spatial universe at constant t , as calculated from the metric (6.60).

One can now quantize the action S_κ for $\kappa = (m+1)^2$, where $m \in \mathbb{N}$ can be interpreted as a winding number. It was further argued in [134] that in the quantum theory one should shift m by $-1/2$ leading to $\kappa = (m + \frac{1}{2})^2$. The classical Hamiltonian corresponding to the effective action (6.61) with $\kappa = (m + \frac{1}{2})^2$ then reads

$$H_m = \Pi_l / \Pi_l + \left(m + \frac{1}{2}\right)^2 \frac{1}{l} + \Lambda l, \quad (6.63)$$

where Π_l is the canonical momentum conjugate to l . To canonically quantize the system we make the standard replacement $\Pi_l \rightarrow -i \frac{\partial}{\partial l}$, yielding⁴

$$\hat{H}_m = -l \frac{\partial^2}{\partial l^2} - \frac{\partial}{\partial l} + \left(m + \frac{1}{2}\right)^2 \frac{1}{l} + \Lambda l. \quad (6.64)$$

One observes that for $m = 0$ this Hamiltonian precisely coincides with the effective quantum Hamiltonian for CDT, i.e. (6.58). An interpretation for $m > 0$ in the context of CDT was given in [126].

⁴For completeness the spectrum of this Hamiltonian is also derived in App. B.2.

Quite remarkably, when computing the propagator,

$$G_\lambda^{(m)}(L_1, L_2; T) = \langle L_2 | e^{-T\hat{H}_m} | L_1 \rangle, \quad (6.65)$$

one observes that

$$\sum_{m=0}^{\infty} (-1)^m (2m+1) \int_0^\infty dT G_\lambda^{(m)}(L_1, L_2; T) = \frac{\sqrt{L_1 L_2}}{L_1 + L_2} e^{-\sqrt{\lambda}(L_1 + L_2)} \quad (6.66)$$

precisely coincides with the two-loop amplitude of *Euclidean* DT [134]. While a summation over the winding number might seem natural, a complete understanding of this relation is still lacking.

Before moving to the next section let us briefly mention that, since in CDT we are using a lattice regularization, the continuum variables are only defined up to a factor of proportionality which should be fixed by comparing to a continuum calculation. Recall that the length l appearing in Nakayama's Hamiltonian is not the physical length, L_{cont} , but L_{cont}/π . Hence, since both models are described by the same effective quantum Hamiltonian, it is natural to also define the physical length $L_{cont} = \pi L$ for CDT. We will use this assignment in Chap. 8 when discussing the emergence of a semiclassical background in the context of CDT.

6.6 | Physical observables: Comparing CDT and DT

As in the case of DT one of the simplest observables is the disc function or Hartle-Hawking wave function which describes the amplitude of creation of a universe from nothing. The result is given by (6.51), i.e

$$W_\lambda(X) = \frac{1}{X + \sqrt{\lambda}}. \quad (6.67)$$

The corresponding Euclidean expression (5.28), here labeled with a superscript (*eu*) to distinguish from the analogous CDT expressions, is

$$W_\lambda^{(eu)}(X) = (X - \frac{1}{2}\sqrt{\lambda})\sqrt{X + \sqrt{\lambda}}. \quad (6.68)$$

Another interesting quantity to calculate is the Hausdorff dimension d_H of the quantum geometry formally defined as

$$\langle V(T) \rangle \sim T^{d_H} \quad \text{for } T \rightarrow \infty. \quad (6.69)$$

We saw that in Euclidean DT we had a fractal dimension of $d_H = 4$ which was related to the non-canonical scaling of time. We already observed above that in CDT time scales canonically and we therefore expect the Hausdorff dimension to be $d_H = 2$. In the following we will check this by a simple calculation.

From (6.53) we have

$$G_\Lambda(T) \sim e^{-2\sqrt{\Lambda}T} \quad \text{for } T \rightarrow \infty. \quad (6.70)$$

From this we obtain

$$\langle V(T) \rangle = -\frac{1}{G_\Lambda(T)} \frac{\partial}{\partial \Lambda} G_\Lambda(T) \sim \frac{T}{\sqrt{\Lambda}}. \quad (6.71)$$

This equation reflects the fact that at large T the quantum geometry looks effectively one-dimensional. Further we see from this expression that the average spatial length of the quantum geometry at intermediate T behaves as

$$\langle L \rangle = \frac{\langle V(T) \rangle}{T} \sim \frac{1}{\sqrt{\Lambda}}. \quad (6.72)$$

Hence for typical time scales of $T \sim 1/\sqrt{\Lambda}$ we have

$$\langle V(T) \rangle \sim T^2 \quad \text{for } T \sim \frac{1}{\sqrt{\Lambda}} \quad (6.73)$$

which yields a Hausdorff dimension of $d_H = 2$. In this sense the quantum geometry of CDT is much better behaved as a model of two-dimensional quantum gravity in contrary to DT which has a fractal dimension of $d_H = 4$.

To get a better picture of the quantum geometry of CDT it is instructive to look at a typical space-time geometry (Fig. 6.2). We see that in contrast to the Euclidean model there are no spatial topology changes. Further, as we have already seen above the average spatial length of the quantum geometry behaves as

$$\langle L \rangle \sim \frac{1}{\sqrt{\Lambda}}. \quad (6.74)$$

A simple calculation as will be presented in Chap. 8 reveals that also the fluctuations scale as

$$\langle \Delta L \rangle \equiv \sqrt{\langle L^2 \rangle - \langle L \rangle^2} \sim \langle L \rangle \sim \frac{1}{\sqrt{\Lambda}}. \quad (6.75)$$

Hence we see that the two-dimensional quantum geometry is purely governed by quantum fluctuations and there does not exist a sensible semiclassical background geometry. We will see in Chap. 8 how this situation changes when one of the boundaries is taken to infinity and the geometry becomes non-compact.

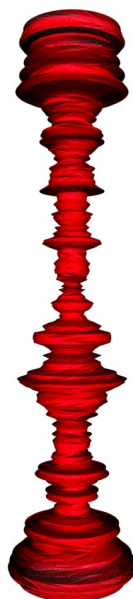


Figure 6.2: A typical two-dimensional Lorentzian space-time. The compactified direction shows the spatial hypersurfaces of length $\langle L \rangle$ and the vertical axis labels proper time T . Technically, the picture was generated by a Monte-Carlo simulation, where a total volume of $N = 18816$ triangles and a total proper time of $t = 168$ steps was used. Further, initial and final boundary has been identified.

6.7 | Summary and outlook to higher dimensions

In this chapter we introduced two-dimensional Lorentzian quantum gravity defined through CDT.

The triangulations used in CDT have a global time-slicing without spatial topology changes. This is unlike DT where spatial topology changes are naturally present. The global notion of time enables us to define a gravitational Wick rotation. We solved the combinatorial problem and performed the continuum limit. As a result we saw that two-dimensional CDT and DT are distinct theories. Whereas the continuum dynamics of DT is completely dominated by spatial topology changes leading to a fractal dimension of $d_H = 4$, the situation is different in CDT where we have $d_H = 2$. In this sense two-dimensional CDT is arguably better suited as a model of two-dimensional quantum

gravity than DT. Before discussing several relations between both theories in the next chapter, let us first comment on the results for higher dimensions.

In contrast to the disappointing situation for DT in higher dimensions, as described in the previous chapter, CDT lead to very interesting results for both $d = 3$ [135, 136, 137, 138, 139, 140, 141] as well as $d = 4$ [142, 143, 144, 145, 146, 147] (see also [21, 20, 145, 148] for a general overview).

Let us briefly mention some of the numerical results obtained from Monte Carlo simulations in 3+1 dimensions. A very important non-trivial test for every non-perturbative formulation of quantum gravity is whether it can reproduce a sensible classical limit at macroscopic scales. The numerical results indicate that the scaling behavior of the spatial volume as a function of space-time volume is that of a four-dimensional universe at large scales, a first indication of sensible classical behavior [142]. Moreover, after integrating out all dynamical variables apart from the spatial volume as a function of proper time, one can derive the scale factor whose dynamics is described by the simplest minisuperspace model used in quantum cosmology [143, 145, 146, 147]. In Chap. 8 we will describe an analogous model in two dimensions where a semi-classical background emerges from quantum fluctuations when the geometries become non-compact.

Having passed the first consistency checks regarding the *macroscopical* structure of space-time it is very interesting what predictions one can make for the quantum nature of the *microstructure* of space-time. One important observable which has been measured is the spectral dimension of space-time which is the dimension a diffusion process would feel on the space-time ensemble. Surprisingly, this quantity depends on the scale at which it is measured. More precisely, one observes a dimensional reduction from four at large scales to two at small scales within measurement accuracy [144]. This gives an indication that non-perturbative quantum gravity defined through CDT provides an effective ultraviolet cut-off through a dynamical dimensional reduction of space-time and might therefore be non-perturbatively renormalizable. The origin of the renormalizability could be a nontrivial fixed point scenario as described by Weinberg [16]. It is interesting to note that similar results were also obtained in the exact renormalization group flow method for Euclidean quantum gravity in the continuum [149, 150, 151, 152, 153].

An interesting observation at this point is that such an effective ultraviolet cut-off through a dynamical dimensional reduction of space-time provides us with a non-

perturbative mechanism which regulates the theory. To come back to the discussion in Part I of this thesis, this means in particular that it is priori not necessary to introduce a fundamental cut-off such as the fundamental discreteness scale by hand.

Relating Euclidean and causal dynamical triangulations

In the previous two chapters we introduced two-dimensional Euclidean quantum gravity defined through DT and two-dimensional Lorentzian quantum gravity defined through CDT. Even though both theories have some physically very distinct features such as the Hausdorff dimension it is nevertheless possible to establish certain relations between them. In particular, following [19, 125], we describe how CDT and DT can be related by respectively introducing or “integrating out” baby universes, i.e. spatial topology changes.

7.1 | Introducing spatial topology changes: From CDT to DT

In this section we discuss the incorporation of spatial topology changes into the discretized framework of CDT and show how this model relates to DT in the continuum limit. Although there exist several ways of implementing spatial topology changes on the discrete level, they all lead to the same continuum description [19].

Before constructing the model let us first discuss some Lorentzian aspects of spatial topology changes. While in the Euclidean model the presence of baby universes was natural, their appearance in the Lorentzian model is far from obvious. Even though the metrics are Wick rotated from Lorentzian to Euclidean signature, one in general still has

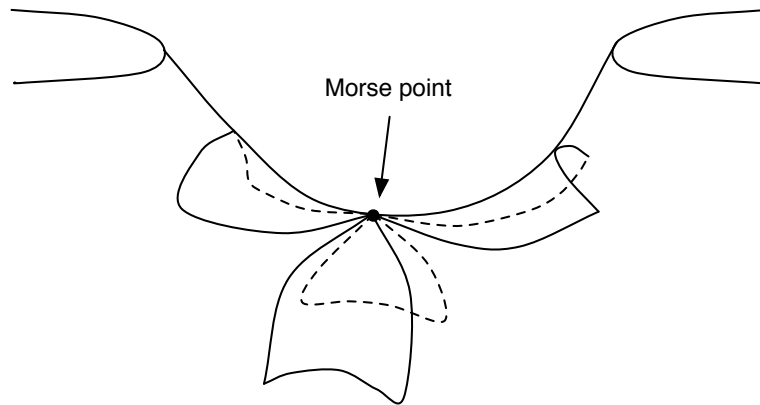


Figure 7.1: Illustration of the double light cone causal structure at a Morse point in an up-side down trousers geometry.

to perform an inverse Wick rotation. However, this is not so easy for geometries with baby universes, since these geometries do not admit a Lorentzian metric everywhere, as we already mentioned above. This is related to the fact that it is not possible to find a non-vanishing vector field everywhere. However, since the geometry is compact there are only finitely many isolated points where this is not possible. These are so-called Morse points [154, 155, 156, 157, 158]. If one imagines the splitting of a spatial universe into two, there is a Morse point precisely at the moment where the spatial topology is that of a “figure eight”. Embedded in \mathbb{R}^3 the two-dimensional geometry looks like an up-side down trousers and the Morse point precisely corresponds to the saddle point. Contrary to a generic point on the manifold, such a Morse point does not have a unique timelike vector field perpendicular to its spatial slice. In fact it has two future, and two past light cones which is referred to as a double light cone structure [158] and the resulting geometry is called causally discontinuous. Such a double light cone structure is illustrated in Fig. 7.1 for the case of the up-side down trousers. One observes that both legs of the trousers carry a future light cone belonging to the Morse point at the splitting, while the mother universe carries the two past light cones.

Since there are indications that the Einstein-Hilbert action develops complex valued singularities at these Morse points [159], it is not a priori clear that the Wick rotation as employed in CDT is valid at these points. However, since we want to relate our model to Euclidean DT, we can confine ourselves to the Euclidean sector of CDT. In Chap. 9 we present a generalized model of CDT which includes spatial topology changes, and

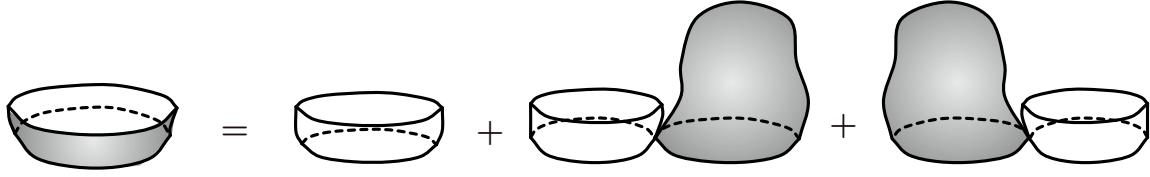


Figure 7.2: Illustration of the one-step propagator with an off-splitting “baby universe”.

where one in principle would like to Wick rotate back to the Lorentzian sector. However, in this model there is a coupling constant associated to every splitting which might be used to absorb possible divergencies.

Let us now, after this short digression, focus on the explicit construction of the discretized CDT model with spatial topology changes. The first step is to generalize the one-step propagator by allowing the initial loop to have topology of a “figure eight”. One possibility to do so is to non-locally identify two points of an initial spatial universe with topology S^1 . For a boundary of length l_1 this so-called pinching leads to a combinatorial factor of l_1 in the full one-step propagator. A baby universe is then created by assigning a disc function to one of the loops of the “figure eight” and the initial loop of a “bare” one-step propagator to the other one (see Fig. 7.2). Putting the above relation into formulas, we see that the new, or “dressed”, one-step propagator is related to the old, or “bare”, one-step propagator as follows

$$G_\lambda(l_1, l_2; t=1) = G_\lambda^{(b)}(l_1, l_2; t=1) + 2 \sum_{l=1}^{l_1-1} l_1 w(l, g) G_\lambda^{(b)}(l, l_2; t=1), \quad (7.1)$$

where $w(l, g)$ denotes the so far undetermined disc function and the factor of two comes again from the two different ways of attaching the disc function. One observes the analogy to the peeling equation for the fixed geodesic distance two-loop amplitude in DT.

It is readily checked that the “dressed” one-step propagator obeys the usual semi-group property, i.e. (6.36),

$$G_\lambda(l_1, l_2; t_1 + t_2) = \sum_l G_\lambda(l_1, l; t_1) G_\lambda(l, l_2; t_2). \quad (7.2)$$

Making the standard choice $t_1 = 1$ and $t_2 = t - 1$ to relate to the one-step propagator we obtain

$$G_\lambda(l_1, l_2; t) = \sum_l G_\lambda(l_1, l; 1) G_\lambda(l, l_2; t-1), \quad (7.3)$$

or in terms of generating functions

$$G(x, y; g; t) = \oint \frac{dz}{2\pi i z} \left[G_\lambda^{(b)}(x, z^{-1}; 1) + 2x \frac{\partial}{\partial x} \left(w(g, x) G_\lambda^{(b)}(x, z^{-1}; 1) \right) \right] G(z, y; g; t-1). \quad (7.4)$$

Inserting the explicit solution for the “bare” one-step propagator $G^{(b)}(x, z; g; 1)$, i.e. (6.38), as derived in the previous chapter, we get

$$G(x, y; g; t) = \left[1 + 2x \frac{\partial w(g, x)}{\partial x} + 2xw(g, x) \frac{\partial}{\partial x} \right] \frac{gx}{1-gx} G\left(\frac{g}{1-gx}, y; g; t-1\right). \quad (7.5)$$

At this point neither the dressed disc amplitude $w(g, x)$ nor the propagator $G(x, y; g; t)$ are known. In particular, $w(g, x)$ is *not* fixed to be the Euclidean disc function. In the following we will show how one can use scaling arguments to uniquely determine the continuum propagator $G_\lambda(X, Y; T)$ and the continuum disc amplitude $W_\lambda(X)$ from this equation. Let us assume the standard scaling relations for the boundary and bulk cosmological constants as used in DT and the “bare” CDT model,

$$g = \frac{1}{2} e^{-a^2 \Lambda}, \quad x = e^{-aX}, \quad y = e^{-aY}. \quad (7.6)$$

Inserting the scaling relations into (7.5) and setting $t=0$ we obtain the initial condition

$$G_\lambda(X, Y; T=0) = \frac{1}{X+Y} \quad (7.7)$$

where we introduced the following wave function renormalization

$$G_\lambda(X, Y; T) = a G_\lambda(x, y; t) \quad (7.8)$$

or in terms of the lengths variables

$$G_\lambda(L_1, L_2; T) = a^{-1} G_\lambda(l_1, l_2, t). \quad (7.9)$$

Extracting the scaling of the disc function is more difficult, since it actually depends on the scaling of time. To do so Ambjørn and Loll used the following combinatorial identity

$$g \frac{\partial w(g, x)}{\partial g} = \sum_t \sum_l G(x, l; g; t) l w(l, g), \quad (7.10)$$

which in terms of the generating functions reads

$$g \frac{\partial w(g, x)}{\partial g} = \sum_t \oint \frac{dz}{2\pi i z} G(x, z^{-1}; g; t) \frac{\partial w(g, z)}{\partial z}. \quad (7.11)$$

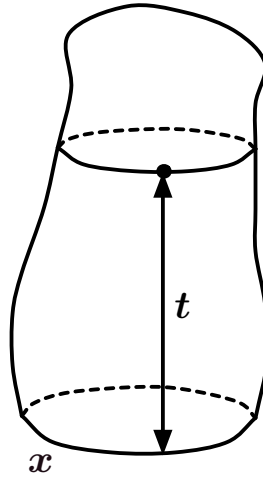


Figure 7.3: Decomposition of the disc function with a marked point in the bulk into a propagator with arbitrary time and a disc function with a mark on the boundary.

Fig. 7.3 illustrates this relation: If we introduce a mark in the bulk by taking a derivative with respect to the fugacity g , the disc function can be decomposed into a propagator and a smaller disc function which has this mark on its boundary. Further, one sums over all t to ensure that the mark can be anywhere in the bulk.

Recall from Chap. 5 and Chap. 6 that the disc function for DT scales as

$$w^{(eu)}(g, x) = w_{ns} + a^{3/2} W_{\Lambda}^{(eu)}(X) \quad (7.12)$$

while the disc function for CDT scales as

$$w^{(b)}(g, x) = a^{-1} W_{\Lambda}^{(b)}(X). \quad (7.13)$$

Hence, we make the following general ansatz for the scaling relation which includes both cases

$$w(g, x) = w_{ns} + a^{\eta} W_{\Lambda}(X) + \text{less singular terms.} \quad (7.14)$$

Further, the general scaling ansatz for the time variable reads

$$T = a^{\varepsilon} t, \quad \varepsilon > 0. \quad (7.15)$$

which describes both the non-canonical scaling of time for DT, i.e. $\varepsilon = 1/2$ as well as the canonical scaling of time for CDT, i.e. $\varepsilon = 1$. Below we show that by allowing

the branching into baby universes to contribute in the continuum limit one is led to a non-canonical scaling of time as for DT.

Inserting the scaling relations (7.6), (7.14) and (7.15) into the combinatorial identity (7.11) we obtain

$$\begin{aligned} \frac{\partial W_{ns}}{\partial g} - 2a^{\eta-2} \frac{\partial W_\Lambda(X)}{\partial \Lambda} = \\ \frac{1}{a^\varepsilon} \int dT \int dZ G_\Lambda(X, -Z; T) \left[\frac{\partial W_{ns}}{\partial z} - a^{\eta-1} \frac{1}{z_c} \frac{\partial W_\Lambda(Z)}{\partial Z} \right], \end{aligned} \quad (7.16)$$

where we have $(x, g) = (x_c, g_c)$ in the non-singular part.

From the last equation and the requirement that $\varepsilon > 0$ it follows that there are only two consistent choices for η :

- *Scaling 1: $\eta < 0$*

In this range the non-scaling part does not survive the continuum limit and Eq. (7.16) becomes

$$a^{\eta-2} \frac{\partial W_\Lambda(X)}{\partial \Lambda} = \frac{a^{\eta-1}}{2a^\varepsilon} \int dT \int dZ G_\Lambda(X, -Z; T) \frac{1}{z_c} \frac{\partial W_\Lambda(Z)}{\partial Z}. \quad (7.17)$$

Hence, we conclude that $\varepsilon = 1$ as in the case of CDT. We observe that whenever the non-scaling part of the disc function is not present in the continuum result time must scale canonically.

- *Scaling 2: $1 < \eta < 2$*

In this range Eq. (7.16) splits into two equations

$$-a^{\eta-2} \frac{\partial W_\Lambda(X)}{\partial \Lambda} = \frac{1}{2a^\varepsilon} \frac{\partial W_{ns}}{\partial z} \Big|_{z=x_c} \int dT \int dZ G_\Lambda(X, -Z; T), \quad (7.18)$$

and

$$\frac{\partial W_{ns}}{\partial g} \Big|_{g=g_c} = -\frac{a^{\eta-1}}{a^\varepsilon} \int dT \int dZ G_\Lambda(X, -Z; T) \frac{1}{z_c} \frac{\partial W_\Lambda(Z)}{\partial Z}. \quad (7.19)$$

From the first equation we see that $a^{\eta-2} = 1/a^\varepsilon$ while from the second equation we have $a^{\eta-1}/a^\varepsilon = 1$. Combining these requirements we get $\varepsilon = 1/2$ and $\eta = 3/2$ which precisely correspond to the scaling relations of DT, i.e (5.46) and (5.27). Further, we observe that using $\varepsilon = 1/2$ and $\eta = 3/2$ Eq. (7.18) reads

$$-\frac{\partial W_\Lambda(X)}{\partial \Lambda} \sim \int_0^\infty dT G_\Lambda(X, L_2 = 0, T). \quad (7.20)$$

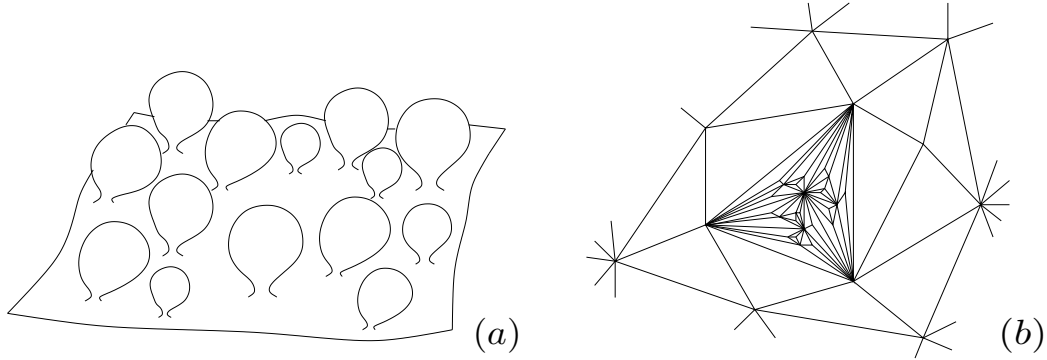


Figure 7.4: (a) At every point in the quantum geometry there is an infinitesimal baby universe. (b) When trying to draw the baby universes on a plane one is forced to draw smaller and smaller triangles reflecting the fractal structure of the geometry.

which is nothing but the relation between the disc function and the propagator as obtained in DT, i.e. (5.55). In addition for $\varepsilon = 1/2$ and $\eta = 3/2$ Eq. (7.19) becomes

$$\int dT \int dZ G_\Lambda(X, -Z; T) \frac{\partial W_\Lambda(Z)}{\partial Z} = \text{const}, \quad (7.21)$$

where the constant is related to the non-scaling part of the disc function and does not play any role in the continuum theory.

The relation (7.20) has an interesting interpretation in terms of baby universes, namely, it shows that at any mark in the bulk there is a baby universe whose boundary is of length of the cut-off. Further, since the mark can be anywhere, we conclude that *near every point of the quantum geometry there is a baby universe with cut-off size boundary*. This situation is illustrated in Fig. 7.4 (a). Mapping the picture into the plane, as shown in Fig. 7.4 (b), clearly visualizes the fractal structure of the quantum geometry. Another indication for the importance of geometries with infinitesimal boundaries comes from the Laplace transform of (7.21), i.e.

$$\int dT \int dL G_\Lambda(L, L'; T) L' W_\Lambda(L') \sim \delta(L). \quad (7.22)$$

Essentially, this equation shows that the distribution of geometries is peaked around universes that have infinitesimal boundary length.

Using the above scaling relations one can now analyze the scaling limit of (7.5) to obtain a differential equation for the dressed propagator. In order for the scaling limit of the equation to exist, the critical values x_c , g_c and w_{ns} must satisfy two relations which can be straightforwardly determined from (7.5). The remaining continuum differential equation reads

$$a^\varepsilon \frac{\partial}{\partial T} G_\Lambda(X, Y; T) = -a \frac{\partial}{\partial X} \left[(X^2 - \Lambda) G_\Lambda(X, Y; T) \right] - 2a^{\eta-1} \frac{\partial}{\partial X} \left[W_\Lambda(X) G_\Lambda(X, Y; T) \right]. \quad (7.23)$$

The first term on the right-hand-side of (7.23) is related to the bare CDT model, while the second term corresponds to the creation of baby universes as is also present in DT. In particular, we saw in the previous chapter that the first term was related to the effective quantum Hamiltonian of CDT and hence represents the kinetic term of the more general model (7.23).

In the case where $\eta \leq 0$ (more precisely $\eta \leq 1$) the last term in (7.23) diverges. This reflects the fact that the bare model is incompatible with spatial topology changes. However, dropping the divergent term, i.e. excluding spatial topology changes we have already seen that for $\eta \leq 0$ we need to have that $\varepsilon = 1$ leaving us with the continuum differential equation for the propagator of the bare CDT model, i.e. (6.41), as a *unique* solution

$$\frac{\partial}{\partial T} G_\Lambda(X, Y; T) = -\frac{\partial}{\partial X} \left[(X^2 - \Lambda) G_\Lambda(X, Y; T) \right]. \quad (7.24)$$

For the second possible scaling, where $1 < \eta < 2$, the last term on the right-hand-side of (7.23) will dominate over the first while still being compatible with the time derivative term. Hence, the kinetic term of the model does *not* survive the continuum limit and *the dynamics is entirely governed by the off-splitting baby universes*, or as Ambjørn and Loll express it, *once we allow for the creation of baby universes, this process will completely dominate the continuum limit*. We have seen above that the only scaling consistent with $1 < \eta < 2$ is $(\eta, \varepsilon) = (3/2, 1/2)$. Inserting the corresponding scaling relation into (7.23) we obtain the following differential equation

$$\frac{\partial}{\partial T} G_\Lambda(X, Y; T) = -2 \frac{\partial}{\partial X} \left[W_\Lambda(X) G_\Lambda(X, Y; T) \right]. \quad (7.25)$$

This is precisely of the form of the differential equation (5.47) for the propagator of DT. However, at this stage $W_\Lambda(X)$ and with that $G_\Lambda(X, Y; T)$ are still undetermined. In the following we want to show how this equation combined with Eq. (7.20), completely

determines the continuum disc function $W_\Lambda(X)$ to be that of DT. Integrating (7.25) with respect to T and using the initial condition

$$G_\Lambda(X, Y; T=0) = \frac{1}{X+Y} \quad (7.26)$$

i.e. in Laplace transform language

$$G_\Lambda(X, L_2=0; T=0) = 1, \quad (7.27)$$

we obtain

$$-1 = \frac{\partial}{\partial X} \left[W_\Lambda(X) \frac{\partial}{\partial \Lambda} W_\Lambda(X) \right]. \quad (7.28)$$

From dimensional analysis one can easily see that $W_\Lambda(X)$ must have mass dimension $-3/2$ and hence can be written as $W_\Lambda^2(X) = X^3 F(\sqrt{\Lambda}/X)$. This condition implies the following general form for the solution of the disc function

$$W_\Lambda(X) = \sqrt{-2\Lambda X + b^2 X^3 + c^2 \Lambda^{3/2}}. \quad (7.29)$$

We can further fix one of the two constants by noting that $W_\Lambda(X)$ is not allowed to have any singularities or cuts for $\Re(X) > 0$. This requirement is essentially the same as saying that the inverse Laplace transform of (7.29), i.e. $W_\Lambda(L)$, should be bounded for $L \rightarrow \infty$. This completely fixes the analytic structure of the disc function, yielding

$$W_\Lambda(X) = b \left(X - \frac{\sqrt{2}}{b\sqrt{3}} \sqrt{\Lambda} \right) \sqrt{X + \frac{2\sqrt{2}}{b\sqrt{3}} \sqrt{\Lambda}}. \quad (7.30)$$

Upon rescaling of the boundary and bulk cosmological constants we can absorb the constant b and obtain the disc function of DT, i.e. (5.28),

$$W_\Lambda(X) = \left(X - \frac{1}{2} \sqrt{\Lambda} \right) \sqrt{X + \sqrt{\Lambda}}. \quad (7.31)$$

7.2 | Integrating out baby universes: From DT to CDT

In the previous section we showed how to obtain DT from CDT by introducing spatial topology changes, i.e. by allowing baby universes to appear. In the following we want to show the opposite, namely how to obtain CDT from DT by “integrating out” the baby universes [125]. Since the baby universes completely dominate the continuum dynamics of DT such a relationship has to be established on the discrete level.

We remind the reader of the following differential equation for the discrete fixed geodesic distance two-loop function in DT, i.e. (5.41), which we obtained from the peeling procedure,

$$\frac{\partial}{\partial t} G^{(eu)}(z, w; g; t) = -2 \frac{\partial}{\partial z} [f^{(eu)}(g, z) G^{(eu)}(z, w; g; t)], \quad (7.32)$$

where we defined

$$f^{(eu)}(g, z) = -\frac{1}{2}(z - gz^2) + w^{(eu)}(g, z). \quad (7.33)$$

The initial condition of this differential equation was given in (5.36), i.e.

$$G(z, w; g; 0) = \frac{1}{zw} \frac{1}{zw - 1}. \quad (7.34)$$

Here the first term in (7.33) corresponded to the first decomposition move, e.g. removing a triangle, while the second term corresponded to the second move, where a double link was removed and a baby universe (disc function) splits off. A first idea for integrating out the baby universes would therefore be to drop the second term in (7.33). However, as we are using unrestricted triangulations (recall Fig. (5.3) (b)) also double links are present. Hence, there could still be off-splitting branched polymers which correspond to zero volume disc functions, i.e. (5.14),

$$w^{(bp)}(z) \equiv w^{(eu)}(g=0, z) = \frac{1}{2} \left(z - \sqrt{z^2 - 4} \right). \quad (7.35)$$

Thus we integrate out the (non-zero volume) baby universes by simply replacing the term $w^{(eu)}(g, z)$ in (7.33) by $w^{(bp)}(z)$, yielding

$$\frac{\partial}{\partial t} G(z, w; g; t) = -2 \frac{\partial}{\partial z} [f(g, z) G(z, w; g; t)], \quad (7.36)$$

with

$$f(g, z) = -\frac{1}{2}(z - gz^2) + w^{(bp)}(z), \quad (7.37)$$

subject to the same initial conditions (7.34). Fig. 7.5 illustrates the peeling equation (7.36).

We now want to show how to obtain the continuum CDT propagator by taking a suitable continuum limit of (7.36). It is natural to use the standard scaling relations for the boundary and bulk cosmological constants which were applicable for both DT and CDT,

$$g = g_c e^{-a^2 \Lambda}, \quad z = z_c e^{aZ}, \quad w = z_c e^{aW}, \quad (7.38)$$

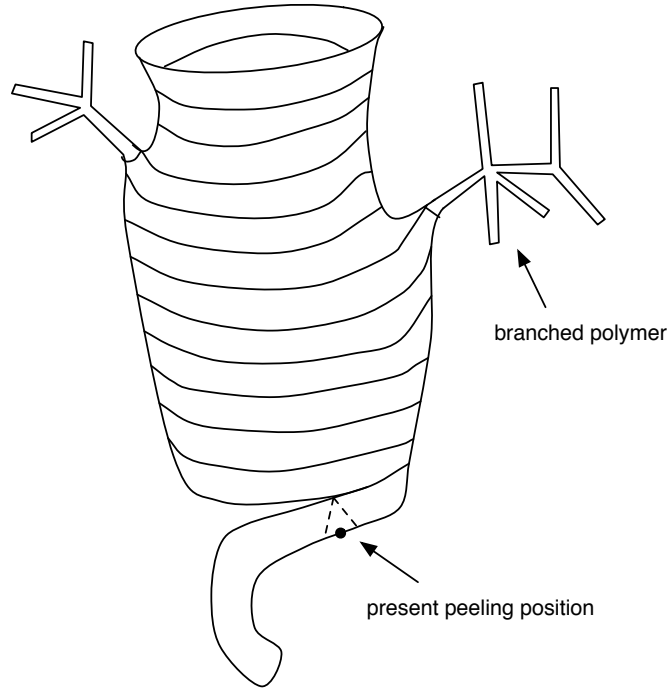


Figure 7.5: Illustration of the peeling relation (7.36). In each step of the decomposition either a triangle is removed or a double link which results into an off-splitting of a branched polymer.

As before the demanded continuum initial condition

$$G_\Lambda(Z, W; T=0) = \frac{1}{Z + W}, \quad (7.39)$$

already fixed the wave function renormalization of the propagator, i.e.

$$G_\Lambda(Z, W; T) = aG(z, w; g; t). \quad (7.40)$$

Further, we note that to obtain a non-trivial continuum dynamics we demand that $f(g, z) \sim \mathcal{O}(a^2)$. This requirement completely fixed the scaling relations: Firstly, from $f(g, z) \sim \mathcal{O}(a^2)$ and the scaling relations (7.38) it follows that

$$T \sim at \quad (7.41)$$

as it is the case for CDT. Secondly, the requirement that the order one and order a part of $f(g, z)$ should vanish determines

$$g_c = \frac{1}{4}, \quad z_c = 1. \quad (7.42)$$

Inserting the complete scaling relations into (7.36) yields (under rescaling of the couplings)

$$\frac{\partial}{\partial T} G_\Lambda(Z, W, T) = -\frac{\partial}{\partial Z} [(Z^2 - \Lambda)G_\Lambda(Z, W, T)] \quad (7.43)$$

with the above initial conditions. This differential equation precisely coincides with the differential equation for the propagator of CDT, i.e. (6.41). Hence we showed how to obtain CDT from DT by integrating out baby universes.

7.3 | The renormalization relation

As an interesting relation between DT and CDT, it was shown in [125] that it is possible to “renormalize” the couplings and time of DT in such a way that the differential equation for the DT propagator is matched to the one of the CDT propagator. This “renormalization” relation can be established both in the discrete as well as in the continuum [125]. We will in the following only derive the continuum relation.

Let us for the remainder of this chapter label all Euclidean quantities with a tilde. The differential equation for the Euclidean propagator thus reads,

$$\frac{\partial}{\partial \tilde{T}} \tilde{G}_\Lambda(\tilde{X}, \tilde{Y}; \tilde{T}) = -2\frac{\partial}{\partial \tilde{X}} [\tilde{W}_\Lambda(\tilde{X})\tilde{G}_\Lambda(\tilde{X}, \tilde{Y}; \tilde{T})], \quad (7.44)$$

where

$$\tilde{W}_\Lambda(\tilde{X}) = (\tilde{X} - \frac{1}{2}\sqrt{\tilde{\Lambda}})\sqrt{\tilde{X} + \sqrt{\tilde{\Lambda}}} \quad (7.45)$$

was the Euclidean disc function. The corresponding equation in the framework of CDT reads

$$\frac{\partial}{\partial T} G_\Lambda(X, Y; T) = -\frac{\partial}{\partial X} [\hat{W}_\Lambda(X)G_\Lambda(X, Y; T)] \quad (7.46)$$

with

$$\hat{W}_\Lambda(X) = X^2 - \Lambda. \quad (7.47)$$

Here the hat (not to be confused with the tilde) should remind ourselves that $\hat{W}_\Lambda(X)$ is not the disc function of CDT but rather related to the effective quantum Hamiltonian of the system.

To relate (7.44) and (7.46) we make the following ansatz for the renormalization relations of the couplings and time

$$\tilde{X} = \tilde{X}(X, \Lambda), \quad \tilde{T} = b\Lambda^{1/4} T, \quad \tilde{\Lambda} = \tilde{\Lambda}(\Lambda), \quad (7.48)$$

where b is a constant and the factor of $\Lambda^{1/4}$ in front of the T has been chosen for dimensional reasons. To map the differential equation (7.44) for DT into the differential equation (7.46) for CDT using the relations (7.48), we must have the following wave function renormalizations

$$G_\Lambda(X, Y; T) = \left(\frac{\partial X}{\partial \tilde{X}} \right)^{-1} \tilde{G}_{\tilde{\Lambda}(\Lambda)}(\tilde{X}(X, \Lambda), \tilde{Y}(Y, \Lambda); b \Lambda^{1/4} T) \quad (7.49)$$

and

$$\hat{W}_\Lambda(X) = 2 b \Lambda^{1/4} \left(\frac{\partial X}{\partial \tilde{X}} \right) \tilde{W}_{\tilde{\Lambda}(\Lambda)}(\tilde{X}(X, \Lambda)). \quad (7.50)$$

Integrating the second relation gives

$$2 b \Lambda^{1/4} \int \frac{dX}{\hat{W}_\Lambda(X)} = \int \frac{\tilde{X}}{\tilde{W}_{\tilde{\Lambda}}(\tilde{X})} + k. \quad (7.51)$$

Since we require that $\tilde{X} \rightarrow \infty$ should imply $X \rightarrow \infty$ the integration constant must be $k = 0$. Inserting (7.45) and (7.47) into (7.51) with $k = 0$ and performing the integrals gives

$$\frac{b}{\sqrt[4]{\Lambda}} \log \left(\frac{X + \sqrt{\Lambda}}{X - \sqrt{\Lambda}} \right) = \sqrt{\frac{2}{3}} \frac{1}{\sqrt[4]{\tilde{\Lambda}}} \log \left(\frac{\sqrt{\frac{2}{3}} \tilde{\Lambda}^{1/4} \sqrt{\tilde{X} + \sqrt{\tilde{\Lambda}} + \sqrt{\tilde{\Lambda}}}}{\sqrt{\frac{2}{3}} \tilde{\Lambda}^{1/4} \sqrt{\tilde{X} + \sqrt{\tilde{\Lambda}} - \sqrt{\tilde{\Lambda}}}} \right) \quad (7.52)$$

To further simplify this expression we perform a rescaling of both X and $\sqrt{\Lambda}$ to choose

$$\sqrt{\Lambda} = \frac{3}{2} b^2 \sqrt{\tilde{\Lambda}}. \quad (7.53)$$

Using this relation (7.53) becomes

$$\frac{X}{\sqrt{\Lambda}} = \sqrt{\frac{2}{3}} \frac{\sqrt{\tilde{X} + \sqrt{\tilde{\Lambda}}}}{\tilde{\Lambda}^{1/4}}. \quad (7.54)$$

Together with

$$T = \frac{\tilde{T}}{b \Lambda^{1/4}} \quad (7.55)$$

these equations determine the whole set of renormalization relations.

These renormalization relations map the differential equation of the DT propagator (7.44) to the corresponding differential equation of the CDT propagator (7.46). Further, it shows that the process of “integrating out” baby universes which we discussed in the

previous section can be understood as a renormalization of the cosmological constants and the time variable combined with a dressing of the propagator.

It is interesting to notice that the relation (7.54) is similar to one encountered in regularized bosonic string theory in dimensions $d \geq 2$ [160, 85, 161], where the world sheet degenerates into so-called branches polymer. The two-point function of these branched polymers is related to the ordinary two-point function of the free relativistic particle by chopping off (i.e. integrating out) the branches, just leaving for each branched polymer connecting two points in target space one *path* connecting the two points. The mass-parameter of the particle is then related to the corresponding parameter in the partition function for the branched polymers as $X/\sqrt{\Lambda}$ to $\tilde{X}/\sqrt{\tilde{\Lambda}}$ in (7.54).

7.4 | Discussion and outlook

In this chapter we explained several relations between two-dimensional Euclidean quantum gravity defined through DT and two-dimensional Lorentzian quantum gravity defined through CDT.

It was shown that when introducing spatial topology changes into the framework of CDT one arrives at a continuum differential equation for the gravitational propagator which only allows for two possible scalings. In the first scaling time scales canonically and spatial topology changes, i.e. off-splitting baby universes are forbidden. This scaling leads back to the ‘bare’ model of CDT without spatial topology changes as described in the previous chapter. However, in the second scaling where time scales non-canonical spatial topology changes are possible and the model naturally leads to DT. Further, we observed how in this scaling the baby universes completely dominate the continuum limit, explaining the fractal structure of two-dimensional Euclidean quantum gravity.

In the Sec. 7.2 of this chapter we showed the opposite relation, namely, when integrating out the baby universes in DT one recovers CDT. This was done by introducing a new peeling equation similar to the one used to calculate the fixed geodesic distance two-loop function in Sec. 5.3.2, where outgrowing baby universes are replaced by branched polymers, i.e. zero-volume baby universes.

In the last section of this chapter we showed how the process of ‘‘integrating out’’ baby universes could be understood as a renormalization of the cosmological constants and the time variable combined with a dressing of the propagator.

In summary, we showed many relations between CDT and DT by respectively introducing or “integrating out” baby universes. An unsatisfactory situation at this point is that we were in a sense not able to “regularize” the spatial topology changes. Either baby universes are absent as in CDT or the average number of baby universes is infinite as in DT which completely dominates the continuum dynamics. In Chap. 9 we show how one can naturally introduce a coupling which regulates spatial topology changes, leading to a finite number of baby universes in the continuum. Further, this formulation lead to the discovery of many other relations between CDT and DT within the framework of matrix models as will be discussed in Part IV.

The emergence of background geometry in two dimensions

In the previous chapters we studied both Euclidean as well as causal dynamical triangulations with compact geometries. In particular, we saw that the quantum geometry in both cases does not possess a semiclassical background, but is rather dominated entirely by quantum fluctuations. In this chapter we show how this situation changes when one studies the case of non-compact space-times. Before moving to our prime interest of non-compact space-times in CDT [129, 162] let us first review some results of the Euclidean model [163].

8.1 | Two-dimensional Euclidean quantum gravity with non-compact space-time

In this thesis we have so far only considered two-dimensional Euclidean and Lorentzian quantum gravity with compact space-time. The study of two-dimensional Euclidean quantum gravity with non-compact space-time was initiated by the Zamolodchikovs (ZZ) in the context of Liouville theory [164]. In particular, they showed how to use conformal bootstrap and the cluster-decomposition properties to quantize Liouville theory on the pseudo-sphere, i.e. the Poincaré disk.

It was later shown by Martinec [75] and Seiberg et al. [165, 166] how the work of the Zamolodchikovs fitted into the framework of non-critical string theory, where the ZZ-theory could be reinterpreted as special branes, now called ZZ-branes. Particularly, they found that the ZZ-brane of two-dimensional Euclidean gravity was associated with the zero of the disc function,

$$W_{\Lambda}^{(eu)}(X) = \left(X - \frac{1}{2}\sqrt{\Lambda}\right)\sqrt{X + \sqrt{\Lambda}}. \quad (8.1)$$

In [163, 167, 168] it was shown how this could be understood in terms of worldsheet geometry, i.e. from a two-dimensional quantum gravity point of view. Let us briefly describe the main idea. We can use the fixed geodesic distance two-loop function, i.e. (5.48), to compute the average length of the final boundary,

$$\langle L(T) \rangle_{X,Y,T} = -\frac{1}{G_{\Lambda}(X, Y; T)} \frac{\partial G_{\Lambda}(X, Y; T)}{\partial Y} = \frac{1}{\bar{X}(T, X) + Y}. \quad (8.2)$$

Further, we see from this that the average length of the boundary of a disc with a marked point in the bulk at geodesic distance T to the boundary is given by

$$\langle L(T) \rangle_{Y,T} = \frac{1}{\bar{X}(T) + Y} \quad (8.3)$$

with $\bar{X}(T) \equiv \bar{X}(T, X = \infty)$. Viewing $\bar{X}(T)$ as a “running” boundary cosmological constant with scale T , we see that both geodesic distance and boundary length diverge simultaneously if we choose $Y = -\bar{X}(\infty) = -\sqrt{\Lambda}/2$ which was precisely determined by $0 = W_{\Lambda}(\bar{X}(\infty))$ (recall Eq. (5.49)). Hence, the geodesic distance from a generic point on the disk to the boundary diverges and in this way effectively creates a non-compact space-time.

In this chapter we show that the same phenomenon occurs in the framework of two-dimensional Lorentzian quantum gravity defined by CDT.

8.2 | The emergence of background geometry

Recall from Sec. 6.4 that the propagator of CDT is given by

$$G_{\Lambda}(X, Y; T) = \frac{\bar{X}^2(T, X) - \Lambda}{X^2 - \Lambda} \frac{1}{\bar{X}(T, X) + Y}, \quad (8.4)$$

where $\bar{X}(T, X)$ is the solution of the characteristic equation

$$\frac{d\bar{X}}{dT} = -(\bar{X}^2 - \Lambda), \quad \bar{X}(0, X) = X. \quad (8.5)$$

The explicit solution to this equation was given by (6.46) which can be rewritten as

$$\bar{X}(t, X) = \sqrt{\Lambda} \coth \sqrt{\Lambda}(t + t_0), \quad X = \sqrt{\Lambda} \coth \sqrt{\Lambda} t_0. \quad (8.6)$$

As described above we can view $\bar{X}(T)$ as a “running” boundary cosmological constant, with T being the scale. For $X > -\sqrt{\Lambda}$ we have $\bar{X}(T) \rightarrow \sqrt{\Lambda}$ for $T \rightarrow \infty$, i.e. $\sqrt{\Lambda}$ can be seen as a “fixed point”, or in other words a zero of the “ β -function” $-(\bar{X}^2 - \Lambda)$ in Eq. (8.5).¹

Using the semi-group property of the marked propagator

$$G_\Lambda(X, Y; T_1 + T_2) = \int_0^\infty dL G_\Lambda(X, L; T_1) G(L, Y, T_2). \quad (8.7)$$

we can now calculate the expectation value of the length of the spatial slice at intermediate proper time $t \in [0, T]$:

$$\langle L(t) \rangle_{X, Y, T} = \frac{1}{G_\Lambda(X, Y; T)} \int_0^\infty dL G_\Lambda(X, L; t) L G_\Lambda(L, Y; T - t). \quad (8.8)$$

Since the classical action is trivial, there is no reason to expect $\langle L(t) \rangle$ to have a classical limit. We have already seen in Sec. 6.5 and Sec. 6.6 that for a generic situation the system is purely governed by quantum fluctuations. Except for boundary effects these quantum fluctuations are determined by the ground state of the effective quantum Hamiltonian \hat{H}_X as introduced in Sec. 6.5. More precisely, an explicit calculation using (8.8) shows that in the situation where X and Y are larger than $\sqrt{\Lambda}$ and where $T \gg 1/\sqrt{\Lambda}$ the system has forgotten everything about the boundaries and the expectation value of $L(t)$ is, up to corrections of order $e^{-2\sqrt{\Lambda}t}$ or $e^{-2\sqrt{\Lambda}(T-t)}$, determined by the ground state of the effective Hamiltonian \hat{H}_X .

We will now study the situation where a non-compact space-time is obtained as a limit of the compact space-time in the same manner as described in the previous subsection for the case of DT. Hence we want to take $T \rightarrow \infty$ and at the same time also take the length of the outer boundary at time T to infinity. Following the same reasoning as above, we see that the only choice of the boundary cosmological constant

¹Note that here $\hat{W}_\Lambda = \bar{X}^2 - \Lambda$ is not the disc function of CDT, as it was for the analogous term in DT.

Y independent of T where the length $\langle L(T) \rangle_{X,Y,T}$ goes to infinity for $T \rightarrow \infty$ is the “fixed point” $Y = -\sqrt{\Lambda}$, since

$$\langle L(T) \rangle_{X,Y,T} = -\frac{1}{G_\Lambda(X, Y; T)} \frac{\partial G_\Lambda(X, Y; T)}{\partial Y} = \frac{1}{\bar{X}(T, X) + Y} \quad (8.9)$$

which differs from the analogous DT expression, i.e. (8.2), only in the definition of $\bar{X}(T, X)$.

Inserting $Y = -\sqrt{\Lambda}$ into (8.8) one obtains in the limit $T \rightarrow \infty$:

$$\langle L(t) \rangle_X = \frac{1}{\sqrt{\Lambda}} \sinh(2\sqrt{\Lambda}(t + t_0(X))), \quad (8.10)$$

where $t_0(X)$ is inversely defined through Eq. (8.6).

At this point we want to remind the reader that starting from a lattice regularization and taking the continuum limit the length L is only determined up to a constant of proportionality which should be fixed by comparing with a continuum effective action. In Sec. 6.5 we made such a comparison with a continuum calculation by Nakayama and concluded that L has to be identified with L_{cont}/π . We thus have

$$L_{cont}(t) \equiv \pi \langle L(t) \rangle_X = \frac{\pi}{\sqrt{\Lambda}} \sinh(2\sqrt{\Lambda}(t + t_0(X))). \quad (8.11)$$

We now consider the line element of the classical surface where the intrinsic geometry is defined by proper time t and spatial length $L_{cont}(t)$ at constant t

$$ds^2 = dt^2 + \frac{L_{cont}^2}{4\pi^2} d\theta^2 = dt^2 + \frac{\sinh^2(2\sqrt{\Lambda}(t + t_0(X)))}{4\Lambda} d\theta^2. \quad (8.12)$$

Here $t \geq 0$ and $t_0(X)$ is a function of the boundary cosmological constant X at the boundary corresponding to $t=0$ (see (8.6)). A remarkable observation about Eq. (8.12) is that the surfaces for different boundary cosmological constants X can be viewed as sections of the same surface, namely the Poincaré disk with curvature $R = -8\Lambda$, since t can be continued to $t = -t_0$. The whole Poincaré disk is then obtained in the limit $X \rightarrow \infty$, where the initial boundary is shrunken to a point and $t_0 = 0$.

8.3 | The classical effective action

Even though the classical action of our theory is trivial, we discussed in Sec. 6.5 that the effective quantum Hamiltonian of CDT can be derived from the following classical

effective action

$$S_\kappa = \int_0^T dt \left(\frac{(l(t))^2}{4l(t)} + \Lambda l(t) + \frac{\kappa}{l} \right). \quad (8.13)$$

With respect to this it is interesting to see in how far the results of this chapter relate to the classical solutions of this effective action. Solving the equations of motion of (8.13) gives

$$l(t) = \frac{\sqrt{\kappa}}{\sqrt{\Lambda}} \sinh 2\sqrt{\Lambda}t, \quad \kappa > 0 \text{ elliptic case}, \quad (8.14)$$

$$l(t) = \frac{\sqrt{-\kappa}}{\sqrt{\Lambda}} \cosh 2\sqrt{\Lambda}t, \quad \kappa < 0 \text{ hyperbolic case}, \quad (8.15)$$

$$l(t) = e^{2\sqrt{\Lambda}t}, \quad \kappa = 0 \text{ parabolic case}. \quad (8.16)$$

One observes that all solutions correspond to cylinders with constant negative curvature -8Λ . In the elliptic case, there is a conical singularity at $t = 0$ unless $\kappa = 1$ for which the geometry is regular at $t = 0$ and corresponds precisely to the Poincaré disc as described by (8.12). However, $\kappa = 1$ is exactly the value for which Nakayama's Hamiltonian corresponds to the effective quantum Hamiltonian of CDT. Concluding, we see that upon the required identification $L_{cont}(t) = \pi l(t)$ the classical solution of Nakayama's effective action coincides with (8.11).

8.4 | Quantum fluctuations

In the considerations above we fixed the outer boundary cosmological constant to a specific value, namely the “fixed point” of the running boundary cosmological constant, rather than fixing the outer length of the boundary to a specific value. Since the boundary length and the boundary cosmological constant are conjugate variables, one pays the price that the fluctuations of the boundary size are large. In particular, it can be checked from (8.9) that the fluctuations are of order of the average length of the boundary itself, as was also true for the compact case

$$\langle L^2(T) \rangle_{X,Y;T} - \langle L(T) \rangle_{X,Y;T}^2 = -\frac{\partial \langle L(T) \rangle_{X,Y;T}}{\partial Y} = \langle L(T) \rangle_{X,Y;T}. \quad (8.17)$$

The same relation also holds for DT as was shown by Ambjørn et al. [163]. These large fluctuations are not only present at the outer boundary as described by (8.17), but also at $t < T$. From this point of view it is even more remarkable that the emergent semiclassical background has such a nice interpretation in terms of the Poincaré disc.

In the following we want to analyze the situation, where we by hand fix the boundary lengths L_1 and L_2 instead of the boundary cosmological constants. This is done in the Hartle-Hawking Euclidean path integral when the geometries $[g]$ are fixed at the boundaries [72]. Recall from the previous chapters that the boundary geometry is complete specified by its length and that amplitudes with fixed boundary cosmological constants can be related to amplitudes with fixed boundary lengths by a Laplace transformation. Let us in the following analyze the temporal correlations between two spatial slices at intermediate times t and $t + \Delta$ with $0 < t \leq t + \Delta < T$. For simplicity we only consider the situation where the entrance loop is shrunken to a point, i.e. $L_1 = 0$. The temporal correlations are determined by the so-called connected loop-loop correlator

$$\langle L(t)L(t+\Delta) \rangle_{L_2, T}^{(c)} \equiv \langle L(t+\Delta)L(t) \rangle_{L_2, T} - \langle L(t) \rangle \langle L(t+\Delta) \rangle_{L_2, T}. \quad (8.18)$$

Using the semi-group property (8.7) and the length version of the propagator (8.4) one obtains

$$\begin{aligned} \langle L(t)L(t+\Delta) \rangle_{L_2, T}^{(c)} &= \frac{2 \sinh^2 \sqrt{\Lambda} t \sinh^2 \sqrt{\Lambda} (T - (t + \Delta))}{\Lambda \sinh^2 \sqrt{\Lambda} T} + \\ &\frac{2L_2 \sinh^2 \sqrt{\Lambda} t \sinh \sqrt{\Lambda} (t + \Delta) \sinh \sqrt{\Lambda} (T - (t + \Delta))}{\sqrt{\Lambda} \sinh^3 \sqrt{\Lambda} T}. \end{aligned} \quad (8.19)$$

In comparison the average length is given by

$$\langle L(t) \rangle_{L_2, T} = \frac{2 \sinh \sqrt{\Lambda} t \sinh \sqrt{\Lambda} (T - t)}{\sqrt{\Lambda} \sinh \sqrt{\Lambda} T} + L_2 \frac{\sinh^2 \sqrt{\Lambda} t}{\sinh^2 \sqrt{\Lambda} T}. \quad (8.20)$$

For fixed L_2 and $T \rightarrow \infty$, i.e. in the situation of compact geometries, we obtain

$$\langle L(t)L(t+\Delta) \rangle_{L_2}^{(c)} = \frac{1}{2\Lambda} e^{-2\sqrt{\Lambda}\Delta} \left(1 - e^{-2\sqrt{\Lambda}t}\right)^2 \quad (8.21)$$

and

$$\langle L(t) \rangle_{L_2} = \frac{1}{\sqrt{\Lambda}} \left(1 - e^{-2\sqrt{\Lambda}t}\right). \quad (8.22)$$

These equations precisely agree with the picture presented above, namely that except for small t , where we are close to the initial boundary we have $\langle L(t) \rangle_{L_2} = 1/\sqrt{\Lambda}$, i.e. the dynamics is determined by the ground state of the effective quantum Hamiltonian. Further, the quantum fluctuations are

$$(\Delta L(t))^2 = \langle L(t)L(t) \rangle^{(c)} \equiv \langle L^2(t) \rangle - \langle L(t) \rangle^2 \sim \langle L(t) \rangle^2 \sim \frac{1}{\sqrt{\Lambda}}. \quad (8.23)$$

Thus the quantum geometry is entirely governed by quantum fluctuations as is illustrated in Fig. 6.2. The time correlation between two slices $L(t)$ and $L(t + \Delta)$ is also dictated by the same scale $1/\sqrt{\Lambda}$. Particularly, we observe that temporal correlations between “elementary” spatial elements of size $1/\sqrt{\Lambda}$, separated in time by Δ fall off exponentially as $e^{-2\sqrt{\Lambda}\Delta}$. This is precisely what one would expect from the two-dimensional Einstein-Hilbert action with boundary terms, i.e.

$$S[g] = \Lambda \int \int dxdt \sqrt{g(x, t)} + X \oint dl_1 + Y \oint dl_2. \quad (8.24)$$

If we force T to be large and choose a generic Y at which $\langle L_2(T) \rangle$ is not large, the quantum geometry will look like a thin tube which except close to the boundaries is “classically” of zero spatial extension, but due to quantum fluctuations has average spatial length $1/\sqrt{\Lambda}$.

Let us now repeat the above analysis for the case of non-compact geometries. Recall that only when the boundary cosmological constant was chosen to $Y = -\sqrt{\Lambda}$ one obtains a non-compact geometry in the limit $T \rightarrow \infty$. To implement this “critical value” of Y in a situation where L_2 is fixed instead of Y we fix $L_2(T)$ to the average value (8.9) for $Y = -\sqrt{\Lambda}$, i.e.

$$L_2(T) = \langle L(T) \rangle_{X, Y = -\sqrt{\Lambda}; T} = \frac{1}{\sqrt{\Lambda}} \frac{1}{\coth \sqrt{\Lambda} T - 1}. \quad (8.25)$$

From (8.19) and (8.20) one obtains in the limit $T \rightarrow \infty$ the following expression for the average length at intermediate time t

$$\langle L(t) \rangle = \frac{1}{\sqrt{\Lambda}} \sinh 2\sqrt{\Lambda} t \quad (8.26)$$

which agrees with (8.10) as expected. Further, the loop-loop correlator equates to

$$\langle L(t + \Delta)L(t) \rangle^{(c)} = \frac{2}{\Lambda} \sinh^2 \sqrt{\Lambda} t = \frac{1}{\sqrt{\Lambda}} \left(\langle L(t) \rangle - \frac{1}{\sqrt{\Lambda}} (1 - e^{-2\sqrt{\Lambda} t}) \right). \quad (8.27)$$

In contrast to the analogue expression for compact geometries, one observes that (8.27) is independent of Δ . In particular, using $\Delta = 0$ we see that the quantum fluctuations for $t \gg 1/\sqrt{\Lambda}$ are given by

$$(\Delta L(t))^2 \equiv \langle L^2(t) \rangle - \langle L(t) \rangle^2 \sim \frac{1}{\sqrt{\Lambda}} \langle L(t) \rangle. \quad (8.28)$$

As in the case of compact geometries we can give an interpretation of (8.28) in terms of correlations between “elementary” spatial elements of size $1/\sqrt{\Lambda}$. More precisely, we can view the curve of length $L(t)$ as consisting of $N(t) \approx \sqrt{\Lambda}L(t) \approx e^{2\sqrt{\Lambda}t}$ independently fluctuating “elementary” spatial elements of size $1/\sqrt{\Lambda}$, each with a fluctuation of size $1/\sqrt{\Lambda}$, i.e. each corresponding to a section of compact geometry. Thus the fluctuation $\Delta L(t)$ of the total spatial slice $L(t)$ are of order $\sqrt{N(t)}/\sqrt{\Lambda}$, i.e.

$$\frac{\Delta L(t)}{\langle L(t) \rangle} \sim \frac{1}{\sqrt{\sqrt{\Lambda} \langle L(t) \rangle}} \sim e^{-\sqrt{\Lambda}t}. \quad (8.29)$$

Thus the fluctuations of $L(t)$ around $\langle L(t) \rangle$ are small for $t \gg 1/\sqrt{\Lambda}$. In the same way we can understand the independence of the loop-loop correlator of Δ as the combined result, where $L(t + \Delta)$ is growing exponentially in length with $e^{2\sqrt{\Lambda}\Delta}$ and the correlation between “elementary” spatial elements of $L(t)$ and $L(t + \Delta)$ is exponentially decreasing with $e^{-2\sqrt{\Lambda}\Delta}$, causing a correlation constant in Δ .

8.5 | Discussion and outlook

In this chapter we described the transition from compact to non-compact quantum geometries within the framework of two-dimensional CDT. In particular, the resulting quantum geometry can be viewed as the Poincaré disk dressed with quantum fluctuations. Remarkably, it was shown that the quantum fluctuations of $L(t)$ are small compared to the average value of $L(t)$. In contrast to the analogous construction in the context of DT, this enables us to view the average geometry as a true semiclassical background.

The main idea underlying this construction is similar to the appearance of ZZ-branes when described from a worldsheet perspective, i.e. from a two-dimensional quantum gravity point of view [163]. In DT the non-compactness arose when the running boundary cosmological constant $\bar{X}(T)$ approached its fixed point described by $W_{\Lambda}^{(eu)}(\bar{X}(\infty)) = 0$, i.e. to $\bar{X}(\infty) = \sqrt{\Lambda}/2$ (see (8.1)). In the case of CDT the transition occurs in exactly the same manner, namely when the running boundary cosmological constant $\bar{X}(T)$ goes to $\sqrt{\Lambda}$ for $T \rightarrow \infty$ which is determined by $\hat{W}_{\Lambda}(\bar{X}(\infty)) = 0$. However, in the case of CDT $\hat{W}_{\Lambda}(X)$ is not the disc function, but is related to the effective quantum Hamiltonian of the system. It is interesting to observe that both processes are essentially the same, since both fixed points can be related by the mapping between

the coupling constants of both theories as derived in the previous chapter, i.e. (7.54),

$$\frac{X}{\sqrt{\Lambda}} = \sqrt{\frac{2}{3}} \frac{\sqrt{\tilde{X} + \sqrt{\tilde{\Lambda}}}}{\tilde{\Lambda}^{1/4}}, \quad (8.30)$$

where the Euclidean couplings are labeled with a tilde again. From this expression we can see that $X \rightarrow \sqrt{\Lambda}$ corresponds precisely to $\tilde{X} \rightarrow \sqrt{\tilde{\Lambda}}/2$.

Another interesting observation is that the geometries described by (8.12), for different initial boundary conditions, are all sections of the same surface, namely the Poincaré disc. Hence, they obey the Euclidean Hartle-Hawking no-boundary condition. This is particularly surprising, since before rotating to the Euclidean sector we initially started with a path integral over entirely Lorentzian geometries. It would be interesting to investigate whether this also holds in higher dimensional CDT. So far, the computer simulations, as briefly described in Sec. 6.7, seem to be compatible with this condition.

Part III

Third quantization of 2D causal dynamical triangulations

A field theoretic perspective of spatial topology changes

In the second part of this thesis we introduced causal dynamical triangulations from a two-dimensional quantum gravity point of view in which the two-dimensional geometries were interpreted as a toy model for four-dimensional space-time. Taking the string theoretic point of view we see the surfaces as worldsheets of propagating strings. Using this interpretation one is naturally lead to the idea of formulating a third-quantization of the theory, a so-called string field theory, in which strings can be annihilated, and created from the vacuum. Models of string field theory (SFT) have been intensively studied in the framework of the Euclidean model [90, 169, 92, 170, 94, 171]. In this part of the thesis we develop an analogous formulation also for the Lorentzian theory. While in this chapter we compute certain “Feynman diagrams” of the model [130], we will in the next chapter introduce the whole string field theoretic framework.

9.1 | Taming spatial topology changes

In Chap. 7 we described how to introduce spatial topology changes into CDT. We saw that when viewing them as a purely geometric process¹, one obtains Euclidean quan-

¹By this we mean that each distinct geometry (distinct in the sense of Euclidean geometry) appears with equal weight in the sum over two-dimensional geometries.

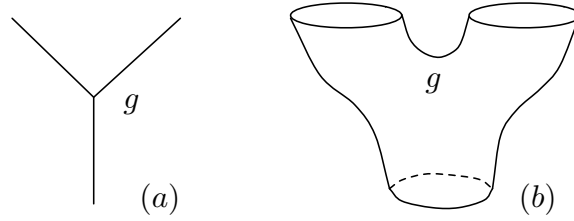


Figure 9.1: Feynman rules: (a) shows a vertex of φ^3 -theory which is assigned a coupling g . (b) shows the analogous interaction term for a splitting string. Similar to φ^3 -theory we assign a string coupling g to this interaction.

tum gravity. In particular, we recall from Sec. 7.1 that there are two possible scaling relations entering the differential equation for the propagator (7.23), i.e.

$$a^\varepsilon \frac{\partial}{\partial T} G_\Lambda(X, Y; T) = -a \frac{\partial}{\partial X} \left[(X^2 - \Lambda) G_\Lambda(X, Y; T) \right] - 2a^{\eta-1} \frac{\partial}{\partial X} \left[W_\Lambda(X) G_\Lambda(X, Y; T) \right]. \quad (9.1)$$

In the scaling described by

$$w(g, x) \xrightarrow{a \rightarrow 0} a^\eta W_\Lambda(X), \quad \eta < 0, \quad (9.2)$$

$$t \xrightarrow{a \rightarrow 0} T/a^\varepsilon, \quad \varepsilon = 1. \quad (9.3)$$

the creation of baby universes is forbidden, leading back to the “bare” CDT model. Further, in the scaling with

$$w(g, x) \xrightarrow{a \rightarrow 0} w_{ns} + a^\eta W_\Lambda(X), \quad \eta = 3/2 \quad (9.4)$$

$$t \xrightarrow{a \rightarrow 0} T/a^\varepsilon, \quad \varepsilon = 1/2, \quad (9.5)$$

the baby universes completely dominate the continuum limit, leading to Euclidean quantum gravity described by DT.

Taking a string field theoretic perspective, however, one can view each spatial topology change as a vertex of a Feynman diagram of the corresponding string field theory (see Fig. 9.1). In this spirit it is natural to assign a string coupling g to this process. This is in analogy to the coupling g in front of the interaction term of zero-dimensional φ^3 -theory, described by the action

$$S[\varphi] = \frac{1}{2}\varphi^2 - \frac{g}{3!}\varphi^3. \quad (9.6)$$

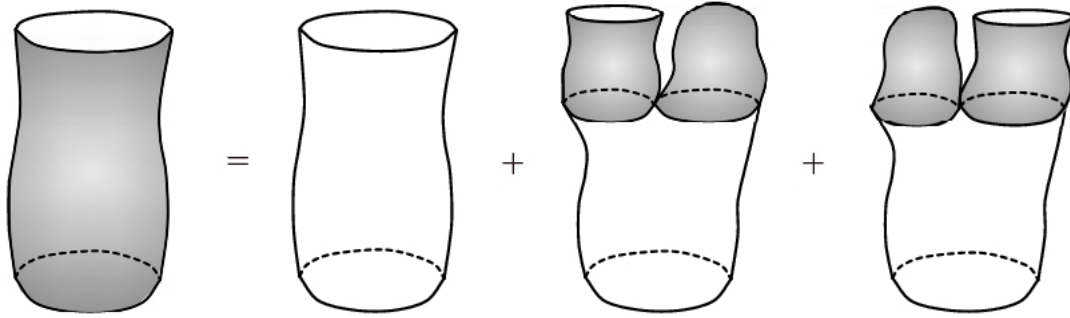


Figure 9.2: In all four graphs, the geodesic distance from the final to the initial loop is given by T . Differentiating with respect to T leads to eq. (9.8). Shaded parts of graphs represent the full, g_s -dependent propagator and disc amplitude, and non-shaded parts the CDT propagator.

While in the Euclidean model such a coupling is absent² we will see in the following that in the case of CDT it can be used to regulate the number of baby universes. From renormalization arguments one expects the coupling g also to scale, i.e. to be a non-constant function $g = g(a)$ of the cut-off a . A geometric interpretation of this assignment will be given in the discussion at the end of this chapter. Since we are interested in a theory which smoothly recovers CDT in the limit as $g \rightarrow 0$, it is natural to assume that $\eta = -1$, as in CDT. Consequently, the only way to obtain a non-trivial consistent equation is to assume that g scales to zero with the cut-off a according to

$$g = g_s a^3, \tag{9.7}$$

where g_s is a coupling constant of mass dimension three, which is kept constant when $a \rightarrow 0$ [130]. With this choice, (9.1) is turned into

$$\frac{\partial}{\partial T} G_{\Lambda, g_s}(X, Y; T) = -\frac{\partial}{\partial X} \left[\left((X^2 - \Lambda) + 2g_s W_{\Lambda, g_s}(X) \right) G_{\Lambda, g_s}(X, Y; T) \right]. \tag{9.8}$$

The graphical representation of (9.8) is shown in Fig. 9.2. Differentiating the integral equation corresponding to this figure with respect to the time T one obtains (9.8). The disc amplitude $W_{\Lambda, g_s}(X)$ is at this stage unknown.

Note that one could in principle have considered an a priori more general branching process, where more than one baby universe is allowed to sprout at any given time step T . However, one observes from the scaling relation (9.7) that the corresponding

²This is also reflected in the Hamiltonian of the string field theory [90].

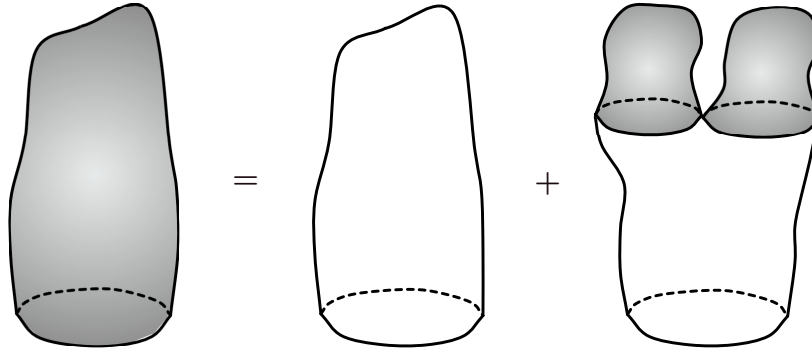


Figure 9.3: Graphical illustration of eq. (9.10). Shaded parts represent the full disc amplitude, unshaded parts the CDT disc amplitude and the CDT propagator.

extra terms in relation (9.1) would be suppressed by higher orders of a and therefore play no role in the continuum limit.

In the next section we show that the quantum geometry, in the sense defined above, together with the requirement of recovering standard CDT in the limit as $g_s \rightarrow 0$, uniquely determines the disc amplitude and thus $G_{\Lambda, g_s}(X, Y; T)$.

9.2 | The disc amplitude

The disc amplitude of CDT was calculated in Sec. 6.4, i.e. (6.50). In (6.48) it was determined directly by integrating $G_{\Lambda}(L_1, L_2 = 0; T)$ over all times. This decomposition is unique, since by assumption T is a global time and no baby universes can be created. In Sec. 7.2 it was shown that it could also be obtained from Euclidean quantum gravity (DT) by peeling off baby universes in a systematic way. By either method we found

$$W_{\Lambda}(X) = \frac{1}{X + \sqrt{\Lambda}} \quad (9.9)$$

for the disc amplitude as function of the boundary cosmological constant X . In the present, generalized case we allow for baby universes, leading to a graphical representation of the decomposition of the disc amplitude as shown in Fig. 9.3. It translates into the equation

$$W_{\Lambda, g_s}(X) = W_{\Lambda, g_s}^{(b)}(X) + g_s \int_0^{\infty} dT \int_0^{\infty} dL_1 dL_2 (L_1 + L_2) G_{\Lambda, g_s}^{(b)}(X, L_1 + L_2; T) W_{\Lambda, g_s}(L_1) W_{\Lambda, g_s}(L_2) \quad (9.10)$$

for the full propagator $W_{\Lambda, g_s}(X)$, where we have introduced a superscript (b) to indicate the “bare” CDT amplitudes, that is,

$$W_{\Lambda, g_s}^{(b)}(X) \equiv W_{\Lambda, g_s=0}(X) = W_{\Lambda}(X), \quad (9.11)$$

and similarly for $G_{\Lambda, g_s}^{(b)}$, quantities which were defined in eqs. (9.9) and (8.4) respectively. The integrations in (9.10) can be performed, yielding

$$W_{\Lambda, g_s}(X) = \frac{1}{X + \sqrt{\Lambda}} + \frac{g_s}{X^2 - \Lambda} \left(W_{\Lambda, g_s}^2(\sqrt{\Lambda}) - W_{\Lambda, g_s}^2(X) \right). \quad (9.12)$$

Solving for $W_{\Lambda, g_s}(X)$ we find

$$W_{\Lambda, g_s}(X) = \frac{-(X^2 - \Lambda) + \hat{W}_{\Lambda, g_s}(X)}{2g_s}, \quad (9.13)$$

where we have defined

$$\hat{W}_{\Lambda, g_s}(X) = \sqrt{(X^2 - \Lambda)^2 + 4g_s \left(g_s W_{\Lambda, g_s}^2(\sqrt{\Lambda}) + X - \sqrt{\Lambda} \right)}. \quad (9.14)$$

The sign of the square root is fixed by the requirement that $W_{\Lambda, g_s}(X) \rightarrow W_{\Lambda}(X)$ for $g_s \rightarrow 0$, and $W_{\Lambda, g_s}(X)$ is determined up to the value $W_{\Lambda, g_s}(\sqrt{\Lambda})$. We will now show that this value is also determined by consistency requirements of the quantum geometry. If we insert the solution (9.13) into (9.8) we obtain

$$\frac{\partial}{\partial T} G_{\Lambda, g_s}(X, Y; T) = -\frac{\partial}{\partial X} \left[\hat{W}_{\Lambda, g_s}(X) G_{\Lambda, g_s}(X, Y; T) \right]. \quad (9.15)$$

In analogy with (6.44) and (6.45), this is solved by

$$G_{\Lambda, g_s}(X, Y; T) = \frac{\hat{W}_{\Lambda, g_s}(\bar{X}(T, X))}{\hat{W}_{\Lambda, g_s}(X)} \frac{1}{\bar{X}(T, X) + Y}, \quad (9.16)$$

where $\bar{X}(T, X)$ is the solution of the characteristic equation for (9.15),

$$\frac{d\bar{X}}{dT} = -\hat{W}_{\Lambda, g_s}(\bar{X}), \quad \bar{X}(T=0, X) = X, \quad (9.17)$$

such that

$$T = \int_{\bar{X}(T)}^X \frac{dY}{\hat{W}_{\Lambda, g_s}(Y)}. \quad (9.18)$$

Physically, we require that T can take values from 0 to ∞ , as opposed to just in a finite interval. From expression (9.18) for T this is only possible if the polynomial under the

square root in the defining equation (9.13) has a double zero, which fixes the function $\hat{W}_{\Lambda, g_s}(X)$ to

$$\hat{W}_{\Lambda, g_s}(X) = (X - C)\sqrt{(X + C)^2 - 2g_s/C}, \quad (9.19)$$

where

$$C = U\sqrt{\Lambda}, \quad U^3 - U + \frac{g_s}{\Lambda^{3/2}} = 0. \quad (9.20)$$

In order to have a physically acceptable $W_{\Lambda, g_s}(X)$, one has to choose the solution to the third-order equation which is closest to 1. Quite remarkably, one can also derive (9.19) from (9.13) by demanding that the inverse Laplace transform $W_{\Lambda, g_s}(L)$ falls off exponentially for large L . In this region $W_{\Lambda, g_s}(X)$ equals $W_{\Lambda, g_s}^{(b)}(X)$ plus a convergent power series in the dimensionless coupling constant $g_s/\Lambda^{3/2}$.

One can check the consistency of the quantum geometry by using (9.16) in

$$-\frac{\partial}{\partial \Lambda} W_{\Lambda, g_s}(X) = \int_0^\infty dT \int_0^\infty dL G_{\Lambda, g_s}(X, L; T) L W_{\Lambda, g_s}(L) \quad (9.21)$$

which comes from the decomposition of a disc function with a mark in the bulk (see Fig. 7.3), i.e. the continuum version of (7.10). Integrating (9.21) gives

$$\frac{\partial W_{\Lambda, g_s}(X)}{\partial \Lambda} = \frac{W_{\Lambda, g_s}(X) - W_{\Lambda, g_s}(C)}{\hat{W}_{\Lambda, g_s}(X)}, \quad (9.22)$$

which is indeed satisfied by the solution (9.13).

9.3 | The loop-loop amplitude and the consistency condition

We mentioned earlier that the propagator can be regarded as a building block for other, more conventional “observables” in two-dimensional quantum gravity. One of the most beautiful illustrations of this and at the same time a non-trivial example of what we have called quantum geometry is the calculation in two-dimensional Euclidean quantum gravity of the loop-loop amplitude from the fixed geodesic distance two-loop amplitude [97]. The full loop-loop amplitude is obtained by summing over all Euclidean two-dimensional geometries with two boundaries, without any particular restriction on the boundaries’ mutual position. This amplitude was first calculated using matrix model techniques (for cylinder topology) [172].

To appreciate the underlying construction, consider a given geometry of cylindrical topology. Its two boundaries will be separated by a geodesic distance t , in the sense

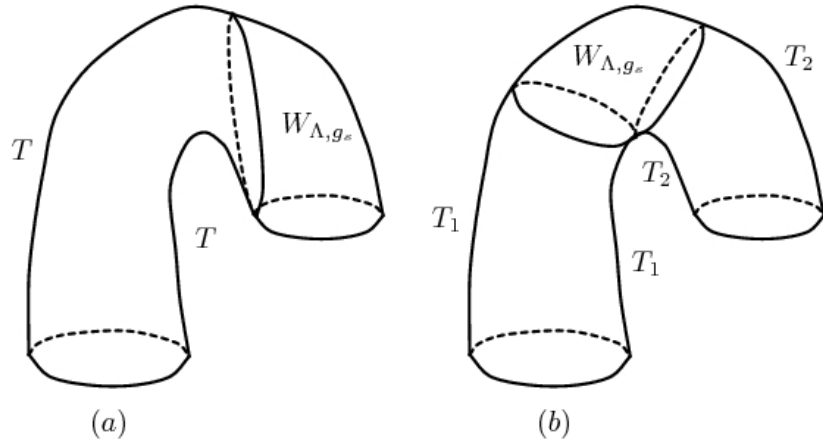


Figure 9.4: Two different ways of decomposing the loop-loop amplitude into proper-time propagators and a disc amplitude. Two points touch in the disc amplitude W , pinching the boundary to a figure-8, which combinatorially implies a substitution $W_{\Lambda, g_s}(L) \rightarrow L W_{\Lambda, g_s}(L)$ in the formulas. The time variables are related by $T_1 + T_2 = T$.

of minimal distance of any point on the final loop to the initial loop. It follows that we can consider the geometry as composed of a cylinder where the entire final loop (i.e. *each* of its points) has a distance t from the initial one and a “cap” related to the disc amplitude, as illustrated in Fig. 9.4 (a). One can now obtain the loop-loop amplitude by integrating over all T and all gluings of the cap (we refer to [97] for details). An intriguing aspect of the construction is that the decomposition of a given geometry into cylinders and caps is not unique. One can choose another decomposition consisting of two cylinders of length T_1 and T_2 , with $T_1 + T_2 = T$, joined by a cap, as illustrated in Fig. 9.4 (b). As shown in [97], the end result is indeed independent of this decomposition.

The whole construction can be repeated for our new, generalized CDT model, in this way *defining* a loop-loop amplitude. More precisely, although an exact equality of amplitudes corresponding to different decompositions like those depicted in Fig. 9.4 (a) and (b) is not immediately obvious at the level of the triangulations of the discretized theory³, the continuum ansatz (9.23) below is self-consistent, in the sense that it leads to a non-trivial symmetric expression for the amplitude with a well-defined $g_s \rightarrow 0$ limit. The algebra is similar to that of [97].

We will denote the loop-loop amplitude by $W_{\Lambda, g_s}(X, Y)$, and its Laplace transform by

³because of the different arrangements of the proper-time slicings

$W_{\Lambda, g_s}(L_1, L_2)$. The integral equation corresponding to Fig. 9.4 (a) is given by

$$W_{\Lambda, g_s}(L_1, L_2) = \int_0^\infty dT \int_0^\infty dL G_{\Lambda, g_s}(L_1, L; T) L W_{\Lambda, g_s}(L + L_2). \quad (9.23)$$

Laplace-transforming eq. (9.23), the integrals can be performed using eqs. (9.16)-(9.19). After some non-trivial algebra one obtains

$$W_{\Lambda, g_s}(X, Y) = \frac{1}{f(X)f(Y)} \frac{1}{4g_s} \left(\frac{[(X+C) + (Y+C)]^2}{(f(X) + f(Y))^2} - 1 \right), \quad (9.24)$$

where we are using the notation

$$f(X) = \sqrt{(X+C)^2 - 2g_s/C} = \hat{W}_{\Lambda, g_s}(X)/(X-C). \quad (9.25)$$

In the limit $g_s \rightarrow 0$ one finds

$$W_{\Lambda, g_s=0}^{(b)}(X, Y) = \frac{1}{2\sqrt{\Lambda}(X + \sqrt{\Lambda})^2(Y + \sqrt{\Lambda})^2}, \quad (9.26)$$

a result which could of course also have been obtained directly from (9.23) using (6.44), (6.45) and (9.9). We note that the corresponding expression in the case of Euclidean two-dimensional quantum gravity is given by

$$W_\Lambda^{(eu)}(X, Y) = \frac{1}{2h(X)h(Y)(h(X) + h(Y))^2}, \quad h(X) = \sqrt{X + \sqrt{\Lambda}}, \quad (9.27)$$

which can be obtained from expressions similar to (9.16)-(9.19), only with $\hat{W}_{\Lambda, g_s}(X)$ replaced by the Euclidean disc function

$$W_\Lambda^{(eu)}(X) = (X - \sqrt{\Lambda}/2) h(X). \quad (9.28)$$

We observe a structural similarity between (9.24) and (9.28), with the function $f(X)$ having the same relation to $\hat{W}_{\Lambda, g_s}(X)$ as $h(X)$ has to $W_\Lambda^{(eu)}(X)$.

Let us now prove the consistency condition that the two composition of the two-loop as shown in Fig. 9.4 lead to the same result. Decomposing as in Fig. 9.4 (a) leads to

$$W_{\Lambda, g_s}(L_1, L_2; T) = \int_0^\infty dL G_{\Lambda, g_s}(L_1, L; T) L W_{\Lambda, g_s}(L + L_2). \quad (9.29)$$

while the decompositions of Fig. 9.4 (b) reads

$$W_{\Lambda, g_s}(L_1, L_2; T) = \int_0^\infty dL \int_0^\infty dL' G_{\Lambda, g_s}(L_1, L; T_1) L W_{\Lambda, g_s}(L + L') L_2 G_{\Lambda, g_s}(L', L_2; T - T_1). \quad (9.30)$$

Thus we arrive at the consistency condition:

$$0 = \frac{\partial}{\partial T_1} \int_0^\infty dL \int_0^\infty dL' G_{\Lambda, g_s}(L_1, L; T_1) L W_{\Lambda, g_s}(L + L') L_2 G_{\Lambda, g_s}(L', L_2; T - T_1). \quad (9.31)$$

This condition was checked for the Euclidean model in [90]. Remarkably, it is also satisfied in the our case. After a Laplace transformation eq. (9.31) reads:

$$0 = \frac{\partial^2}{\partial X \partial Y} \frac{\partial}{\partial T_1} \int_{-i\infty+c}^{i\infty+c} \frac{dZ}{2\pi i} G_{\Lambda, g_s}(X, -Z; T_1) W_{\Lambda, g_s}(Z) G_{\Lambda, g_s}(Y, -Z; T - T_1). \quad (9.32)$$

Using the explicit form of $G_{\Lambda, g_s}(X, Y; T)$, eq. (9.16), we can perform the Z -integration in eq. (9.32). Using (9.12) we can express $W_{\Lambda, g_s}(X)$ in terms of $\hat{W}_{\Lambda, g_s}(X)$ given by (9.10) and finally using (9.17) we can differentiate after T_1 . The result is⁴

$$0 = \frac{\partial^2}{\partial X \partial Y} \left(\bar{X}^2(T_1, X) - \bar{Y}^2(T - T_1, Y) \right), \quad (9.33)$$

which is satisfied.

The existence of well-defined, symmetric expressions for the unrestricted loop-loop amplitudes in our generalized CDT model (at genus 0) and thus in standard two-dimensional CDT, formulas (9.24) and (9.26), gives strong support to the claims that (i) the proper-time propagator does indeed encode the complete information on the quantum-gravitational system, and (ii) following the arguments given in [97] concerning the decomposition invariance of the loop-loop amplitude (c.f. Fig. 9.4), the continuum theory is diffeomorphism-invariant.

9.4 | Discussion and outlook

The generalized CDT model of two-dimensional quantum gravity we have defined in this chapter is a perturbative deformation of the original model in the sense that it has

⁴The corresponding equation in the case of non-critical string theory is

$$0 = \frac{\partial^2}{\partial X \partial Y} \left(\bar{X}(T_1, X) - \bar{Y}(T - T_1, Y) \right).$$

Again one obtains the remarkable result that the amplitude $W_\Lambda^{(eu)}(X, Y; T)$ is independent of the subdivision of $T = T_1 + T_2$ as shown in Fig. 9.4. In addition we have in the non-critical SFT setting the additional consistency test that $\int_0^\infty dT W_\Lambda^{(eu)}(X, Y; T) = W_\Lambda^{(eu)}(X, Y)$, where $W_\Lambda^{(eu)}(X, Y)$ is the so-called universal loop-loop correlator calculated from matrix model [172, 173], i.e. (9.27). This was verified in [90].

a convergent power expansion of the form

$$W_{\Lambda, g_s}(X) = \sum_{n=0}^{\infty} c_n(X, \Lambda) \left(\frac{g_s}{\Lambda^{3/2}} \right)^n \quad (9.34)$$

in the dimensionless coupling constant $g_s/\Lambda^{3/2}$ [130]. This implies in particular that the average number $\langle n \rangle$ of “causality violations” in a two-dimensional universe described by this model is finite, a property already observed in previous two-dimensional models with topology change [174, 175, 128, 176]. The expectation value of the number n of branchings can be computed according to

$$\langle n \rangle = \frac{g_s}{W_{\Lambda, g_s}(X)} \frac{dW_{\Lambda, g_s}(X)}{dg_s}, \quad (9.35)$$

which is finite as long as we are in the range of convergence of $W_{\Lambda, g_s}(X)$. As already mentioned, this coincides precisely with the range where the function $W_{\Lambda, g_s}(X)$ behaves in a physically acceptable way, namely, $W_{\Lambda, g_s}(L)$ goes to zero exponentially in terms of the length L of the boundary loop. The same is true for the other functions considered, namely, $G_{\Lambda, g_s}(L_1, L_2; T)$ and $G_{\Lambda, g_s}(L_1, L_2)$.

The behaviour (9.35) should be contrasted with that in two-dimensional Euclidean quantum gravity, and is reflected in the different scaling behaviours (9.3) and (9.5) for the time t . These scaling relations show that the effective continuum “time unit” in Euclidean quantum gravity is much longer than in CDT, giving rise to infinitely many causality violations for a typical space-time history which appears in the path integral when the cut-off a is taken to zero. This phenomenon was discovered in the seminal paper [95].

As we will see in the next chapter, the calculations presented here should be seen as pertaining to the genus-0 sector of a generalized CDT model, which also includes a sum over space-time topologies. Although we have not given a precise definition of the higher-genus amplitudes in this chapter, one would expect them to be finite order by order. If the handles are as scarce as are the baby universes in the genus-0 amplitudes, it might even be that the sum over all genera is uniquely defined. Whether or not this is so will clearly also depend on the combinatorics of allowed handle configurations.

In the context of higher-genus amplitudes, it is natural to associate each handle with a “string coupling constant”, because one may think of it as a process where (one-dimensional) space splits and joins again, albeit as a function of an intrinsic proper time, rather than the time of any embedding space. An explicit calculation reveals that

in the generalized CDT model this process is related with a coupling constant g_s^2 (see next chapter), which one may think of as two separate factors of g_s , associated with the splitting and joining respectively.

How does the disc amplitude fit into this picture? From a purely Euclidean point of view all graphs appearing in Fig. 9.3 have the fixed topology of a disc. However, from a Lorentzian point of view, which comes with a notion of time, it is clear that the branching of a baby universe is associated with a change of the *spatial* topology, a singular process in a Lorentzian space-time [159]. One way of keeping track of this in a Wick-rotated, Euclidean picture is as follows. Since each time a baby universe branches off it also has to end somewhere, we may think of marking the resulting “tip” with a puncture. From a gravitational viewpoint, each new puncture corresponds to a topology change and receives a weight $1/G_N$, where G_N is Newton’s constant, because it will lead to a change by precisely this amount in the two-dimensional (Euclidean) Einstein-Hilbert action

$$S_{EH} = -\frac{1}{2\pi G_N} \int d^2\xi \sqrt{g} R. \quad (9.36)$$

Identifying the dimensionless coupling constant in eq. (9.1) with $g(a) = e^{-1/G_N(a)}$, one can introduce a *renormalized* gravitational coupling constant by

$$\frac{1}{G_N^{ren}} = \frac{1}{G_N(a)} + \frac{3}{2} \ln \Lambda a^2. \quad (9.37)$$

This implies that the *bare* gravitational coupling constant $G_N(a)$ goes to zero like $1/|\ln a^3|$ when the cut-off vanishes, $a \rightarrow 0$, in such a way that the product $e^{1/G_N^{ren}}/\Lambda^{3/2}$ is independent of the cut-off a . We can now identify

$$e^{-1/G_N^{ren}} = g_s/\Lambda^{3/2} \quad (9.38)$$

as the genuine coupling parameter in which we expand.

This renormalization of the gravitational (or string) coupling constant is reminiscent of the famous double-scaling limit in non-critical string theory⁵. In that case one also has $g_s \propto e^{-1/G_N^{ren}}$, the only difference being that relation (9.37) is changed to

$$\frac{1}{G_N^{ren}} = \frac{1}{G_N(a)} + \frac{5}{4} \ln \Lambda a^2, \quad (9.39)$$

⁵It is called the double-scaling limit since from the point of view of the discretized theory it involves a simultaneous renormalization of the cosmological constant Λ and the gravitational coupling constant G_N . In this article we have already performed the renormalization of the cosmological constant. For details on this in the context of CDT we refer to [19].

whence the partition function of non-critical string theory appears precisely as a function of the dimensionless coupling constant $g_s/\Lambda^{5/4}$.

CHAPTER 10

A causal string field theory

In the previous chapter we introduced a generalization of CDT by incorporating spatial topology changes regularized by a coupling g_s . Using certain Feynman rules for propagation and splitting of strings (spatial universes) we were able to solve the genus zero disc function to all orders in g_s . In this chapter we embed these results in a broader framework of a causal string field theory [131].

10.1 | The string field theory framework

In quantum field theory particles can be created and annihilated if the process does not violate any conservation law of the theory. In string field theories one operates in the same way with operators which can create and annihilate strings. From the two-dimensional quantum gravity point of view we thus have a third-quantization of gravity: one-dimensional universes can be created and destroyed. In [90, 169, 92, 170, 94, 171] such a formalism was developed for non-critical strings (or two-dimensional Euclidean quantum gravity). We will follow the formalism developed there closely and develop a string field theory or third quantization for CDT which will allow us in principle to calculate any amplitude involving creation and annihilation of universes [131].

The starting point is the assumption of a vacuum from which universes can be

created. We denote this state $|0\rangle$ and define creation and annihilation operators:

$$[\Psi(L), \Psi^\dagger(L')] = L\delta(L - L'), \quad \Psi(L)|0\rangle = \langle 0|\Psi^\dagger(L) = 0. \quad (10.1)$$

This assignment corresponds to working with spatial universes where a point has been marked. This avoids putting in certain combinatorial factors by hand when gluing together universes. The operators $\Psi(L)$ and $\Psi^\dagger(L)$ will be assigned dimensions $\dim[\Psi] = \dim[\Psi^\dagger] = 0$.

We could alternatively have chosen creation and annihilation operators which create and annihilate universes without such a mark. Then instead of (10.1) one would have

$$[\Psi(L), \Psi^\dagger(L')] = L^{-1}\delta(L - L'), \quad \Psi(L)|0\rangle = \langle 0|\Psi^\dagger(L) = 0, \quad (10.2)$$

and the dimensional assignment would be $\dim[\Psi] = 1$ and $\dim[\Psi^\dagger] = 1$. One could even let Ψ^\dagger create marked universes and Ψ annihilate unmarked universes if one just compensates for missing combinatorial factors by hand. Here we will use the assignment (10.1).

Let us write the differential equation for the finite time propagator derived in (6.41) using the boundary length rather than the boundary cosmological constant as variable

$$\frac{\partial}{\partial T} G_\Lambda^{(m)}(L_1, L_2; T) = L_1 \left(\frac{\partial^2}{\partial L_1^2} - \Lambda \right) G_\Lambda^{(m)}(L_1, L_2; T), \quad (10.3)$$

For convenience we have in (10.3) also marked the exit-loop L_2 in order to have symmetry between loops at the initial time and the loop at the final time, i.e. $G_\Lambda^{(m)}(L_1, L_2; T) = L_2 G_\Lambda(L_1, L_2; T)$, where $G_\Lambda(L_1, L_2; T)$ was given by (6.47).

We can now also write

$$G_\Lambda^{(m)}(L_1, L_2; T) = \langle L_2 | e^{-TH_0(L)} | L_1 \rangle, \quad H_0(L) = -L \frac{\partial^2}{\partial L^2} + \Lambda L, \quad (10.4)$$

where $H_0(L)$ was derived in (6.56).¹ Associated with the spatial universe we have a Hilbert space on the positive half-line, and a corresponding scalar product making $H_0(L)$ self-adjoint (see App. B.2 for more details)

$$\langle \psi_1 | \psi_2 \rangle = \int \frac{dL}{L} \psi_1^*(L) \psi_2(L). \quad (10.5)$$

¹We changed the notation from \hat{H}_L in (6.56) to $H_0(L)$ in (10.4) to indicate that it is the first-quantized Hamiltonian.

The introduction of the operators $\Psi(L)$ and $\Psi^\dagger(L)$ in (10.1) can be thought of as analogous to the standard second quantization in many-body theory. The single particle Hamiltonian becomes in our case the “single universe” Hamiltonian H_0 . It has eigenfunctions $\psi_n(L)$ with corresponding eigenvalues $E_n = 2n\sqrt{\Lambda}$, $n = 1, 2, \dots$:

$$\psi_n(L) = L e^{-\sqrt{\Lambda}L} p_{n-1}(L), \quad H_0(L)\psi_n(L) = E_n\psi_n(L), \quad (10.6)$$

where $p_{n-1}(L)$ is a polynomial of order $n-1$.² We now introduce creation and annihilation operators a_n^\dagger and a_n corresponding to these states, acting on the Fock-vacuum $|0\rangle$ and satisfying $[a_n, a_m^\dagger] = \delta_{n,m}$. We define

$$\Psi(L) = \sum_n a_n \psi_n(L), \quad \Psi^\dagger(L) = \sum_n a_n^\dagger \psi_n^*(L), \quad (10.7)$$

and from the orthonormality of the eigenfunctions with respect to the measure dL/L we recover (10.1). The “second-quantized” Hamiltonian is

$$\hat{H}_0 = \int_0^\infty \frac{dL}{L} \Psi^\dagger(L) H_0(L) \Psi(L), \quad (10.8)$$

and the propagator $G_\Lambda^{(m)}(L_1, L_2; T)$ is now obtained as

$$G_\Lambda^{(m)}(L_1, L_2; T) = \langle 0 | \Psi(L_2) e^{-T\hat{H}_0} \Psi^\dagger(L_1) | 0 \rangle. \quad (10.9)$$

While this is trivial, the advantage of the formalism is that it automatically takes care of symmetry factors (like in the many-body applications in statistical field theory) both when many spatial universes are at play and when they are joining and splitting. We can follow [90] and define the following Hamiltonian, describing the interaction between spatial universes:

$$\begin{aligned} \hat{H} = \hat{H}_0 &- g_s \int dL_1 \int dL_2 \Psi^\dagger(L_1) \Psi^\dagger(L_2) \Psi(L_1 + L_2) \\ &- \alpha g_s \int dL_1 \int dL_2 \Psi^\dagger(L_1 + L_2) \Psi(L_2) \Psi(L_1) - \int \frac{dL}{L} \rho(L) \Psi(L), \end{aligned} \quad (10.10)$$

where the different terms of the Hamiltonian are illustrated in Fig. 10.1. Here g_s is the coupling constant we have already encountered in Chap. 9 of mass dimension 3. The factor α is just inserted to be able to identify the action of the two g_s -terms in (10.10)

²The precise form of $p_{n-1}(L)$ is not of relevance here, but it can be readily obtained from the general formulas in App. B.2.

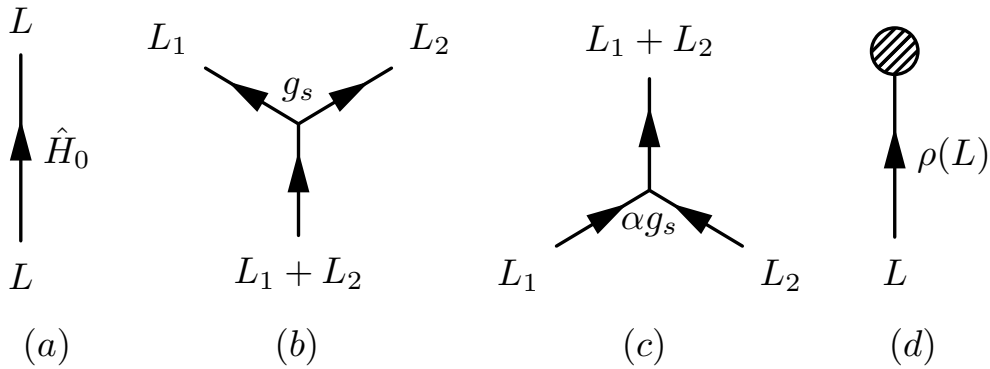


Figure 10.1: The elementary terms of the string field theory Hamiltonian (10.10): (a) the single spatial universe propagator, (b) the term corresponding to splitting into two spatial universes, (c) the term corresponding to the merging of two spatial universes and (d) the tadpole term.

when expanding in powers of g_s . We will think of $\alpha = 1$ unless explicitly stated differently. Note that the sign of all the interaction terms in (10.10) is negative. This reflects that we want these terms to represent the insertion of new geometric structures compared to the “free” propagation generated by \hat{H}_0 . These structures should thus appear with positive weight when we expand $e^{-T\hat{H}}$. \hat{H} is hermitian except for the presence of the tadpole term. It tells us that universes can vanish, but not be created from nothing. The meaning of the two interaction terms is as follows: the first term replaces a universe of length $L_1 + L_2$ with two universes of length L_1 and L_2 . This is precisely the process shown in Fig. 9.2. The second term represents the opposite process where two spatial universes merge into one, i.e. the time-reversed picture. The coupling constant g_s seems to play the role of a string coupling constant: one factor g_s for splitting spatial universes, one factor g_s for merging spatial universes and thus a factor g_s^2 when the space-time topology changes.

In a certain way the appearance of a tadpole term is more natural in the CDT framework than in the original Euclidean framework in [90]. Recall the discussion in Chap. 9: In a Lorentzian setting there is no regular disc geometry, it has to end in a “puncture”. The tadpole term is a formal realization of this process. Also recall that we could associate this process with a gravitational coupling constant, in this way linking it to g_s . It was done by observing that to each splitting off of a baby universe we have a puncture where the baby universe ends. Thus the coupling constant g_s related to the splitting

of spatial universes could be identified with the vanishing of universes. This shift can be made explicit in our string field Hamiltonian \hat{H} in (10.10). In (10.10) the coupling constant g_s is associated with splitting and joining of spatial universes. No coupling constant is associated with the tadpole term, i.e. the vanishing of a spatial universe. However we can redefine Ψ and Ψ^\dagger :

$$\bar{\Psi} = g_s \Psi, \quad \bar{\Psi}^\dagger = \frac{1}{g_s} \Psi^\dagger. \quad (10.11)$$

With this substitution the coupling constant g_s is shifted from the splitting term to the tadpole term, i.e. precisely the shift mentioned above. In addition the term associated with the joining of spatial universes will have the coupling constant g_s^2 , which matches a change in topology.

Finally, let us identify the real coupling constant appearing in (10.10): let us measure everything in terms of $1/\sqrt{\Lambda}$ which is the natural length scale of our universe. Introducing the dimensionless length variable $\tilde{L} = L\sqrt{\Lambda}$, the dimensionless boundary cosmological constant $\tilde{X} = X/\sqrt{\Lambda}$, the dimensionless time variable $\tilde{T} = T\sqrt{\Lambda}$, the dimensionless tadpole density $\tilde{\rho}(\tilde{L}) = \rho(L)/\sqrt{\Lambda}$, the dimensionless coupling constant $\tilde{g}_s = g_s/\Lambda^{3/2}$ (already introduced in eq. (9.34)) and finally the dimensionless Hamiltonian $\tilde{H} = \hat{H}/\sqrt{\Lambda}$, we can write

$$\hat{H}_0 = \sqrt{\Lambda} \tilde{H}_0, \quad \tilde{H}_0 = \int \frac{d\tilde{L}}{\tilde{L}} \tilde{\Psi}^\dagger(\tilde{L}) H_0(\tilde{L}) \tilde{\Psi}(\tilde{L}), \quad (10.12)$$

where $\tilde{\Psi}(\tilde{L}) = \Psi(L)$ and $\tilde{\Psi}^\dagger(\tilde{L}) = \Psi^\dagger(L)$ satisfy the same commutation relation as $\Psi(L), \Psi^\dagger(L)$ when expressed in terms of \tilde{L} , and $\hat{H} = \sqrt{\Lambda} \tilde{H}$, where

$$\begin{aligned} \tilde{H} = \tilde{H}_0 - \tilde{g}_s \int d\tilde{L}_1 \int d\tilde{L}_2 \tilde{\Psi}^\dagger(\tilde{L}_1) \tilde{\Psi}^\dagger(\tilde{L}_2) \tilde{\Psi}(\tilde{L}_1 + \tilde{L}_2) \\ - \alpha \tilde{g}_s \int d\tilde{L}_1 \int d\tilde{L}_2 \tilde{\Psi}^\dagger(\tilde{L}_1 + \tilde{L}_2) \tilde{\Psi}(\tilde{L}_2) \tilde{\Psi}(\tilde{L}_1) - \int \frac{d\tilde{L}}{\tilde{L}} \tilde{\rho}(\tilde{L}) \tilde{\Psi}(\tilde{L}). \end{aligned} \quad (10.13)$$

From this equation it is clear that the real coupling constant in the theory is the dimensionless \tilde{g}_s , precisely the "double scaling" coupling constant which already appeared in the calculation of $W_{\Lambda, g_s}(X)$ and $G_{\Lambda, g_s}(X, Y; T)$ (i.e. (9.34)). From the discussion above we also observe that the expansion parameter for topology change of space-time is $\tilde{g}_s^2 = g_s^2/\Lambda^3$.

In principle we can now calculate the process where we start out with m spatial universes at time 0 and end with n universes at time T , represented as

$$G_{\Lambda, g_s}(L_1, \dots, L_m; L'_1, \dots, L'_n; T) = \langle 0 | \Psi(L'_1) \dots \Psi(L'_n) e^{-T\hat{H}} \Psi^\dagger(L_1) \dots \Psi^\dagger(L_m) | 0 \rangle. \quad (10.14)$$

10.2 | The genus zero limit

10.2.1 | The disc amplitude

Let us consider the simplest amplitude: a single spatial universe which disappears in the vacuum. This is precisely the disc-amplitude considered in the previous chapter. The topology of space-time was not allowed to change in the calculation in Chap. 9. We can incorporate that in the SFT-picture by choosing $\alpha = 0$ in (10.10), i.e. the genus zero limit. The disc-amplitude can then be expressed as:

$$W_{\Lambda, g_s}(L) = \lim_{T \rightarrow \infty} W_{\Lambda, g_s}(L, T) = \lim_{T \rightarrow \infty} \langle 0 | e^{-T\hat{H}(\alpha=0)} \Psi^\dagger(L) | 0 \rangle. \quad (10.15)$$

It will describe all possible ways in which a spatial loop can develop in time and disappear in the vacuum without changing the topology of space-time. Note that the tadpole term in (10.10) is needed in order that the amplitude (10.15) is different from zero since the state $|L\rangle = \psi^\dagger(L)|0\rangle$ is orthogonal to the vacuum state $|0\rangle$. We note that if $\alpha = 0$ we have

$$\begin{aligned} \langle 0 | e^{-T\hat{H}(\alpha=0)} \Psi^\dagger(L_1) \cdots \Psi^\dagger(L_m) | 0 \rangle = & \quad (10.16) \\ \langle 0 | e^{-T\hat{H}(\alpha=0)} \Psi^\dagger(L_1) | 0 \rangle \langle 0 | e^{-T\hat{H}(\alpha=0)} \Psi^\dagger(L_2) | 0 \rangle \cdots \langle 0 | e^{-T\hat{H}(\alpha=0)} \Psi^\dagger(L_m) | 0 \rangle, \end{aligned}$$

this factorization being a consequence of the fact that if we start out with m spatial universes there is no way they can merge at any time if $\alpha = 0$ (it is easy to prove (10.16) using the algebra of the Ψ 's).

Following [90] we obtain an equation for $W_{\Lambda, g_s}(L)$ by differentiating (10.15) with respect to T and using $\hat{H}|0\rangle = 0$:

$$0 = \lim_{T \rightarrow \infty} \frac{\partial}{\partial T} W_{\Lambda, g_s}(L, T) = \lim_{T \rightarrow \infty} \langle 0 | e^{-T\hat{H}(\alpha=0)} [\hat{H}(\alpha=0), \Psi^\dagger(L)] | 0 \rangle. \quad (10.17)$$

The commutator can readily be calculated and after a Laplace transformation eq. (10.17) reads

$$\frac{\partial}{\partial X} ((X^2 - \Lambda)W_{\Lambda, g_s}(X) + g_s W_{\Lambda, g_s}^2(X)) = \rho(X), \quad (10.18)$$

where the last term on the left-hand-side of (10.18) is a consequence of the factorization (10.16).

Eq. (10.18) has the generalized CDT solution (9.19)-(9.20) discussed in Chap. 9 if

$$\rho(X) = 1, \quad \text{i.e.} \quad \rho(L) = \delta(L), \quad (10.19)$$

which is a reasonable physical requirement: the spatial universe can only vanish in the vacuum when the length of the universe goes to zero.

10.2.2 | Inclusive amplitudes

Above we have understood how to reproduce the generalized CDT disc amplitude $W_{\Lambda, g_s}(X)$ as the connected amplitude arising in SFT in the limit $\alpha = 0$. We now want to understand how to reproduce the proper-time propagator $G_{\Lambda, g_s}^{(m)}(X, Y; T)$ in the context of SFT. We have an “entrance” loop at time $T = 0$ and an “exit” loop at time T . However, the propagator $G_{\Lambda, g_s}^{(m)}(X, Y; T)$ allows baby-universes to split off and propagate further than time T if they only vanish into the vacuum eventually (see Fig. 9.2).

We can reproduce this result in the $\alpha = 0$ limit of SFT by introducing the “inclusive” Hamiltonian [90]. Since we are working in the $\alpha = 0$ limit, we only have universes branching, not merging, during the time evolution, and all the branching universes except one have to vanish in the vacuum. The branching process is dictated by the term

$$g_s \int dL_1 \int dL_2 \Psi^\dagger(L_1) \Psi^\dagger(L_2) \Psi(L_1 + L_2) \quad (10.20)$$

in the Hamiltonian \hat{H} , eq. (10.10). Once the branching has occurred, only one of the two universes can connect to the exit loop at time T , the other universe has to continue until it eventually vanishes in the vacuum, a process which is allowed to occur a time later than T . This scenario is captured by the replacement

$$\Psi^\dagger(L_1) \Psi^\dagger(L_2) \rightarrow W_{\Lambda, g_s}(L_1) \Psi^\dagger(L_2) + \Psi^\dagger(L_1) W_{\Lambda, g_s}(L_2) \quad (10.21)$$

in eq. (10.20). Thus we arrive at the following “inclusive Hamiltonian”

$$\hat{H}_{incl} = \int \frac{dL}{L} \Psi^\dagger(L) H_0(L) \Psi(L) - 2g_s \int dL_1 \int dL_2 W_{\Lambda, g_s}(L_1) \Psi^\dagger(L_2) \Psi(L_1 + L_2), \quad (10.22)$$

and we obtain the following representation of $G_{\Lambda, g_s}^{(m)}(L_1, L_2; T)$

$$G_{\Lambda, g_s}^{(m)}(L_1, L_2; T) = \langle 0 | \Psi(L_2) e^{-T \hat{H}_{incl}} \Psi^\dagger(L_1) | 0 \rangle. \quad (10.23)$$

Differentiating eq. (10.23) with respect to T , commuting \hat{H}_{incl} to the right to $|0\rangle$ (and using $\hat{H}_{incl}|0\rangle = 0$) one obtains after a Laplace transformation and removal of the mark on the final boundary (9.8). Thus the generalized CDT proper-time propagator also has a simple SFT description.

10.3 | Dyson-Schwinger equations

The disc amplitude is one of a set of functions for which it is possible to derive Dyson-Schwinger equations (DSE). Here we consider a more general class of functions. Define the generating function:

$$Z(J; T) = \langle 0 | e^{-T\hat{H}} e^{\int dL J(L)\Psi^\dagger(L)} | 0 \rangle. \quad (10.24)$$

We have

$$\langle 0 | e^{-T\hat{H}} \Psi^\dagger(L_1) \cdots \Psi^\dagger(L_n) | 0 \rangle = \left. \frac{\delta^n Z(J; T)}{\delta J(L_1) \cdots \delta J(L_n)} \right|_{J=0}. \quad (10.25)$$

We have already seen that in the case where the coupling constant $\alpha = 0$ we had factorization:

$$Z(J, T; \alpha = 0) = e^{\int dL J(L)W_{\Lambda, g_s}(L, T)} \quad (10.26)$$

where $W_{\Lambda, g_s}(L, T)$ denotes the disk amplitude where the universe decays into the vacuum before or at time T , and where $W_{\Lambda, g_s}(L, T = \infty)$ was the disc amplitude we already calculated.

Following [90] we can obtain the DSE in the same way as for the disc amplitude, the only difference being that when the constant α is no longer zero these equations do not close but connect various amplitudes of more complicated topology. However, the equations can be solved iteratively. We denote

$$Z(J) \equiv \lim_{T \rightarrow \infty} Z(J; T), \quad (10.27)$$

$Z(J)$ being the generating functional for universes that disappear in the vacuum. We now have

$$0 = \lim_{T \rightarrow \infty} \frac{\partial}{\partial T} \langle 0 | e^{-T\hat{H}} e^{\int dL J(L)\Psi^\dagger(L)} | 0 \rangle = \lim_{T \rightarrow \infty} \langle 0 | e^{-T\hat{H}} \hat{H} e^{\int dL J(L)\Psi^\dagger(L)} | 0 \rangle. \quad (10.28)$$

Commuting the $\Psi(L)$'s in \hat{H} past the source term effectively replaces these operators by $LJ(L)$, after which they can be moved to the left of any $\Psi^\dagger(L)$ and outside $\langle 0 |$. After that the remaining $\Psi^\dagger(L)$'s in \hat{H} can be replaced by $\delta/\delta J(L)$ and also moved outside $\langle 0 |$, leaving us with an integro-differential operator acting on $Z(J)$:

$$0 = \int_0^\infty dL J(L) O \left(L, J, \frac{\delta}{\delta J} \right) Z(J) \quad (10.29)$$

where

$$O\left(L, J, \frac{\delta}{\delta J}\right) = H_0(L) \frac{\delta}{\delta J(L)} - \delta(L) - g_s L \int_0^L dL' \frac{\delta^2}{\delta J(L') \delta J(L-L')} - \alpha g_s L \int_0^\infty dL' L' J(L') \frac{\delta}{\delta J(L+L')} \quad (10.30)$$

$Z(J, T)$ is a generating functional which also includes totally disconnected universes which never “interact” with each other. It is of more interest to restrict ourselves to the study of “connected universes”, i.e. universes where space-time is connected. The generating functional for connected universes is obtained in the standard way from field theory by taking the logarithm of $Z(J, T)$. Thus we write:

$$F(J, T) = \log Z(J, T), \quad (10.31)$$

and we have

$$\langle 0 | e^{-T\hat{H}} \Psi^\dagger(L_1) \cdots \Psi^\dagger(L_n) | 0 \rangle_{con} = \frac{\delta^n F(J, T)}{\delta J(L_1) \cdots \delta J(L_n)} \Big|_{J=0}, \quad (10.32)$$

and we can readily transfer the DSE (10.29)-(10.30) into an equation for the connected functional

$$F(J) = \lim_{t \rightarrow \infty} F(J, T). \quad (10.33)$$

From (10.29)-(10.30) we obtain

$$0 = \int_0^\infty dL J(L) \left\{ H_0(L) \frac{\delta F(J)}{\delta J(L)} - \delta(L) - g_s L \int_0^L dL' \frac{\delta^2 F(J)}{\delta J(L') \delta J(L-L')} - g_s L \int_0^L dL' \frac{\delta F(J)}{\delta J(L')} \frac{\delta F(J)}{\delta J(L-L')} - \alpha g_s L \int_0^\infty dL' L' J(L') \frac{\delta F(J)}{\delta J(L+L')} \right\}. \quad (10.34)$$

From (10.34) one obtains the DSE by differentiating (10.34) after $J(l)$ a number of times and then taking $J(L) = 0$.

10.4 | Application of the DSE

Let us introduce the notation

$$W(L_1, \dots, L_n) \equiv \frac{\delta^n F(J)}{\delta J(L_1) \cdots \delta J(L_n)} \Big|_{J=0} \quad (10.35)$$

as well as the Laplace transform

$$W(X_1, \dots, X_n) \equiv \int_0^\infty dL_1 \cdots \int_0^\infty dL_n e^{-X_1 L_1 - \cdots - X_n L_n} W(L_1, \dots, L_n) \quad (10.36)$$

for the higher loop amplitudes.

Let us differentiate eq. (10.34) after $J(L)$ one, two and three times, then take $J(L) = 0$ and Laplace transform the obtained equations. We obtain the following three equations (where $H_0(X)f(X) = \partial_X[(X^2 - \Lambda)f(X)]$):

$$0 = H_0(X)W(X) - 1 + g_s \partial_X (W(X, X) + W(X)W(X)), \quad (10.37)$$

$$\begin{aligned} 0 = & (H_0(X) + H_0(Y))W(X, Y) + g_s \partial_X W(X, X, Y) + g_s \partial_Y W(X, Y, Y) \\ & + 2g_s (\partial_X [W(X)W(X, Y)] + \partial_Y [W(Y)W(X, Y)]) \\ & + 2\alpha g_s \partial_X \partial_Y \left(\frac{W(X) - W(Y)}{X - Y} \right) \end{aligned} \quad (10.38)$$

$$\begin{aligned} 0 = & (H_0(X) + H_0(Y) + H_0(Z))W(X, Y, Z) \\ & + g_s \partial_X W(X, X, Y, Z) + g_s \partial_Y W(X, Y, Y, Z) + g_s \partial_Z W(X, Y, Z, Z) \\ & + 2g_s \partial_X [W(X)W(X, Y, Z)] + 2g_s \partial_Y [W(Y)W(X, Y, Z)] \\ & + 2g_s \partial_Z [W(Z)W(X, Y, Z)] + 2g_s \partial_X [W(X, Y)W(X, Z)] \\ & + 2g_s \partial_Y [W(X, Y)W(Y, Z)] + 2g_s \partial_Z [W(X, Z)W(Y, Z)] \\ & + 2\alpha g_s \left(\partial_X \partial_Y \frac{W(X, Z) - W(Y, Z)}{X - Y} + \partial_X \partial_Z \frac{W(X, Y) - W(Y, Z)}{X - Z} \right. \\ & \left. + \partial_Y \partial_Z \frac{W(X, Y) - W(X, Z)}{Y - Z} \right) \end{aligned} \quad (10.39)$$

The structure of the DSE should now be clear.

We can solve the DSE iteratively. For this purpose let us introduce the expansion of $W(X_1, \dots, X_n)$ in terms of the coupling constants g_s and α :

$$W(X_1, \dots, X_n) = \sum_{k=n-1}^{\infty} \alpha^k \sum_{m=k-1}^{\infty} g_s^m W(X_1, \dots, X_n; m, k). \quad (10.40)$$

The amplitude $W(X_1, \dots, X_n)$ starts with the power $(\alpha g_s)^{n-1}$ since we have to perform n mergings during the time evolution in order to create a connected geometry if we begin with n separated spatial loops. Thus one can find the lowest order contribution

to $W(X_1)$ from (10.37), use that to find the lowest order contribution to $W(X_1, X_2)$ from (10.38) and use this again in (10.39) which involves $W(X_1, X_2, X_3)$, etc. Returning to eq. (10.37) we can use the lowest order expression for $W(X_1, X_2)$ to find the next order correction to $W(X_1)$, use this and the lowest order correction for $W(X_1, X_2, X_3)$ to find the next order correction to $W(X_1, X_2)$, etc.

Two remarks are in order: firstly, the integration constants which come by integrating (10.37)-(10.39) and the corresponding higher order equations are uniquely fixed by the requirement that the correlation functions fall off for the lengths $L_i \rightarrow \infty$, i.e. the requirement that the Laplace transformed amplitude $W(X_1, \dots, X_n)$ is analytic for $X_i > 0$. Secondly, the expressions obtained for $W(X_1, \dots, X_n)$ can of course be obtained directly from a diagrammatic expansion, using the interaction rules shown in Fig. 10.1, the propagation being defined by \hat{H}_0 , and then integrating in a suitable way over the times T_i involved.

Let us just list the first few orders:

$$W(X; 0, 0) = \frac{1}{X + \sqrt{\Lambda}}, \quad (10.41)$$

$$W(X; 1, 0) = \frac{X + 3\sqrt{\Lambda}}{\Lambda(X + \sqrt{\Lambda})^3}, \quad (10.42)$$

$$W(X, Y; 1, 1) = \frac{1}{2\sqrt{\Lambda}(X + \sqrt{\Lambda})^2(Y + \sqrt{\Lambda})^2}. \quad (10.43)$$

$$W(X, Y, Z; 2, 2) = \frac{7\Lambda^{\frac{3}{2}} + 5\Lambda(X + Y + Z) + 3\sqrt{\Lambda}(XY + XZ + YZ) + XYZ}{4\Lambda^{\frac{3}{2}}(\sqrt{\Lambda} + X)^3(\sqrt{\Lambda} + Y)^3(\sqrt{\Lambda} + Z)^3} \quad (10.44)$$

These amplitudes involve no change in space-time topology. The genus one and genus two amplitudes to lowest order in g_s , i.e. without any additional baby universes, become, using the results (10.41)-(10.44) in the iteration as described above,

$$W(X; 2, 1) = \frac{15\Lambda^{\frac{3}{2}} + 11\lambda X + 5\sqrt{\Lambda}X^2 + X^3}{32\Lambda^{\frac{5}{2}}(\sqrt{\Lambda} + X)^5}. \quad (10.45)$$

$$W(X; 3, 2) = \frac{1}{2048\Lambda^{\frac{11}{2}}(\sqrt{\Lambda} + X)^9} \left(11319\Lambda^{\frac{7}{2}} + 19951\Lambda^3 X + 21555\Lambda^{\frac{5}{2}} X^2 + 16955\Lambda^2 X^3 + 9765\Lambda^{\frac{3}{2}} X^4 + 3885\Lambda X^5 + 945\sqrt{\Lambda} X^6 + 105X^7 \right). \quad (10.46)$$

In terms of diagrams this genus 2 amplitude corresponds to the following three dia-

grams (integrated suitably over the times T_i):

$$W(X; 3, 2) = \begin{array}{c} \text{diagram 1} \\ \text{diagram 2} \\ \text{diagram 3} \end{array} .$$

As mentioned above the amplitude $W(X_1, \dots, X_n)$ starts with the power $(\alpha g_s)^{n-1}$ coming from merging the n disconnected spatial universes. The rest of the powers of αg_s will result in a topology change of the resulting, connected worldsheet. From a Euclidean point of view it is thus more appropriate to reorganize the series as follows

$$W(X_1, \dots, X_n) = (\alpha g_s)^{n-1} \sum_{h=0}^{\infty} (\alpha g_s^2)^h W_h(X_1, \dots, X_n) \quad (10.47)$$

$$W_h(X_1, \dots, X_n) = \sum_{j=0}^{\infty} g_s^j W(X_1, \dots, X_n; n-1+2h+j, n-1+h) \quad (10.48)$$

and aim for a topological expansion in αg_s^2 , at each order solving for all possible baby-universe creations which at some point will vanish into the vacuum. Thus $W_h(X_1, \dots, X_n)$ will be a function of g_s although we do not write it explicitly. The DSE allow us to obtain the topological expansion iteratively, much the same way we already did as a power expansion in g_s .

Since we have $W(X, Y) = O(\alpha)$ this term does not contribute to the lowest order and from the DSE (10.37) we obtain a closed equation for $W_0(X)$:

$$H_0(X)W_0(X; g_s) + g_s \partial_X W_0^2(X; g_s) = 1, \quad (10.49)$$

This equation is of course just eq. (10.17) and we have

$$W_0(X) = W_{\Lambda, g_s}(X). \quad (10.50)$$

Knowing $W_0(X)$ allows us to obtain $W_0(X, Y)$ from (10.38) since $W(X, Y, Z)$ is of order $O(\alpha^2)$. Thus the 3-loop term does not contribute to the lowest α order of eq. (10.38), which is $O(\alpha)$, and we have to the lowest order:

$$\begin{aligned} \left(H_0(X) + 2g \partial_X W_0(X) + H_0(Y) + 2g_s \partial_Y W_0(Y) \right) W_0(X, Y) &= \\ &= -2 \partial_X \partial_Y \left(\frac{W_0(X) - W_0(Y)}{X - Y} \right) \end{aligned} \quad (10.51)$$

Thus $W_0(X, Y)$ is entirely determined by the knowledge of $W_0(X)$. We note that using the definition (9.12) we can simplify (10.51):

$$\begin{aligned} \frac{\partial}{\partial X} \left(\hat{W}_{\Lambda, g_s}(X) W_0(X, Y) \right) + \frac{\partial}{\partial Y} \left(\hat{W}_{\Lambda, g_s}(Y) W_0(X, Y) \right) &= \\ &= -\frac{1}{g_s} \frac{\partial^2}{\partial X \partial Y} \left(\frac{\hat{W}_{\Lambda, g_s}(X) - \hat{W}_{\Lambda, g_s}(Y)}{X - Y} \right) \end{aligned} \quad (10.52)$$

The solution $W_0(X, Y)$ can readily be found from eq. (10.52), yielding

$$W_0(X, Y) = \frac{1}{f(X)f(Y)} \frac{1}{4g_s} \left(\frac{[(X+C) + (Y+C)]^2}{[f(X) + f(Y)]^2} - 1 \right), \quad (10.53)$$

where

$$f(x) = \sqrt{(x+C)^2 - 2g_s/C} = \hat{W}_{\Lambda, g_s}(x)/(x-C). \quad (10.54)$$

and

$$C = U\sqrt{\Lambda}, \quad U^3 - U + \frac{g_s}{\Lambda^{3/2}} = 0. \quad (10.55)$$

as in Sec. 9.2.

In fact this solution was already found in Sec. 9.3 since we by definition have

$$W_0(X, Y) = \int_0^\infty dT W_{\Lambda, g_s}(X, Y; T), \quad (10.56)$$

where $W_{\Lambda, g_s}(X, Y; T)$ is the Laplace transform of the loop-loop function $W_{\Lambda, g_s}(L_1, L_2; T)$ defined in (9.30) with $T_1 = T/2$. When expanded to lowest order in g_s we reproduce (10.43).

It should now be clear that one can iterate the DSE in a systematic way as a power series in the number of handles of the world sheet exactly the same way as we iterated the DSE as a function of the coupling constant g_s : As an instructive example we calculate the genus one amplitude $W_1(X)$. We expand

$$\begin{aligned} W(X) &= W_0(X) + \alpha g_s^2 W_1(X) + \alpha^2 g_s^4 W_2(X) + \dots \\ W(X, Y) &= \alpha g_s W_0(X, Y) + \alpha^2 g_s^3 W_1(X, Y) + \dots \end{aligned} \quad (10.57)$$

While (10.49) was the 0th order in α of eq. (10.37), the 1st order reads

$$\frac{\partial}{\partial X} \left(\hat{W}_{\Lambda, g_s}(X) W_1(X) + W_0(X, X) \right) = 0, \quad (10.58)$$

where $W_0(X, X)$ is given by (10.53). The integration constant is fixed by the requirement that $W_1(x)$ is analytic for $X > 0$, i.e. that $W_1(L)$ falls off as $L \rightarrow \infty$. We then obtain

$$W_1(X) = \frac{W_0(C, C) - W_0(X, X)}{\hat{W}_{\lambda, g_s}(X)} = \frac{(X + 3C)(X^2 + 2CX + 5C^2 - 4g_s/C)}{4(2C^3 - g_s)((X + C)^2 - 2g_s/C)^{5/2}}. \quad (10.59)$$

It is seen that if we expand $W_1(X)$ in powers of g_s , the first term will reproduce (10.45).

10.5 | Discussion

We have developed here a string-field theory based on the CDT quantization of two-dimensional quantum gravity. It shares many properties with the original non-critical SFT, and the whole formalism was borrowed from non-critical SFT. Yet, it is different and in some ways simpler. The tad-pole term is simpler. It is simply $\rho(L) = \delta(L)$, telling us that universes can only disappear in the vacuum if they have zero spatial “volume”. This is in accordance with the interaction between spatial universes, which preserves the total length (the total spatial volume). In non-critical SFT the evolution in proper time results in a process where the original spatial universe at proper time $T = 0$ spawn an infinity of (infinitesimal) baby universe during the time evolution. This is linked to the fact that the proper time in non-critical SFT has the anomalous length dimension $1/2$. In our new CDT-based SFT the situation is different. The proper time T has the canonical dimension 1, and the number of baby universes created during the time evolution is finite (see (9.35)).

As discussed in Chap. 9 it is not possible to connect the non-critical SFT and the CDT-based SFT by a simple analytic continuation in the coupling constant g_s , not even in the $\alpha = 0$ limit. As already shown in Chap. 7, starting out with a discretized, regularized version of the theory, the Euclidean theory (quantum Liouville theory) is obtained if the “bare” dimensionless coupling constant g is of order one. However, the relation between the bare coupling constant and the dimensionful continuum coupling constant g_s used here and in the previous chapter is, as mentioned in Sec. 9.1,

$$g = g_s a^3 \quad (10.60)$$

As discussed in Sec. 9.1 the generalized CDT continuum limit corresponds to g_s fixed, $a \rightarrow 0$, and thus to $g(a) \rightarrow 0$. The fact that $g(a)$ goes to zero in CDT SFT is of course

related to the finite number of baby universes generated in this theory. In contrast we have an infinite number of baby universes generated in non-critical SFT where g is of order one.

However, there is clearly a deep connection between the Euclidean theory and the CDT theory awaiting to be fully understood. In Sec. 7.2 it was shown that if one integrate out the “excessive spawn” of baby universes in Euclidean two-dimensional quantum gravity one recovers the CDT theory and the mapping between the dimensionless variables $X/\sqrt{\Lambda}$ in the two theories was found, i.e. (7.54). This mapping was later discovered by Seiberg et al. [165] as the uniformization map from the algebraic surface representing the “semiclassical” non-critical string to the complex plane. The singular points of the algebraic surface corresponds to ZZ-branes where there is a transition from compact to non-compact topology [163, 167, 168]. These singular points are mapped to points in the complex plane where one has a similar transition from compact to non-compact geometry in CDT context as discussed in Chap. 8.

It is interesting to try to generalize the present CDT-based SFT to include the coupling to matter. In particular, the presence of a $c = 1$ barrier can then be addressed. Since the $c = 1$ barrier partly can be understood as the result of an excessive creation of baby universes, such that the two-dimensional worldsheet is torn apart [161, 177] it is clear that the CDT theory may behave differently at $c = 1$. Numerical simulations hint that there still might be a barrier for large c [178], but nothing is presently known with certainty and CDT-based SFT may provide a useful analytic tool. Work in this direction is in progress.

Equally interesting is the possibility of performing a summation over wordsheets of all genera. Again, since the double-scaling limit in CDT-based SFT is different from the double-scaling limit in non-critical string theory and the penalty for creation of a higher genus surface is larger in the sense mentioned above, viewing the creation a higher genus worldsheet as a successive creation and annihilation of a baby universe, one could hope the result of such a summation is better behaved and less ambiguous than was the case in non-critical string theory. Work in this direction is also in progress.

Part IV

Matrix models for 2D causal dynamical triangulations

CHAPTER 11

Matrix models for two-dimensional Euclidean quantum gravity

In the previous chapter we computed higher-loop and higher-genus amplitudes in the framework of a SFT for the continuum model of generalized CDT. An earlier formulation for DT was introduced by Kawai et al. [90] as discussed above. If one would like to perform similar calculations in the discrete framework of DT one could either formulate a discrete STF as has been done in [94] or make use of so-called matrix models and loop equations derived from them.

In this chapter we want to introduce the use of matrix models to solve combinatorial counting problems of DT on the discretized level. Those techniques are very powerful, since they allow for many generalizations especially in the context of matter couplings.

11.1 | Counting triangulations with matrix models

In the following we want to give a short introduction to how certain matrix integrals can be used as generating functionals for random triangulation. The basic idea underlying this construction goes back to the seminal work by 't Hooft [179] on the large- N limit of QCD, followed by work on the saddle point approximation [84, 180]. For further references the reader is referred to several reviews [74, 181, 73, 18].

Before entering the discussion of matrix integrals let us first briefly recall the Feyn-

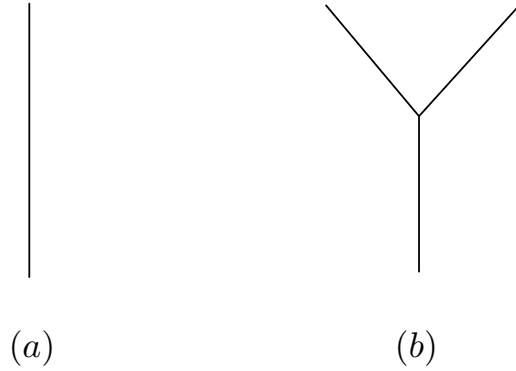


Figure 11.1: Building blocks for Feynman graphs: (a) the scalar propagator and (b) the scalar three-point vertex.

man expansion of zero-dimensional φ^3 field theory whose action we already mentioned in (9.6),

$$Z(g) = \int_{-\infty}^{\infty} \frac{d\varphi}{\sqrt{2\pi}} e^{-\frac{1}{2}\varphi^2 + \frac{g}{3!}\varphi^3} = \sum_{n=0}^{\infty} I_n(g) \quad (11.1)$$

with

$$I_n(g) = \int_{-\infty}^{\infty} \frac{d\varphi}{\sqrt{2\pi}} e^{-\frac{1}{2}\varphi^2} \frac{1}{n!} \left(\frac{g}{3!}\varphi^3 \right)^n. \quad (11.2)$$

The integral (11.1) is formal since it is clearly not convergent until some analytic continuation is performed. In terms of Wick contractions the integral (11.2) counts all possible ways of connecting n three-valent vertices (Fig. 11.1 (b)) by pairings, represented by the propagator $\langle \varphi\varphi \rangle$ (Fig. 11.1 (a)). These Feynman diagrams already look very much alike the dual triangulations in DT. However, to represent Riemannian geometry more structure is needed. This structure is provided when replacing the usual Feynman graphs by so-called “fat-graphs” as shown in Fig. 11.2 In terms of the integral expression (11.2) this means that we replace the field φ by traces over $N \times N$ Hermitian matrices $\phi = (\phi_{\alpha\beta})$, i.e.

$$Z(g, N) = \int d\phi e^{-N(\frac{1}{2}\text{tr}\phi^2 - \frac{g}{3}\text{tr}\phi^3)} = \sum_{n=0}^{\infty} I_n(g, N) \quad (11.3)$$

with

$$I_n(g, N) = \int d\phi e^{-\frac{N}{2}\text{tr}\phi^2} \frac{1}{n!} \left(\frac{Ng}{3}\text{tr}\phi^3 \right)^n. \quad (11.4)$$

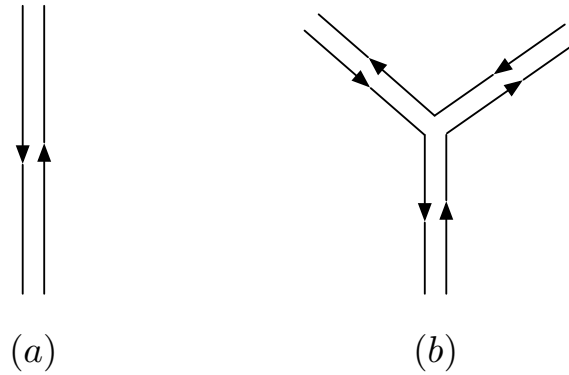


Figure 11.2: Building blocks for fat-graphs: (a) the Hermitian matrix propagator and (b) the Hermitian matrix three-point vertex.

Here the integration measure is defined using the matrix elements

$$d\phi = \prod_{\alpha \leq \beta} d\Re \phi_{\alpha\beta} \prod_{\alpha < \beta} d\Im \phi_{\alpha\beta}. \quad (11.5)$$

The propagators become now oriented links (see Fig. 11.2 (a))

$$\langle \phi_{\alpha\beta} \phi_{\alpha'\beta'} \rangle = \delta_{\alpha,\beta} \delta_{\alpha',\beta'} \quad (11.6)$$

and the three-valent vertices become also oriented (Fig. 11.2(b)). From this we see that the integral (11.4) accounts for all closed, possibly disconnected, unrestricted triangulations with n triangles (recall Fig. 5.3). Since each vertex comes with a factor of gN and each propagator with a factor $1/N$ one can convince oneself that the contribution of a given triangulation with n triangles carries a factor

$$C^{-1}(T) g^n N^{\chi(T)}, \quad (11.7)$$

where the Euler characteristic of the triangulation is given by $\chi(T) = 2 - 2h$, with h being the genus of the triangulation.¹ Further, it is noted that the factor $1/n!$ in (11.4) combines with the number of permutation of the vertices yielding the factor $1/C(T)$ which already appeared in (5.5). To make contact with dynamical triangulations we

¹The relation (11.7) is also valid for the case of triangulations with boundaries, where the Euler characteristic becomes $\chi(T) = 2 - 2h - b$ with b being the number of boundary components.

see that we have to assign g with the bare dimensionless cosmological constant and N with the bare dimensionless Newton's constant G_N as follows²:

$$g = e^{-\lambda}, \quad N = e^{1/G_N}. \quad (11.8)$$

Eq. (11.7) now corresponds to the Boltzmann weight of the triangulation. We conclude that the partition function for dynamical triangulations is given by

$$\mathcal{Z}(g, N) = \frac{\log Z(g, N)}{\log Z(0, N)}, \quad (11.9)$$

where the logarithm is introduced to precisely account for the number of *connected* (non-restricted) triangulations. Here $Z(g, N)$ as introduced in (11.3) is commonly written as

$$Z(g, N) = \int d\phi e^{-N \text{tr} V(\phi)}, \quad V(\phi) = \frac{1}{2}\phi^2 - \frac{g}{3}\phi^3, \quad (11.10)$$

where $V(\phi)$ is called the potential of the matrix model. From (11.7) we see that $\mathcal{Z}(g, N)$ has the expected topological expansion

$$\mathcal{Z}(g, N) = \sum_{h=0}^{\infty} N^{2-2h} \mathcal{Z}_h(g). \quad (11.11)$$

In the so-called planar or large- N limit one takes $N \rightarrow \infty$ and obtains the genus zero partition function

$$\mathcal{Z}_0(g) = N^{-2} \mathcal{Z}(g, N) + \mathcal{O}(1/N^2). \quad (11.12)$$

We have seen how to represent the partition function of DT as an integral over Hermitian matrices. One of the strengths of using matrix models is that it allows for many generalizations. One possible generalization is to replace the potential $V(\phi)$ in (11.10) by

$$Z(g_1, \dots, N) = \int d\phi e^{-N \text{tr} V(\phi)}, \quad V(\phi) = \frac{1}{2}\phi^2 - \sum_{j=1}^{\infty} \frac{g_j}{j} \phi^j. \quad (11.13)$$

This integral counts for closed, possibly disconnected, general non-restricted triangulations which include j -gons, each weighted by the corresponding coupling g_j . Generalizing (11.7) to arbitrary potential gives

$$C^{-1}(T) N^{\chi(T)} \prod_{j=1}^{\infty} g_j^{N(j)}, \quad (11.14)$$

²The relation for g is the same as used in previous chapters, only that we sometimes written it in terms of the bare dimensionfull cosmological constant, i.e $g = e^{-a^2\lambda}$.

where $N(j)$ is the number of j -gons in the triangulation.

Having established the connection between matrix models and dynamical triangulations we now want to show how to actually calculate certain quantities, such as the disc function, within this framework.

11.2 | Loop equations from matrix models

Let us for the following consider the matrix model with general potential as described in (11.13). We abbreviate the set of couplings by $\underline{g} = (g_1, g_2, g_3, \dots)$.

Denoting the expectation value by

$$\langle O_1(\phi) \cdots O_n(\phi) \rangle = \frac{\int d\phi O_1(\phi) \cdots O_n(\phi) e^{-N \text{tr} V(\phi)}}{\int d\phi e^{-N \text{tr} V(\phi)}} \quad (11.15)$$

we see that

$$w_l(\underline{g}, N) = \frac{1}{N} \langle \text{tr} \phi^l \rangle \quad (11.16)$$

accounts for the disc function for general non-restricted triangulations with boundary length l and arbitrary genus.³ We can now also introduce the generating function

$$w(\underline{g}, N, z) = \sum_{l=0}^{\infty} w_l(\underline{g}, N) z^{-l-1} = \frac{1}{N} \left\langle \text{tr} \frac{1}{z - \phi} \right\rangle \quad (11.17)$$

It is sometimes useful to further express the disc function in terms of the density of eigenvalues $\rho(\lambda)$ defined as

$$\rho(\lambda) = \left\langle \sum_{i=1}^N \delta(\lambda - \lambda_i) \right\rangle, \quad (11.18)$$

where λ_i , $i = 1, 2, \dots, N$ are the eigenvalues of the matrix ϕ . We can now write the disc function as

$$w_l(\underline{g}, N) = \int_{-\infty}^{\infty} d\lambda \rho(\lambda) \lambda^l, \quad w(\underline{g}, N, z) = \int_{-\infty}^{\infty} d\lambda \frac{\rho(\lambda)}{z - \lambda}. \quad (11.19)$$

In the limit $N \rightarrow \infty$ the density of eigenvalues has finite support $[c_-, c_+]$ on the real axis. This implies that the analytic continuation of $w(\underline{g}, N, z)$ is well defined on $\mathbb{C}/[c_-, c_+]$ and we can invert (11.19) as follows

$$2\pi i \rho(\lambda) = \lim_{\epsilon \rightarrow 0} (w(\underline{g}, N, \lambda - i\epsilon) - w(\underline{g}, N, \lambda + i\epsilon)). \quad (11.20)$$

³The factor of $1/N$ is introduced to cancel the factor N^{2-b} , $b=1$ coming from the Euler characteristic. This is done to make the leading order in the large- N limit of order one.

To derive the loop equations for the disc function from the matrix model [182, 172, 173] we will make an infinitesimal change in the field variable of the functional integral. This is a standard method employed in field theories. Let us consider the following infinitesimal field redefinition

$$\delta : \phi \rightarrow \phi + \epsilon \frac{1}{z - \phi}, \quad (11.21)$$

where $\epsilon > 0$ is an infinitesimal parameter. In the limit $N \rightarrow \infty$ this field redefinition is well defined for $z \in \mathbb{C}/[c_-, c_+]$. Under this field redefinition the measure and the potential transform to first order in ϵ as

$$d\phi \rightarrow d\phi \left(1 + \epsilon \operatorname{tr} \frac{1}{z - \phi} \operatorname{tr} \frac{1}{z - \phi} \right) \quad (11.22)$$

and

$$\operatorname{tr} V(\phi) \rightarrow \operatorname{tr} V(\phi) + \epsilon \operatorname{tr} \left(\frac{1}{z - \phi} V'(\phi) \right). \quad (11.23)$$

Using that $\log Z(\underline{g}, N)$ as given in (11.13) should be invariant under the transformation δ we obtain the following identity

$$\delta \log Z(\underline{g}, N) = Z^{-1}(\underline{g}, N) \int d\phi \left\{ \left(\operatorname{tr} \frac{1}{z - \phi} \right)^2 - N \operatorname{tr} \left(\frac{1}{z - \phi} V'(\phi) \right) \right\} e^{-N \operatorname{tr} V(\phi)} = 0. \quad (11.24)$$

The first term in the brackets is by definition (see (11.40))

$$\left\langle \left(\operatorname{tr} \frac{1}{z - \phi} \right)^2 \right\rangle = N^2 w^2(\underline{g}, N, z) + w(\underline{g}, N, z, z), \quad (11.25)$$

where $w(\underline{g}, N, z_1, z_2)$ is the two-loop amplitude, i.e. the sum over all triangulations with two-boundaries with boundary cosmological constants z_1 and z_2 . The second term can be evaluated using the density of eigenvalues,

$$\frac{1}{N} \left\langle \operatorname{tr} \frac{V'(\phi)}{z - \phi} \right\rangle = \int_{-\infty}^{\infty} d\lambda \rho(\lambda) \frac{V'(\lambda)}{z - \lambda} = \oint_C \frac{dw}{2\pi i} \frac{V'(w)}{z - w} w(\underline{g}, N, z), \quad (11.26)$$

where the first equality follows from (11.19) and the second equality from (11.20). The contour C encloses counterclockwise the cut $[c_-, c_+]$ of $w(\underline{g}, N, z)$ but not z as shown in Fig. 11.3. As discussed above (11.19) for this relation to hold we must have $N \rightarrow \infty$ which implies finiteness of $[c_-, c_+]$. Inserting (11.25) and (11.26) into (11.24) yields the loop equation

$$\oint_C \frac{dw}{2\pi i} \frac{V'(w)}{z - w} w(\underline{g}, N, z) = w^2(\underline{g}, N, z) + \frac{1}{N^2} w(\underline{g}, N, z, z). \quad (11.27)$$

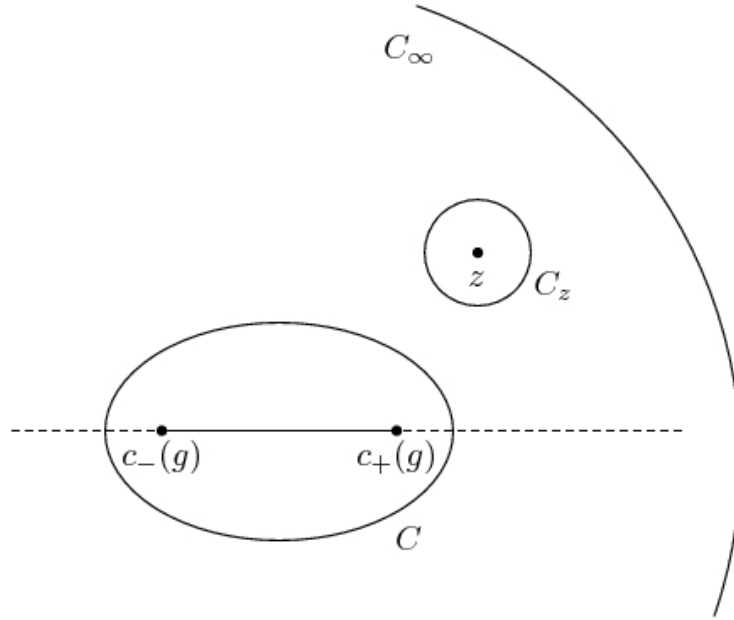


Figure 11.3: The contour C encloses counterclockwise the cut $[c_-, c_+]$ but not z .

Since we are only interested in the genus zero disc function we can take the large- N limit which allows us to drop the last term from (11.27), yielding

$$\oint_C \frac{dw}{2\pi i} \frac{V'(w)}{z-w} w(\underline{g}, z) = w^2(\underline{g}, z). \quad (11.28)$$

The solution to (11.28) reads

$$w(\underline{g}, z) = \frac{1}{2} \left(V'(z) - M(\underline{g}, z) \sqrt{(z - c_+(\underline{g}))(z - c_-(\underline{g}))} \right), \quad (11.29)$$

where $M(z)$ is a polynomial whose degree is one less than $V'(z)$. Further the density of eigenvalues reads

$$\rho(\lambda) = \frac{1}{2\pi} M(\underline{g}, \lambda) \sqrt{(c_+(\underline{g}) - \lambda)(\lambda - c_-(\underline{g}))}. \quad (11.30)$$

As for the loop equations of DT, the solution for the disc function (11.29) is completely determined by the requirement that $w(\underline{g}, z) = 1/z + \mathcal{O}(1/z^2)$. In particular, one can derive the following equations by imposing this requirement for (11.29) and using (11.28) (see for example [18] for more details):

$$M(\underline{g}, z) = \oint_{C_\infty} \frac{dw}{2\pi i} \frac{V'(w)}{w-z} \frac{1}{\sqrt{(w - c_+)(w - c_-)}} \quad (11.31)$$

and

$$M_{-1}(\underline{g}, c_-, c_+) = 2, \quad M_0(\underline{g}, c_-, c_+) = 0, \quad (11.32)$$

where we defined

$$M_k(\underline{g}, c_-, c_+) = \oint_C \frac{dw}{2\pi i} \frac{V'(w)}{(w - c_+)^{k+1/2}(w - c_-)^{1/2}}. \quad (11.33)$$

Here the first equation (11.31) determines the polynomial $M(\underline{g}, z)$ as a function of c_-, c_+ and the couplings \underline{g} , while the second equation (11.32) yields two algebraic equations which determine $c_-(\underline{g})$ and $c_+(\underline{g})$ as functions of the couplings \underline{g} .

Let us now look at two specific cases of the potential. For

$$V(\phi) = \frac{1}{2}\phi^2 \quad (11.34)$$

we expect to obtain the generating function for rooted branched polymers. Inserting $V'(z)$ into (11.29) and using the conditions (11.31)-(11.32) for the requirement that $w(z) = 1/z + \mathcal{O}(1/z^2)$ we obtain

$$w(z) = \frac{1}{2} \left(z - \sqrt{(z-2)(z+2)} \right), \quad (11.35)$$

which is precisely (5.14). Further, using (11.30) one gets for the density of eigenvalues

$$\rho(\lambda) = \frac{1}{2\pi} \sqrt{(z-2)(z+2)} \quad (11.36)$$

which is Wigner's semicircle law for the eigenvalue distribution of Hermitian matrices [183, 184].

For the potential

$$V(\phi) = \frac{1}{2}\phi^2 - \frac{g}{3}\phi^3 \quad (11.37)$$

we expect, according to the considerations made above, to obtain DT. Inserting (11.37) into (11.29) we get using (11.31)-(11.32)

$$w(g, z) = \frac{1}{2} \left(z - gz^2 - (gz - c(g)) \sqrt{(z - c_+(g))(z - c_-(g))} \right) \quad (11.38)$$

which coincides with (5.2.2), where $c(g)$, $c_-(g)$ and $c_+(g)$ are determined by the same algebraic equations as in (5.2.2).

We have seen how matrix models can be used to count generalized triangulations. Further, we showed how we can obtain DT from matrix models for the specific potential $V(\phi) = \phi^2/2 - g\phi^3/3$. In particular, we computed the disc function. In the following section we want to extend our results by calculating higher-loop amplitudes.

11.3 | The loop insertion operator and higher loop amplitudes

Even though in Chap. 5 we only calculated the one-loop amplitude for DT (disc function), we already encountered higher loop amplitudes in this thesis, namely the two-loop amplitude for DT in the continuum, i.e. (9.27).

Matrix model higher-loop amplitudes, i.e. amplitudes for generalized triangulations with b boundaries of lengths l_1, l_2, \dots, l_b , can be defined as follows

$$w_{l_1, \dots, l_b}(\underline{g}) = N^{b-2} \langle (\text{tr } \phi^{l_1}) \cdots (\text{tr } \phi^{l_b}) \rangle_c, \quad (11.39)$$

where $\langle \dots \rangle_c$ denotes the connected expectation value defined as

$$\langle O_1(\phi) \cdots O_n(\phi) \rangle_c = \langle O_1(\phi) \cdots O_n(\phi) \rangle - \langle O_1(\phi) \rangle \cdots \langle O_n(\phi) \rangle. \quad (11.40)$$

Equivalently one can also use the generating functional for the higher-loop amplitudes

$$w(\underline{g}, z_1, \dots, z_b) = N^{b-2} \left\langle \left(\text{tr } \frac{1}{z_1 - \phi} \right) \cdots \left(\text{tr } \frac{1}{z_b - \phi} \right) \right\rangle_c. \quad (11.41)$$

To calculate the higher loop amplitudes we introduce the so-called loop insertion operator [172, 185]

$$\frac{d}{dV(z)} = \sum_{j=1}^{\infty} \frac{j}{z^{j+1}} \frac{d}{dg_j}. \quad (11.42)$$

For a given potential with fixed coupling constants g_j^0 one uses these relations in the following way. Assume that g_j can vary, one now acts with the loop insertion operator $d/dV(z_2)$ say on the disc function $w(\underline{g}, z_1)$, and then set $g_j = g_j^0$ again. Each term in the summation over j has the effect that it removes a j -sided polygon⁴, leaving a marked boundary of length j to which the new boundary cosmological constant is assigned.

We now obtain the higher-loop amplitudes by successive action of the loop insertion operator on the disc function

$$w(\underline{g}, z_1, \dots, z_b) = \frac{d^{n-1}}{dV(z_b) \cdots dV(z_2)} w(\underline{g}, z_1). \quad (11.43)$$

⁴We showed above that each triangulation comes with a weight proportional to $\prod_{i=1}^{\infty} g_i^{N(i)}$, where $N(i)$ is the number of i -gons in the triangulation. Acting with d/dg_j therefore reduces the number of j -gons by one. Further it brings down a factor of $N(j)$ which precisely accounts for the number of possibilities to choose a specific j -gon.

Inserting the solution for the disc function (11.29) into (11.43) one obtains for $b=2$ the two-loop amplitude for general potential [182, 172, 173],

$$w(\underline{g}, z_1, z_2) = \frac{1}{2} \frac{1}{(z_1 - z_2)^2} \left(\frac{z_1 z_2 - \frac{1}{2}(c_- + c_+)(z_1 + z_2) + c_- c_+}{\sqrt{(z_1 - c_-)(z_1 - c_+)} \sqrt{(z_2 - c_-)(z_2 - c_+)}} - 1 \right). \quad (11.44)$$

The dependence on the potential is implicit through $c_-(\underline{g})$ and $c_+(\underline{g})$. For the case of DT this expression can be used to derive the continuum two-loop amplitude (9.27).

We will make further use of the loop insertion operator in Chap. 13, where we will look at higher genus contributions. It is clear from the loop equation (11.27) and the genus expansion

$$w(\underline{g}, N, z) = \sum_{h=0}^{\infty} N^{-2h} w_h(\underline{g}, z) \quad (11.45)$$

that to calculate the higher genus disc function higher-loop amplitudes are needed. This is similar to the situation when calculating higher genus amplitudes from the SFT in Chap. 10. We will see in Chap. 13 that this is not a coincidence, since the CDT-based SFT can be described by a matrix model.

11.4 | Discussion and outlook

In this chapter we introduced matrix models to facilitate combinatorial counting problems in DT. Matrix model techniques are very powerful to compute many quantities on the discrete level and to study further generalizations of those.

We explicitly saw how the disc function and higher-loop functions can be computed within this context. This construction can also be extended to higher genus contributions of the disc function and higher-loop amplitudes as we also commented on above (see, for instance, [185] or the more recent papers [186, 187]).

Further, we saw that matrix model techniques generalize easily to arbitrary potentials. This interesting fact allows one to study simple matter models, so-called *minimal models*, coupled to the quantum geometry (see [188] for the simplest example). In the continuum limit of the pure DT matrix model the first moment of the potential was tuned to zero while the second moment was non-zero. This situation corresponds to the so-called *2nd multi-critical hypersurface* in the space of coupling constants. Being able to introduce higher terms in the potential we can generalize this situation by going to the m th multi-critical hypersurface, where the first k moments, $k < m$ of the potential

are zero. It was seen that those minimal models correspond to so-called $(2, 2m - 1)$ -conformal field theories coupled to two-dimensional Euclidean quantum gravity.

The so-called two-matrix model allows for further applications with respect to matter coupling [189, 190, 191, 192, 193, 194, 195]. This model is used to study the Ising model coupled to two-dimensional Euclidean quantum gravity, where the two matrices are used to describe the triangles with up-pointing and down-pointing spins respectively. We will further comment on this in the final discussion of this thesis.

CHAPTER 12

A loop equation and matrix model for CDT

Matrix model techniques have been a useful tool in the field of DT. However, until recently [133, 196, 197] no matrix model for two-dimensional CDT has been found. In this chapter we introduce a newly discovered matrix model for discretized CDT [196, 197]. After motivating geometrical loop equations for the “bare” CDT model in the next section, we see that to make the link to matrix models it is important to include (weighted) spatial topology changes. In particular, we present a matrix model derivation of the generalized CDT disc function as derived in Chap. 9 purely from continuum methods.

12.1 | Geometrical loop equations for CDT

In this section we compute the generating function for a set $w_{l,N}$ of triangulations which are somewhat similar to the original set of causal triangulations and which lead to the same continuum physics: Let N denote the number of triangles and l the number of links at the boundary (which has one marked link), and assume the topology is that of the disk and denote the generating function $\tilde{w}(g, x)$:

$$\tilde{w}(g, x) = \sum_{l, N=0}^{\infty} w_{l,N} g^N x^l = \sum_{l=0}^{\infty} w_l(g) x^l. \quad (12.1)$$

Here we adopted the definition of the generating function as used in (5.9), where g is the fugacity of a triangle and x is the fugacity of a boundary edge. The triangulations

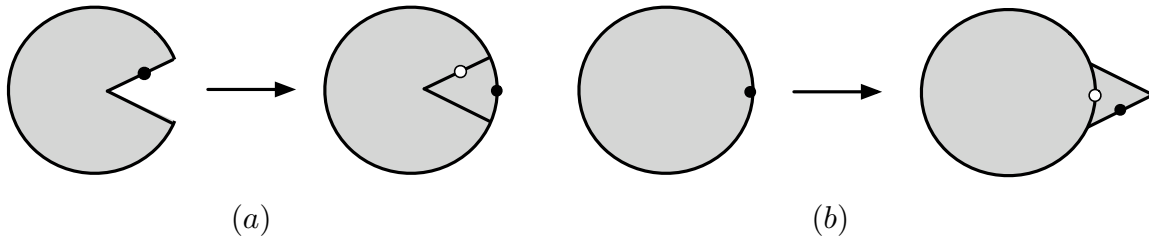


Figure 12.1: Illustration of the two composition moves to add a triangle. The white dot on the right-hand-side shows the position of the mark before the triangle was added whereas the black dot shows the mark after the triangle was added.

considered here do not have the strict time-sliced structure as those considered in Chap. 6 (e.g. see Fig. 6.1), but have a spiral structure, since they are derived using loop equations, i.e. through a peeling procedure (see Fig. 7.5). Nevertheless, we will see that this construction leads to the same continuum expressions as obtained in Chap. 6. This is similar to the derivation of the fixed geodesic distance two-loop function for DT considered in Sec. 5.3, where both the transfer matrix method and the peeling procedure lead to the same continuum results.

The triangulations can be generated by recursively adding triangles. In our model there are two possible moves. Firstly, one can glue two edges of the additional triangle to the triangulation, one to the marked edge and the other one next to it in the clockwise direction (Fig. 12.1 (a)). Secondly, one can add a triangle by simply gluing one of its edges to the marked edge of the triangulation and assigning the new mark to the new edge further clockwise (Fig. 12.1 (b)). Together, the two moves give the following generating equation for large n and l (see Fig. 12.2),

$$\tilde{w}(g, x) = 1 + \frac{g}{x} (\tilde{w}(g, x) - w_1(g)x - 1) + gx\tilde{w}(g, x). \quad (12.2)$$

The one in front and the subtraction of $w_1(g)x + 1$ are related to the initial conditions.

Equation (12.2) is a simple linear equation and the solution is given by

$$\tilde{w}(g, x) = g \left(\frac{1 - (1/g - w_1(g))x}{gx^2 - x + g} \right), \quad (12.3)$$

where as in previous situations $w_1(g)$ can be determined by demanding that the singularity structure of (12.3) does not change discontinuously near $g = 0$. The poles of

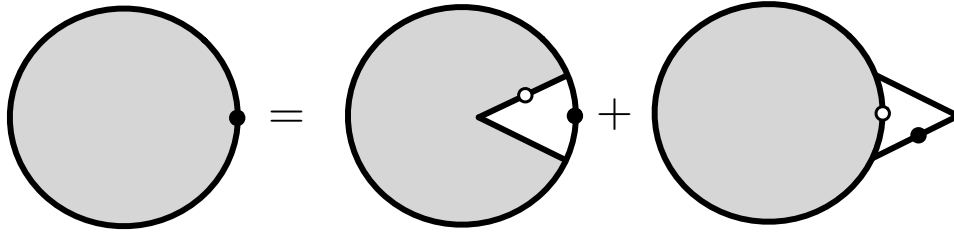


Figure 12.2: Graphical representation of the loop equation (12.2).

(12.3) are located at

$$x_{\pm} = \frac{1 \pm \sqrt{1 - 4g^2}}{2g}, \quad 1/g - x_- = x_+. \quad (12.4)$$

Since the expansion of $w_1(g)$ needs to be a power series, we have that $w_1 = x_-$. Hence the disc function is given by the following simple expression

$$\tilde{w}(g, x) = \frac{1}{1 - w_1(g)x}, \quad w_l(g) = w_1(g)^l. \quad (12.5)$$

Using the same scaling relations as in the transfer matrix formalism of CDT,

$$g = \frac{1}{2}e^{-a^2\Lambda/2}, \quad x = e^{-aX}, \quad (12.6)$$

we reproduce the continuum disc amplitude of CDT, e.g. (6.51),

$$W_{\Lambda}(X) = \frac{1}{X + \sqrt{\Lambda}}, \quad W_{\Lambda}(L) = e^{-\sqrt{\Lambda}L}. \quad (12.7)$$

12.2 | A matrix model for generalized 2D causal quantum gravity

To include weighted spatial topology changes, as has been done in Chap. 9 in the continuum, we reintroduce the quadratic term in the loop equation (12.2)

$$\tilde{w}_{\beta}(g, x) = 1 + \frac{g}{x} (\tilde{w}_{\beta}(g, x) - w_1(g, \beta)x - 1) + gx\tilde{w}_{\beta}(g, x) + \beta x^2 \tilde{w}_{\beta}(g, x)^2, \quad (12.8)$$

where β is a coupling constant that determines the rate of the spatial topology fluctuations (see Fig. 12.3).

To conform with matrix model conventions it is useful to introduce the following notation

$$w_{\beta}(g, z) = \frac{\tilde{w}_{\beta}(g, x = 1/z)}{z}, \quad (12.9)$$

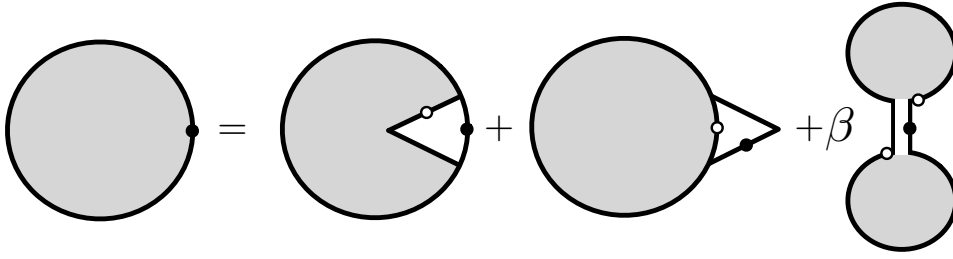


Figure 12.3: Graphical representation of the loop equation (12.8).

which has already been employed in (5.11).

With these conventions the loop equation is given by

$$\beta w_\beta(g, z)^2 - V'(z)w_\beta(g, z) + Q_\beta(g, z) = 0, \quad (12.10)$$

where

$$V(z) = -gz + \frac{1}{2}z^2 - \frac{1}{3}gz^3, \quad V'(z) = -g + z - gz^2, \quad (12.11)$$

and

$$Q_\beta(g, z) = 1 - g(w_1(g, \beta) + z). \quad (12.12)$$

The solution of the loop equation (12.10) is of the following form

$$w_\beta(g, z) = \frac{1}{2\beta} \left(V'(z) - \sqrt{V'(z)^2 - 4\beta Q_\beta(g, z)} \right). \quad (12.13)$$

At this stage the solution of the disc function is still implicit since it depends on $w_1(g, \beta)$ through (12.12). Demanding the solution to have only one cut in the complex z plane, as discussed in Sec. 11.2, gives the explicit solution

$$w_\beta(g, z) = \frac{1}{2\beta} \left(-g + z - gz^2 + (gz - c) \sqrt{(z - c_+)(z - c_-)} \right), \quad (12.14)$$

where c is the solution of a third order polynomial,

$$2c^3 - 3c^2 + (2g^2 + 1)c = g^2(1 - 2\beta), \quad (12.15)$$

and

$$c_\pm = \frac{1 - c \pm \sqrt{2}\sqrt{(1 - c)c - g^2}}{g}. \quad (12.16)$$

Written in the form of (12.10) it is easily seen from the considerations in Sec. 11.2 that this equation corresponds to the loop equation of a simple matrix model,

$$Z_\beta(g, N) = \int d\phi \exp\left(-\frac{N}{\beta} \text{tr} V(\phi)\right), \quad (12.17)$$

where ϕ is a $N \times N$ Hermitian matrix and the functional form of the potential $V(\phi)$ is given by

$$V(\phi) = -g\phi + \frac{1}{2}\phi^2 - \frac{1}{3}g\phi^3. \quad (12.18)$$

We see that in comparison with the matrix model of DT, i.e. (11.37), we have an additional linear term in the potential. For later convenience we also took the factor $1/\beta$ out of the potential, but alternatively one could have included it in the potential to be in accordance with the conventions used in (11.13).

12.3 | Taking the continuum limit

In the continuum limit of DT, as described in Sec. 5.2.2, or equivalently of the matrix model for DT, the critical value for the boundary cosmological constant z coincides with the critical value of c_+ only, i.e. $z_c = c_+(g_c)$. As a result, this standard limit has the peculiar feature that it leaves a non-scaling term as a memory of the discrete theory, since

$$w^{(eu)}(g, z) = w_{ns} + a^{3/2} W_\Lambda^{(eu)}(Z) + \mathcal{O}(a^2), \quad (12.19)$$

where $w_{ns} = (z - gz^2)/2$ is non-scaling part and $W_\Lambda^{(eu)}(X)$ the continuum disc function of DT

$$W_\Lambda^{(eu)}(Z) = \left(Z - \frac{\sqrt{\Lambda}}{2}\right) \sqrt{Z + \sqrt{\Lambda}} \quad (12.20)$$

In our specific model the matrix potential is such that the critical points of $c_+(g_c)$ and $c_-(g_c)$ coincide. This leads us naturally to the universality class of two-dimensional CDT implying the same scaling relations as before (12.6), provided one also scales the coupling constant β in exactly the same way as described in (9.7),

$$\beta = \frac{1}{2} g_s a^3, \quad c = \frac{1}{2} e^{aC}. \quad (12.21)$$

Contrary to the standard continuum limit of the one matrix model as employed by DT our new continuum limit is free from leading non-scaling contributions. Inserting the

scaling relations of the bare model (12.6), i.e.

$$g = \frac{1}{2} e^{-a^2 \Lambda / 2}, \quad z = e^{aZ}, \quad (12.22)$$

and (12.21) into (12.14) yields

$$w_\beta(g, z) = \frac{1}{a} W_{\Lambda, g_s}(Z) + \mathcal{O}(a^0), \quad (12.23)$$

where the continuum disc function $W_{\Lambda, g_s}(Z)$ is given by

$$W_{\Lambda, g_s}(Z) = \frac{1}{2g_s} \left(-(Z^2 - \Lambda) + (Z - C) \sqrt{(Z + C)^2 - 2g_s/C} \right). \quad (12.24)$$

Inserting the scaling relations (12.22) and (12.21) into the algebraic equation for c (12.15) further gives

$$C^3 - \Lambda C + g_s = 0. \quad (12.25)$$

We see that (13.1) and (13.1) agree precisely with the solution for the generalized CDT model as derived in Chap. 9 purely in a continuum framework, i.e. (9.19)-(9.20).

12.4 | The finite time propagator

Having derived the disc function of generalized CDT from a matrix model we can now also implement the decomposition moves of the above loop equation into an corresponding peeling equation for the finite time propagator. This is in analogy to the calculation of the fixed geodesic distance two-loop function in DT which has been described in Sec. 5.3.2.

Recall from Sec. 5.3.2 that in the peeling procedure it is natural to interpret the loop equation as a time dependent process [94, 125, 198], where each decomposition move on a boundary of length l is seen as a “ $1/l$ -th” part of a time step. Following [197] we can obtain an equation for the finite time propagator similar to (5.39) and (5.40) for DT. For large h_1 we have

$$\begin{aligned} \frac{\partial}{\partial t} G_\beta(h_1, l_2; g; t) &= g h_1 G_\beta(h_1 - 1, l_2; g; t) - h_1 G_\beta(h_1, l_2; g; t) + g h_1 G_\beta(h_1 + 1, l_2; g; t) + \\ &+ 2\beta h_1 \sum_{l=0}^{\infty} w_l(g, \beta) G_\beta(h_1 - l - 2, l_2; g; t). \end{aligned} \quad (12.26)$$

Here the first term on the right-hand-side is new in comparison with (5.39) and it precisely corresponds to the new move in the loop equation. In terms of the generating function we have

$$\frac{\partial}{\partial t} G_\beta(z, w; g; t) = \frac{\partial}{\partial z} [(-g + z - gz^2 - 2\beta w_\beta(g, z)) G_\beta(z, w; g; t)]. \quad (12.27)$$

Using the scaling relations defined above, i.e. (12.22) and (12.21), and letting time scale as

$$T \sim t a \quad (12.28)$$

we obtain

$$\frac{\partial}{\partial T} G_{\Lambda, g_s}(X, Y; T) = -\frac{\partial}{\partial X} [(X^2 - \Lambda + 2g_s W_{\Lambda, g_s}(X)) G_{\Lambda, g_s}(X, Y; T)]. \quad (12.29)$$

This is precisely the result obtained in Chap. 9. However, whereas in Chap. 9 we were generalizing CDT within a continuum framework, we now found an underlying discrete theory reproducing those results.

12.5 | Discussion and outlook

In this chapter we developed a loop equation and a matrix model for generalized CDT [196, 197]. For the continuum limit of this matrix model it is important that both endpoints of the cut are taken to the same critical point, i.e. $c_+(g_c) = c_-(g_c) = z_c$. To accomplish this it is essential that the matrix model has a linear term in the potential with the same coupling as the cubic term. We gave an interpretation of this linear term in terms of a new move in the loop equation.

In the next chapter we will see an intriguing aspect of this new matrix model continuum limit, namely, that it does not require N to scale with the cutoff in the so-called double scaling limit [199, 200, 201]. Moreover the continuum results are also described by a matrix model. This matrix model has of course both an expansion in the coupling constants g_s and Λ , as well as a large- N expansion in powers of $1/N^2$, which reorganizes the power expansions in g_s and Λ in convergent “subseries”. By comparing with the generalized causal dynamical triangulation model the powers of N^{-2h+2} in the large N expansion can be identified with the continuum causal dynamical surfaces of genus h [133]. In this sense our new continuum limit leads to a picture that is much closer in spirit to the original idea by 't Hooft [179] for QCD.

An advantage of having a matrix model description is its computational strength. Until now, only the transfer matrix formalism has been available for analytical computations in CDT. Here we extended the available tools and presented new, more powerful, matrix model and loop equation methods. Importantly, these new methods allow one to analytically study simple matter models coupled to two-dimensional causal quantum gravity, such as minimal models or the Ising model. Several of these models are currently under investigation.

It is interesting that two-dimensional CDT without spatial topology change is not described by a matrix model. Pure CDT is only recovered when taking the limit $g_s \rightarrow 0$ of the loop equations for generalized CDT. There exists a rather complicated matrix model description for the one-step propagator of three-dimensional CDT [137, 139]. It seems quite plausible that if one allows for branching baby universes weighted by a coupling g_s the matrix model could greatly simplify.

CHAPTER 13

A continuum matrix model for CDT

In the previous chapter we found a matrix model for two-dimensional causal quantum gravity defined through CDT. In this chapter we show that not only the discrete, but also the continuum model of CDT can be described by a matrix model [133]. This is a very interesting result, since in the DT context matrix models have only been used on the discretized level and not in the continuum.

13.1 | Mapping the DSE

One interesting observation is that the *continuum* expression of the disc function for generalized CDT (9.19), as derived in Chap. 9, is very similar to the expression of the disc function obtained from matrix models, i.e. (11.29). Writing (9.19) in the following way it becomes more obvious:

$$W_{\Lambda, g_s}(X) = \frac{1}{2g_s} \left(-(X^2 - \Lambda) + (X - C) \sqrt{(X - C_-)(X - C_+)} \right). \quad (13.1)$$

where the constants C , C_{\pm} are determined by

$$C^3 - \Lambda C + g_s = 0, \quad C_{\pm} = -C \pm \sqrt{2g_s/C}. \quad (13.2)$$

This analogy can be pushed much further. Introducing the notation

$$V'(X) = \frac{1}{g_s}(\Lambda - X^2), \quad V(X) = \frac{1}{g_s} \left(\Lambda X - \frac{1}{3} X^3 \right), \quad (13.3)$$

we can rewrite the DSE from the CDT-based SFT, i.e. (10.37)-(10.39), in the following way

$$0 = \partial_X \left(-V'(X)W(X) + W^2(X) + \alpha W(X, X) \right) - \frac{1}{g_s}, \quad (13.4)$$

$$\begin{aligned} 0 = & \partial_X \left([-V'(X) + 2W(X)]W(X, Y) + \alpha W(X, X, Y) \right) + \\ & \partial_Y \left([-V'(Y) + 2W(Y)]W(X, Y) + \alpha W(X, Y, Y) \right) + \\ & + 2\partial_X \partial_Y \left(\frac{W(X) - W(Y)}{X - Y} \right), \end{aligned} \quad (13.5)$$

$$\begin{aligned} 0 = & \partial_X \left([-V'(X) + 2W(X)]W(X, Y, Z) + \alpha W(X, X, Y, Z) \right) + \\ & \partial_Y \left([-V'(Y) + 2W(Y)]W(X, Y, Z) + \alpha W(X, Y, Y, Z) \right) + \\ & \partial_Z \left([-V'(Z) + 2W(Z)]W(X, Y, Z) + \alpha W(X, Y, Z, Z) \right) + \\ & 2\partial_X [W(X, Y)W(X, Z)] + 2\partial_Y [W(X, Y)W(Y, Z)] + \\ & 2\partial_Z [W(X, Z)W(Y, Z)] + 2 \left(\partial_X \partial_Y \frac{W(X, Z) - W(Y, Z)}{X - Y} + \right. \\ & \left. \partial_X \partial_Z \frac{W(X, Y) - W(Y, Z)}{X - Z} + \partial_Y \partial_Z \frac{W(X, Y) - W(X, Z)}{Y - Z} \right). \end{aligned} \quad (13.6)$$

Let us introduce the expansion¹

$$W(X_1, \dots, X_n) = \sum_{h=0}^{\infty} \alpha^h W_h(X_1, \dots, X_n). \quad (13.7)$$

As shown in Chap. 10, h can be interpreted as the number of handles of the worldsheet, and the equations above can be solved iteratively in h . More precisely, the equations at order α^0 allow us to determine $W_0(x)$, $W_0(x, y)$, ..., and similarly the equations at general order α^h determine $W_h(x)$, $W_h(x, y)$, etc. For example, one finds

$$W_0(X) = \frac{1}{2} \left(V'(X) + \frac{1}{g_s} (X - C) \sqrt{(X - C_-)(X - C_+)} \right), \quad (13.8)$$

$$W_0(X, Y) = \frac{1}{2} \frac{1}{(X - Y)^2} \left(\frac{XY - \frac{1}{2}(C_- + C_+)(X + Y) + C_- C_+}{\sqrt{(X - C_-)(X - C_+)} \sqrt{(Y - C_-)(Y - C_+)}} - 1 \right), \quad (13.9)$$

¹Note that both W and W_h are still g_s -dependent, although we do not write the dependence explicitly here.

where the constants C and C_{\pm} are defined as in (13.2) above.

Writing the amplitudes in this fashion leads one to the surprising realization that $W_0(X)$ and $W_0(X, Y)$ indeed coincide with the large- N limit of the disc function and two-loop function of a Hermitian matrix model

$$Z_{g_s}(\Lambda, N) = \int d\Phi e^{-N \text{tr} V(\Phi)} \quad (13.10)$$

with potential

$$V(\Phi) = \frac{\Lambda}{g_s} \Phi - \frac{1}{3g_s} \Phi^3. \quad (13.11)$$

This is a potentially exciting result, because so far no standard formulation in terms of matrix models has been found for a continuum model of quantum gravity. We will in the following section show a more general result which identifies the Dyson-Schwinger equations derived above with the loop equations of a Hermitian matrix model with the cubic potential (13.11).

13.2 | Matrix loop equations

In Sec. 11.3 we explained how in a matrix model context loop equations for higher-loop amplitudes can be derived from the loop equation of the disc function by applying the loop insertion operator sufficiently many times, as summarized in (11.43). In order to compare with the Dyson-Schwinger equations of our string field theory, we differentiate the equations obtained with respect to X . For the potential (13.11) we arrive at the following equations

$$0 = \partial_X \left(-V'(X)W(X) + W^2(X) + \frac{1}{N^2} W(X, X) \right) - \frac{1}{g_s}, \quad (13.12)$$

$$0 = \partial_X \left([-V'(X) + 2W(X)]W(X, Y) + \frac{1}{N^2} W(X, X, Y) \right) + \partial_X \partial_Y \left(\frac{W(X) - W(Y)}{X - Y} \right), \quad (13.13)$$

$$0 = \partial_X \left([-V'(X) + 2W(X)]W(X, Y, Z) + \frac{1}{N^2} W(X, X, Y, Z) \right) + 2\partial_X \left(W(X, Z)W(X, Y) \right) + \partial_X \partial_Y \left(\frac{W(X, Z) - W(Y, Z)}{X - Y} \right) + \partial_X \partial_Z \left(\frac{W(X, Y) - W(Z, Y)}{X - Z} \right). \quad (13.14)$$

Using that $W(X_1, \dots, X_n)$ is a symmetric function of its arguments, we see that eqs. (13.12)-(13.14) lead to exactly the same coupled equations for W as do (13.4)-(13.6) if we identify

$$\alpha = \frac{1}{N^2}. \quad (13.15)$$

In this case the discussion surrounding the expansion (13.7) is nothing but the standard discussion of the large- N expansion

$$W(X_1, \dots, X_n) = \sum_{h=0}^{\infty} N^{-2h} W_h(X_1, \dots, X_n) \quad (13.16)$$

of the multi-loop correlators (see [185] or for more recent developments [186, 187]). The iterative solution of these loop equations is uniquely determined by $W_0(X)$ provided that $W(X_1, \dots, X_n)$ is analytic in those X_i that do not belong to the cut of the matrix model.

13.3 | Relation to the discrete matrix model

In the previous chapter we saw how the *discretized* model of CDT could be described by a matrix model with the following partition function and action

$$Z_{\beta}^{(d)}(g, N) = \int d\phi e^{-S^{(d)}[\phi]}, \quad S^{(d)}[\phi] = \frac{N}{\beta} \text{tr} \left(-g\phi + \frac{1}{2}\phi^2 - \frac{1}{3}g\phi^3 \right). \quad (13.17)$$

In comparison, in this chapter, we obtained a matrix model for the *continuum* model of CDT, described by

$$Z_{g_s}^{(c)}(\Lambda, N) = \int d\Phi e^{-S^{(c)}[\Phi]}, \quad S^{(c)}[\Phi] = \frac{N}{g_s} \text{tr} \left(\Lambda\Phi - \frac{1}{3}\Phi^3 \right). \quad (13.18)$$

It is a very surprising result that both matrix models can be related by taking the continuum limit on the level of the action. Inserting the standard scaling relations

$$\beta = \frac{1}{2}g_s a^3, \quad g = \frac{1}{2}e^{-a^2\Lambda/2} \quad (13.19)$$

together with a scaling of the matrices

$$\phi = e^{a\Phi} = \sum_{n=0}^{\infty} \frac{1}{n!} (a\Phi)^n, \quad \Phi^0 = 1_{N \times N} \quad (13.20)$$

into the action (13.17) of the matrix model for the discrete CDT model gives

$$S^{(d)}[\phi] = \frac{N}{g_s} \text{tr} \left(\Lambda \Phi - \frac{1}{3} \Phi^3 \right) + \text{const.} + \mathcal{O}(a). \quad (13.21)$$

Hence we see that the matrix model for continuum CDT follows from the one for the discrete model by simply taking the continuum limit on the level of the action.

This situation is very different to the one encountered in the matrix model for DT. Due to the absence of the coupling β one has to perform a *double scaling limit* in which N scales as

$$N(a) \equiv e^{1/G_N(a)} = \Lambda^{-5/4} a^{-5/2} \quad (13.22)$$

such that the dimensionless Newton's constant

$$\frac{1}{G_N^{\text{ren}}} = \frac{1}{G_N(a)} + \frac{5}{4} \log(\Lambda a^2) = \log(N(a) a^{5/2}) \quad (13.23)$$

remains finite as $a \rightarrow 0$ and $N \rightarrow \infty$. In contrary, in our continuum CDT matrix model N does not have to scale with the cut-off.

13.4 | Discussion and Outlook

Let us consider the matrix model corresponding to the potential (13.11). We can perform a simple change of variables $\Phi \rightarrow -\Phi - \sqrt{\Lambda}$ in the matrix integral to obtain a standard matrix integral

$$Z_{g_s}(m, N) = \int d\Phi e^{-N \text{tr} V(\Phi)}, \quad (13.24)$$

where the new potential (up to an irrelevant constant term) is given by

$$V(\Phi) = \frac{1}{g_s} \left(\frac{1}{2} m \Phi^2 + \frac{1}{3} \Phi^3 \right), \quad m = 2\sqrt{\Lambda}. \quad (13.25)$$

It is amusing to note that the matrix integral (13.24) is precisely the kind of matrix integral considered in the so-called Dijkgraaf-Vafa correspondence [202, 203], where in this case $V(\Phi)$ is the tree-level superpotential of the adjoint chiral field Φ , which breaks the supersymmetry of the unitary gauge theory from $\mathcal{N} = 2$ to $\mathcal{N} = 1$. If one demands that this tree-level potential correspond to a renormalizable theory, its form is essentially unique, and precisely of the form (13.25) originally used by Dijkgraaf and Vafa, with g_s a dimension-three coupling constant coming from topological string

theory and in the DV-correspondence related to the glueball superfield condensate in the gauge theory.

In the “old” matrix model representation of non-critical strings and two-dimensional gravity one had to perform a fine-tuning of the coupling constants in order to obtain a continuum string or quantum gravity theory. This implemented the gluing of triangles (or, more generally, of squares, pentagons, etc.) which served as a regularization of the worldsheet. The fine-tuning of the coupling constants reflected the fact that the link length of the triangles (the lattice spacing of the dynamical lattice) was taken to zero in the continuum limit. The situation here is different. Although CDT can be constructively defined as the continuum limit of a dynamical lattice, we have in the present work been dealing only with the associated continuum theory. Thus in our case the matrix model with the potential (13.11) (or (13.24)) already describes a *continuum* theory of two-dimensional quantum gravity. Its coupling constants can be viewed as continuum coupling constants and the role of N is exactly as in the original context of QCD, namely, to *reorganize* the expansion in the coupling constant g_s . 't Hooft's large- N expansion of QCD is a reorganization of the perturbative series in the Yang-Mills coupling g_{YM} , with $1/N$ taking the role of a new expansion parameter. In this framework, after the coefficient of the term $1/N^{2h}$ of some observable has been calculated as function of the 't Hooft coupling $g_H^2 = g_{\text{YM}}^2 N$, one must take $N = 3$ for $SU(3)$, say. The situation in CDT string field theory is entirely analogous: starting from a perturbative expansion in the “string coupling constant” g_s (in fact, in the dimensionless coupling constant $g_s/\Lambda^{3/2}$, as described in previous chapters), we can reorganize it as a topological expansion in the genus of the worldsheet by introducing the expansion parameter α . For the multi-loop correlators this expansion is exactly the large- N expansion of the matrix model (13.11) and the coefficients, the functions $W_h(X_1, \dots, X_n)$, are exactly the multi-loop correlators for genus- h worldsheets of the CDT string field theory with $\alpha = 1$.

As a “bonus” for our treatment of generalized (and therefore slightly causality-violating) geometries, we also obtain a matrix formulation of the original two-dimensional CDT model as discussed in Chap. 6, where the spatial universe was *not* allowed to split. Working out the limit as $g_s \rightarrow 0$ of the various expressions derived above, we see that this model corresponds to the large- N limit of the matrix model where the coupling constants go to infinity, but at the same time the cut shrinks to a point in such a way

that the resolvent (or disk amplitude) survives, that is,

$$W_0(X) \rightarrow \frac{1}{X + \sqrt{\Lambda}} = W_\Lambda^{(cdt)}(X). \quad (13.26)$$

The existence of a matrix model describing the algebraic structure of the DSE leads automatically to the existence of Virasoro-like operators L_n , $n \geq -1$ [182, 172], which can be related to redefinitions of the time variable T in the string field theory. This line of reasoning has already been pursued by Ishibashi, Kawai and collaborators in the context of non-critical string field theory. It would be interesting to perform the same analysis in the CDT model and show that reparametrization under the change of time-variable will reappear in a natural way in the model via the operators L_n . The results should be simpler and more transparent than the corresponding results in non-critical string field theory since we have a non-trivial free Hamiltonian H_0 in the CDT model.

CHAPTER 14

Summary and conclusions

In this thesis we discussed the incorporation of causality in models of random geometry.

In the first part of this thesis we introduced causal sets as a simple and instructive model of causal random geometry. Using a phenomenological model where causal sets are faithfully embedded in a fixed continuum space-time, we proposed a measure for the maximal entropy of spherically symmetric spacelike space-time regions. Using this entropy measure, a bound for the entropy contained in such a region was derived from a counting of potential “degrees of freedom” associated with the Cauchy horizon of its future domain of dependence. For different spherically symmetric spacelike regions in Minkowski spacetime of arbitrary dimension, we showed that this proposal leads, in the continuum approximation, to Susskind’s and Bekenstein’s well-known spherical entropy bound up to a numerical factor. It was interesting to observe how the interplay between causality and discreteness leads to holography and finite entropy in the continuum approximation.

In the remaining parts of this thesis we focused on the causal dynamical triangulations (CDT) approach to quantum gravity.

In Chap. 4 we gave a brief introduction to path integrals. After a short exposition of the path integral for the relativistic particle and the relativistic string, we discussed problems one encounters when defining a path integral for quantum gravity.

In Chap. 5 we described dynamical triangulations (DT) as a non-perturbative definition of the path integral for two-dimensional Euclidean quantum gravity. We showed an analytical solution and discussed the resulting quantum geometries. An intriguing aspect is the fractal structure of the two-dimensional geometries and the related Hausdorff dimension $d_H = 4$. This behavior can be explained in terms of an excessive off-splitting of baby universes. We commented on how this proliferation of spatial topology changes leads to problems when trying to obtain a sensible continuum limit of DT in dimensions higher than two.

In Chap. 6 we introduced two-dimensional Lorentzian quantum gravity which can be defined through causal dynamical triangulations (CDT). The triangulations used in CDT have a global time-slicing without spatial topology changes, i.e. off-splitting baby universes. This is in contrast to DT where spatial topology changes are naturally present. The global notion of time enables us to define a gravitational Wick rotation. We described how to solve the combinatorial problem analytically using transfer matrix techniques and performed the continuum limit. As a result one observes that two-dimensional CDT and DT are distinct theories. Whereas the continuum dynamics of DT is completely dominated by spatial topology changes leading to a fractal dimension of $d_H = 4$, in CDT one has $d_H = 2$. We briefly commented on results in higher dimensions, where the causality constraint is essential to obtain a sensible continuum limit.

In Chap. 7 we explained several relations between both models. In particular, we showed how CDT and DT can be related by respectively introducing or “integrating out” baby universes, i.e. spatial topology changes.

In Chap. 8 we analyzed two-dimensional CDT with non-compact space-times. In this situation a semi-classical background emerges from quantum fluctuations yielding a simple model of two-dimensional quantum cosmology.

In the following part of this thesis we introduced a generalized CDT model which was formulated as a third quantization of two-dimensional CDT, i.e. a model in which spatial universes or strings can be annihilated, and created from the vacuum. In Chap. 9 we showed how by introducing a coupling constant g_s to the process of off-splitting baby-universes one can non-perturbatively solve for the disc function with an arbitrary number of baby-universes. In Chap. 10 this result was embedded in the framework of a string field theory (SFT) model of CDT. As an application of the resulting Dyson-Schwinger equations (DSE) of the SFT we calculated amplitudes of higher genus.

One of the biggest achievements of this thesis is the development of a matrix model

for two-dimensional causal quantum gravity defined through CDT. After a short introduction to matrix model techniques employed in DT in Chap. 11, we formulated a matrix model to solve combinatorial problems of the discretized CDT model in Chap. 12. In Chap. 13 we showed that also the generalized CDT model in the continuum is described by a matrix model. Interestingly, both matrix models can be related by taking a continuum limit already on the level of the action. Subsequently, the continuum theory also has a large- N expansion in which terms with powers N^{-2h+2} can be identified with continuum causal surfaces of genus h . In this sense, the role of N is exactly as in the original context of 't Hooft's large- N expansion of QCD, namely, to reorganize the expansion in the coupling constant g_s .

One advantage of having a matrix model is the computational strength. Until now, only transfer matrix techniques have been available for analytical computations in CDT. Here we extend the available tools by introducing powerful matrix model techniques for CDT.

One possible application is to lift the analytical methods to higher-dimensional CDT. In fact, there already exists a matrix model for three-dimensional CDT [137, 139]. However, this model is rather complicated which is partially related to the fact that it does not allow for off-splitting baby universes. From the discussion above, it seems quite plausible that if one allows for the outgrowth of baby universes weighted by a coupling g_s the matrix model could greatly simplify.

Another important application comes from the fact that the new matrix model allows one in principle to analytically study simple matter models coupled to two-dimensional causal quantum gravity, such as minimal models or the Ising model. Several of these models are currently under investigation.

With respect to applying the matrix model to couple the Ising model to CDT there is a very interesting feature, namely, that the triangulations appearing in CDT are much more regular than the triangulations appearing in DT. In particular, we observed that a generic triangulation appearing in DT has a fractal dimension $d_H = 4$, while a generic triangulation appearing in CDT has a Hausdorff dimension $d_H = 2$. If one couples the Ising model to DT the critical exponents will change from the Onsager-values (see for instance [204, 205, 206]) to the so-called KPZ-values [190, 191]. This change can be traced to the very fractal structure of generic triangulations in DT. However, we have seen that generic triangulations in CDT do not have this fractal structure and we expect the critical exponents to be much more similar to those of the flat case. Notably,

it has been shown in numerical simulations that the critical exponents for the Ising model coupled to CDT are precisely given by the Onsager-values [207, 178, 208]. By generalizing the one-matrix model of CDT, as presented in this thesis, to a two-matrix model one should be able to prove analytically that the critical exponents are indeed given by the Onsager-values. In fact, if possible, this would be by far the simplest derivation of the Onsager exponents from an Ising-lattice model. Work in this direction is in progress.

We hope to have convinced the reader that the incorporation of causality in models of random geometry leads to interesting models of causal quantum gravity and to fascinating new results. As described above there are still many interesting challenges and we will hopefully report on them soon.

APPENDIX A

Annexes: Causal sets

A.1 | Basic definitions regarding the causal structure

In this appendix we state some of the basic concepts regarding the causal structure of continuum spacetimes. For further references the reader is referred to [209, 210], where we follow the conventions of [209].

Let (\mathcal{M}, g) be a time orientable spacetime. We define a differentiable curve $\lambda(t)$ to be a *future directed timelike curve* if at each point $p \in \lambda$ the tangent t^a is a future directed timelike vector. Further, $\lambda(t)$ is called a *future directed causal curve* if at each $p \in \lambda$ the tangent t^a is a future directed timelike or null vector.

Using this definition one can define the chronological future (past) and causal future (past) of a spacetime event or a set of spacetime events. The *chronological future* of $p \in \mathcal{M}$, denoted by $I^+(p)$, is defined as

$$I^+(p) = \{q \in \mathcal{M} \mid \exists \text{ future directed timelike curve } \lambda(t) \text{ s.t. } \lambda(0) = p \text{ and } \lambda(1) = q\} \quad (\text{A.1})$$

For any subset $\Sigma \subset \mathcal{M}$ we thus define

$$I^+(\Sigma) = \bigcup_{p \in \Sigma} I^+(p) \quad (\text{A.2})$$

In analogy to $I^+(p)$ and $I^+(\Sigma)$ we can also define the *chronological past* $I^-(p)$ and $I^-(\Sigma)$ by simply replacing “future” by “past” in (A.1).

In analogy to the chronological future we can also define the *causal future* of a point $p \in \mathcal{M}$, denoted by $J^+(p)$, by replacing “future directed timelike curve” by “future directed causal curve” in (A.1). The definition of $J^+(\Sigma)$, $J^-(p)$ and $J^-(\Sigma)$ then follow accordingly.

Very important for the formulation of the entropy bound stated in Sec. 3.2 is the concept of the domain of dependence of a spacetime region.

Let Σ be any spacelike hypersurface of \mathcal{M} . We define the *future domain of dependence* of Σ , denoted by $D^+(\Sigma)$, by

$$D^+(\Sigma) = \{p \in \mathcal{M} \mid \text{every past inextendible causal curve through } p \text{ intersects } \Sigma\}. \quad (\text{A.3})$$

Analogously, one can define the *past domain of dependence* of Σ , denoted by $D^-(\Sigma)$, by simply replacing “past” by “future” in (A.3).

Using the definitions above one can then define the future and past Cauchy horizon. Let Σ be any spacelike hypersurface of \mathcal{M} . The *future Cauchy horizon* of Σ , denoted by $H^+(\Sigma)$, is defined as

$$H^+(\Sigma) = \overline{D^+(\Sigma)} \setminus I^-(D^+(\Sigma)), \quad (\text{A.4})$$

where $\overline{D^+(\Sigma)}$ is the closure of $D^+(\Sigma)$. The *past Cauchy horizon*, $H^-(\Sigma)$, can be defined in analogy to (A.4). The different concepts defined in this subsection are illustrated in Fig. 3.1.

A.2 | Volume of the causal region between two events

In this appendix we calculate the volume of the intersection of the causal future of an event p with the causal past of another event $q \in J^+(p)$ in Minkowski spacetime \mathbb{M}^d , i.e. the Alexandrov region $J^+(p) \cap J^-(q)$. This volume depends only on the proper time τ between p and q and hence we set $\text{Vol}_d(\tau) \equiv \text{Vol}(J^+(p) \cap J^-(q))$.

Note that the volume of a d -dimensional ball with radius r , $S_d(r)$, is given by

$$\text{Vol}(S_d(r)) = \frac{\pi^{\frac{d}{2}} r^d}{\Gamma(\frac{d}{2} + 1)} =: C_d r^d, \quad \text{with} \quad C_d = \frac{\pi^{\frac{d}{2}}}{\Gamma(\frac{d}{2} + 1)}. \quad (\text{A.5})$$

Using this we obtain

$$\begin{aligned}\text{Vol}_d(\tau) &= 2 \int_0^{\frac{\tau}{2}} dt \text{Vol}(S_{d-1}(t)) \\ &= \frac{\pi^{\frac{d-1}{2}}}{2^{d-1} d \Gamma(\frac{d+1}{2})} \tau^d =: D_d \tau^d, \quad \text{with } D_d = \frac{C_{d-1}}{2^{d-1} d}.\end{aligned}\quad (\text{A.6})$$

Specifically we get $\text{Vol}_2(\tau) = \frac{1}{2}\tau^2$, $\text{Vol}_3(\tau) = \frac{\pi}{12}\tau^3$ and $\text{Vol}_4(\tau) = \frac{\pi}{24}\tau^4$.

A.3 | Asymptotics of the generalized hypergeometric function

In this appendix we obtain the asymptotic expansion of the generalized hypergeometric function as given in (3.29) to first order.

We use the general expression for the asymptotic expansion of the generalized hypergeometric function ${}_pF_q$ with $p=q$ which can be derived from [211]

$$\begin{aligned}{}_pF_p(a_1, \dots, a_p; b_1, \dots, b_p; z) &= \left(\prod_{j=1}^p \frac{\Gamma(b_j)}{\Gamma(a_j)} \right) e^z z^\gamma \left(1 + \mathcal{O}\left(\frac{1}{z}\right) \right) + \\ &+ \left(\prod_{j=1}^p \frac{\Gamma(b_j)}{\Gamma(a_j)} \right) \sum_{k=1}^p \frac{\Gamma(a_k) \prod_{j=1, j \neq k}^p \Gamma(a_j - a_k)}{\prod_{j=1}^p \Gamma(b_j - a_k)} (-z)^{-a_k} \left(1 + \mathcal{O}\left(\frac{1}{z}\right) \right), \quad |z| \rightarrow \infty\end{aligned}\quad (\text{A.7})$$

where

$$\gamma = \sum_{k=1}^p a_k - b_k \quad \text{and} \quad a_k \neq a_j \quad \forall \quad k \neq j.\quad (\text{A.8})$$

In the special case of (3.29) we cannot straightforwardly apply (A.7), since $a_{p-1} = a_p$. However, since we are only interested in the first order behavior and $a_1 < a_j$ with $a_1 \neq a_j$ for all $2 \leq j \leq p$, we can obtain the asymptotic expansion of (3.29) to first order, yielding

$$\begin{aligned}{}_{\frac{d}{2}+1}F_{\frac{d}{2}+1} \left(\frac{2}{d}, \frac{4}{d}, \dots, \frac{d}{d}, 1; \frac{d+1}{d}, \frac{d+3}{d}, \dots, \frac{2d-1}{d}, 2, -2^{1-d}N \right) \\ = \left(\prod_{j=1}^{\frac{d}{2}+1} \frac{\Gamma(b_j)}{\Gamma(a_j)} \right) \frac{\Gamma(a_1) \prod_{j=2}^{\frac{d}{2}+1} \Gamma(a_j - a_1)}{\prod_{j=1}^{\frac{d}{2}+1} \Gamma(b_j - a_1)} (2^{1-d}N)^{-a_1} + \mathcal{O}(N^{-2a_1}), \quad N \rightarrow \infty \\ = \frac{d-1}{d} \frac{2^{\frac{2d-2}{d}} \pi}{\sin\left(\frac{2\pi}{d}\right) \Gamma\left(\frac{2d-2}{d}\right)} N^{-\frac{2}{d}} + \mathcal{O}(N^{-\frac{4}{d}}), \quad N \rightarrow \infty.\end{aligned}\quad (\text{A.9})$$

APPENDIX **B**

Annexes: Causal dynamical triangulations

B.1 | Lorentzian angles and simplicial building blocks

In this appendix, a brief summary of results on Lorentzian angles is presented, where we follow the treatment and conventions of [212].

Since in CDT one considers simplicial manifolds consisting of Minkowskian triangles, Lorentzian angles or “boosts” naturally appear in the Regge action as rotations around vertices. Recall from Section 5.1 that the definition of the Gaussian curvature at a vertex v is given by (5.1),

$$K_v = \frac{\epsilon_v}{V_v}, \quad (\text{B.1})$$

where $\epsilon_v = 2\pi - \sum_{i \supset v} \theta_i$ is the deficit angle at a vertex v and V_v is the dual volume of the vertex v . Recall that the space-like deficit angle ϵ_v can be positive or negative as illustrated in Figure 5.1. Furthermore, if the deficit angle is time-like, as shown in Figure B.1, it will be complex. The time-like deficit angles are still additive, but contribute to the curvature (B.1) with the opposite sign. Hence, both space-like defect and time-like excess increase the curvature, whereas space-like excess and time-like defect decrease it.

The complex nature of the time-like deficit angles can be seen explicitly by noting that the angles θ_i between two edges \vec{a}_i and \vec{b}_i (as vectors in Minkowski space) are

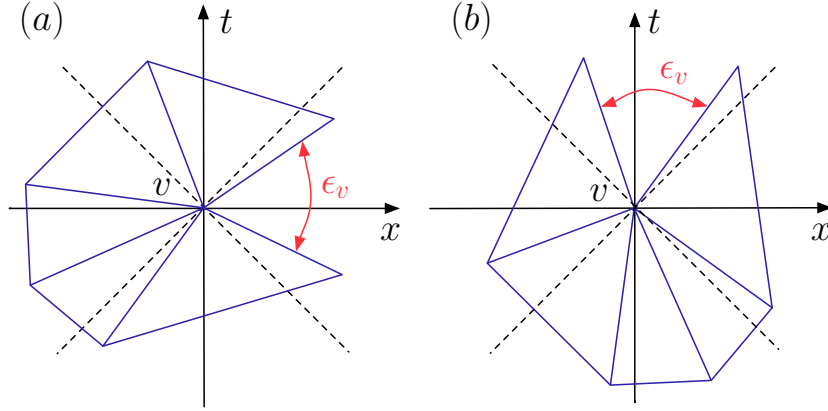


Figure B.1: Illustration of a space-like (a) and a time-like (b) Lorentzian deficit angle ϵ_v at a vertex v .

calculated using

$$\cos \theta_i = \frac{\langle \vec{a}_i, \vec{b}_i \rangle}{\langle \vec{a}_i, \vec{a}_i \rangle^{\frac{1}{2}} \langle \vec{b}_i, \vec{b}_i \rangle^{\frac{1}{2}}}, \quad \sin \theta_i = \frac{\sqrt{\langle \vec{a}_i, \vec{a}_i \rangle \langle \vec{b}_i, \vec{b}_i \rangle - \langle \vec{a}_i, \vec{b}_i \rangle^2}}{\langle \vec{a}_i, \vec{a}_i \rangle^{\frac{1}{2}} \langle \vec{b}_i, \vec{b}_i \rangle^{\frac{1}{2}}}, \quad (\text{B.2})$$

where $\langle \cdot, \cdot \rangle$ denotes the flat Minkowskian scalar product and by definition, the square roots of negative arguments are positive imaginary.

Having given a concrete meaning to Lorentzian angles, we can now use (B.2) to calculate the volume of Minkowskian triangles which we will then use to explicitly compute the volume terms of the Regge action.

The triangulations we are considering consist of Minkowskian triangles with one space-like edge of length squared $l_s^2 = a^2$ and two time-like edges of length squared $l_t^2 = -\alpha a^2$ with $\alpha > 0$. The general argument $\alpha > 0$ is used to give a mathematically precise prescription of the Wick rotation, but it can be set to $\alpha = 1$ after the Wick rotation has been performed. With the use of (B.2) we can calculate the volume of such a Minkowskian triangle, yielding

$$\text{Vol}(\text{triangle}) = \frac{a^2}{4} \sqrt{4\alpha + 1}. \quad (\text{B.3})$$

Now one can define the Wick rotation \mathcal{W} as the analytic continuation of $\alpha \mapsto -\alpha$ through the lower-half plane. One then sees that for $\alpha > \frac{1}{2}$ under this prescription

$i \text{Vol}(\text{triangle}) \mapsto -\text{Vol}(\text{triangle})$ (up to a $\mathcal{O}(1)$ constant which can be absorbed in the corresponding coupling constant in the action). This ensures that

$$\mathcal{W} : e^{i S_{\text{Regge}}(\mathcal{T}^{\text{lor}})} \mapsto e^{-S_{\text{Regge}}(\mathcal{T}^{\text{eu}})}, \quad \alpha > \frac{1}{2}. \quad (\text{B.4})$$

In the following we set $\alpha = 1$ again. Generalizations of this treatment to dimension $d = 3, 4$ can be found in [136].

B.2 | Analyzing Hamiltonians for causal quantum gravity

In this appendix we analyze the properties and spectrum of Hamiltonians which one usually encounters in causal quantum gravity such as discussed in Sec. 6.5. Generally the Hamiltonian appearing in this context are of the form

$$\hat{H}(L, \frac{\partial}{\partial L}) = -c_1 L \frac{\partial^2}{\partial L^2} - c_2 \frac{\partial}{\partial L} + \Lambda L \quad (\text{B.5})$$

where c_1 and c_2 are real constants. In the following we investigate this generalized class of Hamiltonians.

It is immediately checked that the Hamiltonian (B.5) is selfadjoint on the Hilbert space $\mathcal{H} = \mathcal{L}^2(\mathbb{R}_+, d\mu(L))$, where the measure $d\mu(L)$ is given by

$$d\mu(L) = L^\mu dL, \quad \mu = \frac{c_2}{c_1} - 1. \quad (\text{B.6})$$

Further, for the boundary components of the partial integration in $\langle \hat{H}\psi | \phi \rangle = \langle \psi | \hat{H}\phi \rangle$ to vanish, the wave functions on the Hilbert space must satisfy

$$\left[L^{\mu+1} \psi(L) \frac{\partial}{\partial L} \psi(L) \right]_0^\infty = 0 \quad (\text{B.7})$$

To have a Hilbert space with flat measure, one can pull the measure into the wave function by substituting $\Psi(L) = L^{-\frac{\mu}{2}} \psi(L)$, where $\psi(L)$ is the wave function corresponding to (B.5). Commuting $L^{-\frac{\mu}{2}}$ through the Hamiltonian gives

$$\hat{H}^{\text{flat}}(L, \frac{\partial}{\partial L}) = -c_1 L \frac{\partial^2}{\partial L^2} - c_1 \frac{\partial}{\partial L} + \Lambda L + \frac{(c_1 - c_2)^2}{4c_1} \frac{1}{L}, \quad d\mu(L) = dL \quad (\text{B.8})$$

This pulling in and out of the measure is similar to what one does when introducing markings on the boundary loops.

We now consider the eigenvalue problem of the Hamiltonian (B.8),

$$\left(-c_1 L \frac{\partial^2}{\partial L^2} - c_1 \frac{\partial}{\partial L} + \Lambda L + \frac{(c_1 - c_2)^2}{4c_1} \frac{1}{L} - E \right) \Psi(L) = 0. \quad (\text{B.9})$$

Let us perform a change of variables and wave functions,

$$L = \frac{c_1}{2} \varphi^2, \quad \Phi(\varphi) = \sqrt{\varphi} \Psi \left(\frac{\varphi^2}{2} \right), \quad (\text{B.10})$$

where the latter guarantees a flat measure $d\mu(\varphi) = d\varphi$ for $\Phi(\varphi)$. The eigenvalue problem then reads

$$\left(-\frac{1}{2} \frac{\partial^2}{\partial \varphi^2} + \frac{1}{2} \omega^2 \varphi^2 - \frac{1}{8} \frac{A}{\varphi^2} - E \right) \Phi(\varphi) = 0, \quad (\text{B.11})$$

where we set $\omega = \sqrt{c_1 \Lambda}$ and $A = 1 - 4\mu^2 \in (-\infty, 1)$. This is nothing but the eigenvalue problem corresponding to the Hamiltonian of the one-dimensional Calogero model,

$$\hat{H}^{\text{Calogero}} \left(\varphi, \frac{\partial}{\partial \varphi} \right) = -\frac{1}{2} \frac{\partial^2}{\partial \varphi^2} + \frac{1}{2} \omega^2 \varphi^2 - \frac{1}{8} \frac{A}{\varphi^2}, \quad d\mu(\varphi) = d\varphi. \quad (\text{B.12})$$

Note that the parameter range $A = 1 - 4\mu^2 \in (-\infty, 1)$ is the maximum range for which the Calogero Hamiltonian is selfadjoint. Two-dimensional Lorentzian quantum gravity with open boundary conditions corresponds to the value $A = 1$, whereas for circular boundary conditions it corresponds to $A = -3$. The first connection between two-dimensional CDT and the Calogero model was established in [127], where a generalized CDT model was introduced which continuously covered the parameter range $0 \leq A \leq 1$.

The spectrum of the Calogero Hamiltonian is well-known, further it can be related to the spectrum of the radial solution of the three-dimensional Schrödinger equation with potential $U(r) = D_1/r^2 + D_2 r^2$ [213]. Explicitly, the solution of the eigenvalue problem (B.11) can be obtained by doing a variable transformation $\tilde{L} = \omega \varphi^2$, yielding

$$\left(\tilde{L} \frac{\partial^2}{\partial \tilde{L}^2} + \frac{1}{2} \frac{\partial}{\partial \tilde{L}} - \frac{1}{4} \tilde{L} + \frac{E}{2\omega} + \frac{A}{16\tilde{L}} \right) \Phi(\tilde{L}) = 0. \quad (\text{B.13})$$

Note that \tilde{L} is just a scaled version of L , so we could have directly arrived here from (B.9), using the wave function transformation from $\Psi(L)$ to $\Phi(\tilde{L})$. From (B.13) one can see that asymptotically for $\tilde{L} \rightarrow \infty$ the solution should be proportional to $\exp(-\tilde{L}/2)$ and for small $\tilde{L} \rightarrow 0$ it behaves like $\tilde{L}^{1/4+\mu/2}$. Note that these are the only asymptotics compatible with the requirement (B.7) on the wave functions. Hence, we make the

following ansatz for the wave functions $\Phi(\tilde{L}) \propto \exp(-\tilde{L}/2)\tilde{L}^{1/4+\mu/2}\eta(\tilde{L})$. Substituting this into (B.13) yields

$$\tilde{L}\eta''(\tilde{L}) + (1 + \mu - \tilde{L})\eta'(\tilde{L}) + \left(\frac{E}{2\omega} - \frac{1}{2}(\mu + 1)\right)\eta(\tilde{L}) = 0 \quad (\text{B.14})$$

This equation is known as Kummer's equation [214], whose solutions are the confluent hypergeometric functions,

$$\eta(\tilde{L}) = {}_1F_1(-n; 1 + \mu; \tilde{L}), \quad (\text{B.15})$$

where $n = \frac{E}{2\omega} - \frac{1}{2}(1 + \mu)$ must be a nonnegative integer. In this case the power series of the confluent hypergeometric function is truncated to a polynomial of degree n , namely, the generalized Laguerre polynomials [57],

$${}_1F_1(-n; \mu + 1; z) = \frac{\Gamma(n + 1)\Gamma(\mu + 1)}{\Gamma(n + \mu + 1)} L_n^\mu(z), \quad (\text{B.16})$$

with

$$L_n^\mu(z) = \frac{1}{n!} e^z z^{-\mu} \frac{d^n}{dz^n} (e^{-z} z^{n+\mu}) \quad (\text{B.17})$$

$$= \sum_{k=0}^n (-1)^k \frac{\Gamma(n + \mu + 1)}{\Gamma(n - k + 1)\Gamma(\mu + k + 1)} \frac{z^k}{k!}, \quad (\text{B.18})$$

yielding the final expression,

$${}_1F_1(-n; \mu + 1; z) = \sum_{k=0}^n (-1)^k \binom{n}{k} \frac{1}{(\mu + 1)(\mu + 2)\dots(\mu + k)} \frac{z^k}{k!}. \quad (\text{B.19})$$

Since $n = \frac{E}{2\omega} - \frac{1}{2}(1 + \mu)$ must be a nonnegative integer, the spectrum of the Calogero Hamiltonian $\hat{H}^{\text{Calogero}}$ reads

$$E_n = \omega(2n + \mu + 1), \quad n = 0, 1, 2, \dots \quad (\text{B.20})$$

The corresponding eigenfunctions are given by

$$\Phi_n(\varphi) = C_n e^{-\frac{\omega}{2}\varphi^2} \varphi^{\frac{1}{2}+\mu} {}_1F_1(-n; 1 + \mu; \omega\varphi^2), \quad d\mu(\varphi) = d\varphi. \quad (\text{B.21})$$

Further, since the Laguerre polynomials are orthogonal functions, the wave functions form an orthonormal basis of the Hilbert space, where the normalization constant is given by

$$C_n = \sqrt{\frac{2\omega^{\mu+1}\Gamma(n + \mu + 1)}{\Gamma(n + 1)\Gamma(\mu + 1)^2}}, \quad (\text{B.22})$$

where we used the following orthogonal relation for the generalized Laguerre polynomials [57],

$$\int_0^\infty d\tilde{L} e^{-\tilde{L}} \tilde{L}^\mu L_n^\mu(\tilde{L}) L_m^\mu(\tilde{L}) = \begin{cases} 0 & \text{for } n \neq m, \\ \frac{\Gamma(\mu+n+1)}{\Gamma(n+1)} & \text{for } n = m, \end{cases} \quad (\text{B.23})$$

which is valid for $\mu \geq 0$.

Let us now come back to the original problem, analyzing the Hamiltonian

$$\hat{H}(L, \frac{\partial}{\partial L}) = -c_1 L \frac{\partial^2}{\partial L^2} - c_2 \frac{\partial}{\partial L} + \Lambda L, \quad d\mu(L) = L^\mu dL, \quad \mu = \frac{c_2}{c_1} - 1. \quad (\text{B.24})$$

The spectrum is obviously the same as for the Calogero Hamiltonian, hence from (B.20) we get

$$E_n = \sqrt{c_1 \Lambda} (2n + \mu + 1), \quad n = 0, 1, 2, \dots \quad (\text{B.25})$$

Further, the eigenfunctions of $\hat{H}(L, \partial_L)$ can be obtained from (B.21) by a simultaneous variable and wave function transformation, yielding

$$\psi_n(L) = \mathcal{A}_n e^{-\sqrt{\frac{\Lambda}{c_1}} L} {}_1F_1(-n; 1 + \mu; 2\sqrt{\frac{\Lambda}{c_1}} L), \quad d\mu(L) = L^\mu dL \quad (\text{B.26})$$

where the normalization factor is given by

$$\mathcal{A}_n = 2^{\frac{\mu}{2}} c_1^{-\frac{\mu+1}{2}} C_n = \left(\frac{4\Lambda}{c_1} \right)^{\frac{\mu+1}{4}} \sqrt{\frac{\Gamma(n + \mu + 1)}{\Gamma(n + 1)\Gamma(\mu + 1)^2}}. \quad (\text{B.27})$$

Having obtained the eigenfunctions for the class of Hamiltonians $\hat{H}(L, \partial_L)$, we are now able to give an explicit expression for the finite time propagator or loop-loop correlator,

$$G_\Lambda(L_1, L_2; T) = \langle L_2 | e^{-T\hat{H}} | L_1 \rangle. \quad (\text{B.28})$$

Since the eigenfunctions form an orthonormal basis of the Hilbert space, we can insert the unit operator $I = \sum_{n \geq 0} |n\rangle \langle n|$, yielding

$$\begin{aligned} G_\Lambda(L_1, L_2; T) &= \sum_{n=0}^{\infty} \langle L_2 | n \rangle e^{-TE_n} \langle n | L_1 \rangle \\ &= \sum_{n=0}^{\infty} e^{-TE_n} \psi_n^*(L_2) \psi_n(L_1) \end{aligned} \quad (\text{B.29})$$

Upon inserting the energy eigenvalues (B.25) and eigenfunctions (B.26) into (B.29) one obtains

$$G_\Lambda(L_1, L_2; T) = \left(\frac{4\Lambda}{c_1}\right)^{\frac{\mu+1}{2}} e^{-\sqrt{\frac{\Lambda}{c_1}} T} \sum_{n=0}^{\infty} z^{n+\frac{\mu+1}{2}} \frac{\Gamma(n+\mu+1)}{\Gamma(n+1)\Gamma(\mu+1)^2} \times \\ \times {}_1F_1(-n; 1+\mu; 2\sqrt{\frac{\Lambda}{c_1}}L_1) {}_1F_1(-n; 1+\mu; 2\sqrt{\frac{\Lambda}{c_1}}L_2), \quad (\text{B.30})$$

where we used the notation $z = e^{-2\sqrt{c_1\Lambda}T}$. To evaluate the above summation we make use of the following quadratic relation satisfied by the confluent hypergeometric function [57],

$$\sum_{n=0}^{\infty} z^n \frac{\Gamma(n+\mu+1)}{\Gamma(n+1)\Gamma(\mu+1)^2} {}_1F_1(-n; 1+\mu; x) {}_1F_1(-n; 1+\mu; y) = \\ = \frac{1}{1-z} e^{-\frac{z(x+y)}{1-z}} (xyz)^{\frac{-\mu}{2}} I_\mu\left(2\sqrt{\frac{xyz}{1-z}}\right), \quad (\text{B.31})$$

where $I_\mu(x)$ denotes the modified Bessel function of the μ -th kind. Gathering all terms together leads to the final expression for the finite time propagator

$$G_\Lambda(L_1, L_2, T) = \sqrt{\frac{\Lambda}{c_1}} (L_1 L_2)^{-\frac{\mu}{2}} \frac{e^{-\sqrt{\frac{\Lambda}{c_1}}(L_1+L_2)\coth(\sqrt{c_1\Lambda}T)}}{\sinh(\sqrt{c_1\Lambda}T)} I_\mu\left(\frac{2}{\sqrt{c_1}} \frac{\sqrt{\Lambda L_1 L_2}}{\sinh(\sqrt{c_1\Lambda}T)}\right). \quad (\text{B.32})$$

For $\mu = c_1 = 1$, (B.32) corresponds to the “unmarked” propagator for the two-dimensional CDT model with circular boundary conditions, as obtained in (6.33).

Bibliography

- [1] M. Weigel, *Vertex models on random graphs*. PhD thesis, Universität Leipzig, 2002.
- [2] S. Carlip, “Quantum gravity: A progress report,” *Rept. Prog. Phys.* **64** (2001) 885, gr-qc/0108040.
- [3] G. 't Hooft and M. J. G. Veltman, “One loop divergencies in the theory of gravitation,” *Annales Poincare Phys. Theor.* **A20** (1974) 69–94.
- [4] M. B. Green, J. H. Schwarz, and E. Witten, *Superstring Theory. Vol. 1: Introduction*. Cambridge Monographs On Mathematical Physics. Cambridge University Press, 1987.
- [5] M. B. Green, J. H. Schwarz, and E. Witten, *Superstring Theory. Vol 2. Loop Amplitudes, Anomalies and Phenomenology*. Cambridge Monographs On Mathematical Physics. Cambridge University Press, 1987.
- [6] J. Polchinski, *String theory. Vol. 1: An introduction to the bosonic string*. Cambridge University Press, 1998.
- [7] J. Polchinski, *String theory. Vol. 2: Superstring theory and beyond*. Cambridge University Press, 1998.
- [8] L. F. Alday, “Lectures on scattering amplitudes via AdS/CFT,” *Fortsch. Phys.* **56** (2008) 816–823, 0804.0951.
- [9] H. Nicolai, K. Peeters, and M. Zamaklar, “Loop quantum gravity: An outside view,” hep-th/0501114.
- [10] H. Nicolai and K. Peeters, “Loop and spin foam quantum gravity: A brief guide for beginners,” *Lect. Notes Phys.* **721** (2007) 151–184, hep-th/0601129.
- [11] P. A. M. Dirac, *Lectures on quantum mechanics*. Yeshiva University Press, 1964.
- [12] A. Ashtekar, “New variables for classical and quantum gravity,” *Phys. Rev. Lett.* **57** (1986) 2244–2247.
- [13] A. Perez, “Spin foam models for quantum gravity,” *Class. Quant. Grav.* **20** (2003) R43, gr-qc/0301113.

- [14] L. Bombelli, J.-H. Lee, D. Meyer, and R. Sorkin, "Space-time as a causal set," *Phys. Rev. Lett.* **59** (1987) 521.
- [15] R. D. Sorkin, "Causal sets: Discrete gravity," in *Lectures on Quantum Gravity, Proceedings of the Valdivia Summer School, Valdivia, Chile, January 2002*, A. Gomberoff and D. Marolf, eds. Plenum, 2005. gr-qc/0309009.
- [16] S. Weinberg, "Ultraviolet divergences in quantum theories of gravitation," in *General Relativity*, S. Hawking and W. Israel, eds., pp. 790–831. 1980.
- [17] O. Lauscher and M. Reuter, "Asymptotic safety in quantum Einstein gravity: Nonperturbative renormalizability and fractal spacetime structure," in *Quantum gravity*, B. Fauser, ed., pp. 293–313. 2005. hep-th/0511260.
- [18] J. Ambjørn, B. Durhuus, and T. Jonsson, *Quantum geometry. A statistical field theory approach*. No. 1 in Cambridge Monogr. Math. Phys.,. Cambridge University Press, Cambridge, UK, 1997.
- [19] J. Ambjørn and R. Loll, "Non-perturbative Lorentzian quantum gravity, causality and topology change," *Nucl. Phys.* **B536** (1998) 407–434, hep-th/9805108.
- [20] J. Ambjørn, J. Jurkiewicz, and R. Loll, "Quantum gravity, or the art of building spacetime," hep-th/0604212.
- [21] J. Ambjørn, J. Jurkiewicz, and R. Loll, "The self-organized de Sitter universe," 0806.0397.
- [22] S. W. Hawking, A. R. King, and P. J. McCarthy, "A new topology for curved space-time which incorporates the causal, differential, and conformal structures," *J. Math. Phys.* **17** (1976) 174–181.
- [23] D. B. Malament, "The class of continuous timelike curves determines the topology of spacetime," *J. Math. Phys.* **18** (1977) 1399–1404.
- [24] G. 't Hooft, "Quantum gravity: A fundamental problem and some radical ideas," in *Recent Developments in Gravitation (Proceedings of the 1978 Cargese Summer Institute)*, M. Levy and S. Deser, eds. Plenum, 1979.
- [25] J. Myrheim, "Statistical geometry," *CERN-TH-2538* (1978).
- [26] R. D. Sorkin, "First steps with causal sets," in *Proceedings of the ninth Italian Conference on General Relativity and Gravitational Physics, Capri, Italy, September 1990*, R. Cianci, R. de Ritis, M. Francaviglia, G. Marmo, C. Rubano, and P. Scudellaro, eds., pp. 68–90. World Scientific, Singapore, 1991.
- [27] R. D. Sorkin, "Space-time and causal sets," in *Relativity and Gravitation: Classical and Quantum (Proceedings of the SILARG VII Conference, Cocoyoc, Mexico, December 1990)*, pp. 150–173. World Scientific, Singapore, 1991.
- [28] F. Dowker, J. Henson, and R. D. Sorkin, "Quantum gravity phenomenology, Lorentz invariance and discreteness," *Mod. Phys. Lett.* **A19** (2004) 1829–1840, gr-qc/0311055.

- [29] L. Bombelli, J. Henson, and R. D. Sorkin, "Discreteness without symmetry breaking: A theorem," *gr-qc/0605006*.
- [30] L. Bombelli and D. A. Meyer, "The origin of Lorentzian geometry," *Phys. Lett.* **A141** (1989) 226–228.
- [31] J. Noldus, "A Lorentzian Lipschitz, Gromov-Hausdorff notion of distance," *Class. Quant. Grav.* **21** (2004) 839–850, *gr-qc/0308074*.
- [32] D. P. Rideout and R. D. Sorkin, "A classical sequential growth dynamics for causal sets," *Phys. Rev.* **D61** (2000) 024002, *gr-qc/9904062*.
- [33] X. Martin, D. O'Connor, D. P. Rideout, and R. D. Sorkin, "On the 'renormalization' transformations induced by cycles of expansion and contraction in causal set cosmology," *Phys. Rev.* **D63** (2001) 084026, *gr-qc/0009063*.
- [34] D. P. Rideout and R. D. Sorkin, "Evidence for a continuum limit in causal set dynamics," *Phys. Rev.* **D63** (2001) 104011, *gr-qc/0003117*.
- [35] M. Varadarajan and D. P. Rideout, "A general solution for classical sequential growth dynamics of causal sets," *Phys. Rev.* **D73** (2006) 104021, *gr-qc/0504066*.
- [36] D. P. Rideout Private communication.
- [37] M. Ahmed, S. Dodelson, P. B. Greene, and R. D. Sorkin, "Everpresent Lambda," *Phys. Rev.* **D69** (2004) 103523, *astro-ph/0209274*.
- [38] D. Dou and R. D. Sorkin, "Black hole entropy as causal links," *Found. Phys.* **33** (2003) 279–296, *gr-qc/0302009*.
- [39] D. Rideout and S. Zohren, "Evidence for an entropy bound from fundamentally discrete gravity," *Class. Quant. Grav.* **23** (2006) 6195–6213, *gr-qc/0606065*.
- [40] S. Johnston, "Particle propagators on discrete spacetime," *Preprint* (2008) 0806.3083.
- [41] D. Rideout and S. Zohren, "Counting entropy in causal set quantum gravity," in *Proceedings of the Eleventh Marcel Grossmann Meeting on General Relativity*, H. Kleinert and R. T. Jantzen, eds. World Scientific, 2008. *gr-qc/0612074*.
- [42] J. D. Bekenstein, "Black holes and the second law," *Nuovo Cim. Lett.* **4** (1972) 737–740.
- [43] J. D. Bekenstein, "Black holes and entropy," *Phys. Rev.* **D7** (1973) 2333–2346.
- [44] J. D. Bekenstein, "Generalized second law of thermodynamics in black hole physics," *Phys. Rev.* **D9** (1974) 3292–3300.
- [45] S. W. Hawking, "Black hole explosions," *Nature* **248** (1974) 30–31.
- [46] L. Susskind, "The world as a hologram," *J. Math. Phys.* **36** (1995) 6377–6396, *hep-th/9409089*.
- [47] J. D. Bekenstein, "A universal upper bound on the entropy to energy ratio for bounded systems," *Phys. Rev.* **D23** (1981) 287.

- [48] R. Bousso, “Bekenstein bounds in de Sitter and flat space,” *JHEP* **04** (2001) 035, hep-th/0012052.
- [49] R. Bousso, “A covariant entropy conjecture,” *JHEP* **07** (1999) 004, hep-th/9905177.
- [50] R. Bousso, “The holographic principle,” *Rev. Mod. Phys.* **74** (2002) 825–874, hep-th/0203101.
- [51] G. ’t Hooft, “Dimensional reduction in quantum gravity,” in *Salamfestschrift: A collection of talks*, A. Ali, E. Ellis, and S. Randjbar-Daemi, eds., vol. 4 of *World Scientific Series in 20th Century Physics*. World Scientific, 1993. gr-qc/9310026.
- [52] S. Carlip, “Black hole thermodynamics and statistical mechanics,” *Preprint* (2008) 0807.4520.
- [53] R. D. Sorkin, “Forks in the road, on the way to quantum gravity,” *Int. J. Theor. Phys.* **36** (1997) 2759–2781, gr-qc/9706002.
- [54] C. J. Isham, “Prima facie questions in quantum gravity,” in *Canonical Formalism in Classical and Quantum General Relativity*, pp. 1–21. 1993. gr-qc/9310031.
- [55] R. D. Sorkin, “Ten theses on black hole entropy,” *Stud. Hist. Philos. Mod. Phys.* **36** (2005) 291–301, hep-th/0504037.
- [56] T. Goodale, G. Allen, G. Lanfermann, J. Massó, T. Radke, E. Seidel, and J. Shalf, “The cactus framework and toolkit: Design and applications,” in *VECPAR*, pp. 197–227. 2002.
- [57] I. S. Gradshteyn, I. M. Ryzhik, and A. Jeffrey, *Table of Integrals, Series, and Products*. Academic Press, New York and London, fifth ed., 1971.
- [58] K. A. Meissner, “Black hole entropy in loop quantum gravity,” *Class. Quant. Grav.* **21** (2004) 5245–5252, gr-qc/0407052.
- [59] P. A. M. Dirac *Z. Phys. Sov. Union* **3** (1933) 64.
- [60] R. P. Feynman, “Space-time approach to non-relativistic quantum mechanics,” *Rev. Mod. Phys.* **20** (1948) 367.
- [61] H. Kleinert, *Path Integrals in Quantum Mechanics, Statistics, Polymer Physics, and Financial Markets*. World Scientific, 4th ed., 2006.
- [62] L. Brink, P. Di Vecchia, and P. S. Howe, “A locally supersymmetric and reparametrization invariant action for the spinning string,” *Phys. Lett.* **B65** (1976) 471–474.
- [63] T. Goto, “Relativistic quantum mechanics of one-dimensional continuum and subsidiary conditions of dual resonance model,” *Prog. Theor. Phys.* **46** (1971) 1560.
- [64] A. M. Polyakov, “Quantum geometry of bosonic strings,” *Phys. Lett.* **B103** (1981) 207–210.
- [65] J. W. York, “Role of conformal three-geometry in the dynamics of gravitation,” *Phys. Rev. Lett.* **28** (1972), no. 16, 1082–1085.
- [66] G. W. Gibbons and S. W. Hawking, “Action integrals and partition functions in quantum gravity,” *Phys. Rev. D* **15** (1977), no. 10, 2752–2756.

- [67] L. D. Faddeev and A. A. Slavnov, *Gauge fields: Introduction to quantum theory*, vol. 50 of *Front. Phys.* Addison-Wesley Publishing Comp., 1980.
- [68] F. David, “Conformal field theories coupled to 2D gravity in the conformal gauge,” *Mod. Phys. Lett.* **A3** (1988) 1651.
- [69] J. Distler and H. Kawai, “Conformal field theory and 2-D quantum gravity or who’s afraid of Joseph Liouville?,” *Nucl. Phys.* **B321** (1989) 509.
- [70] E. Mottola, “Functional integration over geometries,” *J. Math. Phys.* **36** (1995) 2470–2511, hep-th/9502109.
- [71] A. Dasgupta and R. Loll, “A proper-time cure for the conformal sickness in quantum gravity,” *Nucl. Phys.* **B606** (2001) 357–379, hep-th/0103186.
- [72] J. B. Hartle and S. W. Hawking, “Wave function of the universe,” *Phys. Rev.* **D28** (1983) 2960–2975.
- [73] P. H. Ginsparg and G. W. Moore, “Lectures on 2-D gravity and 2-D string theory,” in *TASI 92*, pp. 277–470. 1993. hep-th/9304011.
- [74] P. Di Francesco, P. H. Ginsparg, and J. Zinn-Justin, “2-d gravity and random matrices,” *Phys. Rept.* **254** (1995) 1–133, hep-th/9306153.
- [75] E. J. Martinec, “The annular report on non-critical string theory,” *Preprint* (2003) hep-th/0305148.
- [76] R. Loll, “Discrete approaches to quantum gravity in four dimensions,” *Living Rev. Rel.* **1** (1998) 13, gr-qc/9805049.
- [77] T. Regge, “General relativity without coordinates,” *Nuovo Cim.* **19** (1961) 558–571.
- [78] M. Roček and R. M. Williams, “Quantum Regge calculus,” *Phys. Lett.* **B104** (1981).
- [79] J. Fröhlich, “Regge calculus and discretized gravitational functional integrals,” in *Non-perturbative quantum field theory*, J. Fröhlich, ed., pp. 523–545. 1994.
- [80] W. T. Tutte, “A census of hamiltonian polygons,” *Can. J. Math.* **14** (1962) 402–417.
- [81] W. T. Tutte, “A census of planar triangulations,” *Can. J. Math.* **14** (1962) 21–38.
- [82] W. T. Tutte, “A census of slicings,” *Can. J. Math.* **14** (1962) 798–722.
- [83] W. T. Tutte, “A census of planar maps,” *Can. J. Math.* **15** (1963) 249–271.
- [84] E. Brezin, C. Itzykson, G. Parisi, and J. B. Zuber, “Planar diagrams,” *Commun. Math. Phys.* **59** (1978) 35.
- [85] J. Ambjørn, B. Durhuus, and J. Fröhlich, “Diseases of triangulated random surface models, and possible cures,” *Nucl. Phys.* **B257** (1985) 433.
- [86] J. Ambjørn, B. Durhuus, J. Fröhlich, and P. Orland, “The appearance of critical dimensions in regulated string theories,” *Nucl. Phys.* **B270** (1986) 457.

- [87] F. David, "A model of random surfaces with nontrivial critical behavior," *Nucl. Phys.* **B257** (1985) 543.
- [88] A. Billoire and F. David, "Scaling properties of randomly triangulated planar random surfaces: A numerical study," *Nucl. Phys.* **B275** (1986) 617.
- [89] V. A. Kazakov, A. A. Migdal, and I. K. Kostov, "Critical properties of randomly triangulated planar random surfaces," *Phys. Lett.* **B157** (1985) 295–300.
- [90] N. Ishibashi and H. Kawai, "String field theory of noncritical strings," *Phys. Lett.* **B314** (1993) 190–196, [hep-th/9307045](#).
- [91] N. Ishibashi and H. Kawai, "String field theory of $c \leq 1$ noncritical strings," *Phys. Lett.* **B322** (1994) 67–78, [hep-th/9312047](#).
- [92] N. Ishibashi and H. Kawai, "A background independent formulation of noncritical string theory," *Phys. Lett.* **B352** (1995) 75–82, [hep-th/9503134](#).
- [93] M. Fukuma, N. Ishibashi, H. Kawai, and M. Ninomiya, "Two-dimensional quantum gravity in temporal gauge," *Nucl. Phys.* **B427** (1994) 139–157, [hep-th/9312175](#).
- [94] Y. Watabiki, "Construction of noncritical string field theory by transfer matrix formalism in dynamical triangulation," *Nucl. Phys.* **B441** (1995) 119–166, [hep-th/9401096](#).
- [95] H. Kawai, N. Kawamoto, T. Mogami, and Y. Watabiki, "Transfer matrix formalism for two-dimensional quantum gravity and fractal structures of space-time," *Phys. Lett.* **B306** (1993) 19–26, [hep-th/9302133](#).
- [96] S. S. Gubser and I. R. Klebanov, "Scaling functions for baby universes in two-dimensional quantum gravity," *Nucl. Phys.* **B416** (1994) 827–849, [hep-th/9310098](#).
- [97] H. Aoki, H. Kawai, J. Nishimura, and A. Tsuchiya, "Operator product expansion in two-dimensional quantum gravity," *Nucl. Phys.* **B474** (1996) 512–528, [hep-th/9511117](#).
- [98] J. Ambjørn and Y. Watabiki, "Scaling in quantum gravity," *Nucl. Phys.* **B445** (1995) 129–144, [hep-th/9501049](#).
- [99] V. G. Knizhnik, A. M. Polyakov, and A. B. Zamolodchikov, "Fractal structure of two-dimensional quantum gravity," *Mod. Phys. Lett.* **A3** (1988) 819.
- [100] J. Ambjørn, J. Jurkiewicz, and Y. Watabiki, "On the fractal structure of two-dimensional quantum gravity," *Nucl. Phys.* **B454** (1995) 313–342, [hep-lat/9507014](#).
- [101] J. Ambjørn, D. Boulatov, J. L. Nielsen, J. Rolf, and Y. Watabiki, "The spectral dimension of 2D quantum gravity," *JHEP* **02** (1998) 010, [hep-th/9801099](#).
- [102] J. Ambjørn, B. Durhuus, and T. Jonsson, "Three-dimensional simplicial quantum gravity and generalized matrix models," *Mod. Phys. Lett.* **A6** (1991) 1133–1146.
- [103] M. E. Agishtein, R. Benav, A. A. Migdal, and S. Solomon, "Numerical study of a two point correlation function and Liouville field properties in two-dimensional quantum gravity," *Mod. Phys. Lett.* **A6** (1991) 1115–1132.

- [104] D. V. Boulatov and A. Krzywicki, "On the phase diagram of three-dimensional simplicial quantum gravity," *Mod. Phys. Lett.* **A6** (1991) 3005–3014.
- [105] J. Ambjørn, D. V. Boulatov, A. Krzywicki, and S. Varsted, "The vacuum in three-dimensional simplicial quantum gravity," *Phys. Lett.* **B276** (1992) 432–436.
- [106] J. Ambjørn and J. Jurkiewicz, "Four-dimensional simplicial quantum gravity," *Phys. Lett.* **B278** (1992) 42–50.
- [107] M. E. Agishtein and A. A. Migdal, "Simulations of four-dimensional simplicial quantum gravity," *Mod. Phys. Lett.* **A7** (1992) 1039–1062.
- [108] S. Varsted, "Four-dimensional quantum gravity by dynamical triangulations," *Nucl. Phys.* **B412** (1994) 406–414.
- [109] J. Ambjørn, J. Jurkiewicz, and C. F. Kristjansen, "Quantum gravity, dynamical triangulations and higher derivative regularization," *Nucl. Phys.* **B393** (1993) 601–632, [hep-th/9208032](#).
- [110] M. E. Agishtein and A. A. Migdal, "Critical behavior of dynamically triangulated quantum gravity in four-dimensions," *Nucl. Phys.* **B385** (1992) 395–412, [hep-lat/9204004](#).
- [111] J. Ambjørn, S. Jain, J. Jurkiewicz, and C. F. Kristjansen, "Observing 4-d baby universes in quantum gravity," *Phys. Lett.* **B305** (1993) 208–213, [hep-th/9303041](#).
- [112] B. Brugmann, "Nonuniform measure in four-dimensional simplicial quantum gravity," *Phys. Rev.* **D47** (1993) 3330–3338, [hep-lat/9210001](#).
- [113] B. V. de Bakker and J. Smit, "Curvature and scaling in 4-d dynamical triangulation," *Nucl. Phys.* **B439** (1995) 239–258, [hep-lat/9407014](#).
- [114] S. Catterall, J. B. Kogut, and R. Renken, "Phase structure of four-dimensional simplicial quantum gravity," *Phys. Lett.* **B328** (1994) 277–283, [hep-lat/9401026](#).
- [115] S. Warner, S. Catterall, and R. Renken, "Phase diagram of three-dimensional dynamical triangulations with a boundary," *Phys. Lett.* **B442** (1998) 266–272, [hep-lat/9808006](#).
- [116] S. Catterall, "Simulations of dynamically triangulated gravity: An algorithm for arbitrary dimension," *Comput. Phys. Commun.* **87** (1995) 409–415, [hep-lat/9405026](#).
- [117] B. V. de Bakker, "Further evidence that the transition of 4d dynamical triangulation is 1st order," *Phys. Lett.* **B389** (1996) 238–242, [hep-lat/9603024](#).
- [118] S. Warner and S. Catterall, "Phase diagram of four-dimensional dynamical triangulations with a boundary," *Phys. Lett.* **B493** (2000) 389–394, [hep-lat/0008015](#).
- [119] S. Zohren, "Analytic results in 2D causal dynamical triangulations," Master's thesis, Utrecht University, 2005.
- [120] W. Westra, *Topology change and the emergence of geometry in two dimensional causal quantum gravity*. PhD thesis, Utrecht University, 2007.

- [121] C. Teitelboim, "Causality versus gauge invariance in quantum gravity and supergravity," *Phys. Rev. Lett.* **50** (1983) 705.
- [122] C. Teitelboim, "The proper time gauge in quantum theory of gravitation," *Phys. Rev.* **D28** (1983) 297.
- [123] J. Ambjørn, J. Jurkiewicz, and R. Loll, "Lorentzian and Euclidean quantum gravity: Analytical and numerical results," in *M-Theory and Quantum Gravity*, L. Thorlacius and T. Jonsson, eds., NATO Science Series, pp. 382–449. Kluwer Academic Publishers, 2000. [hep-th/0001124](#).
- [124] J. Ambjørn, R. Loll, J. L. Nielsen, and J. Rolf, "Euclidean and Lorentzian quantum gravity: Lessons from two dimensions," *Chaos Solitons Fractals* **10** (1999) 177–195, [hep-th/9806241](#).
- [125] J. Ambjørn, J. Correia, C. Kristjansen, and R. Loll, "On the relation between Euclidean and Lorentzian 2D quantum gravity," *Phys. Lett.* **B475** (2000) 24–32, [hep-th/9912267](#).
- [126] P. Di Francesco, E. Guitter, and C. Kristjansen, "Integrable 2D Lorentzian gravity and random walks," *Nucl. Phys.* **B567** (2000) 515–553, [hep-th/9907084](#).
- [127] P. Di Francesco, E. Guitter, and C. Kristjansen, "Generalized Lorentzian gravity in (1+1)D and the Calogero Hamiltonian," *Nucl. Phys.* **B608** (2001) 485–526, [hep-th/0010259](#).
- [128] R. Loll, W. Westra, and S. Zohren, "Taming the cosmological constant in 2D causal quantum gravity with topology change," *Nucl. Phys.* **B751** (2006) 419–435, [hep-th/0507012](#).
- [129] J. Ambjørn, R. Janik, W. Westra, and S. Zohren, "The emergence of background geometry from quantum fluctuations," *Phys. Lett.* **B641** (2006) 94–98, [gr-qc/0607013](#).
- [130] J. Ambjørn, R. Loll, W. Westra, and S. Zohren, "Putting a cap on causality violations in CDT," *JHEP* **12** (2007) 017, [arXiv:0709.2784](#) [[gr-qc](#)].
- [131] J. Ambjørn, R. Loll, Y. Watabiki, W. Westra, and S. Zohren, "A string field theory based on causal dynamical triangulations," *JHEP* **05** (2008) 032, [0802.0719](#).
- [132] J. Ambjørn, R. Loll, Y. Watabiki, W. Westra, and S. Zohren, "Topology change in causal quantum gravity," in *Proceedings of the 17th Workshop on General Relativity and Gravitation in Japan*. 2008. [arXiv:0802.0896](#) [[hep-th](#)].
- [133] J. Ambjørn, R. Loll, Y. Watabiki, W. Westra, and S. Zohren, "A matrix model for 2D quantum gravity defined by causal dynamical triangulations," *Phys. Lett.* **B665** (2008) 252–256, [0804.0252](#).
- [134] R. Nakayama, "2-D quantum gravity in the proper time gauge," *Phys. Lett.* **B325** (1994) 347–353, [hep-th/9312158](#).
- [135] J. Ambjørn, J. Jurkiewicz, and R. Loll, "Nonperturbative 3d Lorentzian quantum gravity," *Phys. Rev.* **D76** (2001) 044011, [hep-th/0011276](#).
- [136] J. Ambjørn, J. Jurkiewicz, and R. Loll, "Dynamically triangulating Lorentzian quantum gravity," *Nucl. Phys.* **B610** (2001) 347–382, [hep-th/0105267](#).

- [137] J. Ambjørn, J. Jurkiewicz, R. Loll, and G. Vernizzi, “Lorentzian 3d gravity with wormholes via matrix models,” *JHEP* **09** (2001) 022, [hep-th/0106082](#).
- [138] J. Ambjørn, J. Jurkiewicz, and R. Loll, “3d Lorentzian quantum gravity, dynamically triangulated quantum gravity,” *Nucl. Phys. Proc. Suppl.* **106** (2002) 980–982, [hep-lat/0201013](#).
- [139] J. Ambjørn, J. Jurkiewicz, R. Loll, and G. Vernizzi, “3d Lorentzian quantum gravity from the asymmetric ABAB matrix model,” *Acta Phys. Polon.* **B34** (2003) 4667–4688, [hep-th/0311072](#).
- [140] J. Ambjørn, J. Jurkiewicz, and R. Loll, “Renormalization of 3d quantum gravity from matrix models,” *Phys. Lett.* **B581** (2004) 255–262, [hep-th/0307263](#).
- [141] D. Benedetti, R. Loll, and F. Zamponi, “(2+1)-dimensional quantum gravity as the continuum limit of causal dynamical triangulations,” *Phys. Rev.* **D76** (2007) 104022, [0704.3214](#).
- [142] J. Ambjørn, J. Jurkiewicz, and R. Loll, “Emergence of a 4D world from causal quantum gravity,” *Phys. Rev. Lett.* **93** (2004) 131301, [hep-th/0404156](#).
- [143] J. Ambjørn, J. Jurkiewicz, and R. Loll, “Semiclassical universe from first principles,” *Phys. Lett.* **B607** (2005) 205–213, [hep-th/0411152](#).
- [144] J. Ambjørn, J. Jurkiewicz, and R. Loll, “Spectral dimension of the universe,” *Phys. Rev. Lett.* **95** (2005) 171301, [hep-th/0505113](#).
- [145] J. Ambjørn, J. Jurkiewicz, and R. Loll, “Reconstructing the universe,” *Phys. Rev.* **D72** (2005) 064014, [hep-th/0505154](#).
- [146] J. Ambjørn, A. Görlich, J. Jurkiewicz, and R. Loll, “Planckian birth of the quantum de Sitter universe,” *Preprint* (2007) [arXiv:0712.2485](#) [[hep-th](#)].
- [147] J. Ambjørn, A. Görlich, J. Jurkiewicz, and R. Loll, “The nonperturbative quantum de Sitter universe,” [0807.4481](#).
- [148] J. Ambjørn, J. Jurkiewicz, and R. Loll, “The universe from scratch,” *Contemp. Phys.* **47** (2006) 103–117, [hep-th/0509010](#).
- [149] W. Souma, “Non-trivial ultraviolet fixed point in quantum gravity,” *Prog. Theor. Phys.* **102** (1999) 181–195, [hep-th/9907027](#).
- [150] M. Reuter and F. Saueressig, “A class of nonlocal truncations in quantum Einstein gravity and its renormalization group behavior,” *Phys. Rev.* **D66** (2002) 125001, [hep-th/0206145](#).
- [151] M. Reuter and F. Saueressig, “Renormalization group flow of quantum gravity in the Einstein-Hilbert truncation,” *Phys. Rev.* **D65** (2002) 065016, [hep-th/0110054](#).
- [152] D. F. Litim, “Fixed points of quantum gravity,” *Phys. Rev. Lett.* **92** (2004) 201301, [hep-th/0312114](#).
- [153] O. Lauscher and M. Reuter, “Fractal spacetime structure in asymptotically safe gravity,” *JHEP* **10** (2005) 050, [hep-th/0508202](#).
- [154] F. Dowker and S. Surya, “Topology change and causal continuity,” *Phys. Rev.* **D58** (1998) 124019, [gr-qc/9711070](#).

- [155] A. Borde, H. F. Dowker, R. S. Garcia, R. D. Sorkin, and S. Surya, "Causal continuity in degenerate spacetimes," *Class. Quant. Grav.* **16** (1999) 3457–3481, [gr-qc/9901063](#).
- [156] H. F. Dowker, R. S. Garcia, and S. Surya, "K-causality and degenerate spacetimes," *Class. Quant. Grav.* **17** (2000) 4377–4396, [gr-qc/9912090](#).
- [157] H. F. Dowker, R. S. Garcia, and S. Surya, "Morse index and causal continuity: A criterion for topology change in quantum gravity," *Class. Quant. Grav.* **17** (2000) 697–712, [gr-qc/9910034](#).
- [158] F. Dowker, "Topology change in quantum gravity," in *The future of theoretical physics and cosmology*, G. Gibbons, E. Shellard, and S. Rankin, eds. Cambridge Univ. Press, Cambridge, UK, 2002. [gr-qc/0206020](#).
- [159] J. Louko and R. D. Sorkin, "Complex actions in two-dimensional topology change," *Class. Quant. Grav.* **14** (1997) 179–204, [gr-qc/9511023](#).
- [160] B. Durhuus, J. Fröhlich, and T. Jonsson, "Critical behavior in a model of planar random surfaces," *Nucl. Phys.* **B240** (1984) 453.
- [161] J. Ambjørn and B. Durhuus, "Regularized bosonic strings need extrinsic curvature," *Phys. Lett.* **B188** (1987) 253.
- [162] J. Ambjørn, R. Janik, W. Westra, and S. Zohren, "The emergence of AdS(2) from quantum fluctuations," in *Proceedings of the Eleventh Marcel Grossmann Meeting on General Relativity*, H. Kleinert and R. T. Jantzen, eds. World Scientific, 2008. [gr-qc/0610101](#).
- [163] J. Ambjørn, S. Arianos, J. A. Gesser, and S. Kawamoto, "The geometry of ZZ-branes," *Phys. Lett.* **B599** (2004) 306–312, [hep-th/0406108](#).
- [164] A. B. Zamolodchikov and A. B. Zamolodchikov, "Liouville field theory on a pseudosphere," [hep-th/0101152](#).
- [165] N. Seiberg and D. Shih, "Branes, rings and matrix models in minimal (super)string theory," *JHEP* **02** (2004) 021, [hep-th/0312170](#).
- [166] D. Kutasov, K. Okuyama, J.-W. Park, N. Seiberg, and D. Shih, "Annulus amplitudes and ZZ branes in minimal string theory," *JHEP* **08** (2004) 026, [hep-th/0406030](#).
- [167] J. Ambjørn and J. A. Gesser, "World-sheet dynamics of ZZ branes," *Phys. Lett.* **B653** (2007) 439–444, [0706.3231](#).
- [168] J. Ambjørn and J. A. Gesser, "The nature of ZZ branes," *Phys. Lett.* **B659** (2008) 718–722, [0707.3431](#).
- [169] M. Ikehara, N. Ishibashi, H. Kawai, T. Mogami, R. Nakayama, and N. Sasakura, "String field theory in the temporal gauge," *Phys. Rev.* **D50** (1994) 7467–7478, [hep-th/9406207](#).
- [170] M. Ikehara, N. Ishibashi, H. Kawai, T. Mogami, R. Nakayama, and N. Sasakura, "A note on string field theory in the temporal gauge," *Prog. Theor. Phys. Suppl.* **118** (1995) 241–258, [hep-th/9409101](#).

- [171] J. Ambjørn and Y. Watabiki, “Non-critical string field theory for 2d quantum gravity coupled to (p,q) -conformal fields,” *Int. J. Mod. Phys. A* **12** (1997) 4257–4289, [hep-th/9604067](#).
- [172] J. Ambjørn, J. Jurkiewicz, and Y. M. Makeenko, “Multiloop correlators for two-dimensional quantum gravity,” *Phys. Lett. B* **251** (1990) 517–524.
- [173] J. Ambjørn and Y. M. Makeenko, “Properties of loop equations for the Hermitean matrix model and for two-dimensional quantum gravity,” *Mod. Phys. Lett. A* **5** (1990) 1753–1764.
- [174] R. Loll and W. Westra, “Sum over topologies and double-scaling limit in 2D Lorentzian quantum gravity,” [hep-th/0306183](#).
- [175] R. Loll and W. Westra, “Space-time foam in 2D and the sum over topologies,” *Acta Phys. Polon. B* **34** (2003) 4997–5008, [hep-th/0309012](#).
- [176] R. Loll, W. Westra, and S. Zohren, “Nonperturbative sum over topologies in 2D Lorentzian quantum gravity,” *AIP Conf. Proc.* **861** (2006) 391–397, [hep-th/0603079](#).
- [177] J. Ambjørn, B. Durhuus, T. Jonsson, and G. Thorleifsson, “Matter fields with $c > 1$ coupled to 2-d gravity,” *Nucl. Phys. B* **398** (1993) 568–592, [hep-th/9208030](#).
- [178] J. Ambjørn, K. N. Anagnostopoulos, and R. Loll, “Crossing the $c = 1$ barrier in 2d lorentzian quantum gravity,” *Phys. Rev. D* **61** (2000) 044010, [hep-lat/9909129](#).
- [179] G. 't Hooft, “A planar diagram theory for strong interactions,” *Nucl. Phys. B* **72** (1974) 461.
- [180] D. Bessis, C. Itzykson, and J. B. Zuber, “Quantum field theory techniques in graphical enumeration,” *Adv. Appl. Math.* **1** (1980) 109–157.
- [181] P. Di Francesco, “2D quantum gravity, matrix models and graph combinatorics,” [math-ph/0406013](#).
- [182] F. David, “Loop equations and nonperturbative effects in two-dimensional quantum gravity,” *Mod. Phys. Lett. A* **5** (1990) 1019–1030.
- [183] E. P. Wigner, “On the statistical distribution of the widths and spacings of nuclear resonance levels,” *Proc. Cambridge Phil. Soc.* **47** (1951) 790.
- [184] E. P. Wigner *Ann. Math.* **53** (1951) 36.
- [185] J. Ambjørn, L. Chekhov, C. F. Kristjansen, and Y. Makeenko, “Matrix model calculations beyond the spherical limit,” *Nucl. Phys. B* **404** (1993) 127–172, [hep-th/9302014](#).
- [186] B. Eynard, “Topological expansion for the 1-Hermitian matrix model correlation functions,” *JHEP* **11** (2004) 031, [hep-th/0407261](#).
- [187] L. Chekhov and B. Eynard, “Hermitean matrix model free energy: Feynman graph technique for all genera,” *JHEP* **03** (2006) 014, [hep-th/0504116](#).
- [188] M. Staudacher, “The Yang-Lee edge singularity on a dynamical planar random surface,” *Nucl. Phys. B* **336** (1990) 349.

- [189] M. L. Mehta, "A method of integration over matrix variables," *Commun. Math. Phys.* **79** (1981) 327–340.
- [190] V. A. Kazakov, "Ising model on a dynamical planar random lattice: Exact solution," *Phys. Lett.* **A119** (1986) 140–144.
- [191] D. V. Boulatov and V. A. Kazakov, "The Ising model on random planar lattice: The structure of phase transition and the exact critical exponents," *Phys. Lett.* **186B** (1987) 379.
- [192] D. J. Gross and A. A. Migdal, "Nonperturbative solution of the Ising model on a random surface," *Phys. Rev. Lett.* **64** (1990) 717.
- [193] M. Staudacher, "Combinatorial solution of the two matrix model," *Phys. Lett.* **B305** (1993) 332–338, hep-th/9301038.
- [194] M. R. Douglas and M. Li, "Free variables and the two matrix model," *Phys. Lett.* **B348** (1995) 360–364, hep-th/9412203.
- [195] S. M. Carroll, M. E. Ortiz, and W. Taylor, "Spin/disorder correlations and duality in the $c = 1/2$ string," *Nucl. Phys.* **B468** (1996) 420–438, hep-th/9510208.
- [196] J. Ambjørn, R. Loll, Y. Watabiki, W. Westra, and S. Zohren, "A causal continuum limit of matrix models." Utrecht preprint, 2008.
- [197] J. Ambjørn, R. Loll, Y. Watabiki, W. Westra, and S. Zohren, "A causal alternative for $c = 0$ strings." to appear in Act. Phys. Pol., 2008.
- [198] M. Arnsdorf, "Relating covariant and canonical approaches to triangulated models of quantum gravity," *Class. Quant. Grav.* **19** (2002) 1065–1092, gr-qc/0110026.
- [199] M. R. Douglas and S. H. Shenker, "Strings in less than one-dimension," *Nucl. Phys.* **B335** (1990) 635.
- [200] E. Brezin and V. A. Kazakov, "Exactly solvable field theories of closed strings," *Phys. Lett.* **B236** (1990) 144–150.
- [201] D. J. Gross and A. A. Migdal, "Nonperturbative two-dimensional quantum gravity," *Phys. Rev. Lett.* **64** (1990) 127.
- [202] R. Dijkgraaf and C. Vafa, "Matrix models, topological strings, and supersymmetric gauge theories," *Nucl. Phys.* **B644** (2002) 3–20, hep-th/0206255.
- [203] R. Dijkgraaf and C. Vafa, "A perturbative window into non-perturbative physics," hep-th/0208048.
- [204] E. Montroll and G. Newell, "On the theory of the Ising model of ferromagnetism," *Rev. Mod. Phys.* **25** (1953) 353.
- [205] B. McCoy and T. Wu, *The two-dimensional Ising model*. Harvard University Press, 1973.
- [206] C. Domb, *The critical point*. Taylor and Francis, 1996.
- [207] J. Ambjørn, K. N. Anagnostopoulos, and R. Loll, "A new perspective on matter coupling in 2d quantum gravity," *Phys. Rev.* **D60** (1999) 104035, hep-th/9904012.

-
- [208] J. Ambjørn, K. N. Anagnostopoulos, R. Loll, and I. Pushkina, "Shaken, but not stirred - Potts model coupled to quantum gravity," *Preprint* (2008) 0806.3506.
- [209] R. M. Wald, *General Relativity*. University Press, Chicago, USA, 1984.
- [210] S. W. Hawking and G. F. R. Ellis, *The Large Scale Structure of Space-time*. Cambridge University Press, 1973.
- [211] Y. L. Luke, *The special functions and their approximations*, vol. 1. Academic Press, New York and London, 1969.
- [212] R. Sorkin, "Time evolution problem in Regge calculus," *Phys. Rev.* **D12** (1975) 385–396.
- [213] L. D. Landau and E. M. Lifshitz, *Quantum Mechanics: Non-Relativistic Theory. Volume 3*. Butterworth-Heinemann, Oxford, UK, 4th rev. english ed., 1998.
- [214] M. Abramowitz and I. A. Stegun, *Handbook of Mathematical Functions, With Formulas, Graphs, and Mathematical Tables*. Dover Publications, 1974.

Index

- φ^3 -theory, 122, 151
- Additive renormalization, 58
- Alexandrov region, 184
- Baby universe, 94
- Bekenstein's entropy bound, 16
- Bekenstein-Hawking formula, 15
- Black hole entropy, 15
- Bousso's entropy bound, 16
- Branched polymers, 56
- Brink-Di Vecchia-Howe action, 40
- $c=1$ barrier, 147
- Cactus, 21
- Calogero Hamiltonian, 190
- Catalan numbers, 56
- Cauchy horizon, 184
 - future, 184
 - past, 184
- Causal dynamical triangulations (CDT), 75
 - classical effective action, 112
 - continuum limit, 81
 - dimensional reduction, 90
 - disc function, 84, 87
 - double scaling limit, 131, 175
 - effective quantum Hamiltonian, 85
 - energy eigenvalues, 192
 - generalized model, 123
 - genus one disc function, 143
 - genus two disc function, 143
 - Hamiltonians, 189
 - Hausdorff dimension, 88
 - higher dimensional, 90
 - loop equations, 163
 - loop-loop amplitude, 128
 - matrix model, 167, 173
 - one-step propagator, 79
 - propagator, 80–82
 - renormalization relation to DT, 104
 - running boundary cosmological constant, 111
 - scaling relations, 81
 - spectral dimension, 90
 - states, 192
 - string coupling constant, 123
 - string field theory, 135
 - two-point function, 84
 - Wick rotation, 77
- Causal future, 184
- Causal past, 184
- Causal sets, 10
 - entropy bound, 19
 - fundamental length scale, 29
 - future, 11
 - maximal element, 11
 - minimal element, 11
 - past, 11
- Chronological future, 183
- Chronological past, 183
- Composition law, 67, 78
- Conformal embedding, 11
- Conformal gauge, 46

- Correlation length, 58
- Covariant entropy bound, 16
- Critical exponent, 58
- Critical phenomena, 58

- Deficit angle, 50
 - Lorentzian, 187
- Dijkgraaf-Vafa correspondence, 175
- Double light cone, 94
- Dynamical triangulations (DT), 52
 - branched polymer phase, 74
 - continuum limit, 58
 - crumpled phase, 74
 - disc function, 53, 70
 - double scaling limit, 131
 - fractal structure, 99
 - Hausdorff dimension, 72
 - higher-dimensional, 73
 - loop equation, 55
 - loop-loop amplitude, 128
 - matrix model, 154
 - non-compact space-times, 109
 - one-step propagator, 70
 - propagator, 65
 - renormalization relation to CDT, 104
 - running boundary cosmological constant, 110
 - scaling relations, 59
 - two-point function, 67
- Dyson-Schwinger equations, 140

- Einstein-Hilbert action, 43
- Euclidean quantum gravity, 45
- Euler's beta function, 24
- Euler-characteristic, 45
- Exponential integral, 21
 - asymptotic expansion, 21

- Faithful embedding, 11
- Fat-graphs, 152
- Feynman propagator, 40
- Fixed geodesic distance two-loop amplitude, 65
- Future domain of dependence, 184

- Gauss-Bonnet theorem, 45
- Generalized CDT, 123
- Generalized hypergeometric function, 24
 - asymptotic expansion, 185
- Generalized Laguerre polynomials, 191
- Generating functional, 56
- Geodesic distance, 60
- Gravitational path integral, 43

- Hartle-Hawking no-boundary condition, 117
- Hartle-Hawking wave functions, 46
- Hasse diagram, 10
- Hausdorff dimension, 72
- Higher loop amplitudes, 159

- Induced action, 86
- Integrating out baby universes, 101
- Ising model, 181

- Klein-Gordon field, 40
- KPZ-values, 181
- Kummer's equation, 191

- Large- N limit, 154
- Liouville field theory, 46
- Loop insertion operator, 159

- Matrix models, 151
 - CDT, 167, 173
 - density of eigenvalues, 155
 - DT, 154
 - loop equations, 155
- Minimal models, 160
- Modified Bessel function, 82
- Morse point, 94

- Nambu-Goto action, 41
- Non-compact space-times, 109
- Non-scaling part, 59

- One-dimensional gravity, 37
- One-step propagator, 68
- Onsager-values, 181

- Partition function, 43
- Past domain of dependence, 184
- Peeling procedure, 62
- Planar limit, 154
- Pochhammer polynomials, 24
- Poincaré disk, 109
- Poisson distribution, 12
- Polyakov action, 42
- Proper time gauge, 86
- Pseudo-sphere, 109

- Random path, 37
- Random surfaces, 41
- Regge action, 51, 73
- Regge calculus, 49
- Relativistic particle, 37
- Relativistic string, 41
- Rigid Regge calculus, 52

- Semi-group property, 67, 78
- Sequential growth models, 12
- Simplicial quantum gravity, 49
- Spatial topology changes, 62, 94
- String field theory, 133
- String worldsheet, 42
- Susskind's spherical entropy bound, 16

- Third-quantization of gravity, 133
- Topological expansion, 45
- Transfer matrix, 68
- Triangulation, 52
 - automorphism group, 52
 - dual, 51
 - Lorentzian, 76, 187
 - non-restricted, 54
- Trousers geometry, 94

- Wave function renormalization, 59
- Wick rotation, 39
 - CDT, 77, 189
 - quantum gravity, 43

- ZZ-brane, 110

Curriculum Vitae

Stefan Zohren was born in Mönchengladbach, Germany on Dec 17, 1980. From 1986 to 1990 he attended the primary school in Birgelen and from 1990 to 2000 the Cusanus Gymnasium grammar school in Erkelenz, followed by civil service at the German Red Cross with training as a rescue medic. From 2001 to 2005 Stefan studied physics with a mathematics extension at the RWTH Aachen University of Technology and Utrecht University with exchanges to Queen Mary, University of London and Universidad Autónoma de Madrid. He graduated as Dipl.-Phys. (cum laude) from RWTH Aachen, MSc. in theoretical physics (cum laude) and MSc. in mathematical sciences (cum laude) from Utrecht University. For his diploma thesis he received the Sprigorum medal and the Schöneborn Prize of the RWTH Aachen. During the time of his undergraduate studies Stefan worked as system administrator at the Department of Economics, RWTH Aachen, and teaching assistant at the Department of Mathematics and the Department of Theoretical Physics, RWTH Aachen, as well as the Department of Physics at Queen Mary, University of London. In the summer 2005 he did an internship at the German Development Cooperation in Brazil, followed later by a short junior consultant internship. From 2005 to 2008 Stefan was employed as an early stage researcher of the European Research Network on Random Geometries and Random Matrices at the Blackett Laboratory, Imperial College London following his PhD studies in theoretical physics. Besides attendance of numerous international conferences and several short visits to various institutions such as Utrecht University and the Niels Bohr Institute, he was a JSPS fellow at Tokyo Institute of Technology and Ochanomizu University from Oct to Dec 2007. In 2006/2007 Stefan attended a part-time course in economics at the London School of Economics, University of London external program in which he graduated as Diploma for Graduates in Economics (merit) in 2007.

